THE GEOLOGY,GEOCHEMISTRY, GEOCHRONOLOGY AND REGIONAL SETTING OF THE ANNIEOPSQUOTCH COMPLEX AND RELATED ROCKS OF SOUTHWEST NEWFOUNDLAND

GREGORY RALPH DUNNING

CANADIAN THESES ON MICROFICHE

I.S.B.N.

THESES CANADIENNES SUR MICROFICHE

National Library of Canada
Collections Development Branch

Canadian Theses on
Microfiche Service

Ottawa, Canada
K1A 0N4

Bibliothèque nationale du Canada
Direction du développement des collections

Service des thèses canadiennes
sur microfiche

NOTICE

The quality of this microfiche is heavily dependent upon the quality of the original thesis submitted for microfilming. Every effort has been made to ensure the highest quality of reproduction possible.

If pages are missing, contact the university which granted the degree.

Some pages may have indistinct print especially if the original pages were typed with a poor typewriter ribbon or if the university sent us a poor photocopy.

Previously copyrighted materials (journal articles, published tests, etc.) are not filmed.

Reproduction in full or in part of this film is governed by the Canadian Copyright Act, R.S.C. 1970, c. C-30. Please read the authorization forms which accompany this thesis.

AVIS

La qualité de cette microfiche dépend grandement de la qualité de la thèse soumise au microfilmage. Nous avons tout fait pour assurer une qualité supérieure de reproduction.

S'il manque des pages, veuillez communiquer avec l'université qui a conféré le grade.

La qualité d'impression de certaines pages peut laisser à désirer, surtout si les pages originales ont été dactylographiées à l'aide d'un ruban usé ou si l'université nous a fait parvenir une photocopie de mauvaise qualité.

Les documents qui font déjà l'objet d'un droit d'auteur (articles de revue, examens publiés, etc.) ne sont pas microfilmés.

La reproduction, même partielle, de ce microfilm est soumise à la Loi canadienne sur le droit d'auteur, SRC 1970, c. C-30. Veuillez prendre connaissance des formules d'autorisation qui accompagnent cette thèse.

THIS DISSERTATION
HAS BEEN MICROFILMED
EXACTLY AS RECEIVED

LA THÈSE A ÉTÉ
MICROFILMÉE TELLE QUE
NOUS L'AVONS REÇUE

NL-339 (r. 82/08)

Canada

THE GEOLOGY, GEOCHEMISTRY, GEOCHRONOLOGY AND REGIONAL SETTING OF THE ANNIEOPSQUOTCH COMPLEX AND RELATED ROCKS OF SOUTHWEST NEWFOUNDLAND

BY

© Gregory Ralph Dunning, B.Sc., M.Sc.

A thesis submitted to the School of Graduate Studies in partial fulfillment of the requirements for the degree of Doctor of Philosophy

Department of Earth Sciences
Memorial University of Newfoundland

January, 1984

St. John's Newfoundland

Frontispiece

Gabbro of the base of the ophiolite sequence exposed along the northwest edge of the Annieopsquotch Mountains. View to northeast along Lloyds River to Lloyds Lake. Annieopsquotch is the Indian word for "rocky place".

ABSTRACT

The Annieopsquotch Complex is an ophiolite which forms the Annieopsquotch Mountains of southwest Newfoundland. It contains rocks of the critical zone, gabbro zone (2.3 km thick), sheeted dyke zone (1.5 km) and pillow lava zone of a typical ophiolite. The zones trend northeast, face and dip southeast at approximately fifty to seventy degrees and are offset by faults.

Cumulate rocks of the critical zone preserve graded layers, trough structures and slump folds and elsewhere are metamorphosed and deformed. The gabbro zone is heterogeneous and contains many textural varieties of gabbro, pegmatitic pods, layering, trondhjemite pods and amphibolite near the base. It passes through a transition zone to a sheeted dyke zone which extends the full length of the ophiolite. Dykes trend northwest and are aphyric or plagioclase - phyric diabase. The pillow lava zone, besides pillow basalt, contains minor pillow breccia, hyaloclastite and chert.

Major, trace and rare earth element geochemistry and clinopyroxene chemistry indicate that the suite is most similar to Normal - type mid- ocean ridge basalt, low Zr contents being the only unusual feature. Trondhjemites have variable chemistry but elevated contents of trace elements consistent with differentiation from this basalt.

The Annieopsquotch Complex is faulted against an

Ordovician tonalite terrane to the northwest across the Lloyds River Fault and against the Victoria Lake Group to the southeast. It is cut by dykes and sills correlated with both these units. The ophiolite is cut by two late Ordovician gabbro - diorite intrusions and a granite intrusion of presumed Devonian age and is unconformably overlain by early Silurian terrestrial sedimentary and volcanic rocks.

Two U-Pb ages for zircon from trondhjemite (477.5, 481.4 Ma) indicate that formation of the Annieopsquotch Complex occurred in Arenigian time. Zircon ages for the Bay of Islands (485.7 Ma) and Betts Cove Complexes (488.6 Ma) show them to be time equivalents, likewise Arenigian, refuting previous interpretations. A survey of ages of other ophiolites suggests that only oceanic crust (s.l.) formed over a limited time range is preserved in the Appalachian - Caledonian Mountain Belt.

Other ophiolitic fragments, most intruded by or included in the tonalite, are preserved in a belt from Shanadithit Brook to King George IV Lake. Because of lithologic and chemical similarities, they are included in the Annieopsquotch ophiolite belt. Basalts of the Victoria Lake Group also have very similar chemistry suggesting a genetic link. Common orientations of sheeted dykes in the fragments suggest that they may have comprised one allochthon of Iapetus oceanic crust. This allochthon was emplaced over the Ordovician continental margin of North America during the Taconic Orogeny and intruded by

tonalitic melts at that time.

ACKNOWLEDGMENTS

I am grateful to my supervisor, John Malpas, for discussions and critical comments and for financial support from his NSERC grant. He has also stimulated my interest in world travel.

Mapping during 1978,1979,1980 and 1981 was supported entirely and major element analyses were performed by the Geological Survey of Canada through project 770026 of Dr. Richard Herd. Thanks to J.C. McGlynn for financial support for expenses incurred during the U-Pb dating program at the Royal Ontario Museum. Without these considerable funds, completion of the thesis would have been impossible.

Able field assistance was provided by M.A. Best, K. Cameron, W.P. Carew, P. Carter, R. Jackson, J. MacManus, G.T. Noah and M. Thompson. Equally important, their friendship guaranteed four enjoyable and memory-filled summers. Wayne Carew was certainly the most daring of these people and our high speed 'traverses' on Honda mini bikes will be long remembered.

Helpful discussions were had with Richard Herd throughout the four years. Some of his less conventional ideas about the Puddle Pond map area now appear to have been the most shrewd. Others who contributed helpful advice during many discussions are L.B. Chorlton, B.J. Fryer, B.F. Kean, T.E. Krogh, R.K. Stevens, D.F.

Strong, H. Williams and D.H.C. Wilton.

Technical assistance was provided by W. Marsh, D.E. Press and H. Longerich at Memorial University and D.W. Davis and B. Podstawskj at the Royal Ontario Museum. W. Howell drafted the maps in Chapter 7.

TABLE OF CONTENTS

CHAPTER 3

GEOLOGY OF THE ANNIEOPSQUOTCH COMPLEX

CHAPTER 6

GEOLOGY AND GEOCHEMISTRY OF THE VICTORIA LAKE GROUP

CHAPTER 7

GEOCHRONOLOGY OF OPHIOLITES
OF THE NEWFOUNDLAND APPALACHIANS

CHAPTER 8

NEW DATA RELEVANT TO NEWFOUNDLAND TECTONICS AND
REGIONAL SYNTHESIS AND TECTONIC INTERPRETATION

LIST OF TABLES

LIST OF FIGURES

CHAPTER 1 INTRODUCTION

1.1 Subject and Scope of Thesis

The subject of this thesis, the Annieopsquotch Complex of southwest Newfoundland is an ophiolite which was, until recently, identified as a gabbro-diorite intrusion into crystalline rocks and the Victoria Lake Group. It is shown as such on the Tectonic Lithofacies Map of the Appalachian Orogen (Williams, 1978 after Riley, 1957). Since much of the geology in the region around the Complex has only recently been mapped, a fairly detailed regional picture is presented in Chapter 2 to familiarize the reader with the general setting of the Complex. This new mapping is incorporated in the Geological map of the island of Newfoundland compiled by Hibbard (1983).

The Annieopsquotch Complex itself was mapped in detail by the author between 1978 and 1980. A detailed description of the Complex is presented in Chapter 3 along with a geological map (Map 1 in pocket).

The petrology of the Complex has been studied in detail by examination of thin and polished thin sections. This data is presented in Chapter 4.

As a result of these studies the Annieopsquotch Complex is now recognised as one of twenty- five or more fragments of ophiolite in a northeast - southwest trending belt, the Annieopsquotch ophiolite belt. Major and trace

element analyses of rocks from the Complex and seven other ophiolitic fragments in the belt are presented and discussed in Chapter 5. These, along with rare earth element analyses of a suite of rocks from the Annieopsquotch Complex are used to characterize the Complex and rationalise its tectonic setting.

The relationship of the Annieopsquotch Complex to the adjacent Victoria Lake Group is important in constructing models for the development of southwest Newfoundland. The results of a petrochemical study of the Group adjacent to the ophiolite, including major, trace and rare earth element analyses, are presented in Chapter 6.

New U/Pb (zircon) dates for the Bay of Islands Complex, Betts Cove Complex and Annieopsquotch Complex are presented in Chapter 7. These are discussed in relation to stratigraphic relationships, previous age determinations and ages of other ophiolites in the Appalachian- Caledonian Mountain Belt.

A discussion and synthesis of knowledge of the Annieopsquotch Complex comprises Chapter 8.

1.2 SETTING OF OPHIOLITES WITHIN NEWFOUNDLAND

Ophiolitic rocks of Newfoundland occur mainly in the Humber and Dunnage tectono- stratigraphic zones of Williams (1978) and within these zones have strongly contrasting relationships to surrounding rocks (Figure 1.1).

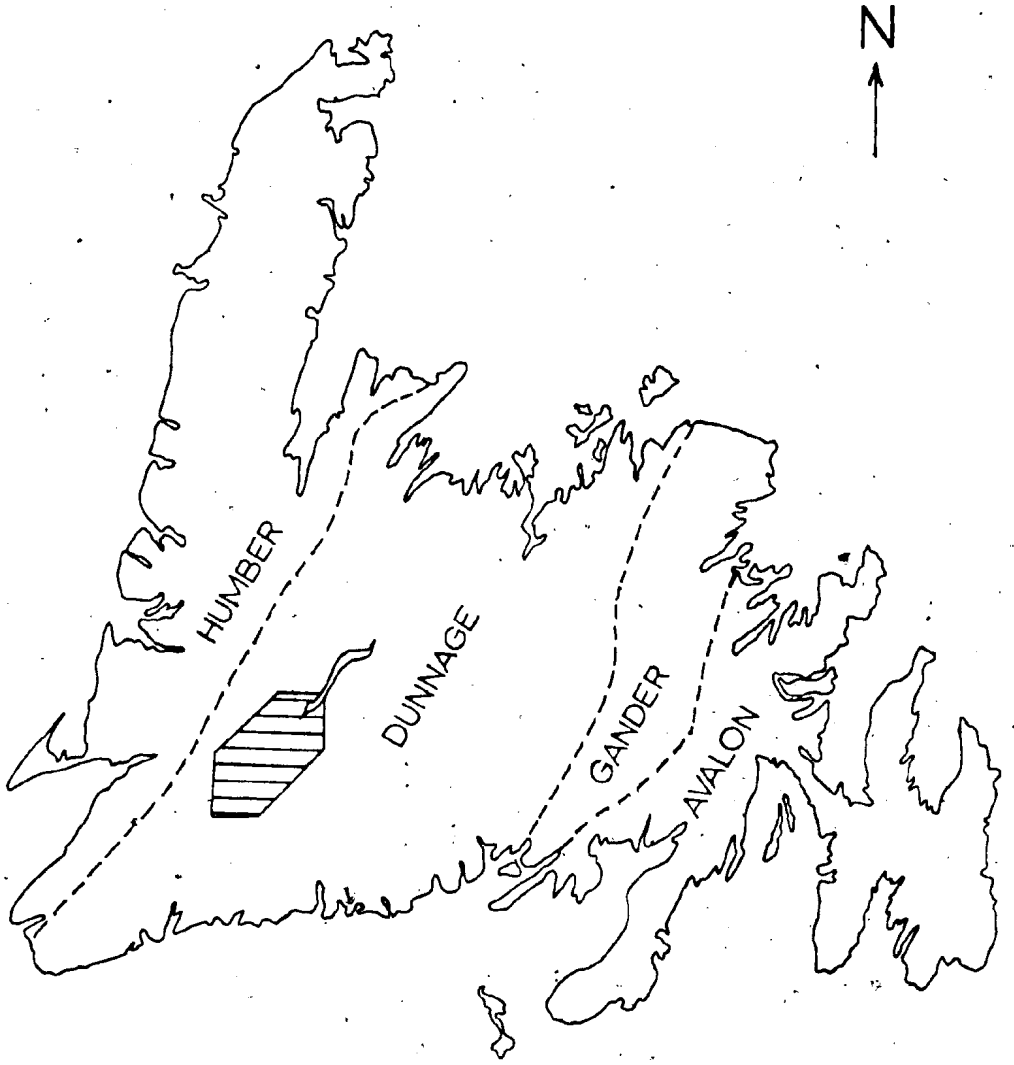

Figure 1.1, Tectonostratigraphic zones of the Newfoundland Appalachians, after Kean (1983). Study area, shown as ruled enclosure, is shown in Figure 2.1 and discussed in Chapter 2.

1.2.1 Humber Zone

Ophiolitic rocks occur as large allochthonous sheets exposed as the uppermost slices of the Humber Arm and Hare Bay Allochthons of west Newfoundland. Both the Bay of Islands and St. Anthony Complexes have at their bases well developed dynamothermal aureoles (Malpas et al., 1973; Malpas, 1979a; Williams and Smyth, 1973; Jamieson, 1982), which are interpreted to have formed during initial displacement of the ophiolite from the oceanic realm and before assembly of the allochthons. Beneath the aureole rocks, which are part of the ophiolite slice, and oceanic sedimentary rocks of lower structural slices, are 'soft' thrust zones occupied by melanges. These are interpreted to have formed by disruption of sediments by the overriding slice and mass wasting of the allochthons during their westward transport and assembly (Stevens, 1970).

The assembled allochthons, after final emplacement on the continental margin, were not affected by further deformational events in the orogen (Williams,1979). Therefore features within the Bay of Islands and St. Anthony Complexes are inferred to have formed in the oceanic realm or during emplacement in Ordovician time (Stevens,1970).

No other ophiolite complexes occur in the Humber Zone as it is now known (see discussion of foliated tonalite terrane on page 20 and compare to Williams, 1979).

1.2.2 Dunnage Zone

In the Dunnage Zone of central Newfoundland ophiolitic rocks occur in abundance on the Baie Verte Peninsula and in the Gander River Ultramafic Belt and as scattered fragments across the Zone. Evidence of mafic and ultramafic xenoliths in acidic intrusions, as well as gravity data have been taken to indicate that the Zone is underlain in great part by mafic crust and mantle lithologies.

The boundaries of the Dunnage Zone in southwest Newfoundland were not clear previous to the recent mapping program. The lines bounding the Zone end in central Newfoundland on most maps (see Williams, 1978). The recent recognition of large areas of ophiolitic rocks in southwest Newfoundland by Dunning and Herd (1980) and Chorlton (1983) indicates that the Dunnage Zone traverses the entire island and emerges as a belt at least fifty kilometres wide at Port aux Basques. The oldest known non-ophiolitic plutonic rocks in this zone are of Ordovician age and cut the ophiolitic rocks (Dunning and Chorlton, 1983). They are similar to plutons in the Dunnage Zone exposed in the Notre Dame Bay area but they are far more extensive in southwest Newfoundland.

Sedimentary rocks of the Fleur de Lys Supergroup, exposed on the Baie Verte Peninsula, are placed in the Humber Zone of Williams (1979). These are interpreted to be deformed remnants of the continental rise prism that mantled the ancient continental margin of North America (Williams, 1978).In southwest Newfoundland however,

sedimentary rocks probably correlative with the Fleur de Lys Supergroup occur together with Ordovician ophiolitic rocks as inclusions in the Ordovician tonalite terrane. Therefore, rocks characteristic of both the Humber and Dunnage Zones, as defined in northern Newfoundland, occur together in southwest Newfoundland. The unifying link between rocks of these two Zones is that they are intruded and engulfed by the Ordovician foliated plutonic rocks. Thus, as both the ophiolitic and foliated plutonic rocks are of Ordovician age and are each interpreted to have formed in the oceanic realm (Chorlton, 1983 and Chapter 2) and because the plutonic rocks have probable equivalents in the Notre Dame Bay area, this whole package of rocks is assigned to the Dunnage Zone.

CHAPTER 2 REGIONAL GEOLOGY

2.1 INTRODUCTION

The geology of the area described in this thesis has been elucidated since 1977. The region is generally remote and inaccessible and its geology was, until recently, amongst the least known in Newfoundland.

Recent work by Herd and Dunning (1979), Dunning and Herd (1980), Dunning (1981), Dunning,Carter and Best (1982) and Kean (1977,1983) has revised much of the earlier interpretation of the area by Riley (1957) and Brown (1975,1976). The new mapping indicates that there is continuity between the geology of the Notre Dame Bay region and that of southwest Newfoundland.

The two most significant modifications to the previously accepted geology of this area are: 1. the recognition that large areas of tonalite and granodiorite in southwest Newfoundland are of Ordovician rather than Precambrian age as previously thought (Brown, 1975) and; 2. that ophiolitic rocks included in the Annieopsquotch ophiolite belt and the Long Range Mafic - Ultramafic Complex underlie a large area of southwest Newfoundland, extending in a belt from near Buchans to Port aux Basques (Figure 2.1).

Most of the regional mapping, cited above, is published only in government publications which have a

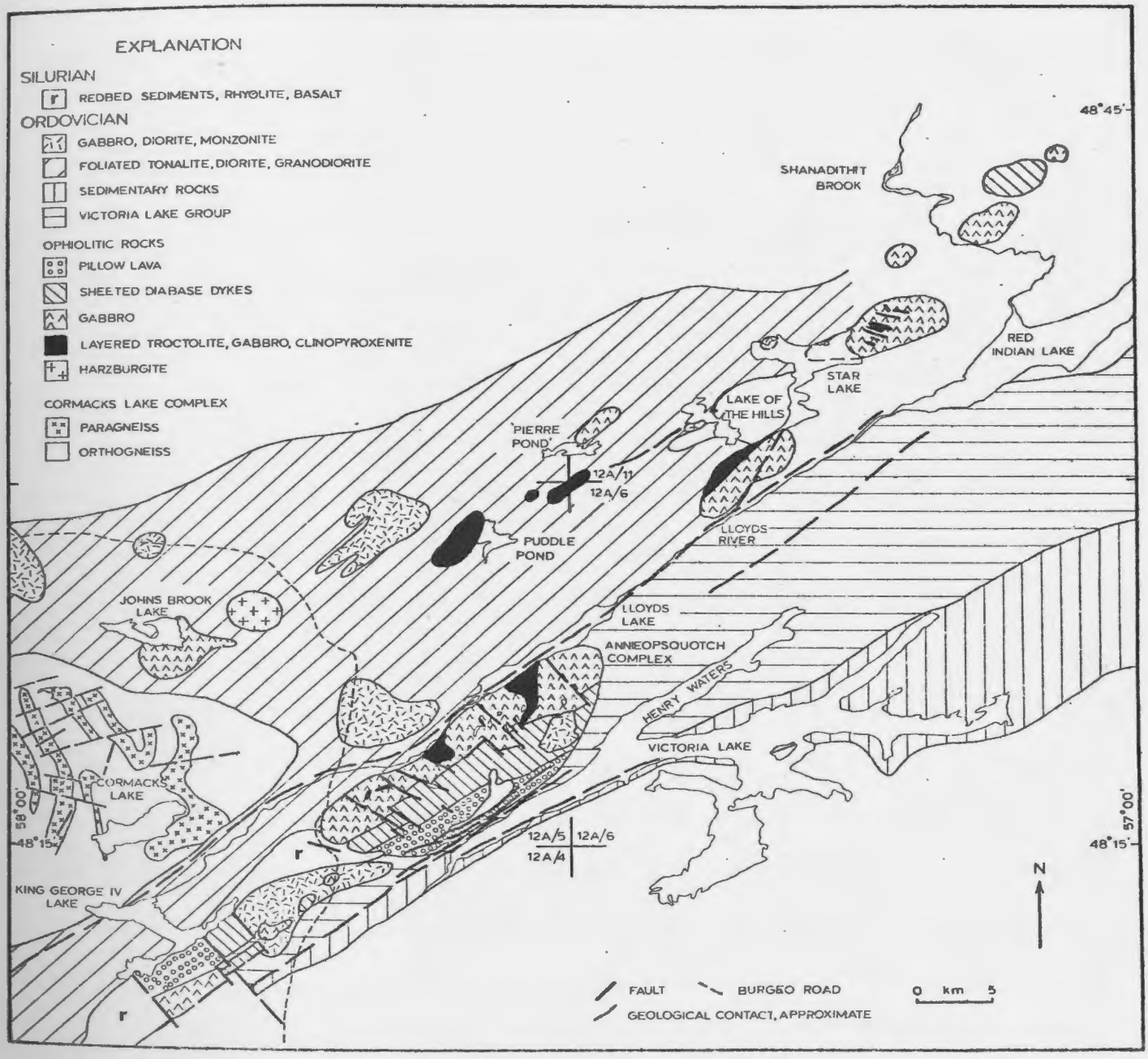

Figure 2.1. Regional Geology.
Compiled from Dunning (1981), Dunning, Carter and Best (1982), Herd and Dunning (1979) and Kean (1977, 1983).

limited distribution. For this reason the geology is reviewed in some detail in this chapter. This should provide an overview of the setting of the Annieopsquotch Complex and other ophiolitic fragments in southwest Newfoundland.

2.2 PHYSIOGRAPHY AND ACCESS

The region described in this chapter is part of the Long Range Mountains of southwest Newfoundland. Relief, to a maximum of 300 metres, is present in the Annieopsquotch Mountains. The country to the northwest of Lloyds River is rugged and forested and is cut by brooks and ponds. The area west and north of Cormacks Lake (Figure 2.1) is predominantly barren rock ridges, glacial deposits and bogs. The area south of the mountains is barren with many shallow ponds, rock ridges and isolated clumps of spruce.

Route 480 to Burgeo crosses the study area, passing close to the southwest end of the Annieopsquotch Mountains. Two ponds in the mountains, informally named Dyke Pond and Loon Echo Pond are large enough to accomodate floatplanes; however most mapping was done from isolated camps supported by helicopter.

2.3 GENERAL STATEMENT

The area of study, the Annieopsquotch Mountains, forms parts of the Puddle Pond, King George IV Lake and Victoria Lake map areas (NTS 12A/5, 12A/4, 12A/6). Limited mapping and sampling was also carried out in the Star Lake map area (12A/11).

The study area and surrounding region can be divided into four contrasting geologic terranes of pre-Ordovician or Ordovician age. These are, from presumed oldest to youngest:

1. the Cormacks Lake Complex, a poly-deformed sequence of metasedimentary rocks and structurally concordant granitoid plutons of possible Precambrian age, metamorphosed to amphibolite and granulite grade;

2. the Annieopsquotch Complex and other ophiolitic fragments of early Ordovician age;

3. the Victoria Lake Group, a volcanic- plutonic and sedimentary rock sequence of early Ordovician age and;

4. a foliated tonalite terrane of mid to late Ordovician age, composed of tonalite, trondhjemite, diorite and granodiorite.

These terranes are separated by major faults but linked by crosscutting intrusions of Ordovician age, and are discussed in more detail below. Several gabbro - diorite plutons of late Ordovician age and granitic plutons, of presumed Devonian age occur in the region, as do red terrestrial sedimentary rocks with interbedded volcanic rocks of Silurian age. The relationships of these units to the Annieopsquotch Complex are discussed below.

2.4 CORMACKS LAKE COMPLEX

The Cormacks Lake Complex (Herd and Dunning,1979) underlies a large area north of the Lloyds River and surrounding Cormacks Lake and continues to the west of the area shown in Figure 2.1. It is composed of foliated granite with structurally concordant layers of rusty-weathering paragneiss and amphibolite. Locally the paragneiss contains quartzite and calcsilicate layers. Hybrid gneiss generally occurs along contacts between foliated granite and paragneiss. The Complex has undergone three phases of folding and fold interference patterns are common in outcrop. The second generation folds are open with axes which strike and plunge southeast, at near right angles to the regional northeast structural trend. These folds define the outcrop pattern.

Riley (1957) suggested that these rocks included metamorphosed volcanic and sedimentary rocks of Cambrian and Ordovician ages. Herd and Dunning (1979) interpreted the Complex to be Grenvillian in age. However, a similar unit to the southwest has been interpreted to be of Ordovician age (Chorlton, 1983). She suggested that some horizons rich in garnet may represent metamorphosed Mn- and Fe- rich pelagic sediments related to the ophiolitic rocks.

The only age determined for this Complex is a K/Ar (hornblende) age of 360+/-25 Ma from amphibolite within the sedimentary sequence (Stevens *et al.*,1982). This age may represent uplift and cooling after the granulite facies

metamorphism. A U/Pb (zircon) age determination is in progress at the Geological Survey of Canada.

2.5 THE ANNIEOPSQUOTCH COMPLEX

The name Annieopsquotch Complex is proposed here for the suite of ophiolitic rocks that underlies an area of 140 square kilometres of the Annieopsquotch Mountains between Lloyds Lake and Victoria Lake (Figure 2.1, Map 1). The Complex is complete from 'critical zone' lithologies (Malpas, 1976), through gabbro and sheeted dykes to pillow lava. The sequence of ophiolitic units faces and dips southeast.

Layered olivine- plagioclase- clinopyroxene cumulates represent the lowest part of the section preserved. These are referred to the 'critical zone' of Malpas (1976) and occur in two areas, separated by 'high-level' gabbro. They are oriented at nearly 90 degrees to the stratigraphy so that the layering is now vertical.

To the southeast of the layered unit, up-section, is the massive or 'high-level' gabbro zone which is composed mainly of plagioclase-clinopyroxene gabbro with local hornblende-rich varieties. Small layered zones, pegmatitic gabbro pods and trondhjemite bodies are common in this zone.

A sheeted dyke zone occurs to the southeast of the gabbro zone. It extends the full strike length of the

ophiolite and contacts with both the gabbro and pillow lavas are offset by faults cutting at high angles across the stratigraphy (Map 1). These faults are interpreted as seafloor features. The great majority of dykes are normal mid- ocean ridge basalt (N-type MORB). Some trondhjemitic dykes are present.

Pillow lava first appears as screens near the top of the sheeted dyke zone. Throughout the pillow lava zone diabase dykes and sills are present. Pillows are massive and non-vesicular and pockets of pillow breccia and hyaloclastite are locally present. Red chert occurs locally as interpillow material. The zone is cut by several major faults which are parallel to that along Victoria Lake, and the pillow lava is reduced to chlorite schist along these fault zones.

The geology of the Annieopsquotch Complex is discussed in more detail in Chapter 3.

2.6 OTHER OPHIOLITIC FRAGMENTS

Ophiolitic fragments occur in a belt extending from near Buchans to the southwest corner of the island (Dunning and Herd,1980, Dunning,1981, Chorlton,1982, Brown,1976). They preserve part of the ophiolite stratigraphy present in the Bay of Islands Complex (Figure 2.2). Most fragments include 'critical zone' lithologies or 'high-level' gabbro containing trondhjemite pods and cut by diabase dykes.

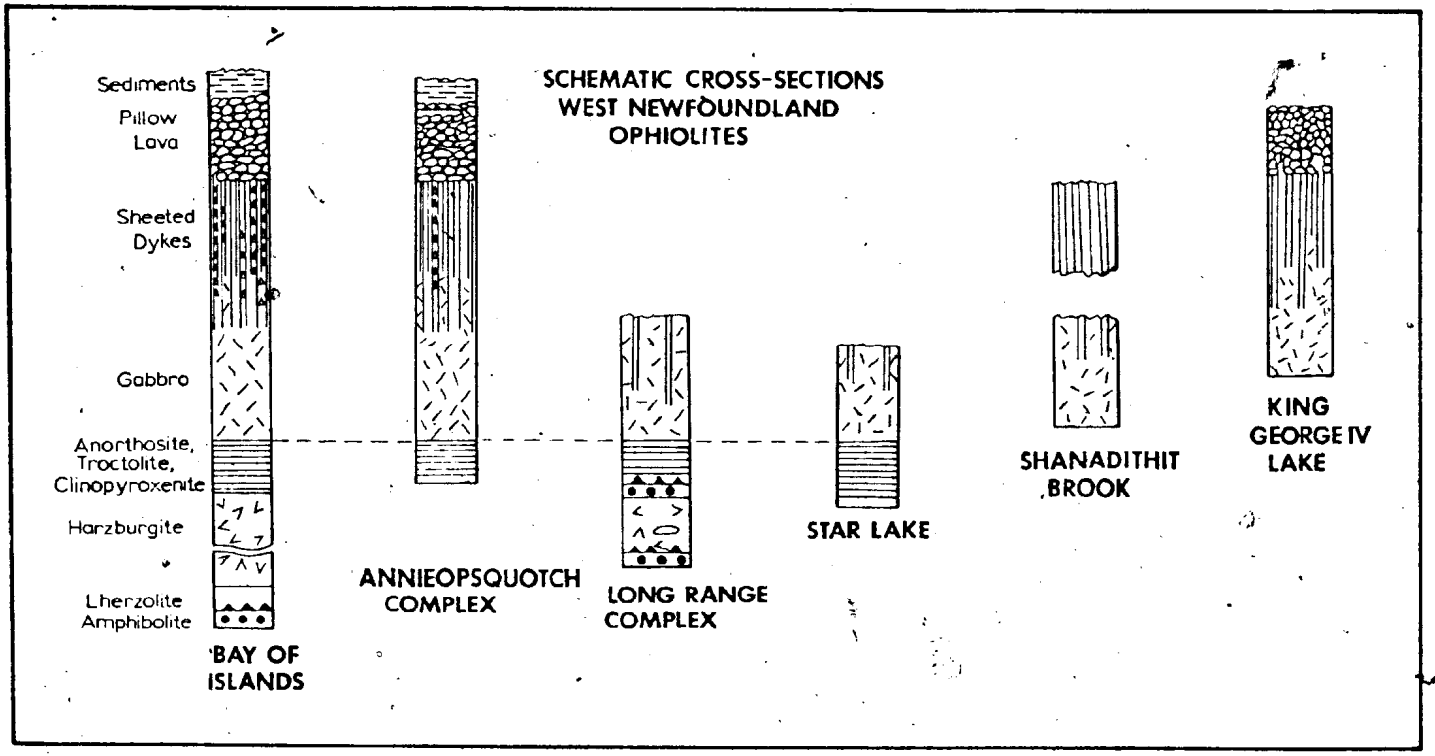

Figure 2.2. Comparison of the stratigraphy of the Annieopsquotch Complex and some ophiolitic fragments of southwest Newfoundland to that of the Bay of Islands Complex (after Malpas and Strong, 1975). Long Range Mafic - Ultramafic Complex after Brown (1976). Modified from figure 2.4 of Dunning (1981). Dashed line shows the top of the 'critical zone'. Sections ignore disruptions due to faulting and the vertical scale is not fixed.

Mantle lithologies occur in only two fragments, sheeted dykes in two and pillow lava in only one. They are discussed, from north to south below.

2.6.1 Star Lake Map Area (NTS 12A/11)

Two large massifs with 200 metres of relief, as well as several smaller hills, at Shanadithit Brook are underlain by ophiolitic rocks (Figure 2.1). Much of the low country in this area, not examined during this study, may comprise ophiolitic rocks as well. The northern massif is composed of sheeted dykes which trend approximately northwest-southeast. They are from 0.5 to 3 metres in width and some are strongly plagioclase porphyritic. They were not examined in detail. The smaller hills are composed mainly of gabbro as is the large massif immediately north of Shanadithit Brook.

The largest ophiolitic fragment in the Star Lake map area occurs as a 200 metre high, flat topped massif immediately northeast of Star Lake. The ophiolitic rocks extend under most of the east arm of the lake and are well exposed on islands there. This body is composed of coarse grained gabbro with a few small trondhjemite pods and cut by diabase dykes. Several irregular areas of fine grained diabase appear similar to those described from the Annieopsquotch Complex in Chapter 3.

At the west side of the massif are five lensoid areas of layered olivine- plagioclase- clinopyroxene cumulate rocks, analogous to those of the critical zone of the

Annieopsquotch Complex. They strike northwest as do igneous layers within them; ie. the same orientation as those of the Annieopsquotch Complex.

The islands and north shore of Star Lake are underlain by layered gabbro (Dunning, Carter and Best,1982), irregular areas of massive gabbro cut by diabase, and amphibolite. On one of the islands, gabbro cut by diabase dykes is further intruded by tonalitic dykes and veins. Nearby, on the central north shore of Star Lake, tonalite engulfs numerous amphibolite fragments forming an agmatite. The fragments are interpreted to be metamorphosed ophiolitic rocks. A small exposure of gabbroic rock is present on the northwest shore of Star Lake. Its full size is unknown as there is an extensive bog- covered area to the northwest.

Harzburgite outcrops in a small area, exagerated in Figure 2.1, on the southwest shore of Lake of the Hills in the tonalite terrane near the contact with a younger granite.

Immediately south of Star Lake and the east end of Lake of the Hills there is a large area of clinopyroxenite and gabbro, with trondhjemite pods, cut by diabase dykes, and forming several hills. Shear zones occur in the gabbro where it is cut by a fault, interpreted to be a splay of the Lloyds River Fault.

Gabbro and a small amount of clinopyroxenite underlie a hill in the southwest corner of the map area about 2 kilometres north of Pierre Pond (informal name). It

appears that the two lithologies are interlayered on a metre scale.

2.6.2 Puddle Pond Map Area (NTS 12A/5)

Three areas of critical zone lithology occur in the northeast corner of the Puddle Pond map area (Figure 2.1). Their outlines are drawn to enclose the minimum area known to be underlain by these rocks. Outcrop is limited in this area so it is possible that more ophiolitic rocks are present than are shown. In these fragments the predominant lithologies are anorthosite, troctolite and olivine gabbro, reflecting changes in the proportions of olivine, plagioclase and clinopyroxene.

Harzburgite occurs with gabbro in the barrens south of the Burgeo road. The harzburgite is foliated less strongly than that in the mantle section of the Bay of Islands Complex and has oikocrysts of bronzite overgrowing olivine. These oikocrysts weather in relief giving the outcrop a knobbly appearance (Dunning and Herd,1980) and in places are aligned giving the appearance of layering.

Gabbro, cut by diabase dykes, outcrops on the shore of Johns Brook Lake and in the high ground to the east where it is intruded by an undeformed granite (Figure 2.1). Layered gabbro and clinopyroxenite occur in the barrens south of the lake. These have been shown as a single large body of gabbro (Herd and Dunning, 1979).

Previous maps (eg. Kean et al., 1981) show a large area of mafic rock immediately north of Lloyds Lake that

has been correlated with that in the Annieopsquotch Mountains. Large cliff faces on the northwest side of the ridge northwest of Lloyds Lake are formed of mafic rock, however it is not known whether it is of ophiolitic affinity or is related to younger gabbro intrusions, discussed below. For this reason the ridge is not shown as an ophiolitic fragment on Figure 2.1. Likewise, a ridge with near vertical northwest facing cliffs, on the south side of Lloyds River Fault northeast of the Annieopsquotch Complex, is composed of gabbro cut by diabase dykes. It is strongly sheared and bleached along the fault but structures and textures are locally recognizable. It could well be ophiolitic, as suggested by Dunning (1981), but since gabbro sills and dykes are common in the adjacent non - ophiolitic Victoria Lake Group this gabbro is not included as an ophiolitic fragment in Figure 2.1.

2.6.3 King George IV Lake Map Area (12A/4)

Southwest of the Annieopsquotch Complex, a late Ordovician intrusion, the Boogie Lake Intrusion (informal name after Sterenberg, pers. comm., 1979), includes three ophiolitic fragments. From north to south they are; coarse grained gabbro cut by diabase dykes, sheeted diabase dykes and coarse grained gabbro. Sheeted dykes strike northwest as they do elsewhere in the Annieopsquotch ophiolite belt (Dunning, 1981). The northern fragment of gabbro is exposed in roadcuts on the Burgeo road.

Southeast of King George IV Lake the second largest

fragment in the belt occurs in several fault bounded blocks. They form a flat topped massif with steep northwest facing cliffs with 200 metres of relief. The blocks are internally undeformed and the sheeted dykes strike northwest and have many of the same features described from the Annieopsquotch Complex below. Pillows are 0.5 to 1 metre in diameter, aphanitic, massive and the interstitial material is basalt, hyaloclastite or minor red chert. Kean (1983) suggested that the pillow lava sequence top is to the west based on basal projections of pillows but the author, having examined the sequence, is not convinced.

2.6.4 Southwest Newfoundland

Ophiolitic fragments and amphibolite with a presumed ophiolitic protolith occur over a considerable area of southwest Newfoundland between the Long Range and Cape Ray Faults. They were assigned to the Long Range Mafic-Ultramafic Complex by Brown (1975,1976) and Chorlton (1982). Detailed mapping in the Grandys Lake map area (NTS 110/11) by Chorlton and Dingwell (1981) and along the Cape Ray Fault by Wilton (1983) has shown that these fragments are intruded and some engulfed by a suite of tonalitic rocks. They do not occur as thrust slices over the tonalites as described by Brown (1976). The general relationship between ophiolitic rocks and tonalite is therefore the same as that in the Annieopsquotch ophiolite belt. Chorlton and Dingwell (1981) have described part of

the ophiolitic- tonalitic terrane in the Grandys Lake map area as agmatitic with numerous variably sized blocks of mafic rock, now mainly amphibolite, engulfed in a large volume of tonalite. They modelled these tonalites as partial melts of hydrated oceanic crust. A similar origin is thought likely for the tonalites intruding rocks of the Annieopsquotch ophiolite belt.

2.7 FOLIATED TONALITE TERRANE

Foliated to massive tonalite, diorite, hornblende gabbro, monzonite and granodiorite of mid to late Ordovician and possibly Silurian age underlie a large area north of the Lloyds River and north and northeast of the Cormacks Lake Complex (Figure 2.1). K/Ar (hornblende and biotite) ages of 455+/-14Ma and 449+/-8Ma (Stevens et al., 1982) are the oldest obtained from this terrane. These rocks are part of an extensive terrane of Lower Paleozoic plutonic rocks, predominantly of intermediate composition, that extends from Port aux Basques to Buchans and has correlatives, as discontinuous units, northeast as far as Notre Dame Bay.

The oldest rocks appear to be strongly foliated biotite and hornblende bearing tonalites which characteristically contain blue quartz in elongate clots. This unit strikes northeast to north-northeast and is cut by northeast trending faults. The tonalite contains

inclusions of harzburgite, troctolite- anorthosite, clinopyroxenite and gabbro. Some gabbro inclusions have rims of amphibolite or contain pods of trondhjemite. In the Star Lake map area the clinopyroxenite and some of the gabbro bodies are surrounded and intruded at their margins by tonalite (Dunning, Carter and Best,1982). The preferred model for the development of this terrane involves extensive partial melting of hydrated oceanic crust that had been imbricated on thrust faults in mid Ordovician time (Dunning and Chorlton,1983). At the present level of exposure a series of coalescing tonalitic plutons intrude the higher ophiolitic sheets. Locally an agmatite of blocks of amphibolite in tonalite is present, although metasedimentary inclusions predominate in some areas of tonalite. It has been suggested that the latter may be Fleur de Lys equivalents (Herd,1978) since, in the region north of Southwest Brook, metasedimentary lithologies comparable to those mapped by Kennedy (1982) occur as inclusions in the early foliated tonalites.

2.8 POST-TONALITE INTRUSIONS

The early foliated tonalites are cut by intrusions of various compositions including hornblende diorite, biotite diorite, hornblende gabbro and norite. These are massive to weakly foliated, generally rounded in outline and 1 to 10 kilometres in diameter (Figure 2.1).

The Boogie Lake Intrusion occurs between the Annieopsquotch Complex and the King George IV Lake ophiolite fragment and includes three large ophiolitic fragments, two of gabbro and one of sheeted dykes. It intrudes volcanic rocks of the Victoria Lake Group in outcrops along the Burgeo Road. While it is elongate parallel to the regional trend, it is not penetratively deformed. The intrusion has differentiates of hornblende diorite and biotite monzonite; the latter contains molybdenite mineralization. Preliminary U/Pb (zircon) data indicate a late Ordovician age for this intrusion.

The Southwest Brook Diorite is a small body, near circular in outline (Figure 2.1). It is coarse grained, well jointed and blocky, and considerably less deformed than the surrounding tonalites. Herd (personal communication, 1981) considers this intrusion to be an inclusion in the tonalite, but because it is less deformed than the tonalite the present writer feels that it postdates the tonalite. U/Pb (zircon) age determinations for both units are underway to resolve the debate.

The westernmost gabbroic body shown in Figure 2.1, the Main Gut Intrusion (Carew,1979), has an uncertain relationship to surrounding units. It apparently cuts the tonalite at the west edge of the Puddle Pond map area and is juxtaposed with anorthosite across the Long Range-Cabot Fault. The intrusion is complex and may consist of two bodies: 1. tholeiitic gabbro to diorite with diabase dykes and 2. an oxide-rich norite unit with local, well

developed, cumulate layering. The rocks are remarkably fresh and undeformed. Preliminary U/Pb (zircon) data indicates a late Ordovician age for this intrusion.

The Annieopsquotch Complex is cut by a small intrusion of diorite at its northeastern end (Figure 2.1). The outline of this diorite is inferred, in part, from the aeromagnetic map (GSC map 250G) on which it is marked by a series of concentric positive anomalies. Its true size is unknown; rafts of pillow lava were noted within the area outlined and possibly only the top of the intrusion is exposed. The age of the body is unknown but it is here tentatively correlated with the other mafic intrusions described above.

2.9 GRANITIC INTRUSIONS

Granitic intrusions, weakly foliated to massive and coarse grained, occur throughout the region (Figure 2.1). They postdate the ophiolitic rocks, tonalite and mafic intrusions. One granite intrusion cuts the pillow lava zone of the Annieopsquotch Complex (Figure 2.1). As exposed in the area of Canoe Scrape Lake (informal name, Map 1) it is coarse grained, equigranular, locally biotite- or hornblende- rich granite to granodiorite. It forms an intrusion breccia along its northwest margin incorporating blocks of fine grained mafic rock, some now amphibolite, and is cut by faults along its southeast contact. These

faults also disrupt the red terrestrial sedimentary rocks described below, so their latest movement is certainly post early Silurian and may be Carboniferous in age. The granite is presumed to be of Devonian age.

2.10 TERRESTRIAL SEDIMENTARY ROCKS

Red clastic sedimentary rocks with interbedded rhyolite and minor basalt outcrop around the southwest end of the Annieopsquotch Mountains and in narrow fault bounded slivers on the southeast slope of the mountains above Victoria Lake (Degrace,1974; Dunning and Herd,1980; Chandler, 1982). A rhyolite dyke 10 metres wide, related to the sequence, cuts the Boogie Lake Intrusion at station 1D025 (Map 2, Chapter 5). The sedimentary rocks extend southwest across the King George IV Lake map area (Figure 2.1) and are correlated with the Windsor Point Group of southwest Newfoundland by Kean (1983).

Riley (1957) mapped the sedimentary rocks around King George IV Lake as Devonian, based on lithologic similarity to known Devonian rocks of the Windsor Point Group in southwest Newfoundland. DeGrace (1974) described the sequence exposed in a small area adjacent to King George IV Lake and concluded that they were Carboniferous, correlating them with those at Red Indian Lake. With new exposures in roadcuts along the Burgeo road, Dunning and Herd (1980) compared the sequence to the Springdale and

Botwood Groups and concluded that it too was of Silurian age. Chandler (1982) noted however that the Silurian age of the latter groups "rests upon slender evidence". Fossil spores in the Windsor Point Group in southwest Newfoundland date those rocks as early Devonian (Emsian according to W.R. Forbes in Chorlton, 1983). A Rb/Sr whole rock age of 377+/-21Ma for a felsic ignimbrite interbedded with the Windsor Point sedimentary rocks confirms this interpretation (Wilton,1983).

A recent U/Pb (zircon) age determination of 431+/-5Ma for the Bear Pond rhyolite, a flow within the sedimentary sequence near the Annieopsquotch Mountains (sample 81D280, Map 2), demonstrates that these sediments are of early Silurian age (Chandler and Dunning,1983). They are therefore not correlative with the Windsor Point Group, but rather are about 50Ma older. Grey, fossil bearing Devonian argillites which unconformably overlie the red sedimentary rocks and granite near King George IV Lake (Chandler,1982; Kean,1983) are, however, likely Windsor Point Group equivalents.

A well exposed unconformity between basal conglomeratic beds of the sedimentary sequence and sheeted dykes of the Annieopsquotch Complex occurs at the southwest end of the mountains (Figure 2.1). Two outliers of red conglomerate occur on the ophiolite and a sub-unconformity weathering of ophiolitic rocks along fractures is present in a valley to the northeast of the present outcrop area of the sedimentary rocks, suggesting that they once covered

more of the ophiolite.

Locally the basal conglomerate is composed of greater than eighty percent gabbro and diabase cobbles. These show imbrication indicating transport towards the present high ground of the ophiolite. This relationship led Chandler (1982) to conclude that the main source of these sediments was to the south and that uplift of the mountains occurred after early Silurian time. This is in agreement with the uplift history determined by Chorlton (1983) for the Grandys Lake map area.

Best (1982) studied the provenance of sandstones in this sequence and found a close relationship between their mineralogy and the nearest basement rocks. The ophiolite, the Boogie Lake Intrusion, granodiorite or felsic volcanic rocks contributed the majority of detritus to the nearest sandstone outcrops. In contrast, the unconformably overlying grey argillites contain abundant detritus from a granitic source and southwest of King George IV Lake they overlie a granite which has a regolithic cover (Chandler,1982).

Chandler (1982) interpreted conglomerates in the red sedimentary sequence to be of alluvial fan or braided fluvial origin and fine clastic rocks to be deposits of the braided regime or flash floods. He suggested an arid environment based on the presence of calcite cement in the clastic sedimentary rocks and the occurrence of limestone at King George IV Lake.

2.11 STRUCTURE

The contrasting terranes discussed above have different structural histories and it is not clear when they were first juxtaposed. All the terranes are separated by major faults for which the movement histories are poorly known. Two of these; the Lloyds River and Victoria Lake Faults (Figure 2.1) are major structures that may extend the entire breadth of Newfoundland.

The Victoria Lake Fault was interpreted by Webb (1969) and Kean (1983) to be an extension through central Newfoundland of the Cape Ray Fault of southwest Newfoundland. Webb suggested that it emerged in Notre Dame Bay as the Reach Fault. The Victoria Lake Fault in the study area is interpreted to underlie the southwest arm of the lake and faults along the north shore of the lake are interpreted to be related to it. It curves to the east and underlies the east arm of Victoria Lake. It likely is the northward continuation of the Cape Ray Fault (Chorlton,1983) but its position to the northeast of Victoria Lake is quite uncertain.

The Lloyds River Fault is marked by the presence of mylonites in the river valley southwest of the Burgeo road bridge (R.K.Herd, pers. comm.,1980), by sheared gabbro in cliffs southeast of the Lloyds River and by the pronounced topographic lineament running along the northwest edge of the Annieopsquotch Mountains. This fault juxtaposes the Annieopsquotch Complex with the foliated plutonic terrane.

It may be that both of these faults were important structures in Ordovician time but this cannot be proven with the evidence currently available. An undated granite cutting the ophiolite and the Silurian sedimentary rocks are both affected by movements on the Victoria Lake Fault, or splays off it, but no younger formations are present which could be used to establish an upper limit on movement. The granite and sedimentary rocks were probably disrupted by normal faulting and tilting of blocks on structures steepened in post- early Ordovician time.

Several large faults cut the tonalites west of the Lloyds River Fault. Their history is unknown; they now dip steeply and some have foliated to mylonitic tonalite along them. Chorlton (1983) suggested that faults that cut both the tonalite and ophiolitic fragments in the Grandys Lake map area originated as thrust faults in Ordovician time. A similar origin is possible for some of the faults cutting tonalite west of the Lloyds River in the Puddle Pond map area.

The sequence of structural deformation of each of the terranes, based on the limited data available, is thought to be: Cormacks Lake Complex, early Ordovician ophiolitic rocks, Ordovician foliated tonalite terrane and early Silurian sedimentary rocks. Such a sequence might also be thought of as pre- Iapetus, Iapetus and post- Iapetus structures. Apart from the structure of the Victoria Lake Group (discussed in Chapter 6), structural development of these terranes is discussed below.

2.11.1 Cormacks Lake Complex

The Cormacks Lake Complex, interpreted to be the oldest unit in the region, appears to be a large block surrounded by tonalites. It has undergone three phases of folding. Early isoclines (F1) are recognizable as detached fold noses and some complete isoclines wrapped around open F2 structures. Type 1 and 3 interference patterns (Ramsay, 1967) occur in the southwest corner of the Complex (Kean, 1983). The F2 folds, which are responsible for the map pattern (Herd and Dunning,1979) are open isoclines. They have amplitudes and wavelengths of 2 to 5 km. Their axial planes strike and plunge southeast. The third generation folds in the Complex are minor crenulations on F2 structures.

Folds, if present, are difficult to recognize in younger units adjacent to the Cormacks Lake Complex. It seems likely that all fold phases in the Complex predate the generation of Iapetus ocean crust and foliated tonalite, although this is not proven. Lack of marker units in the tonalites may preclude the recognition of folds in general.

A northwest trending foliation predominates in the Cormacks Lake Complex and is generally parallel to fold axes in the paragneisses. It is related to the second generation folds (Herd and Dunning,1979).

2.11.2 Ophiolitic Rocks

Folds occur in layered cumulates of the critical zone of the Annieopsquotch Complex and also in the Star Lake fragment. They are intra-layering structures interpreted as syn-magmatic slump features. No folds were observed that are interpreted to represent deformation in the solid state.

The Annieopsquotch Complex appears to have behaved as a rigid block during the early to mid Ordovician Taconic event which formed the regional northeast trending structures in southwest Newfoundland. The exception to this is the southeast part of the pillow lava zone which is cut by faults (Map 1; Figure 2.1). Mafic volcanics are reduced to chlorite schist with a steep northeast trending foliation adjacent to these faults. This relationship is well demonstrated in outcrops on the ridges northwest of Victoria Lake. With the exception of these faults, and associated foliation, all structures in the Complex are interpreted to result from deformation in the oceanic realm. They are therefore unrelated to structures in other units described in this section.

High temperature shear zones near the base of the gabbro zone of the ophiolite contain amphibolite with a northeast trending foliation. The foliation is at a high angle to the shear zone in adjacent gabbro. Relict coarse plagioclase grains and gabbro rafts in the amphibolite indicate that it had a coarse grained gabbro protolith. Gabbro is also foliated parallel to faults which offset the

stratigraphy.

Foliated margins of diabase dykes are common throughout the ophiolite and appear to be related to minor movements along dyke margins during their emplacement as liquids and subsequently in the solid state while hot.

2.11.3 Foliated Tonalite Terrane

The predominant structure in this terrane is a northeast trending foliation. In some of the late tonalite and diorite bodies in this terrane the fabric is either poorly developed or absent, indicating that plutonism outlasted deformation. A northwest trending foliation is present in quartz diorite in the valley of Little Barachois Brook (Herd and Dunning,1979) where it appears to postdate the northeast structural trend. However it is poorly developed generally and the northeast trend predominates.

Late Ordovician gabbro-diorite intrusions are locally foliated at their margins and along shear zones but are otherwise massive, as are crosscutting granite plutons of presumed Devonian age.

2.11.4 Terrestrial Sedimentary Rocks

Silurian terrestrial sedimentary and associated volcanic rocks are undeformed except for shear zones along faults. Fault bounded blocks of sandstone and siltstone caught up in the pillow lava zone of the Annieopsquotch Complex and Victoria Lake Group (Kean,1983 and Figure 2.1) have a steep northeast striking foliation along their

margins but preserve undeformed sedimentary structures internally.

2.12 SUMMARY AND CONCLUSIONS

A strongly deformed sequence of meta- sedimentary and meta- igneous rocks, the Cormacks Lake Complex, locally of granulite facies, occurs in a large fault bounded block west of the Lloyds River Fault. These rocks have been interpreted as possible Precambrian basement but Chorlton (1982) interprets similar high grade meta-sedimentary rocks in southwest Newfoundland to be of Ordovician age.

The rocks of oldest proven age in the region are ophiolitic fragments of early Ordovician age that are distributed over a wide area of southwest Newfoundland.

Tonalites underlie a large area northwest of the Lloyds River and, with associated diorite and granodiorite, comprise an Ordovician batholithic terrane that extends from near Buchans to Port aux Basques. These rocks clearly intrude the Annieopsquotch Complex and ophiolitic fragments at Star Lake and Lake of the Hills and are interpreted as partial melts of imbricated and partially subducted oceanic crust. It is suggested that Fleur de Lys sediments were involved in the melting (Dunning and Chorlton, 1983).

The tonalites and ophiolitic fragments are intruded by massive, undeformed mafic intrusions of apparent late Ordovician age. They are 5 to 10 km. in diameter and are

composed of hornblende gabbro, hornblende diorite, granodiorite and monzonite.

Early Silurian terrestrial clastic sedimentary rocks with bimodal basalt-rhyolite provide evidence for rifting and the formation of small fault bounded basins.

Granitic intrusions, of unknown age (but presumed to be Devonian in this work), cut ophiolitic rocks and tonalite post-tectonically.

The region described above was poorly known until the recent mapping program began in 1977 (Herd, 1978). It was interpreted to be a Precambrian tonalitic basement terrane cut by Paleozoic intrusions (Williams,1978) by analogy with the area to the southwest, mapped by Brown (1975, 1976). Riley (1957) had previously described the area as a Paleozoic plutonic terrane and it was shown as such on the geological map of Newfoundland (Williams,1967). This earlier view is closer to the current interpretation.

Recent work shows that the region is a Paleozoic terrane that contains ophiolitic rocks characteristic of the 'Dunnage Zone' (Williams,1979) and meta-sedimentary rocks similar to those of the Fleur de Lys Supergroup, which are included in the Humber Zone on the Baie Verte Peninsula. However, an extensive area is underlain by tonalitic rocks that are poorly developed or simply not exposed or recognized in northern Newfoundland. There are some likely correlatives to the north, for example; the tonalite gneiss at the west end of Grand Lake, interpreted to be of Grenvillian age by Kennedy (1982) but in fact very

similar to the southwest Newfoundland tonalites, the Hungry Mountain Complex, near Buchans (Thurlow, 1981), the Burlington Granodiorite (Hibbard, in press; Epstein,1983) and parts of the South Lake Igneous Complex (Lorenz and Fountain,1982). Other small bodies of tonalite and trondhjemite exposed in the Dunnage Zone in Notre Dame Bay, such as the Twillingate trondhjemite, might also be correlatives. The true extent of this plutonic terrane might be revealed by further examination and re-interpretation of parts of the Dunnage Zone.

CHAPTER 3 GEOLOGY OF THE ANNIEOPSQUOTCH COMPLEX

3.1 INTRODUCTION

The Annieopsquotch Complex (informal name), which underlies the Annieopsquotch Mountains of southwest Newfoundland, is a well exposed ophiolite which contains most of the stratigraphic units of the sequence defined by the Penrose Conference (1972). No ultramafic rocks analogous to the mantle tectonite of other ophiolite complexes have been found in the Annieopsquotch Mountains.

3.1.1 Contact Relationships

The Complex is fault bounded, to the northwest by the Lloyds River Fault and to the southeast by the Victoria Lake Fault (Map 1, Figure 3.1). The history of movement on these faults is poorly known, especially for the Lloyds River Fault.

There is no field evidence that the Annieopsquotch Complex is bounded by a basal thrust fault. The structural base of the ophiolite is not seen and the best exposed relationship to other Ordovician rocks, that with granodiorite of the foliated tonalite terrane at the southwest end of the mountains, is an intrusive contact.

To the northeast, the poorly exposed contact between the Annieopsquotch Complex and the Victoria Lake Group is interpreted to have been a thrust fault (now steep due to

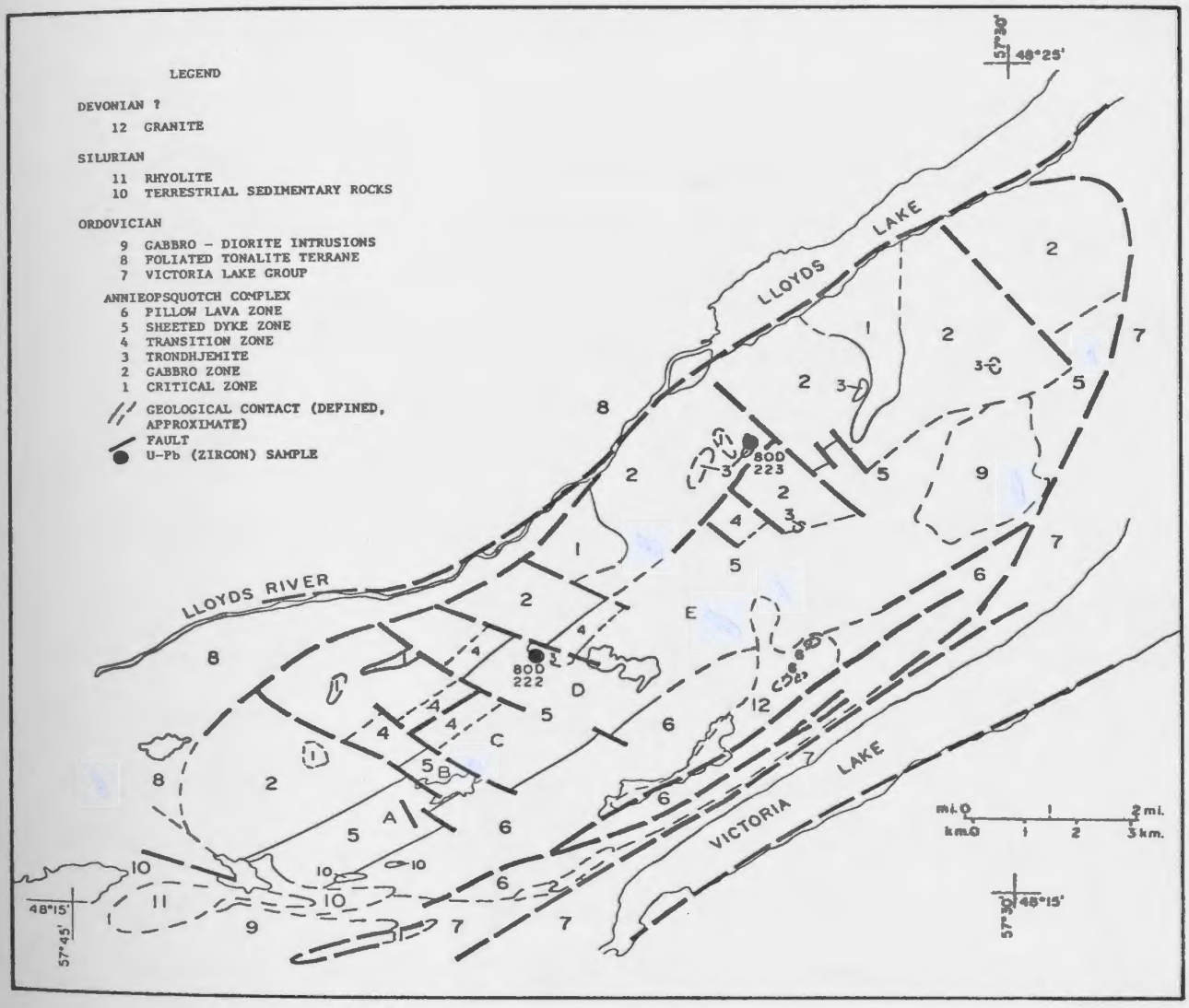

Figure 3.1. Geological map of the Annieopsquotch Complex, simplified after Map 1 (in pocket). A to E refer to stereonets of Figure 3.18.

post Ordovician movement), with the volcanic sequence structurally above the ophiolite.

The granodiorite at the southwest end of the Complex (unit 8) and the ophiolite itself are unconformably overlain by early Silurian terrestrial sedimentary rocks (unit 10). Because of this cover and the presence of the cross- cutting Boogie Lake Intrusion (unit 9), relationships between the Annieopsquotch Complex and other ophiolitic fragments to the south are uncertain. However, it is reasonable to assume that the ophiolitic fragments are correlative with the Complex and that the Boogie Lake Intrusion cuts them all.

A granite of presumed Devonian age, underlying a chain of lakes (Map 1, Figure 3.1, unit 12), cuts the pillow lava zone along a major fault.

Stratigraphic units of the Annieopsquotch Complex face and dip southeast but the dip cannot be accurately determined as no certain paleo-horizontal surfaces are present. It is suggested that the dip of the major contacts is approximately 50 to 70 degrees. The map pattern therefore is approximately a cross section through the stratigraphic units of an ophiolite (Figure 3.1).

3.1.2 Emplacement

Its present topographic expression suggests that the ophiolite is a thrust slice but paleocurrent evidence from the terrestrial sedimentary rocks that unconformably overlie the ophiolite (Chandler, 1982) suggests that uplift

of the mountains is a post early Silurian event. It is suggested that the Annieopsquotch Complex is part of an allochthonous 'Taconic' slice but it is also a horst block uplifted after emplacement of the allochthon. This suggestion will be developed in Chapter 8.

3.1.3 Stratigraphic Units

The ophiolite has been divided into six map units (Map 1, Figure 3.1). These are, from northwest to southeast (base to top): 1. the 'critical zone', composed of olivine-plagioclase-clinopyroxene bearing rocks which are locally well layered; 2. 'high level' gabbro, which is heterogeneous, generally coarse grained, contains pegmatitic pods and is cut by diabase dykes; 3. trondhjemite as pods and intrusion breccia; 4. a transition zone in which the proportion of dykes within gabbro rapidly increases upwards; 5. a sheeted dyke zone in which diabase dykes strike northwest and; 6. a pillow lava zone, in which basaltic pillows, minor hyaloclastite and red chert occur, cut by diabase dykes and sills. These units constitute an ophiolite 'pseudostratigraphy' because younger gabbros may underlie old dykes and lavas. However, throughout this thesis the term 'stratigraphy' will be used for the sake of simplicity. Assuming that the zones dip fifty degrees southeast, the thicknesses are approximately 2.3 km for the gabbro zone and 1.5 km for each of the sheeted dyke zone and pillow lava zone.

3.2 THE CRITICAL ZONE

The term 'critical zone' as used in this thesis follows the usage of Ingerson (1935) and others and refers to the zone defined by Malpas (1976) for the Bay of Islands Complex. It comprises a sequence of olivine, plagioclase and clinopyroxene cumulates at the base of the gabbroic plutonic section. The main difference from the upper part of the gabbro section is the abundance of olivine- rich rocks, including ultramafic cumulates, which exhibit well developed layering. They were interpreted by Malpas (1976) to represent the base of the oceanic crust. He suggested that the top of the critical zone represents the 'seismic MOHO' and a major density contrast. A more significant petrologic break occurs at the base of the critical zone separating cumulates above from tectonized harzburgite below.

3.2.1 Distribution and Contacts

Rocks of the critical zone outcrop in two areas along the northwest edge of the Annieopsquotch Complex (Map 1, Figure 3.1, unit 1). These may represent the basal parts and walls of two discrete intrusions or be remnants of a once continuous unit. The southwest block appears to be bounded to the southwest by a fault, interpreted to be a seafloor feature, which cuts across the stratigraphy at a high angle. The block is intruded by coarse grained gabbro to the northeast and by a few diabase dykes throughout. The southeast contact appears to be intrusive with high

level' gabbro cutting across steeply dipping, north striking layered rocks.

The northeast block of critical zone rocks is surrounded by rocks typical of the 'high level' gabbro zone and it is suggested that the latter intruded and engulfed the block. It is possible that the block was tilted or rotated first along a high angle fault and then intruded by gabbro.

Minor faults cross the critical zone obliquely and appear to be splays off the large faults which offset the stratigraphy of the ophiolite. One of these minor faults is intruded by undeformed coarse grained gabbro indicating that this fault, and probably most, formed in the oceanic realm.

Two sill- like bodies of troctolite and olivine gabbro which appear to cut 'high level' gabbro (Map 1, Figure 3.1) are included in the discussion of the critical zone because of their lithologic similarity.

3.2.2 Magmatic-Sedimentary Structures

Olivine- plagioclase- clinopyroxene cumulates and metacumulates, locally well layered, form the majority of the critical zone (Map 1, unit 1A). The layers strike 160 to 200 degrees in both blocks and are steeply dipping, similar to dyke trends in the sheeted dyke zone. Primary igneous structures, thought to be indicative of a magmatic-sedimentary origin (Jackson,1967; Irvine,1970 and many others) are present in some parts of the critical zone.

These include both isomodal and modally graded layers of Irvine's (1982) terminology. Isomodal layering involves the presence or absence of a mineral phase from layer to layer and results in the sequence anorthosite- gabbro (clinopyroxene in) or gabbro- troctolite (olivine in). Both these sequences are present in the Annieopsquotch Complex.

Modally graded layering is common in the critical zone (Figure 3.2). It involves a change in the proportion of two minerals such as plagioclase and clinopyroxene to give rocks ranging in composition from anorthosite (less than 10% clinopyroxene) through gabbro (near equal proportions of the two minerals) to clinopyroxenite (greater than 90% clinopyroxene). Modally graded layering, involving changes in the proportion of olivine in olivine gabbros, although common is difficult to recognize in most cases as it involves relatively small changes in the colour of the rock.

Well developed layering is discontinuous, passing over short distances into massive olivine gabbro, which may represent thick isomodal layers. As a result it has proven impossible to map out the shape of the intrusion(s) by using attitudes of layering. It is therefore uncertain if rocks within the critical zone , other than those obviously layered, are oriented at a high angle to the ophiolite stratigraphy.

Trough layering occurs rarely; the best example (Figure 3.3) occurs in layered olivine gabbros. It is

Figure 3.2. Modally graded olivine- plagioclase-clinopyroxene metacumulates in the southwest block of the critical zone. Dark layers are olivine gabbro, reddish brown are troctolite and lighter brown are leucotroctolite. Layers strike 348 and dip 84 east. 79HPAD263.

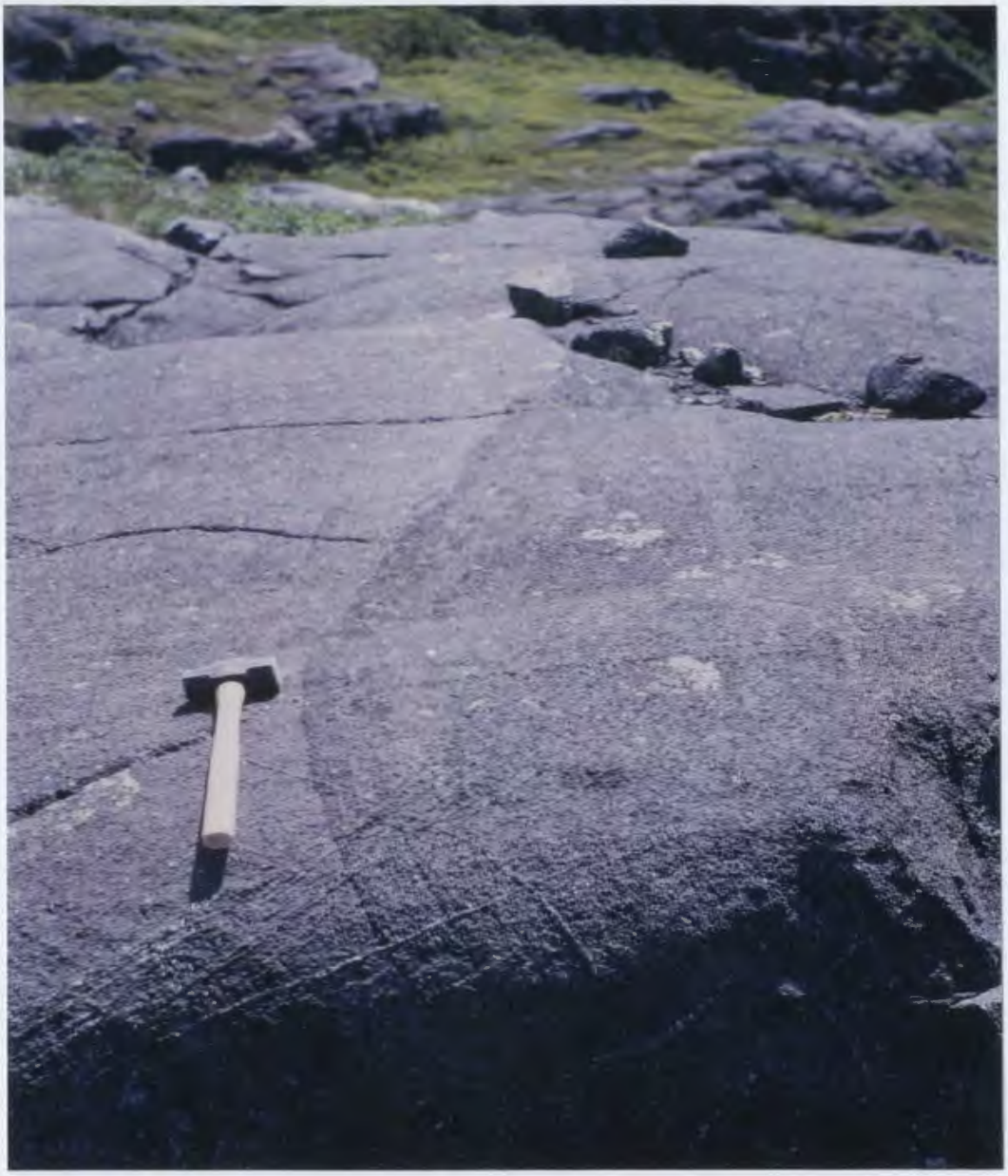

Figure 3.3. Trough structure in layered olivine gabbros of differing clinopyroxene content. Top is to right (west). 79HPAD084.

about two metres across and one half metre deep and layers within the trough, which vary in their olivine content, conform to the contours of the structure.

Angular discordances between sets of igneous layers occur locally in the critical zone. In one example, in the southwest block, gabbro with trondhjemite seams is truncated by olivine gabbro layers (Figure 3.4). The present writer interprets this structure to be a result of magmatic processes, it could be a result of high temperature shear. The texture of the gabbro was not examined in detail.

A 'dropped block' occurs in thick isomodally layered olivine gabbro in the southwest block of the critical zone (Figure 3.5). It is composed of fine grained mafic rock of unknown affinity.

Folds occur rarely in the critical zone. The best example (Figure 3.6) is in olivine gabbro and troctolite of the southwest block. It occurs within a layered sequence and has conformable layers above and below. The rocks are quite fresh and contain subhedral olivine and plagioclase grains. It is interpreted that the fold is the result of slumping of semi- consolidated layers from the wall of a magma chamber.

These structures, though, are not well developed in the zone and the majority of the rock is coarse grained, fairly massive olivine gabbro. Some of this gabbro might represent thick isomodal layers.

Figure 3.4. Angular discordance in the southwest block of the critical zone. Olivine gabbro layers truncate gabbro with trondhjemite seams. 79HPAD037.

Figure 3.5. Olivine gabbro with isomodal layers. Rounded 'dropped block', finer grained than the gabbro, occurs to the right of the hammer head. 79HPAD040.

Figure 3.6. Fold in troctolite-olivine gabbro sequence, interpreted to be formed by slumping of semiconsolidated layers.79HPAD084.

3.2.3 Troctolite Sills

The sill-like body at the southwest end of the Annieopsquotch Complex is composed of troctolite which has minor variations in its mafic mineral content. The rocks are very fresh and contain olivine, plagioclase, clinopyroxene and rare scattered chromite grains. The contact between the grey-brown weathering troctolite and grey-green weathering olivine gabbro to the southeast is sharp but there is no evidence of a chilled margin or even a minor decrease in grain size. The body is estimated to be about a hundred metres thick but it may be the basal part of a magma chamber that includes the overlying olivine gabbros.

A small body of troctolite and olivine gabbro, oriented northwest-southeast, occurs south of the southwest end of Lloyds Lake. It forms a ridge which is separated by a forested cliff from the surrounding gabbros. It appears to be connected to an olivine-porphyritic diabase dyke at its north end and is surrounded by trondhjemite-bearing gabbroic rocks. The contact relationships of the body are enigmatic but it is most likely a sill intrusive into the gabbros. The olivine gabbro is fresh and, in some zones which may be layers, contains bright green chromian diopside oikocrysts up to 5 cm long.

3.2.4 Metamorphism

The layered rocks throughout the northeast block of the critical zone are recrystallized and layer contacts are

not as sharp as those in the southwest block. Plagioclase rich layers are bright white on the weathered surfaces due to formation of albite and are cleaved locally. While the general composition and structure of the layers is preserved, large pyroxene oikocrysts (or porphyroblasts) now overprint layer contacts locally. The layers are also crosscut by rare gabbro or clinopyroxenite dykes and common raised amphibole bearing veinlets (Figure 3.7).

It is this northeast block of the critical zone that is intruded by high- level gabbro and it is suggested that the heat from this intrusion, in addition to the generally high geothermal gradient characteristic of a spreading ridge environment, was the cause of the metamorphism.

3.2.5 Equigranular Rocks

Large areas of the southwest block of the critical zone consist of olivine gabbro in which layering cannot be readily discerned. Within these areas occur irregular masses of fine grained equigranular mafic rock (Map 1, unit 1B). These rocks grade, by increase in grain size and textural heterogeneity, into coarse grained gabbro. This change takes place over a distance of one to ten metres. The equigranular rock is cut by raised 0.1 to 1.0 cm wide green amphibole bearing crisscrossing veinlets (Figure 3.8).

Figure 3.7. Olivine gabbro-troctolite layers, in the northeast block of the critical zone, recrystallized and cut by raised amphibole-bearing alteration veinlets. GSC203551-R. 79HPAD032.

Figure 3.8. Fine grained equigranular mafic rock, cut by raised amphibole-bearing veinlets 0.1 to 1.0 cm. in width, enclosed in olivine gabbro of the southwest block of the critical zone. 79HPAD257.

3.2.6 Interpretation and Discussion

The critical zone lithologies of the Bay of Islands Complex (Malpas,1976) and other ophiolites have generally been interpreted to be the base of the oceanic crust.

The sequence has been described as a cumulate one involving crystallization of various proportions of olivine, chromite, clinopyroxene and plagioclase, commencing crystallization in that order.

The nature of the crystallization mechanism is a matter of discussion; whether due to crystal settling and distribution by currents in a magma chamber (cf. Irvine,1970; Jackson,1967) or by crystallization at the walls of a magma chamber due to element concentration gradients and depletion in the adjacent magma (McBirney and Noyes,1979). However, both viewpoints are based on the assumption that the layering present is a primary feature of magmatic processes.

Casey and Karson (1981) proposed a magma chamber model for North Arm Mountain of the Bay of Islands Complex in which the cumulate units formed with their layering steeply inclined, vertical or overhanging by a process similar to that put forward by McBirney and Noyes (1979).

It has been generally assumed by most workers that layering in the critical zone preserves the original features of magmatic crystallization (Smewing,1981). However, this idea is challenged by Calon and Malpas (pers. comm.,1983) as a result of their work on Table Mountain and North Arm Mountain in the Bay of Islands. Layering in the

critical zone is isoclinally folded on a large scale and the texture of many of the rocks is mylonitic. This suggests to them that the critical zone has undergone significant deformation and Calon (pers. comm.,1983) suggests that this occurred primarily as a result of differential movement (underthrusting) at the mantle : crust boundary. The layering therefore might not be a primary igneous feature but rather a result of metamorphic segregation, although it might be only a modification of primary olivine- rich and plagioclase- rich cumulate layering.

While metamorphic textures and folds are present in the critical zone on North Arm Mountain, textures in layered cumulates in other ophiolites such as the Karmoy Complex of Norway (Pedersen, 1982), the Oman ophiolite (Smewing, 1981) and the Annieopsquotch Complex (Dunning and Herd, 1980 and this work) are comparable to those described from large stratiform intrusions.

In the Annieopsquotch Complex only a small area of critical zone layered rocks is present and, because no ultramafic layers of dunite or peridotite are present, it is suggested that only the upper levels of the critical zone are preserved.

If the suggestion is correct that the deformation structures present on North Arm Mountain are a result of mantle underthrusting relative to the oceanic crust it would seem reasonable to suppose that these effects would be less significant with increasing height in the critical

zone.

It is suggested that such a gradient exists and that this is the reason that relatively undeformed cumulate structures and textures are preserved near the top of the critical zone in the Annieopsquotch Complex and other ophiolites. The recrystallized foliated cumulates likely show the effects of the mantle : crust interaction.

It is interpreted that many metamorphic effects observed are due to heating by the underlying mantle and adjacent 'high level' gabbro. The texture of the equigranular rocks is that of a hornfels and it is suggested that these irregular areas, with gradational boundaries with enclosing gabbro, represent dehydrated mafic rocks metamorphosed by the enclosing gabbro. It is likely that they represent either large blocks engulfed by the gabbro intrusion or parts of the intrusion that solidified first and were then dehydrated and metamorphosed at P-T conditions of the lower part of the oceanic crust. The mineral assemblage, with co-existing equant clinopyroxene and orthopyroxene, indicates that conditions typical of the granulite facies were achieved. Pyroxene equilibration temperatures of approximately 1000 degrees C are recorded in these rocks (Chapter 4).

3.3 GABBRO ZONE

3.3.1 Distribution and Contacts

The gabbro zone occurs along the northwest edge of the mountains (Map 1, Figure 3.1, unit 2) and gabbro occurs as screens in the transition zone and sheeted dyke zone. Gabbro comprises the largest area of the ophiolite and its upper contact with the transition zone or sheeted dyke zone is at different positions along the length of the ophiolite. This appears to be due primarily to offsets along northwest striking faults (Figure 3.1), however it is likely that different intrusions originally extended to different heights in the crust.

Faults cutting the gabbro zone do not extend beyond the ophiolite and therefore are thought to predate its emplacement and the generation of the Ordovician tonalites to the northwest (Chapter 2). The faults cannot be traced with certainty through the sheeted dyke zone in some cases. This could be due to emplacement of diabase dykes along these faults or simply because little deformation resulted from movement along them. The fault at Loon Echo Pond (Figure 3.1) is intruded by an undeformed medium grained trondhjemite which forms an intrusion breccia including blocks of gabbro and diabase. This trondhjemite is chemically related to the ophiolite so it is interpreted that the fault and intrusion are seafloor features.

3.3.2 Components of the Gabbro Zone

The gabbro is predominantly coarse grained and equigranular, composed of near equal proportions of plagioclase and clinopyroxene, or their alteration products, and is correlated with the 'high level' gabbro described from other ophiolite complexes. Many varieties of this gabbro occur along the length of the Annieopsquotch Complex and some likely represent discrete intrusions. The gabbros are texturally heterogeneous. Near the base of the zone, at the northwest edge of the mountains, much of the gabbro has a penetrative foliation. It strikes roughly north to northeast and is steeply dipping. This foliation, which can be extremely pronounced, is defined in outcrop by an alignment of mafic minerals (Figure 3.9). The mafic mineral is almost entirely secondary amphibole. Areas of foliated gabbro occur throughout the gabbro zone. However, much of the gabbro, though variable in grain size and mineral proportions, is not noticeably foliated.

There are zones of amphibolite as well as shear zones near the base of the gabbro zone. Layering also occurs locally and pegmatitic pods and trondhjemite pods are present at or near the top of the gabbro zone. The gabbro : sheeted dyke zone contact is variable along the length of the ophiolite and reflects several different processes that occur at that level. These features of the gabbro zone are discussed in more detail in the following sections.

Figure 3.9. Strongly foliated gabbro near the base of the gabbro zone. Foliation strikes 010 and dips 70 degrees east. 78HPAD202.

3.3.3 Igneous Layering

Modal layering, involving changes in the proportion of plagioclase and clinopyroxene (Irvine,1982) occurs locally in the basal part of the gabbro zone. It is discontinuous, being well developed in sequences up to several metres thick (Figure 3.10) which only extend ten to twenty metres along strike before terminating or pinching out into coarse grained gabbro.

The layers are steeply dipping in most cases and strike at a high angle to the zonal contacts. The layers are curved in some examples suggesting that they may represent trough structures. If their near vertical orientation with respect to the ophiolite stratigraphy is primary, these layered sequences may represent sides of magma chambers where minerals crystallized or were plated on the walls (cf. McBirney and Noyes,1979).

In some examples modally layered sequences contain concordant pegmatitic layers which are undeformed. These indicate that; 1.the layering was not formed or modified by deformation, 2. the layers formed by crystallization from a liquid and 3. the style or rate of crystallization changed during formation of the layers (Figure 3.11).

Rare folds involving isomodal plagioclase-clinopyroxene layers, with parallel concordant layers above and below, are interpreted as syn-magmatic slump features. Figure 3.12 shows such a fold from the Star Lake ophiolitic fragment.

Gabbro in these small layered units is generally

Figure 3.10. Modal layering in `high level' gabbro involving changes in the plagioclase : clinopyroxene ratio. Layering strikes 017 and dips 85 degrees east. 79HPAD036.

Figure 3.11. Modally layered gabbro with concordant pegmatitic layer. 80HPAD057.

Figure 3.12. Fold, interpreted to be a magmatic slump feature, in isomodal plagioclase-clinopyroxene layers of the Star Lake ophiolitic fragment. 80HPAD168.

medium grained and homogeneous relative to the surrounding unlayered gabbro. The layered units have not been found in close spatial association with pegmatitic pods as was reported from the Karmoy Complex by Pedersen (1982).

Recrystallization of some areas of layered rocks has resulted in a coarsening of the grain size with resultant loss of fine textures although the general layered structure is preserved. Large white weathering feldspar patches overgrow layer contacts in some cases.

3.3.4 Amphibolite and Shear Zones

Amphibolite underlies a ridge at the northwest edge of the mountains. The foliation strikes northeast, parallel to the ophiolite stratigraphy and is steeply dipping. The amphibolite is composed of hornblende and plagioclase and contains coarse ragged plagioclase grains. The margins of the amphibolite appear to grade into foliated, then massive, gabbro and the amphibolite is interpreted to represent a high- temperature shear zone. It is suggested that the amphibolite had a gabbro protolith and that the ragged plagioclase grains are relict primary grains.

Shear zones occur locally throughout the Annieopsquotch Complex. Some are parallel to the faults that crosscut the stratigraphy while others are nearly parallel to the stratigraphy. In the gabbro zone, most sheared rocks are composed of amphibole and plagioclase, with epidote, chlorite and albite as less important phases. The amphibole present is either of the actinolite-tremolite

series or is hornblende. The presence of hornblende in an equilibrium texture with plagioclase is taken to indicate the existence of amphibolite facies P-T conditions during formation of some of these zones. Amphibolite bearing shear zones are less than one metre to several metres thick and grade into foliated gabbro with a foliation oblique to the shear zone.

Shear zones, centimetres to 0.5 metre thick, are ubiquitous in the gabbro zone and have widely varying orientations (Figure 3.13). Some diverge from the margins of crosscutting diabase dykes, many of which have foliated margins. Some pegmatitic pods are sheared and crystals within broken or bent.

3.3.5 Pegmatitic Gabbro Pods

Diffuse or sharply bounded patches of very coarse grained to pegmatitic gabbro or hornblende gabbro, locally grading to hornblende trondhjemite occur irregularly in the gabbro zone. Almost all of these pods occur in the southeast part (stratigraphic top) of the zone. They vary from small (less than one metre) pods that are only slightly coarser than the enclosing gabbro to pegmatitic patches of irregular shape, three or more metres across which have zones within them with differing textures and compositions. In one pod, crystals up to twenty-five centimetres in length occur, many arranged at right angles to the edge of the pod suggesting that they grew out from the wall into a pool of magma (Figure 3.14).

Figure 3.13. Small shear zone with gabbro inclusions cutting coarse grained gabbro. 79HPAD040.

Figure 3.14. Pegmatitic pod in 'high level' gabbro, with crystals up to 20 cm long, oriented at a high angle to the walls. South of 80HPAD059.

Some of the pegmatitic gabbro contains more magnetite than the enclosing rocks indicating that the pod was likely a trapped pool of magma which differentiated further than the surrounding gabbro. An increase in the volatile content of the residual magma likely permitted the growth of the coarse crystals and the high fO_2 would stabilize the crystallization of magnetite.

The fact that trondhjemite occurs as the central part of some of the pods indicates that they are the last differentiation product of the gabbroic magma chamber.

Most of the pegmatitic pods do not occur at the top of the gabbro zone but at least ten metres or more below the top. This suggests that the uppermost gabbroic rocks comprise a roof assemblage which formed by underplating of the top of the magma chamber. In some cases, where a fault contact occurs between the gabbro and sheeted dyke zones (Figure 3.1), it is not clear if that was the original top of the gabbro zone or if part has been removed by thrusting.

3.3.6 Trondhjemite Bodies

Small felsic bodies occur locally near the top of the gabbro zone (Map 1, unit 3). It is estimated that they comprise no more than one to two percent of the gabbro zone. They are composed of greater than ninety percent plagioclase with quartz, hornblende, chlorite and biotite as major phases. Epidote, apatite, sphene, zircon and prehnite commonly occur as accessory minerals.

With the exception of this small amount of trondhjemite, occuring in the cores of pegmatitic gabbro pods most trondhjemite forms the matrix of intrusion breccias that contain blocks of both gabbro and diabase, some partially digested (Figure 3.15). The trondhjemite occupies about fifteen to twenty percent of the volume of the breccia as a network of irregular dykes and pods. Some dykes are rooted in the pods and extend a short distance into the host gabbro or overlying sheeted dyke zone (Figure 3.16). Epidote rich assemblages occur along fractures and some large epidosite patches are locally present.

Two trondhjemite bodies, one in the core of a pegmatitic gabbro pod and the other a moderately epidotized intrusion breccia at Loon Echo Pond, yielded zircon for the geochronologic study reported in Chapter 7. The intrusion breccia is slightly older indicating that it is not related to the younger foliated tonalite suite exposed northwest of the Annieopsquotch Complex.

The chemistry of the trondhjemitic rocks is discussed in Chapter 5.

3.3.7 Gabbro - Sheeted Dyke Zone Contact

3.3.7.1 Field Descriptions

In the southwest part of the Annieopsquotch Complex, the gabbro and sheeted dyke zones are separated by a transition zone which displays a somewhat regular increase in the percentage of diabase dykes from northwest to

Figure 3.15. Trondhjemite as matrix to intrusion breccia in the gabbro zone. It includes gabbro and diabase fragments, some partially digested. 79HPAD067.

Figure 3.16. Narrow trondhjemite dykes rooted in a pod of trondhjemite within gabbro. 79HPAD067.

southeast across the zone. This zone is discussed in the next section.

In the northeast part of the Complex, the gabbro and sheeted dyke zones are juxtaposed across a fairly sharp contact that locally is mapped as a fault but elsewhere appears to be conformable. Where conformable, the top of the gabbro zone is texturally heterogeneous and contains a wide variety of gabbro and diabase. This part of the gabbro zone is best exposed and was examined in the most detail between Dyke Pond and Loon Echo Pond.

The most striking feature of the top of the gabbro zone is the structural and textural heterogeneity. Irregular patches, up to several metres wide, of fine grained diabase occur with nebulous, gradational or locally chilled contacts with the coarse grained gabbro. Diabase also fills fractures and occurs as irregular dykes in the same area. Many blocks, small lithic fragments as well as individual crystals of plagioclase and clinopyroxene occur in the pockets of diabase (Figure 3.17) and they appear identical to gabbro forming the walls of the pocket. In fact, in three dimensions, some 'blocks' might well be connected to form a sort of sponge textured host for the diabase. Some of ~~these~~ patches are so charged with crystals and lithic fragments that they can be mistaken for the host gabbro itself. However, close examination reveals that the material between coarse grains and fragments is fine grained diabase, not coarse grained gabbro.

Some aphanitic diabase dykes, which have chilled

Figure 3.17. Irregular patch of fine grained diabase at the top of the gabbro zone. The diabase, enclosing lithic fragments and plagioclase and clinopyroxene crystals, is interpreted to be a quenched pool of basaltic liquid. 80HPAD130.

margins above these pockets, grade into the fine grained diabase within the pocket. In one location, a patch of diabase charged with small lithic fragments and crystals passes upwards into an irregular dyke, full of fragments, which has chilled margins.

Pegmatitic pods, described in section 3.3.5, occur in this top part of the gabbro zone and add further to the textural variability.

3.3.7.2 Discussion and Interpretation

The top of the gabbro zone appears to represent a part of the magma chamber, or chambers, where complex interactions have occurred between solid rock, magma and crystal mushes. It is the area in which stoped blocks, from the overlying roof assemblage rocks and sheeted dykes, would be expected to occur and it is the area where late stage differentiates; the most evolved magmas would solidify. It is also the zone where dyke numbers increase rapidly so it is likely the source for most of the sheeted dyke zone although the magma that fed most of the dykes is not preserved in this zone.

The irregular patches of diabase with gradational contacts with the enclosing gabbro are interpreted to be quenched pools of basaltic liquid in the root zone for some of the diabase dykes of the sheeted dyke zone. They presumably represent late liquid which fed only a few of the late dykes of the sheeted dyke zone. Similar irregular patches of diabase occur in the Star Lake ophiolitic

fragment.

Assimilation of blocks is difficult to prove in this zone as it is so texturally heterogeneous. Water derived from assimilated hydrated mafic crust may be responsible for the generation of pegmatitic pods.

3.4 TRANSITION ZONE

3.4.1 Introduction

Few detailed descriptions exist of the transition zone which separates the gabbro and sheeted dyke zones in ophiolite complexes. Two recent papers have described the rooting of diabase dykes in gabbro in the Oman ophiolite (Rothery,1983) and the complexity present in this zone on North Arm Mountain, Bay of Islands Complex (Rosencrantz,1983). In both these ophiolites one type of transition observed is a downward decrease in the number of dykes, which are seen to merge with gabbro at different depths over a maximum depth range of about two hundred metres. Elsewhere, on North Arm Mountain, the transition occurs abruptly with all dykes grading into gabbro over a zone tens of metres thick and in some locations gabbro cuts the base of the sheeted dykes and contains xenoliths of diabase (Rosencrantz,1983).

All these relationships, and others, are seen within the Annieopsquotch Complex where one has the advantage of exposure of a cross section through the zone.

3.4.2 Distribution and Contacts

The contact between the top of the gabbro zone and the base of the sheeted dyke zone is variable along the length of the ophiolite. In places where gabbro is juxtaposed with close to one hundred percent sheeted dykes across a linear topographic feature, it is shown as faulted (Map 1, Figure 3.1). However, little or no shearing is observed along the line marked.

In the central part of the mountains, the change from the gabbro to sheeted dyke zone is gradational over hundreds of metres. Only this area has been mapped as the transition zone (Map 1, Figure 3.1, unit 4). Within this zone there is a gradual increase in the percentage of dykes from northwest to southeast and the limits of the zone have been arbitrarily set at twenty- five and seventy- five percent diabase dykes in gabbro. This corresponds, roughly, to the D1 unit of Rothery (1983) which he defined as thirty to seventy percent dykes between gabbro seams.

3.4.3 Field Descriptions

Gabbro in the transition zone is coarse grained and heterogeneous composed of varying proportions of plagioclase to clinopyroxene (and their alteration products). At one locality, magnetite rich coarse grained gabbro occurs as screens between dykes within the sheeted dyke zone. This variety of iron rich gabbro is not seen in the transition zone to the southwest.

Many dykes in the transition zone are several metres

wide with coarse grained cores and chilled margins. Where the gradation to a chilled margin is not observed due to lack of exposure, it is not possible in many cases to distinguish between gabbro host and dyke material. Evidence, in the form of blocks of diabase in gabbro, suggests that the gabbro intrudes dykes as well as dykes intruding gabbro in this zone. This is similar to the relationship between the gabbro and sheeted dyke zones on North Arm Mountain as observed by Rosencrantz (1983).

3.4.4 Discussion

The transition zone differs from other areas along the gabbro zone : sheeted dyke zone contact, described above, by the gradual increase in the number of diabase dykes across the zone. While , in places, the contact between the zones may be sharp due to tectonic omission in others it appears to be a primary feature. A similarly sharp boundary was noted in the Bay of Islands Complex by Rosencrantz (1983).

The difference between a gradual increase in dyke abundance in one area and a sharp increase elsewhere might be related to position relative to the underlying magma chamber(s). Possibly, above the centre of the magma chamber the magma pocket closely approaches the sheeted dyke boundary but around the sides dykes penetrate a thicker crystalline gabbroic wall of the magma chamber to reach the sheeted dyke zone. This feature may be of use in delineating magma chambers.

3.5 THE SHEETED DYKE ZONE

3.5.1 Introduction

Recognition of a sheeted dyke zone has been the key to the identification of many mafic- ultramafic complexes as ophiolites and thus to their interpretation as fragments of oceanic crust. The zone, characterized by hundreds to thousands of subparallel, mutually intrusive diabase dykes, is the most distinctive of the ophiolite stratigraphy (Penrose conference participants, 1972).

The recognition of the significance of the dyke zone in terms of sea floor spreading, ie; that it represents one hundred percent extension and likely formed by intrusion processes at an oceanic spreading axis has come fairly recently (Moores and Vine, 1971).

Newfoundland ophiolites at Bay of Islands (Malpas, 1976; Rosencrantz, 1983), Betts Cove (Upadhyay, 1973) and Lushes Bight (Strong, 1973) have well developed sheeted dyke zones, although that at Betts Cove has been truncated or locally removed by thrusting. Several of the fragments in the Annieopsquotch ophiolite belt preserve areas of sheeted dykes and the Annieopsquotch Complex itself has a large, well exposed sheeted dyke zone that extends the length of the mountains. As it is exposed in cross section it is possible to observe variations through the zone, including both its lower and upper boundaries which are transitional into the gabbro (discussed above) and pillow lava zones.

3.5.2 Distribution and Contacts

The sheeted dyke zone forms the central part of the Annieopsquotch Complex. It is broken into several blocks by faults which crosscut the ophiolite stratigraphy, as is the gabbro zone (Map 1, Figure 3.1, unit 5). However, as all dykes trend roughly northwest and are steeply dipping (Map 1), approximately parallel to the faults, it has not been possible to trace all the faults through the sheeted dyke zone.

The northwest contact of the zone is shown as defined where in areas of good exposure or approximate where in areas of poor exposure. In some areas there is a sharp contact between coarse grained gabbro to the northwest and one hundred percent sheeted dykes to the southeast of a topographic lineament. In such areas a faulted contact is inferred, however there is little shearing along this lineament so it is thought to be of only local significance. The contact changes from a faulted to an apparently unfaulted one between the gabbro and sheeted dyke zones, north of Loon Echo Pond.

In the southwest part of the ophiolite, an especially well exposed area, gradational contacts occur between the gabbro zone, transition zone and sheeted dyke zone. However, north of Dyke Pond, a fault marked by a northeast-striking topographic lineament separates the gabbro and sheeted dyke zones.

The southeast boundary of the sheeted dyke zone (stratigraphic top) is placed at the first appearance of

pillow lava screens between dykes, even if they comprise less than ten percent by volume. In general the sheeted dyke zone is approximately two to three kilometres wide in plan view although at Dyke Pond the first appearance of screens of pillow lava is on the south shore of the pond and the sheeted dyke zone is only 1.2 km wide there. It is of a similar width in the southwest block of the zone.

The sheeted dyke zone is cut by two intrusions; 1. the hornblende diorite to granodiorite at the northeast end of the mountains (Map 1, unit 9) and, 2. a lobe of the granite which cuts the pillow lava zone at the southeast side of the ophiolite (Map 1, Figure 3.1, unit 12). The outline of the diorite intrusion is defined on its eastern side by distribution of lithologies in outcrop and on the north and west sides by a pattern of concentric strong positive aeromagnetic anomalies (GSC Map 250G). The age of neither intrusion is known. However, the hornblende diorite is thought to be related to the Boogie Lake Intrusion (see Chapter 2) of late Ordovician age and the granite is thought to be of Devonian age; both are thus thought to significantly postdate formation of the Annieopsquotch Complex.

3.5.3 Field Description of Diabase Dykes

3.5.3.1 Orientation

Dykes in the sheeted dyke zone have a preferred northwest strike varying from approximately 330 to 200 degrees and dip from 60 degrees northeast to the same southwest. The preferred orientation is clearly shown on the stereonets of Figure 3.18 where poles to sheeted dykes are shown for each of the fault- bounded blocks labelled A to E in Figure 3.1. On each stereonet the poles define a broad point maximum indicating that the dykes strike northwest to north- northwest. This orientation is the same as that of sheeted dykes in ophiolitic fragments at King George IV Lake, Shanadithit Brook and those which occur as inclusions in the Boogie Lake Intrusion. The possible significance of this consistent sheeted dyke orientation is discussed in Chapter 8.

3.5.3.2 Continuity of Dykes

Some dykes can be traced one hundred metres or more along strike but many cannot. This is due to several changes that occur along strike such as; 1. pinching out of a dyke, 2. offset along minor faults, 3. sharp high angle turns along fractures or joints and 4. bifurcation to form two or more smaller dykes. This last feature always indicates that the topping direction is to the southeast. In most cases it is not possible to trace out dykes simply because of gaps in exposure between areas of

Figure 3.18. Stereonets (Schmidt equal area, lower hemisphere) for diabase dykes of the sheeted dyke zone. A to E show poles to dykes for each fault - bounded block shown in Figure 3.1. Number of measurements is shown in brackets. F shows orientation of 13 faults which cut the ophiolite stratigraphy at a high angle.

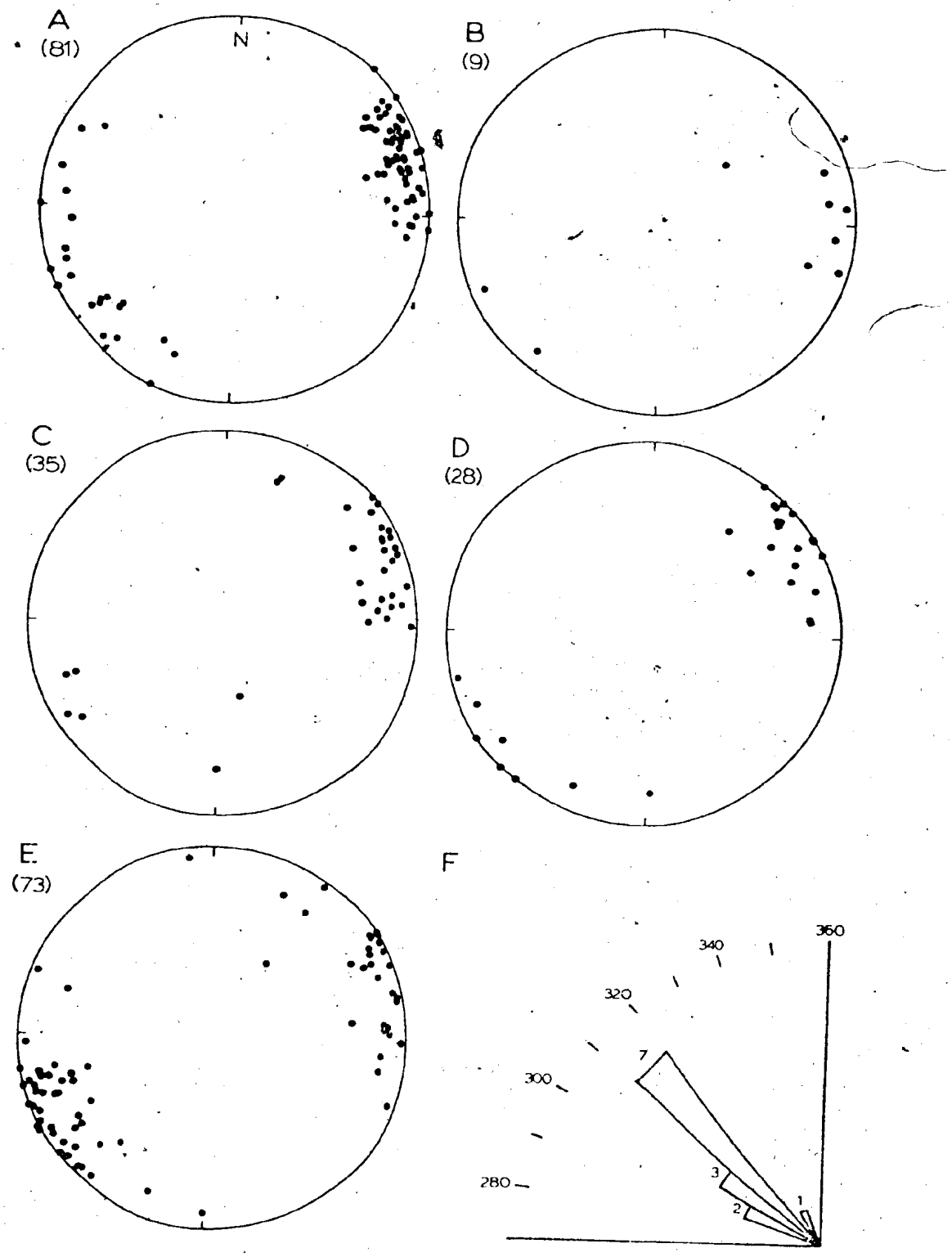
A
(81)
N
B
(9)
C
(35)
D
(28)
E
(73)
F
360
340
320
300
280
7
3
2
1

outcrop of sheeted dykes of identical appearance.

3.5.3.3 Chilling Directions

The proportion of chilled margins facing in one direction over the other in a sheeted dyke zone has been taken by Kidd and Cann (1974), Kidd (1977) and Rosencrantz (1983) to indicate the direction to the paleo-spreading centre of an ophiolite. The idea behind this was that some dykes intruding at the spreading centre were thought to split the preceding dyke down the centre, displacing each half with its chilled margin to its respective side of the ridge. Repeated many times, a segment of crust on one side of the ridge would have a majority of chilled margins facing away from that ridge.

The assumptions made in this model are; 1. that the zone of dyke intrusion is sufficiently narrow so that some dykes split earlier ones, 2. that each dyke is chilled against those it intrudes, 3. that dykes which have chilled margins missing, split by intrusion of later dykes, are half the width of the original dyke and that no split dykes were originally wider than the widest complete dyke observed, 4. that dykes are measured over a sufficiently long section to give statistical credence to the results and, 5. that if dyke one - way chilling directions are consistent over the breadth of an ophiolite complex, it formed at a spreading ridge rather than as a dyke swarm associated with a discrete volcanic centre or some other feature. In addition, for the calculations, Kidd (1977)

assumes dykes less than 0.2 m wide to be veins and apothesis and does not consider them.

In the Annieopsquotch Complex, assumption 3 is not valid because, in many outcrops, numerous late dykes with two chilled margins cut earlier far wider dykes (Figure 3.19).

In the Annieopsquotch Complex, with excellent exposures of the sheeted dyke zone, the chill directions were noted for hundreds of dykes exposed on two topographic ridges. Each ridge is approximately one kilometre in length and trends roughly parallel to the stratigraphy (right angles to the strike of the dykes). No preferred direction of one way chilled margins was noted. Where a chilled margin occurs facing one direction the opposite chilled margin can in most cases be identified on the other side of one or two complete younger dykes. While the older dyke has been split apart by younger ones all slices of the old dyke are in close proximity. Of course, while these younger dykes were being emplaced the spreading centre was at that point. Many such split dykes occur along the length of the sheeted dyke zone. They indicate that the locus of dyke intrusion jumped from one spot to another, probably over a wide zone. While there likely is an overall younging in one direction across the twenty km. long sheeted dyke zone of the Annieopsquotch Complex, this was not proven conclusively by the geochronologic study (Chapter 7).

No quantitative analysis of chilling directions was

Figure 3.19. Sheeted diabase dykes. Early dykes are cut by narrow (.2 to .7 metre) dykes showing dark chilled margins. 79HPAD137.

undertaken in this study.

3.5.3.4 Variation in Dykes Across the Zone

The majority of dykes in the sheeted dyke zone are composed of tholeiitic diabase of N- type MORB affinity (see Chapter 5). Most are one half to three metres in width, however, there is a crude systematic variation in the width of dykes from northwest to southeast (base to top) across the zone.

Near the base of the zone dykes are one to ten metres wide. They vary in grain size from aphanitic to medium grained, from the margin to core of the dyke. In some dykes the margin is only fine grained, rather than aphanitic as is usual higher in the zone. The cores of these dykes are locally as coarse grained as the gabbro in the gabbro zone so that some areas are difficult to interpret unless there is continuous outcrop from the core to chilled margin of a dyke.

Through most of the sheeted dyke zone, dykes have aphanitic chilled margins and fine grained cores (Figure 3.21). Many chilled margins weather in relief as they are more resistant than the bulk of the dyke. Orthogonal sets of cooling fractures are clearly evident in many chilled margins, oriented at near right angles to the wall of the dyke. These margins are medium green on the weathered surface, which is usually about one centimetre thick, and dark green on the fresh surface. The weathered surface of diabase dykes varies from black green or grey green to

Figure 3.20. Narrow aphanitic diabase dykes, with quenched glassy raised chilled margins, cutting wider diabase dyke at the top of the sheeted dyke zone. 79HPAD105.

Figure 3.21. Three late brown- weathering diabase dykes splitting wide grey- green- weathering diabase dyke. 79HPAD107.

medium green. A few dykes have a brown green surface (Figure 3.21). The colour on the fresh surface varies with grain size, being black green for aphanitic samples and progressively lighter with increasing grain size.

At the top of the sheeted dyke zone the diabase dykes are narrower, therefore more numerous per unit area, and are finer grained (Figure 3.20). This is because of bifurcation of dykes as they followed the more numerous fractures and were quickly chilled near the sea floor.

This variation in average width of the diabase dykes through the sheeted dyke zone from base to top is significant in view of the methods used by Kidd and Cann (1974) to estimate dyke width variation in ophiolites. Clearly the average dyke width would vary with the level of the section measured.

Some dykes bend over to cut vertical dykes at a high angle. Dykes split into as many as five dykes as narrow as two centimetres. One dyke appears, in continuous outcrop, to pass into pillow lava. It first develops curved chilled zones which project into the mass of the dyke from the vertical chilled margin. Above this other curved chilled zones cut further into the dyke until at a higher level they join from both margins to separate a mass of basaltic material with the form of a pillow trapped between two diabase dykes.

3.5.3.5 Rock Descriptions

Most diabase dykes are fine grained and massive and are composed of near equal amounts of plagioclase and clinopyroxene in a sub-ophitic texture. In the coarsest or freshest samples this texture can be seen with the naked eye.

Some dykes contain either lithic fragments, or plagioclase or pyroxene phenocrysts. Plagioclase phenocrysts are the most common and vary in size between one millimetre in chilled margins and one centimetre in the cores of the dykes. Rare single plagioclase crystals up to two centimetres long occur but they might be grains entrained from the underlying magma chamber during intrusion.

Clinopyroxene phenocrysts are rare but in one dyke they occur in spectacular fashion with hundreds per square metre of area of the dyke. Clinopyroxene phenocrysts occur sporadically in diabase dykes throughout the zone.

Lithic fragments are abundant in a few dykes (Figure 3.22) and commonly they are aggregates of coarse grained plagioclase and clinopyroxene, and their alteration products, all typical of the underlying gabbro zone. In some cases, individual coarse grains of plagioclase and clinopyroxene in the dykes appear to be disaggregated lithic fragments. However, since gabbro and dyke phenocryst mineralogy are essentially the same it is not possible to determine the origin of single grains. In this study it has been assumed that euhedral to subhedral

Figure 3.22. Dyke containing thousands of lithic fragments, with sharp chilled margins, split by 0.4 metre wide aphanitic diabase dyke. 81HPAD037.

Figure 3.23. Brecciated dyke with angular to rounded fragments of diabase in a matrix of fine grained diabase. Dyke has planar chilled margins. 80HPAD197.

plagioclase of similar grain size, occurring in abundance in a diabase dyke, are (intratelluric) phenocrysts and not xenocrysts brought up from the walls of the magma chamber.

It was earlier reported, based on hand specimen identification, that diabase dykes of the Annieopsquotch Complex rarely contained olivine phenocrysts (Dunning and Herd, 1981). Petrographic examination has failed to confirm this identification.

In several dykes, spherical sulphide globules occur. They make up about one percent of the volume of one dyke.

Two brecciated dykes were noted in the sheeted dyke zone. They both occur near the east end of Dyke Pond and are composed of subangular fragments of diabase in a matrix of fine grained diabase (Figure 3.23). These dykes have regular planar margins composed of chilled diabase which is continuous with the matrix. Williams and Malpas (1972) described similar breccia dykes that they estimated cover an area of sixty- four square km. on North Arm Mountain. Because of the apparent syn- emplacement time of fragmentation and the confinement of fragmentation only to certain dykes and largely to the sheeted dyke zone they suggested that these dykes originated by gas brecciation. Recently Rosencrantz (1983) has remapped these rocks on North Arm Mountain. He suggests that they represent fault breccias rather than dykes. This is incompatible with the angular fragments and lack of deformation noted by Williams and Malpas (1972) so perhaps more than one type of brecciated rock is present. The dykes noted in the

Annieopsquotch Complex are interpreted to have formed by gas brecciation.

3.5.4 Massive Diabase

A large area of fine grained diabase occurs at the east end of the ophiolite within the sheeted dyke zone. No chilled contacts were observed and this body appears to be fine grained throughout. It is a discrete diabase intrusion within the sheeted dyke zone.

Similar bodies occur on North Arm Mountain where they are interpreted by Rosencrantz (1983) to be large lensoid bodies plated to and partly intruding the sheeted dykes above. However, he could not map out their vertical shape accurately.

3.5.5 Field Description of Trondhjemite Dykes

Only a few trondhjemite dykes have been noted in the sheeted dyke zone. Several more occur in the gabbro zone, where they intrude a short distance beyond their source in small trondhjemite pods (Figure 3.16).

Most trondhjemite dykes in the sheeted dyke zone occur on the ridge northeast of Loon Echo Pond. They are closely spaced and likely have a common source in a trondhjemite body in the gabbro zone to the north. They are bright white, almost chalky on the weathered surface and buff to medium grey on the fresh surface.

The dykes are fine to medium grained and have chilled margins only slightly finer grained than the bulk of the

dyke. They are composed of plagioclase and quartz. Epidote and rare minor hornblende are the only other minerals recognizable in the field.

3.6 PILLOW LAVA ZONE

3.6.1 Distribution and Contacts

The pillow lava zone underlies the southeast edge of the Annieopsquotch Mountains and part of the tree covered slope which descends to the northwest shore of Victoria Lake (Map 1, Figure 3.1, unit 6). The contact between the Annieopsquotch Complex and the Victoria Lake Group is nowhere exposed and is interpreted to be a fault. At Wigwam Brook, centimetre scale bedded siliceous argillites occur at the structural base of a sequence of waterlain tuffaceous sediments of the Victoria Lake Group. The argillites occur in open folds overturned toward the ophiolite. These are separated from mafic lavas of the Annieopsquotch Complex by a valley with a ten metre gap in exposure. This valley is interpreted to be a fault zone.

The contact with the sheeted dyke zone is placed at the first occurrence of screens of pillow lava in the dykes. The base of the pillow lava zone is therefore composed primarily of diabase dykes, some of which are probably feeders to lava flows higher in the sequence. Throughout the zone, northwest of the prominent northeast trending faults, the proportions of diabase dykes and

pillow lava are approximately equal.

The base of the pillow lava zone, to the northwest, is offset by several faults. One of these can be traced through the sheeted dyke zone and into the gabbro zone at Dyke Pond (Map 1). North of Canoe Scrape Lake the contact between the pillow lava and sheeted dyke zones is inferred in a forested area of no outcrop. At the northeast end of the ophiolite the boundary between the two zones is faulted. This fault is marked by a northwest facing ridge with ten to twenty metres of relief. At the southwest end of the ophiolite the pillow lava zone is unconformably overlain by basal boulder conglomerate of the early Silurian terrestrial sedimentary sequence.

At the southern edge of the zone, east of the sedimentary rocks, the lavas are cut by an olivine gabbro sill. This appears to occur right at the top of the Annieopsquotch Complex but its age and chemical affinities are unknown.

A porphyritic sill of approximately dacitic composition cuts the pillow lava zone at the southwest end of the ophiolite. It is chemically similar to dacite bombs in agglomerate of the Victoria Lake Group in Henry Waters, Victoria Lake. For this reason it is correlated with this Group and considered to be a post-ophiolite intrusion of Llanvirnian to Llandeilian age. This intrusion provides a link between the Annieopsquotch Complex and Victoria Lake Group in early Ordovician time. The Victoria Lake Group may represent the original ophiolite-conformable cover,

however the present contact is faulted.

The pillow lava zone is cut by a large hornblende and biotite bearing granodiorite to granite (described in Chapter 2) which forms a coarse intrusion breccia at its northwest margin.

Faults cutting the zone might have removed part of the sequence and repeated the stratigraphy locally. A ridge composed in part of sheeted dykes occurs along one fault and vertically dipping terrestrial sedimentary rocks occur in slices along another (Map 1, unit 10).

3.6.2 Field Description

Pillows are round to elongate in cross section and vary from 0.2 to 1 metre in maximum dimension. Their orientations do not indicate an obvious top direction. They are dark green, grey green to medium green or brown on the weathered surface and dark to grey green on the fresh surface. Many have distinct raised chilled margins, and cut by short cooling fractures as are the diabase dykes (Figure 3.24). Neither vesicles nor amygdules were observed in the pillow lava in the field; small holes in some pillows are due to the recessive weathering of plagioclase phenocrysts. About ten percent of the pillows are plagioclase porphyritic. No other phenocryst phases were observed.

Pillows in the southeast, faulted part of the zone are cleaved along their margins and near faults are stretched and penetratively cleaved. In the fault zone they are

Figure 3.24. Undeformed closely packed basaltic pillow lava cut by diabase dyke (at left). The pillows have 1 to 2 centimetre raised dark chilled rims and are aphanitic. 79HPAD106.

reduced to chlorite schist with nebulous light brown patches, interpreted to be remains of less competent basaltic interpillow material (Figure 3.25). Floating within the chlorite schist locally are curved rafts of red chert, original interpillow material that has escaped the deformation due to its greater competence.

Interpillow material is either basaltic lava, hyaloclastite or chert. At the base of the zone there is a considerable space between some pillows that is filled with aphanitic basaltic material. Elsewhere, at the same level, the pillows are moulded together and little or no interpillow material is present.

Hyaloclastite occurs as interpillow material locally in patches up to about one metre in width.

Chert, usually red but rarely grading to white, occurs rarely in pillow interstices where it has a cuspate outline partially wrapping around pillows. Samples of this chert were examined for microfossils but without success. It is the distinctive shape of this interpillow chert, preserved as rafts in chlorite schist, that allows one to identify the protolith of the schist as pillow lava.

Pillow breccia is rare in the Annieopsquotch Complex. Only one location was noted, south of Loon Echo Pond, where it occupies an area of approximately twenty square metres surrounded by pillow lava. The fragments in the breccia are rounded to angular and range from one to twenty centimetres wide.

Dykes and sills of diabase cut the pillow lava zone.

Figure 3.25. Chlorite schist along fault cutting pillow lava zone, southeast part of Annieopsquotch Complex. 79HPAD107.

Diabase dykes comprise the majority of the basal part of the pillow lava zone. They have all the characteristics of diabase dykes of the sheeted dyke zone. They decrease in number with increasing height and are scarce to the southeast of the northeast trending faults. This may indicate that the fault cuts out part of the pillow lava sequence.

Diabase sills cut the pillow lava and comprise approximately twenty percent of the section between the two major northeast trending faults. They are 0.5 to 2 metres thick and dark green to black on the weathered and fresh surface. They strike northeast and dip approximately 85 degrees southeast to 85 degrees northwest.

CHAPTER 4 PETROLOGY OF THE ANNIEOPSQUOTCH COMPLEX

4.1 INTRODUCTION

The mineral assemblages of rocks of the Annieopsquotch Complex result from the effects of two main processes; high temperature igneous crystallization with local metamorphism, and sea floor hydrothermal alteration and metamorphism over a range of temperatures varying with position in the ophiolite stratigraphy. The only post-emplacement effects on the rocks of the Annieopsquotch Complex are contact metamorphism around the diorite intrusion, weathering on the sub- Silurian unconformity and recent post glacial surficial alteration. In the following sections the petrology is discussed separately for each zone.

4.2 THE CRITICAL ZONE

Olivine- plagioclase- clinopyroxene cumulates and meta- cumulates vary in composition from mafic troctolite to leucotroctolite, olivine gabbro to leucogabbro and anorthosite. No pyroxenite layers are present in the Annieopsquotch Complex, however a large area of clinopyroxenite occurs with gabbro in an ophiolitic fragment south of Star Lake (Chapter 2).

The rocks are composed of varying proportions of olivine, plagioclase and clinopyroxene as the major phases. Each occurs with a euhedral to subhedral habit in some rocks (Figure 4.1, 2, 3). However, clinopyroxene usually occurs as angular anhedral grains partially or completely enclosing subhedral olivine or plagioclase. Oikocrysts of clinopyroxene, up to five cm long are common in some layers in the critical zone (Figure 4.3).

In troctolite and olivine gabbro some layers have a preferred orientation of prismatic minerals which is interpreted to be a high temperature foliation rather than a primary igneous lamination. Olivine (with alteration patches of serpentine and magnetite) occurs as anhedral elongate clots that are oriented parallel to layering (Figure 4.4). This is interpreted to be a result of high temperature ductile deformation of the rock and is perhaps related to the tectonic fabric in ophiolitic harzburgites (Girardeau and Nicolas, 1981 and T.J. Calon, pers. comm.,1983) In many rocks, clinopyroxene shows a preferred orientation and sharp grain boundaries with plagioclase. In some layers green chrome bearing clinopyroxene occurs as oikocrysts enclosing many smaller grains of plagioclase and olivine. These do not show a preferred orientation and appear to have overgrown the enclosed grains in a static environment.

Olivine in the critical zone rocks is anhedral and fresh to completely altered to assemblages of serpentine and magnetite or colourless amphibole. All olivine

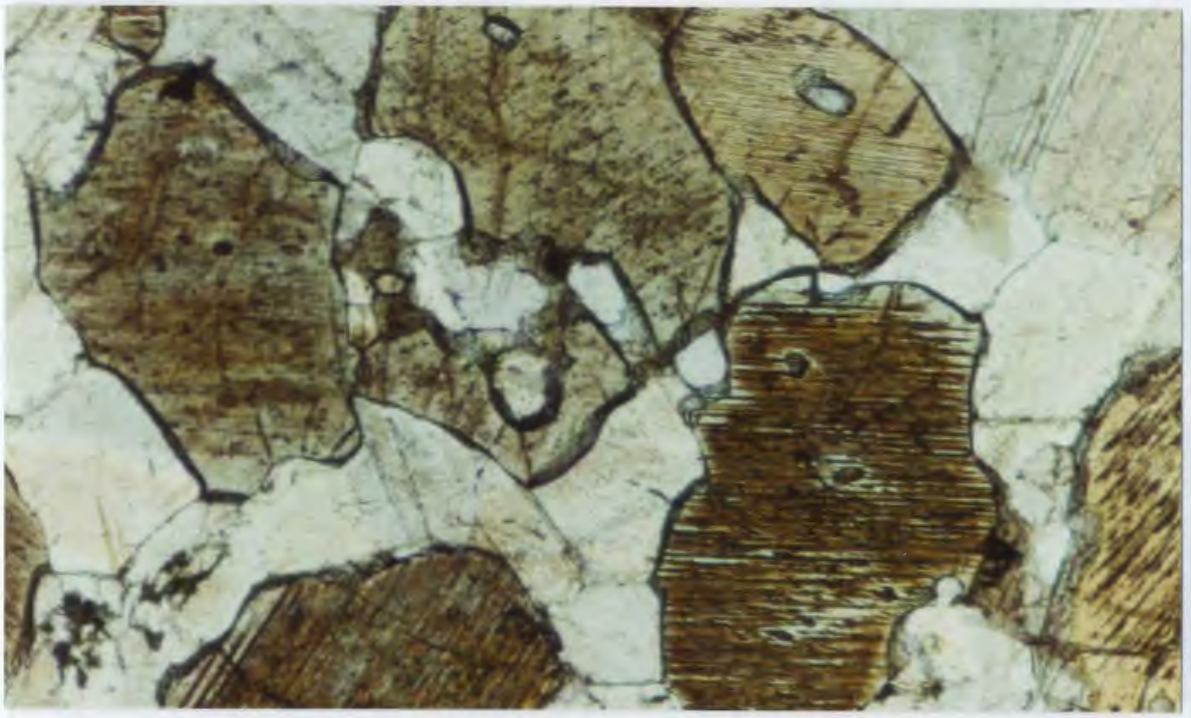

Figure 4.1. Gabbro showing plagioclase and clinopyroxene crystals of an adcumulate layer. Small plagioclase grains enclosed in clinopyroxene. 79HPAD032-3. Plane polarized light. Width = 4 mm.

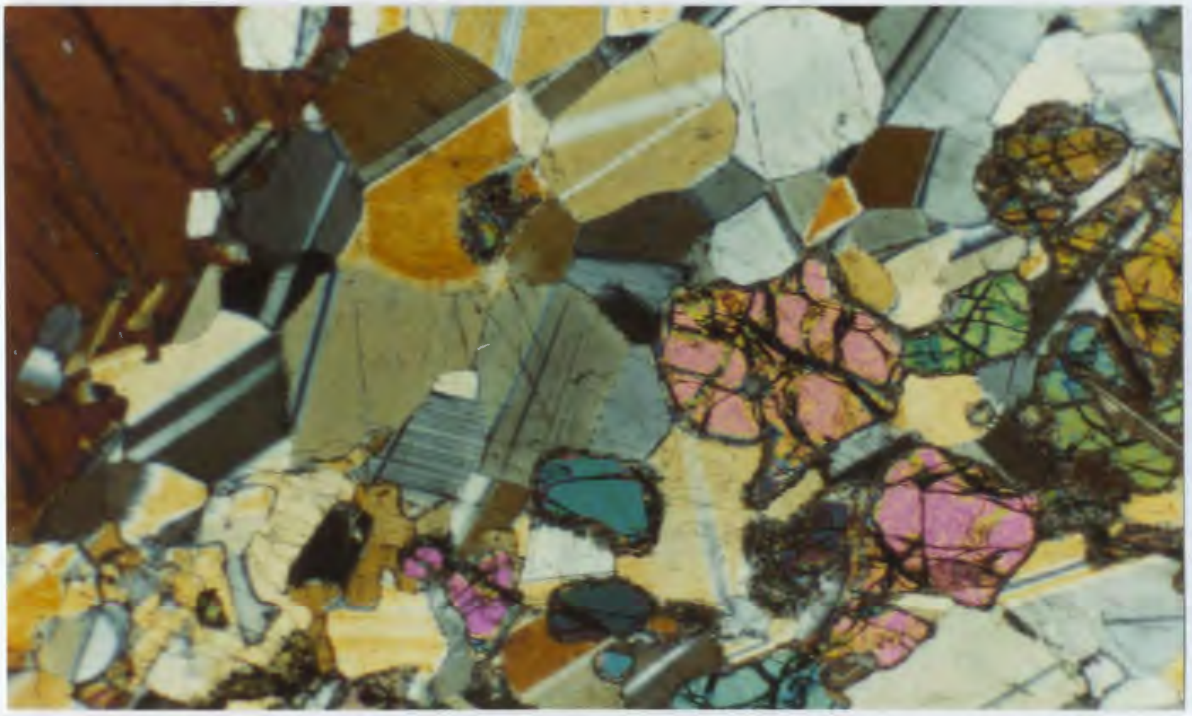

Figure 4.2. Olivine gabbro layer showing equant, subhedral cumulus olivine, cut by veins of serpentine + magnetite, plagioclase with smooth grain margins and triple junctions and oikocryst of Cr-diopside (brown - at left) enclosing small plagioclase grains. 79HPAD263-3. Crossed polars. Width= 4 mm.

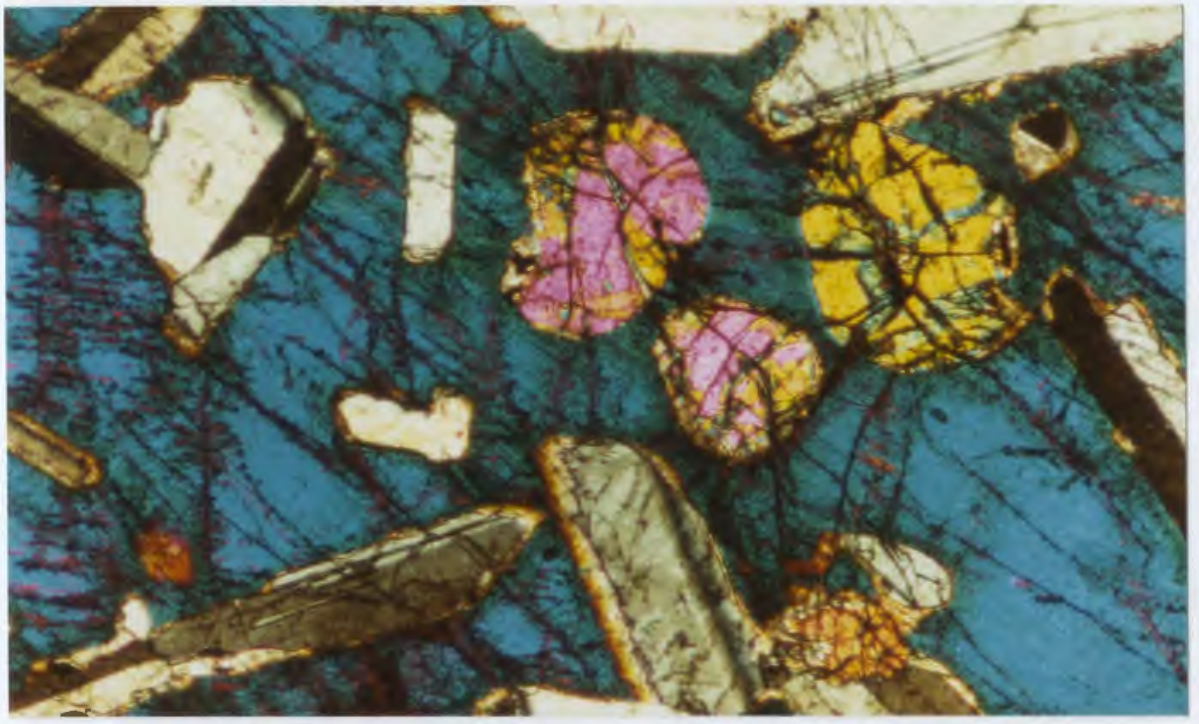

Figure 4.3. Troctolite sill with subhedral `cumulus` olivine and plagioclase grains enclosed in a large Cr - diopside oikocryst (blue). 80HPAD133-5. Crossed polars. Width = 2 mm.

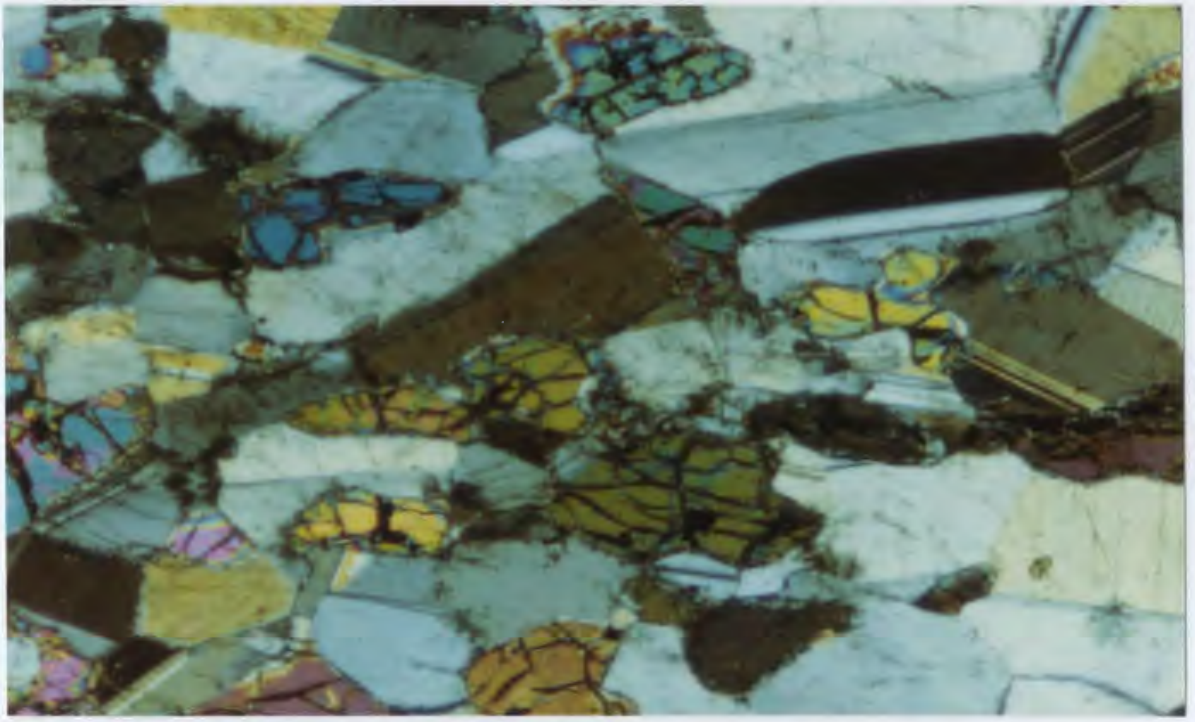

Figure 4.4. Troctolite with oriented elongate anhedral olivine with plagioclase. 79HPAD263-4. Crossed polars. 2 mm.

analysed in this study has compositions in the range Fo76 to Fo86.

Plagioclase in the critical zone, is subhedral to anhedral and coarse to medium grained. The least recrystallized anorthosites and gabbros show classic cumulate and adcumulate textures (Figure 4.5). Euhedral small plagioclase crystals are preserved only within clinopyroxene oikocrysts (Figure 4.3). Albite twins are common and in the recrystallized rocks metamorphic textures, especially polygonalized grains with triple junctions are present. Some recrystallized anorthosite layers have a granular texture.

Minor amounts of orthopyroxene occur as exsolved blebs within or anhedral grains adjacent to large clinopyroxene grains.

Brown amphibole also occurs as narrow anhedral grains which form partial rims around olivine or clinopyroxene (Figure 4.6). This brown amphibole is distinct from both the amphibole in the coronas and that in the alteration patches after clinopyroxene. Therefore, three different types of amphibole are present in the critical zone and it is interpreted that they formed in three different ways.

Chlorite and epidote occur as fine grained alteration products after clinopyroxene and plagioclase. They form irregular patches embaying both minerals.

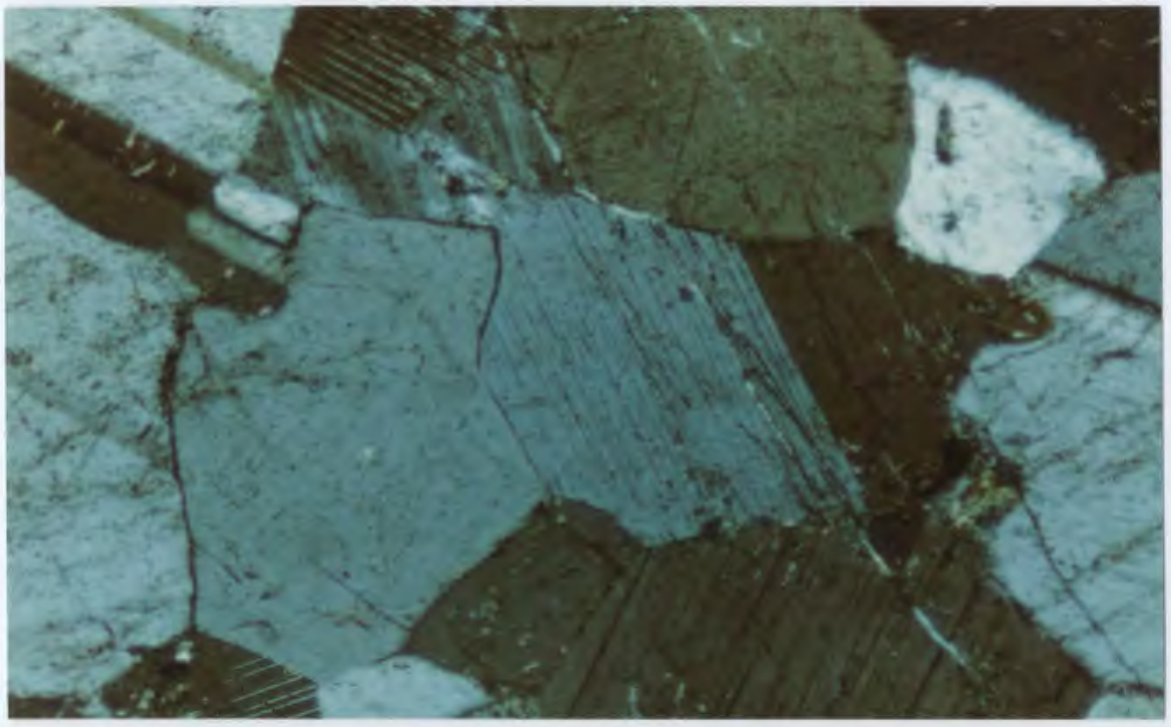

Figure 4.5. Anorthosite with coarse to medium grained plagioclase showing adcumulate texture with smooth grain boundaries and triple junctions. 79HPAD265-4. Plane polars. 2 mm.

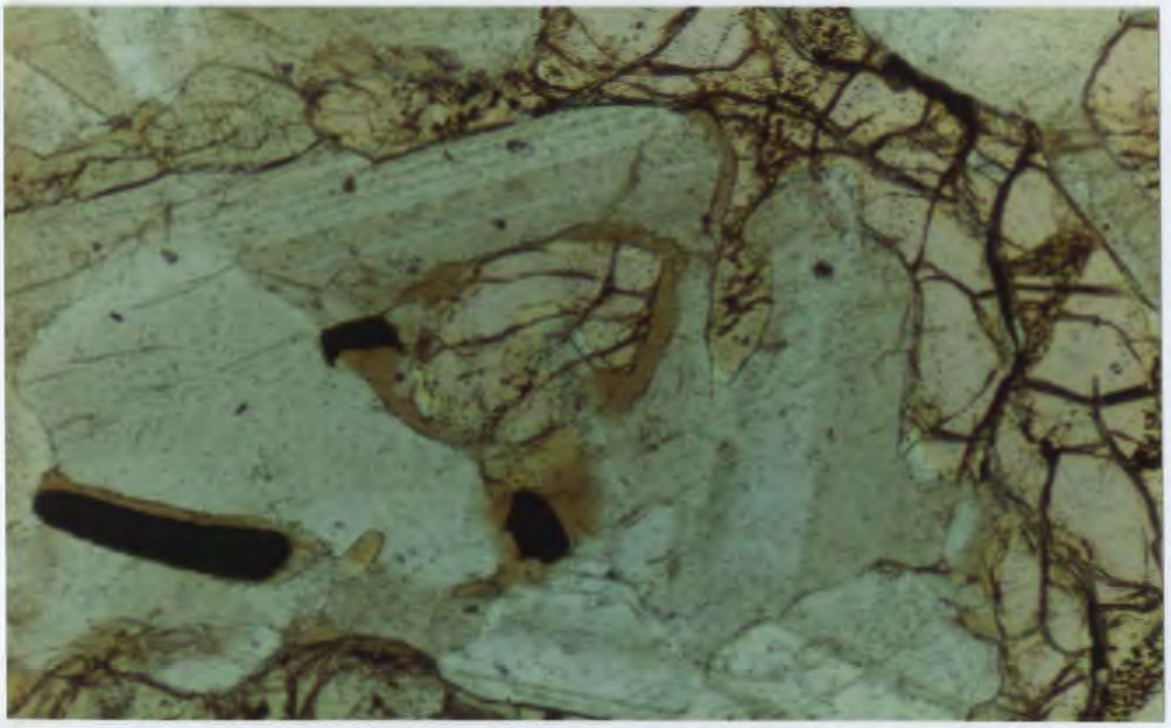

Figure 4.6. Troctolite sill showing olivine, plagioclase, clinopyroxene (upper left), oxide and brown amphibole as partial rims on olivine and oxide. 80HPAD133-5. Plane polars. 1 mm.

4.2.1 Corona Structures

Reaction coronas commonly occur between olivine and plagioclase in the critical zone. They are composed of concentric zones from the relict olivine cores to plagioclase (Figure 4.7) which usually involve; 1.orthopyroxene, a colourless amphibole (probably cummingtonite) and green spinel, 2.pale green amphibole of the tremolite-actinolite series and 3.a zone next to relict plagioclase that is a mixture of albite and an unidentified high relief mineral.

In some samples where only olivine pseudomorphs remain in the core of the coronas, the entire pseudomorph is composed of orthopyroxene and colourless amphibole, the same as the innermost zone of the coronas elsewhere. A polygonal recrystallized texture is common in these orthopyroxene and amphibole cores.

4.2.2 Mafic Granulites

These rocks occur within the critical zone and the gabbro zone and grade into normal coarse grained gabbro. They are fine to medium grained and in thin section have an equigranular texture with polygonal grains of plagioclase, orthopyroxene, clinopyroxene with minor olivine (Figure 4.8). Crosscutting veinlets contain a bright green amphibole and green amphibole poikiloblasts overgrow the other minerals in some samples.

A noticeable feature of these rocks is the presence of abundant magnetite distributed as small grains throughout

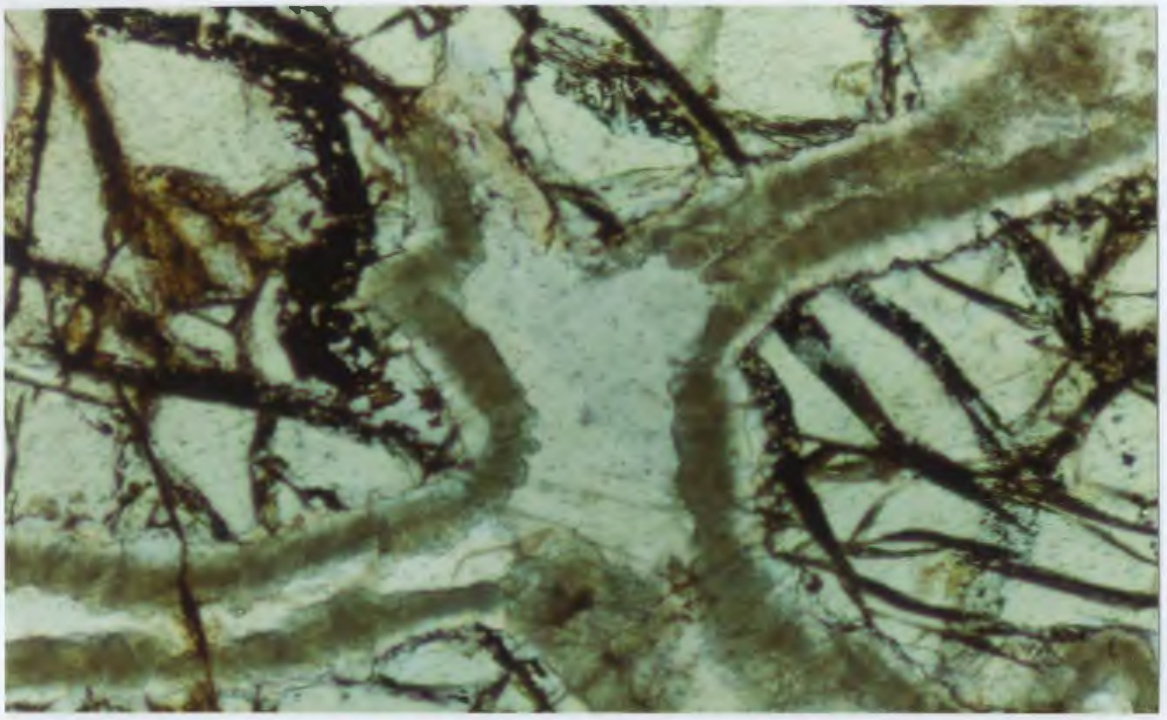

Figure 4.7. Corona texture in troctolite. Coronas separate olivine and plagioclase grains and show concentric zonation. 79HPAD269-3. Plane polars. 1 mm.

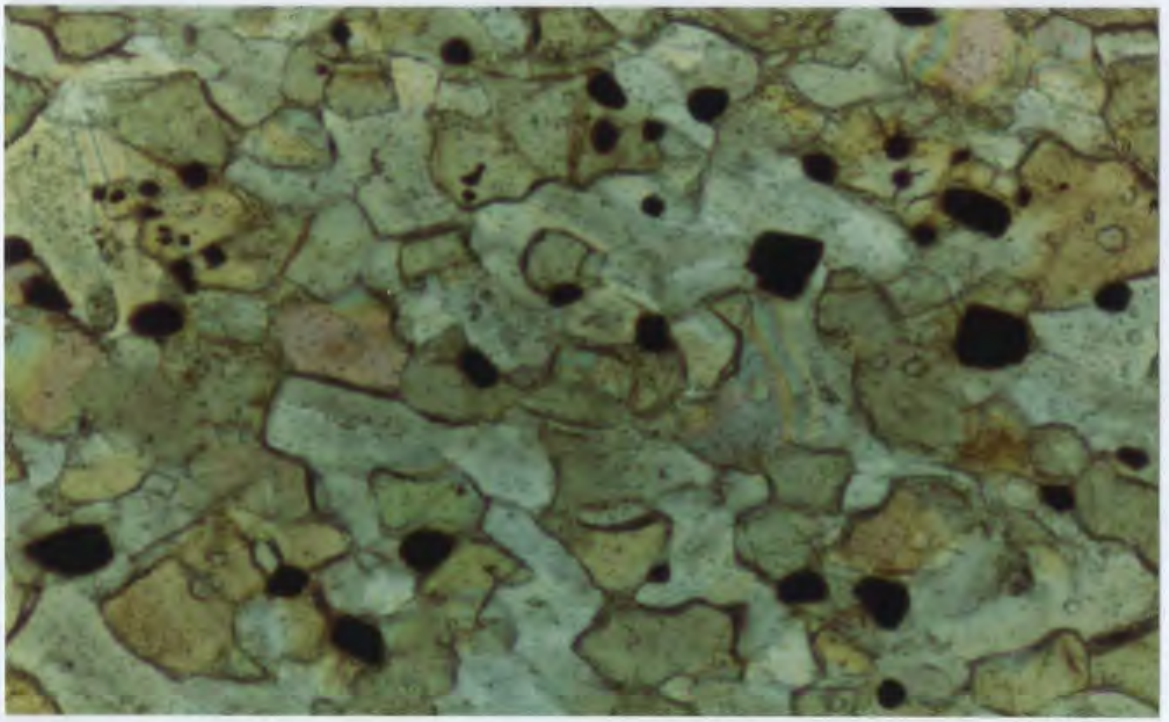

Figure 4.8. Mafic granulite with rounded equant orthopyroxene, clinopyroxene and plagioclase grains. Black grains are magnetite. Pyroxene geothermometry indicates minimum temperature of formation of about 1000 degrees C. 79HPAD153-1. Plane polars. 1 mm.

the rock. In some samples the oxide occurs as small spheres with rims of hematite. Olivine, moderately altered to serpentine and magnetite occurs as poikiloblasts in one sample. It is considerably more Fe-rich than olivine in adjacent rocks of the critical zone.

Clinopyroxene and orthopyroxene both occur as polygonal to rounded fresh grains, the latter often has the characteristic pleochroism of hypersthene. These two minerals in an apparent equilibrium assemblage indicate the achievment of temperatures of the granulite facies of metamorphism (Winkler, 1977). Calculated temperatures for seven orthopyroxene- clinopyroxene pairs, using the method of Wells (1977), range from 940 to 1050 degrees C.

These mafic rocks have clearly been metamorphosed under high temperature static conditions. They have been largely dehydrated, except for some amphibole as poikiloblasts and in crosscutting veinlets. They appear to grade into average coarse grained gabbro but contact relationships are nebulous. It is interpreted that these rocks are blocks of either gabbro or diabase stoped from the walls or roof of the magma chamber. Another possibility is that they represent an early crystallized part of a magma chamber that was subsequently held at high temperature due to the high geothermal gradient or adjacent intrusion of a new magma batch. The gradational contact might be due to; 1. a lessening of metamorphic effects away from the central part of the magma chamber or 2. reaction and recrystallization at the margin of a stoped

block.

4.3 GABBRO ZONE

The gabbro zone contains a wide variety of compositions and textural varieties of gabbro and amphibolite derived from gabbro as well as diabase, diorite and trondhjemite (Chapter 3). Alteration is variable and heterogeneous, even within small outcrop areas. Recrystallization and alteration vary with stratigraphic height in the zone.

Amphibolite high- temperature shear zones occur near the base of the zone whereas shear zones high in the zone contain the assemblage chlorite +/- actinolite +/- epidote +/- albite.

At the top of the zone the mafic alteration minerals are chlorite, actinolite and epidote. These minerals largely replace clinopyroxene and are interpreted to have formed as a result of hydrothermal alteration by seawater. At the base of the gabbro zone the same minerals occur but have a patchy distribution perhaps reflecting the more limited access of seawater to deeper levels of the crust. Commonly, coarse pleochroic hornblende ocuurs at this level and, combined with the assemblage in the shear zones, indicates the general establishment of conditions characteristic of the amphibolite facies.

4.3.1 Gabbro

Gabbro of the 'high level' or 'isotropic' type rarely contains olivine, in contrast to that of the critical zone. In addition it is generally coarser grained and more altered with clinopyroxene replaced by fibrous amphibole of the tremolite-actinolite series and chlorite. This imparts a medium green colour to the replaced pyroxene and thus to the whole rock (Figure 4.9).

Gabbros generally are composed of near equal proportions of plagioclase and clinopyroxene with minor amounts of primary oxides and apatite. Plagioclase is usually subhedral and zoned. It is partially enclosed in large anhedral clinopyroxene grains. In the finer grained gabbro the texture is subophitic; similar to the cores of some wide diabase dykes. Apatite, rarely present, occurs as small subhedral to oval grains interstitial to silicates.

Secondary minerals in the high level gabbro, in approximate order of abundance, are fibrous tremolite-actinolite, chlorite, albite, epidote group minerals, sericite, sphene, carbonate, prehnite and pumpellyite.

The secondary amphiboles replace clinopyroxene as pseudomorphs with their C axes parallel to those of the pyroxenes. Relict clinopyroxene occurs in the cores of some pseudomorphs. The amphiboles vary from near colourless or pale green to medium to dark green grains with a distinct pleochroism. Some blocky grains have a

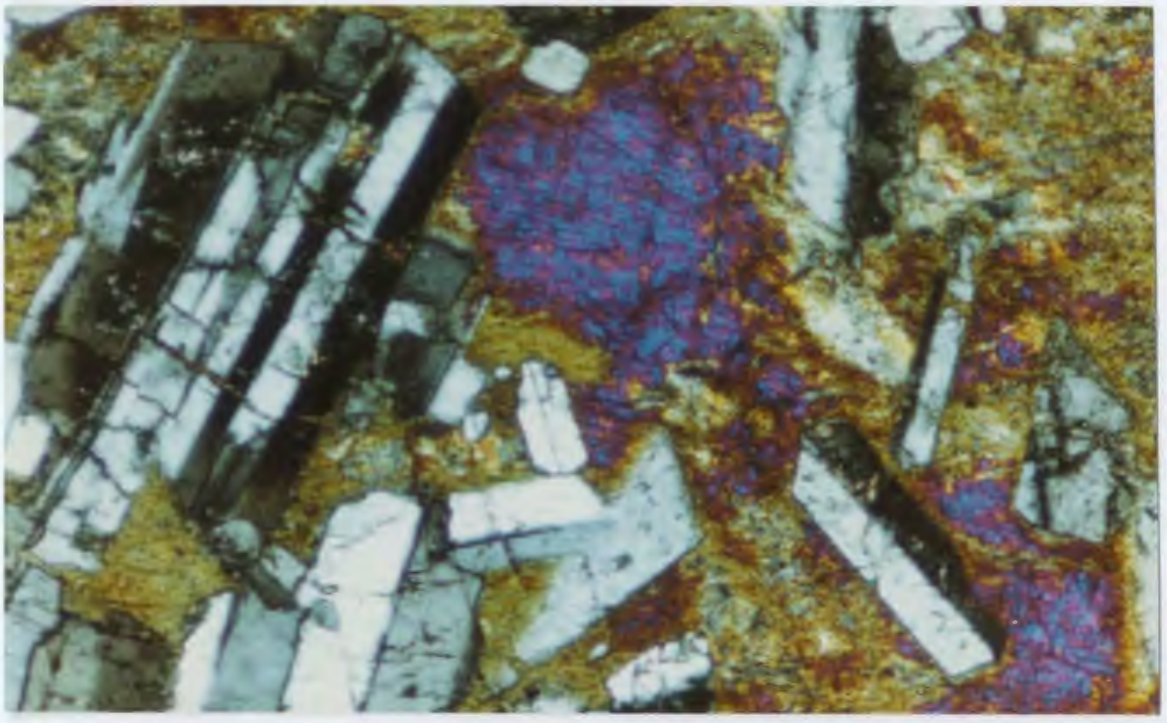

Figure 4.9. Gabbro with euhedral to subhedral plagioclase in fibrous actinolite (green) after clinopyroxene, which is preserved as ragged relicts (blue and orange). 79HPAD143. Crossed polars. 2 mm.

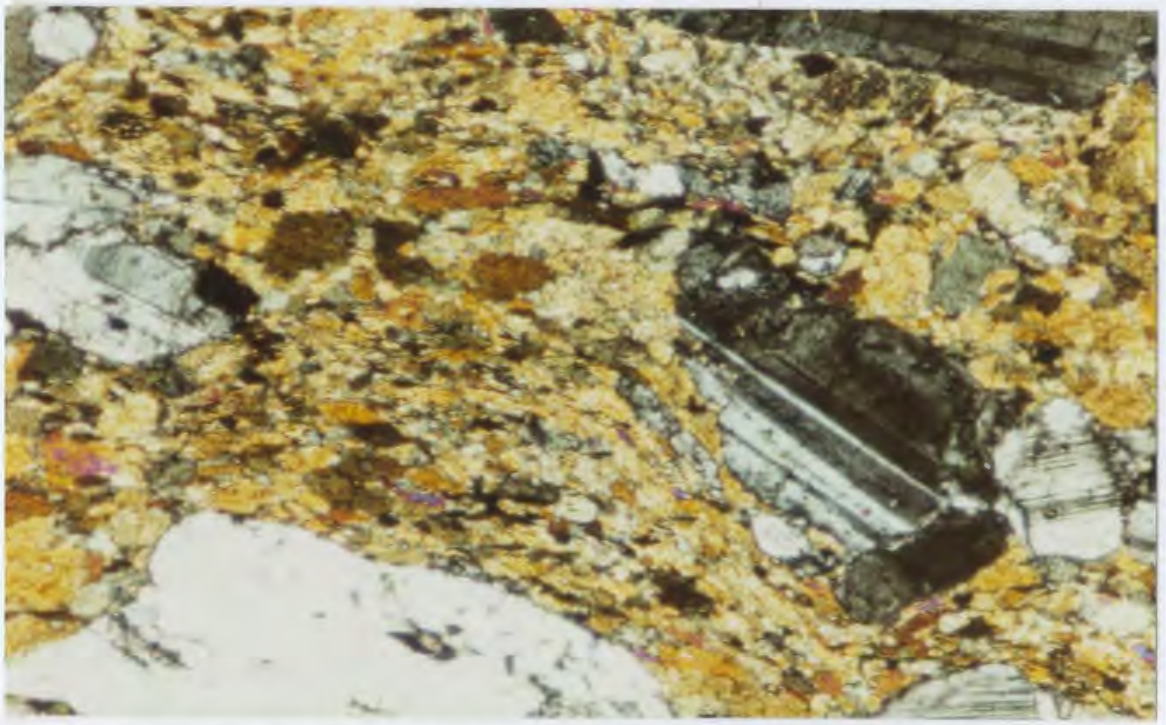

Figure 4.10. Amphibolite composed of near equal amounts of hornblende and plagioclase, and relict primary plagioclase grains which deflect the foliation. 78HPAD202-3. Crossed polars. 2 mm.

strong blue green colour.

Plagioclase grains are weakly to completely altered to a fine grained mixture of minerals that appears light to dark brown in plane polarized light and dark to opaque under crossed polars. This material is a mixture of albite, zoisite, carbonate and fine mica. In some sections with coarser (metamorphic) amphibole the cores of these alteration patches in plagioclase are recrystallized to polygonal mosaics of epidote.

The interstices between plagioclase and clinopyroxene in coarse grained gabbro is composed of a mixture of fine grained chlorite and amphibole of a different habit and colour than that in the pseudomorphs after clinopyroxene. These patches may represent trapped interstitial liquid.

4.3.2 Pegmatitic Pods

Pods and large irregular areas of pegmatitic gabbro occur sporadically throughout the gabbro zone. They are composed of plagioclase and clinopyroxene in near equal proportions with crystals varying from one to fifteen cm in length. Hornblende is abundant in some pods, as is magnetite, which occurs both as euhedral grains and as angular masses interstitial to the silicates. Apatite is abundant in some pods, consistent with the residual nature of the magma forming the pods. No fresh pyroxene was identified in these pegmatitic gabbro pods and epidotization is common.

Textures are variable and heterogeneous within the

pods. Small clots of coarse hornblende or feldspar or quartz- epidote occur locally and large crystals grow radially from the walls of some pods. A core of trondhjemite is present in some pods. The most felsic pockets in these pegmatitic pods contain an intergrowth of feldspar, epidote and quartz with minor apatite and other accessories.

4.3.3 Amphibolite

Amphibolite, medium to coarse grained, occurs in narrow shear zones, especially in the lower part of the gabbro zone. It is composed of near equal proportions of hornblende and plagioclase and usually has a pronounced foliation parallel to the shear zone. Corroded coarse plagioclase grains occur locally (Figure 4.10). These are interpreted to be relict primary igneous crystals. No pyroxene has been identified in the amphibolite. Minor magnetite, epidote, chlorite and carbonate occur.

These amphibolites are interpreted to have formed by recrystallization of gabbro under stress in shear zones at temperatures characteristic of the amphibolite facies of metamorphism.

4.3.4 Trondhjemite and Diorite

Pods of trondhjemite with a marginal zone of diorite gradational into gabbro occur throughout the gabbro zone. They vary considerably from one pod to another and within one pod are commonly texturally and compositionally

heterogeneous.

In general the trondhjemites contain plagioclase, hornblende, quartz, epidote, sphene, apatite and zircon as primary phases and actinolite-tremolite, chlorite, albite, epidote, carbonate and prehnite as alteration minerals. However, models for the generation of trondhjemites in ophiolites call upon the presence of significant amounts of water, either inputed directly in to the magma chamber or, more reasonably, introduced by assimilation of hydrated mafic rock. The effects of fluids on the trondhjemites, including the formation of hydrous minerals, therefore may be late magmatic (deuteric).

Trondhjemite from the body intruded along the fault zone west of Loon Echo Pond (80HPAD222) is medium grained and contains some hornblende and quartz. Most of the body is an intergrowth of angular anhedral feldspar and epidote, with sprays of fibrous grains. Apatite, sphene and zircon are accessory phases; the latter was used to determine the age of the ophiolite (Chapter 7). The sample is cut by a vein of prehnite.

The large area of trondhjemite occurring as intrusion breccia, full of mafic blocks, north of Loon Echo Pond (Figure 3.b) is texturally and compositionally heterogeneous. Most is coarse grained with only a minor mafic mineral content. Sample 80HPAD223-1 (Figure 4.11) is from a pegmatitic trondhjemite pod which contains ten to fifteen percent hornblende, as subhedral crystals up to fifteen cm long. They are twinned and some contain a core

Figure 4.11. Trondhjemite, coarse grained with coarse hornblende (pale green - upper right) and strongly zoned plagioclase, both with ragged margins in groundmass of fine grained anhedral quartz and feldspar. Zircon is euhedral (pink) grain at right. 80HPAD223-1. Crossed polars. 2 mm.

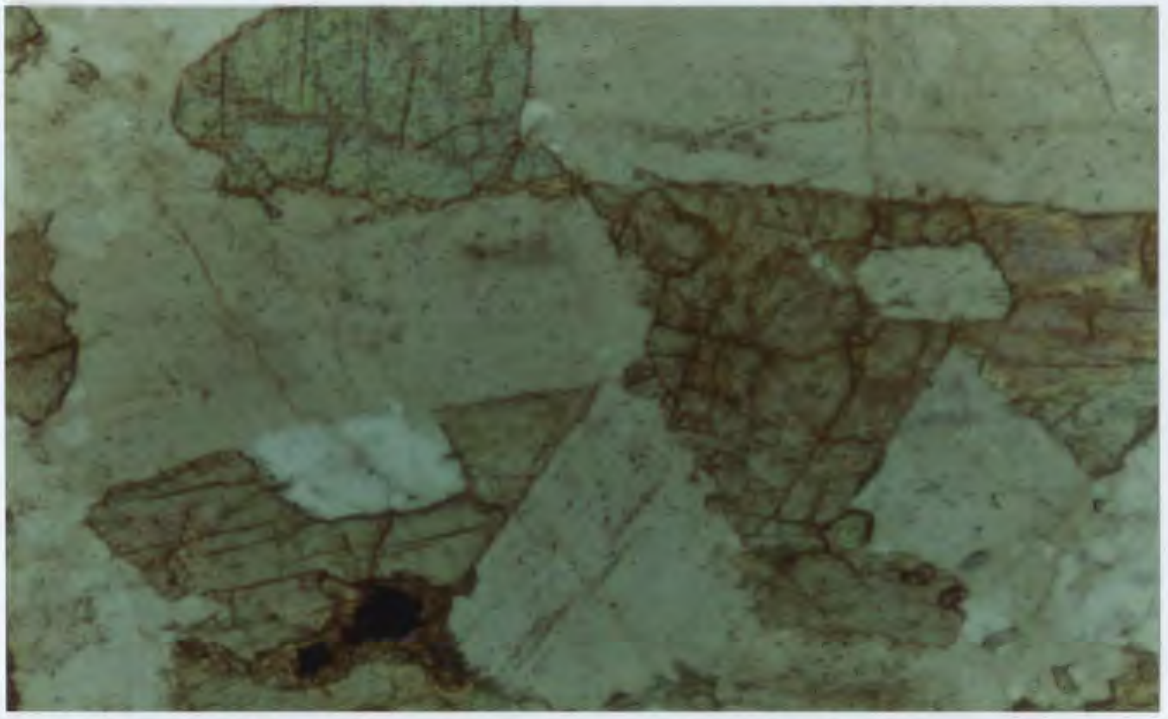

Figure 4.12. Trondhjemite, medium grained, composed of subhedral feldspar and primary epidote in an intersertal texture. Sample contains abundant oxide, rimmed by sphene. 79HPAD212-2. Plane polars. 2 mm.

of biotite. Quartz clots up to twenty-five cm in diameter occur in the pod. Coarse plagioclase grains are subhedral and strongly zoned and are surrounded by a groundmass of fine grained granular feldspar and quartz. Accessory phases are biotite, epidote, apatite and zircon.

A trondhjemite pod occurs at the gabbro:sheeted dyke zone boundary northeast of Loon Echo Pond. It is remarkable for its content of coarse fresh epidote intergrown with plagioclase of equal grain size (Figure 4.12). Quartz is a minor constituent of this sample (79HPAD212) along with sphene and zircon, which both commonly occur with epidote. The rock is undeformed and is a good candidate to be a primary unaltered, trondhjemite.

Several trondhjemite dykes occur in the gabbro and sheeted dyke zones and some of them are seen to be rooted in the trondhjemite pods (Figure 3.16). They are fine grained and consist of either an intergrowth of feldspar, quartz and epidote or spherical radiating clusters of feldspar (albite?) grains. One dyke appears to have tiny vugs between feldspar crystals filled with quartz and epidote needles. This suggests that the latter two minerals crystallized from a volatile rich residual liquid. Minor amounts of tremolite-actinolite occur but minor accessories such as sphene, apatite and zircon, which are common in the pods were not observed in the dykes.

Diorite of the Annieopsquotch Complex is restricted to small areas gradational between gabbro and trondhjemite of the pods. It does not include the diorite intrusion at the

northeast end of the Mountains (Chapter 2). The diorite is really a hornblende rich variety of the trondhjemite with subordinate clinopyroxene and less quartz. It contains sphene and some zircon.

4.3.5 Diabase

Diabase occurs as dykes cutting the gabbro zone and as irregular patches in the transition zone. These are similar to diabase of the sheeted dyke zone and so will not be discussed separately.

4.4 SHEETED DYKE ZONE

Diabase is the only major lithology of the sheeted dyke zone. It occurs in dykes, a few of which are internally brecciated, and as a large mass which is interpreted (Chapter 3) to be an intrusion into the zone.

4.4.1 Diabase Dykes

The diabase dykes of the sheeted dyke zone are remarkably constant in mineralogy, having near equal proportions of plagioclase and clinopyroxene, or their respective alteration products.

The groundmass of the dykes varies with grain size. The cores are composed of blocky equant clinopyroxene grains intergrown with plagioclase laths. Some large clinopyroxene grains enclose plagioclase in a subophitic

texture. In some finer grained dyke rock, very fine grains of clinopyroxene occur as cores of felted amphibole which is of similar grain size to the plagioclase laths. Most diabase dykes have fibrous actinolite as the sole mafic mineral.

In the chilled margins of diabase dykes plagioclase microlites occur in a very fine grained matrix now composed of felted chlorite and actinolite. Groundmass microlites and microphenocrysts show quench textures such as swallow tails and belt buckles (Figure 4.13). These fine plagioclase grains are oriented parallel to the walls of some dykes. Rarely they define a lineation but usually they are randomly oriented about a plane parallel to the margin. Coarse plagioclase phenocrysts in the centre of the dykes generally appear to be randomly oriented. Many dykes have corroded plagioclase laths as the only relicts of the primary mineralogy, the rest of the dyke is generally composed of actinolite and magnetite with minor epidote.

The only other phenocryst phases observed in diabase dykes of the sheeted dyke zone are clinopyroxene (Figure 4.14), commonly altered to actinolite, and rarely hornblende, as twinned subhedral grains similar in appearance to those in the trondhjemite pods. No olivine phenocrysts were observed.

Spherical sulphide globules up to three mm in diameter were noted in the chilled margins of some diabase dykes. These, being of apparent regular shape and composition may

Figure 4.13. Diabase dyke with matrix of fine grained plagioclase laths and felted amphibole. Quenched plagioclase phenocrysts show skeletal `belt buckle` outlines. 78HPAD179. Plane polars. 2 mm.

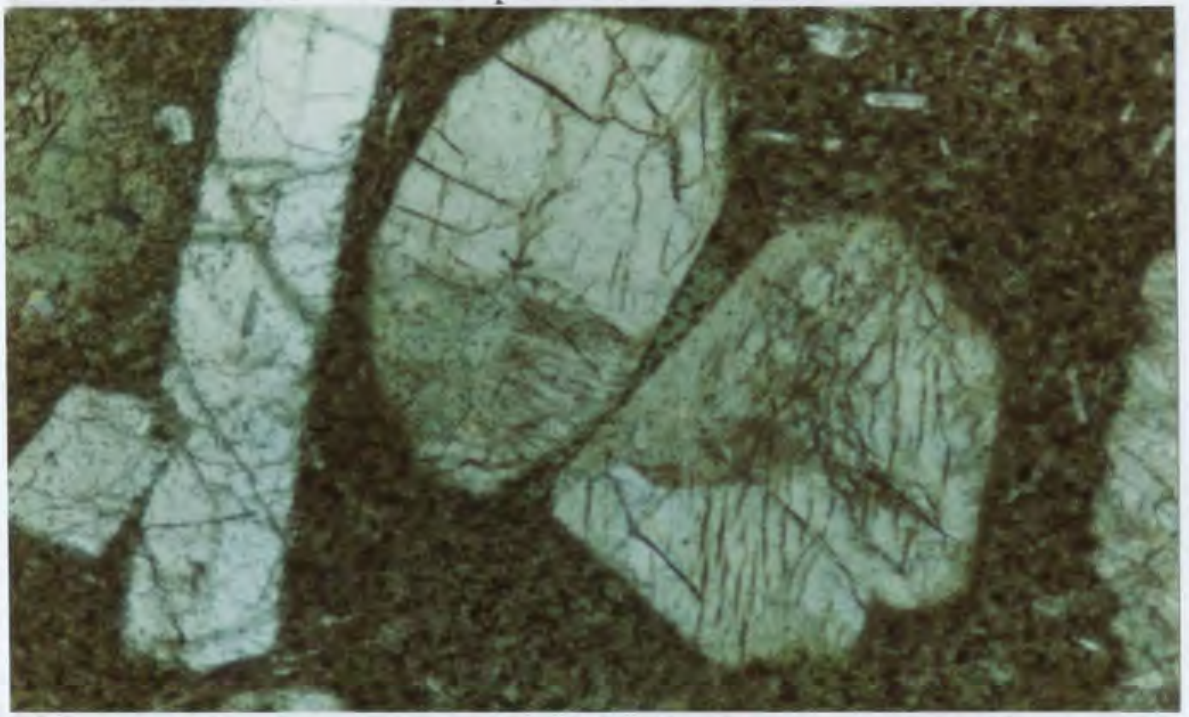

Figure 4.14. Same dyke as above with fine grained matrix and plagioclase and clinopyroxene phenocrysts. Clinopyroxene is partially altered to amphibole. 78HPAD179. Crossed polars. 2 mm.

represent monosulphide solid solution separated as an immiscible liquid from the basalt.

4.4.2 Brecciated Dykes

One diabase dyke contains amygdules filled with chlorite and epidote. The groundmass of the dyke is composed entirely of plagioclase and actinolite. This dyke (79HPAD200-1) is internally brecciated but has planar chilled margins like most dykes. The fragments in the brecciated portion of the dyke are angular to rounded and are of the same grain size and composition as the adjacent intact diabase. The matrix to the fragments is a mixture of chlorite and epidote that appears to be the same as that in the amygdules (Figure 4.15), though these were not analysed. Broken plagioclase crystals and small fragments of diabase occur in the chlorite- epidote matrix.

Williams and Malpas (1972) described dyke breccia from the Bay of Islands Complex which has similar features to that described above. They specifically noted angular to rounded fragments in a fine granular matrix which lacks a cleavage, concluding that they were not formed as a result of deformation but formed during dyke emplacement. Such an interpretation is favoured for the rare brecciated dykes of the Annieopsquotch Complex. A brecciated dyke containing amygdules suggests a high volatile content. It is possible that release of pressure on the magma during intrusion of the dyke to shallow levels permitted the evolution of a gas phase with sufficient force to disrupt the partially

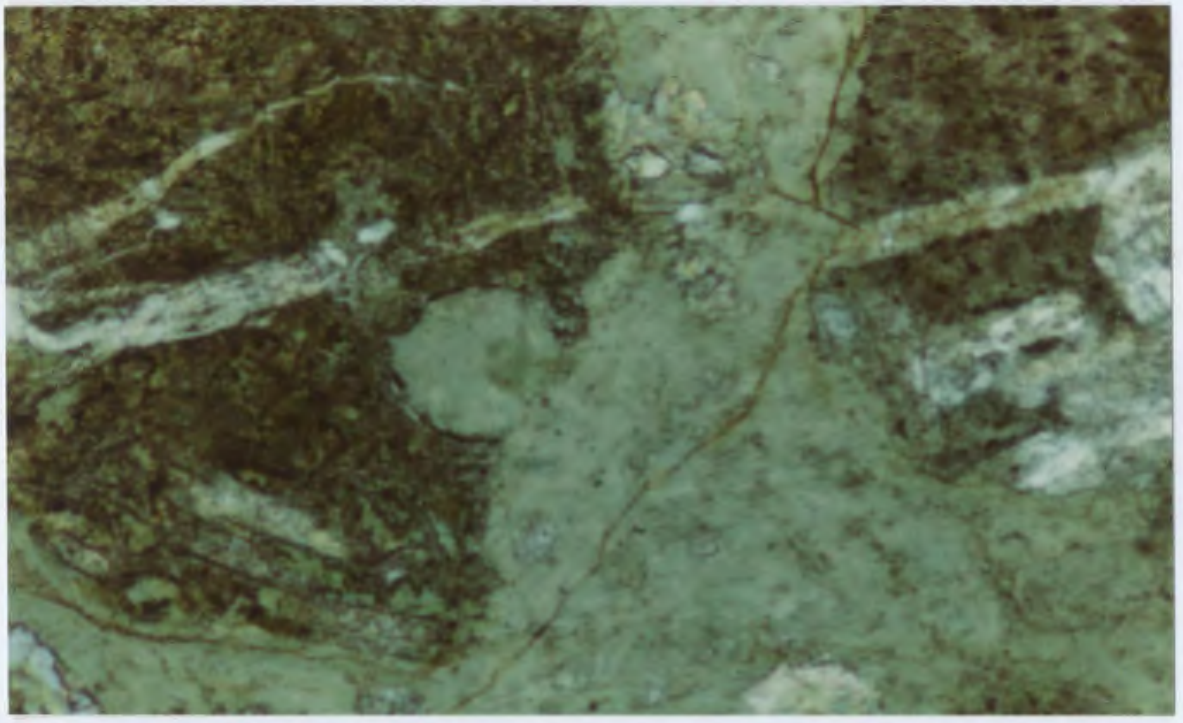

Figure 4.15. Brecciated dyke composed of angular to rounded fragments of fine grained, plagioclase porphyritic diabase (dark) in a matrix of chlorite + epidote (pale green). Spherical amygdules, this one broken into the matrix, also contain chlorite + epidote as does the veinlet cutting the fragment (upper right). 79HPAD200-1. Plane polars. 2 mm.

lithified core of the dyke. The chilled margins, formed first, would be unaffected and would form a conduit for the brecciation.

4.5 PILLOW LAVA ZONE

Pillows are fine grained in the core to aphanitic at the rim. The mineralogy of the rims is unresolvable with the petrographic microscope. Where not opaque, they are composed of cuspate fragments, dark brown or green, set in a matrix of dark brown or green material, presumably devitrified glass. In this matrix radial aggregates of fibrous pumpellyite were recognized in one sample.

No primary pyroxene was recognized; rather the cores of pillows are composed of a fine felted groundmass of relict plagioclase laths, actinolite and chlorite, similar to the chilled margins of the diabase dykes.

Plagioclase is the only phenocryst phase recognized in the pillow lavas. They are small equant to prismatic grains and occur less commonly than in the diabase dykes of the sheeted dyke zone.

The pillow lavas were described as non-vesicular by Dunning and Herd (1980) however very small chlorite and epidote filled amygdules were noted in several thin sections.

4.6 CLASSIFICATION OF MORB

Phenocryst assemblages have been used to define two types of MORB's by Shido et al.(1971) which they termed plagioclase tholeiite and olivine tholeiite.

In a recent classification Bryan (1983) divided MORB's into three groups, consistent with phase equilibria, based on their phenocryst assemblages. These are: 1. olivine- phyric basalts (+/- spinel), 2. olivine- plagioclase- phyric basalts and 3.olivine- plagioclase- pyroxene- phyric basalts. Appearance of phenocrysts is all that is required for this classification, not relative abundance.

Bryan (1983) suggested that many plagioclase tholeiites are type 2 or 3 multiply- saturated basalts that have undergone selective accumulation of plagioclase and that they might be found to contain at least rare microphenocrysts of olivine (+/- clinopyroxene). He further suggested that olivine and olivine- plagioclase- phyric basalts might contain few observable olivine phenocrysts due to their separation from the liquid, even in lava tubes or pillows on the seafloor. In any case, examination of a thirty micron thick section is probably not sufficient grounds for stating that a phenocryst is absent from a rock.

No olivine phenocrysts were observed in diabase dykes or pillow lava of the Annieopsquotch Complex. Plagioclase phenocrysts are virtually ubiquitous and occur in large quantities in some samples suggestive of crystal

accumulation in the magma before entrainment in the dykes.

Free clinopyroxene grains were noted in several dykes. Whether these are true phenocrysts or xenocrysts from the magma chamber is uncertain. As most diabase dykes and pillow lavas of the Annieopsquotch Complex contain plagioclase phenocrysts but no obvious clinopyroxene phenocrysts they likely are the olivine- plagioclase-phyric (group 2) basalts of Bryan (1983).

CHAPTER 5 GEOCHEMISTRY OF THE ANNIEOPSQUOTCH COMPLEX AND RELATED OPHIOLITIC FRAGMENTS

5.1 INTRODUCTION

Analyses were made of diabase dykes from the sheeted dyke zone of the Annieopsquotch Complex and the King George IV Lake and Shanadithit Brook ophiolitic fragments and from ophiolitic inclusions in the Boogie Lake Intrusion. Pillow lava from the Annieopsquotch Complex and the King George IV Lake fragment were also analysed.

Critical zone lithologies and 'high level' gabbro samples from the Annieopsquotch Complex and the Star Lake ophiolitic fragment were also analysed. These show evidence of crystal accumulation (Chapter 3) and do not represent liquid compositions.

Trondhjemites from several pods in the Annieopsquotch Complex were analysed.

All dyke and pillow lava samples are fine grained to aphanitic; weathered surfaces were removed with a saw and phenocryst- rich dykes were avoided. Some samples contain a few plagioclase phenocrysts. Most dyke samples are of chilled margins taken just inside the narrow 1 to 2 cm wide weathered rind. Therefore these samples are interpreted to represent liquid compositions.

Major elements were analysed at the Geological Survey of Canada by X-ray Fluorescence using fused pellets, except

for Na which was analysed by atomic absorption, and Fe2O3 and FeO which were determined by the Pratt titration method. Trace elements abundances were determined by X-ray fluorescence analysis of pressed pellets (10 grams of sample powder) and rare earth elements were analysed by the method of Fryer (1977) at Memorial University of Newfoundland. See Appendices 2,3 and 4 for details of the analytical methods.

Whole rock analyses are reported in Tables 5.1,2,3,4,5,6 and 8 and sample locations are shown on Maps 1 and 2. The ranges of major and trace element contents for each rock type are reported in Table 5.7 and CIPW norms for all rock analyses are reported in Appendix 7.

5.2 SAMPLES FROM THE CRITICAL ZONE

Three samples from a picritic sill of the Annieopsquotch Complex and three from the critical zone of the Star Lake ophiolitic fragment were analysed (Table 5.1). The rocks from the Annieopsquotch Complex are troctolites with abundant plagioclase, while those from Star Lake are part of a lensoid body that could be classified as plagioclase peridotite. Loss on ignition is higher for rocks of the Star Lake ophiolitic fragment due to the presence of serpentine after olivine. Olivine in the sill is very fresh by comparison.

Al2O3 varies between 7.2 and 7.6 wt. % for the Star

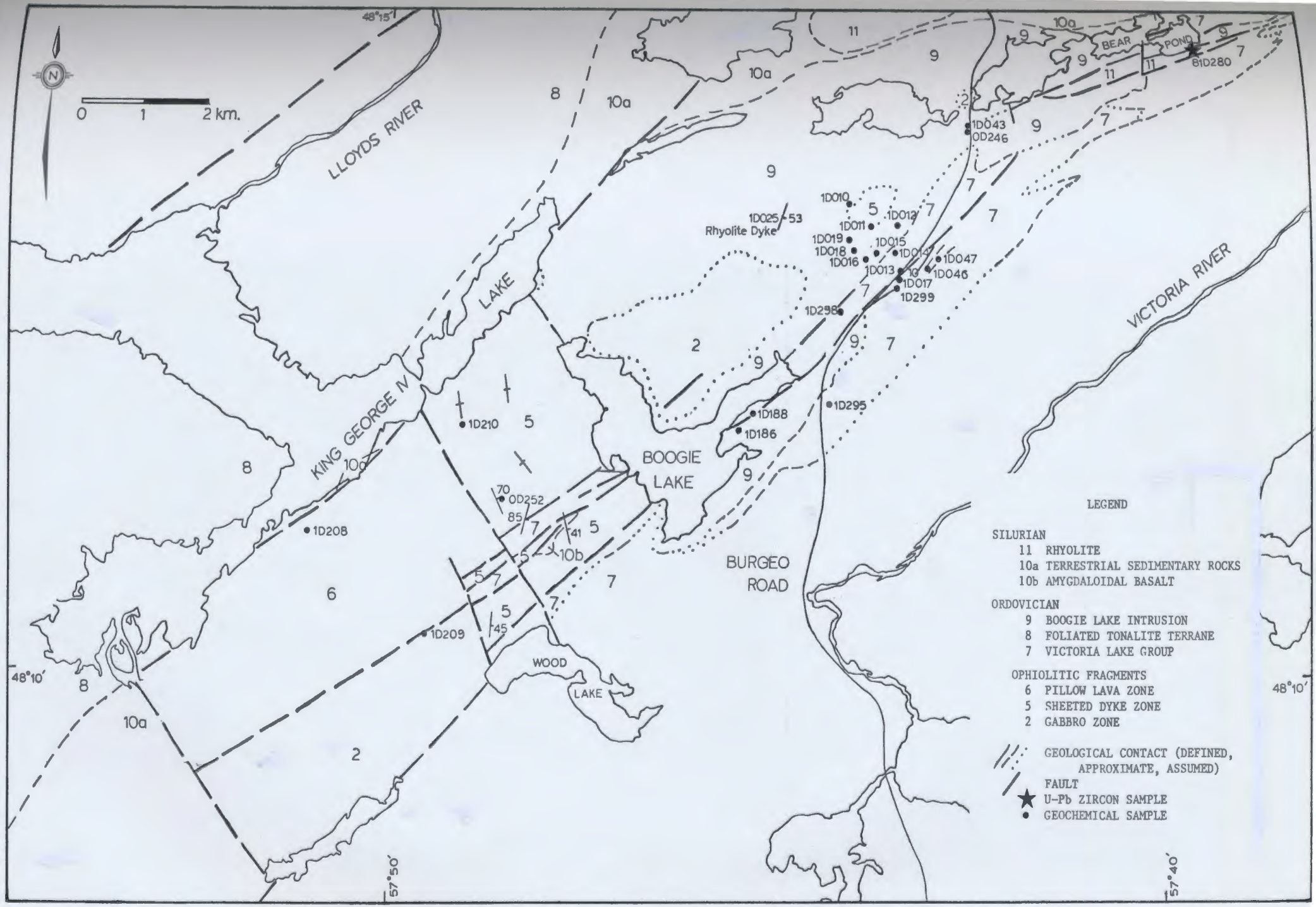

Map 2. Geology of a portion of the King George IV Lake map area (NTS 12A/4), after Kean (1983), showing sample locations.

TABLE 5.1. MAJOR AND TRACE ELEMENT ANALYSES OF ROCKS OF THE TROCTOLITE SILL, ANNIEOPSQUOTCH COMPLEX AND CRITICAL ZONE, STAR LAKE OPHIOLITIC FRAGMENT.

	Annieopsquotch Complex			Star Lake Fragment		
	80D 133-2	80D 133-4	80D 133-5	80D 157-1	80D 168-1	80D 181
SiO_2	43.7	46.6	46.2	40.2	41.7	41.5
TiO_2	0.18	0.16	0.21	0.09	0.16	0.12
Al_2O_3	15.7	20.1	19.2	7.5	7.6	7.2
Fe_2O_3	1.52	0.88	0.88	3.28	4.80	2.01
FeO	5.23	4.66	4.80	7.17	7.03	7.03
MnO	0.12	0.10	0.10	0.17	0.21	0.17
MgO	18.6	12.7	11.8	28.6	24.6	30.4
CaO	10.4	13.3	13.5	6.06	7.58	6.05
Na_2O	0.7	1.0	0.8	0.6	0.2	0.2
K_2O	0.06	0.04	0.02	0.03	0.03	0.01
P_2O_5	0.03	0.03	0.03	0.01	0.03	0.02
L.O.I.	2.97	1.11	0.89	4.63	5.88	4.07
Total	99.21	100.68	98.43	98.34	99.82	98.78
Rb	0	1	0	1	0	0
Sr	50	52	28	15	25	12
Y	7	7	8	1	4	2
Zr	10	3	5	2	4	5
Nb	0	1	0	0	1	0
Zn	57	52	54	67	86	60
Cu	39	78	81	62	88	112
Ni	636	276	294	1246	718	1113
Ba	30	26	28	31	30	38
V	69	73	93	71	104	90
Cr	343	349	764	2353	996	3027

0= not detected

Lake samples and 15.7 and 20.1 wt. % for the sill. This is clearly a function of the greater percentage of plagioclase in the sill.

Likewise CaO varies from 10.4 to 13.5 wt. % in the sill and is significantly lower (6.05 to 7.58 wt. %) in the plagioclase-poor rocks at Star Lake. Na2O is low in both suites but higher (0.7 to 1.0 wt. %) in the sill.

The trace element chemistry of these rocks is easily predictable from their mineralogy. The more MgO rich rocks from Star Lake are enriched in Ni and Cr compared to those of the sill in the Annieopsquotch Complex. Ni is presumably in the olivine, and chromite was observed in thin sections of the Star Lake rocks so the high value of 3027 ppm Cr in sample 80HPAD181 is easily explained.

5.3 SAMPLES FROM THE GABBRO ZONE

Sixteen samples from the gabbro zone of the Annieopsquotch Complex were analysed for major and trace elements and four of these were also analysed for rare earth elements (Table 5.2, 5.9).

These rocks contain pyroxene and amphibole as its predominant alteration product, and plagioclase with secondary albite, carbonate, epidote and chlorite (Chapter 4). Loss on ignition is consistently low for these rocks and ranges from only 1.0 to 1.91 wt. %.

Al2O3 contents vary from 13.6 to 20.7 wt. % and this

TABLE 5.2 MAJOR AND TRACE ELEMENT ANALYSES OF GABBRO

	79D 013-1	79D 014-1	79D 027-1	79D 029-1	79D 143	79D 144-1	79D 144-2	79D 148-1
SiO_2	49.0	50.1	49.2	49.7	48.2	49.4	50.3	50.6
TiO_2	0.31	0.56	0.31	1.43	0.52	0.34	0.48	0.74
Al_2O_3	15.9	17.3	15.3	15.5	20.7	17.1	16.4	13.9
Fe_2O_3	1.50	0.88	2.07	3.36	1.33	1.57	1.41	1.41
FeO	5.71	5.64	6.68	7.39	4.39	4.33	5.02	7.24
MnO	0.17	0.15	0.18	0.21	0.11	0.12	0.14	0.21
MgO	10.5	7.31	9.86	7.25	7.28	9.28	9.12	8.71
CaO	13.8	14.0	12.8	12.3	14.6	15.4	14.7	12.6
Na_2O	1.4	2.2	2.0	2.3	1.4	1.7	1.3	2.0
K_2O	0.06	0.09	0.06	0.06	0.10	0.06	0.16	0.08
P_2O_5	0.01	0.03	0.02	0.07	0.05	0.03	0.06	0.05
L.O.I.	1.10	1.5	1.31	1.0	1.6	1.24	1.10	1.62
Total	99.46	99.76	99.79	100.57	100.28	100.57	100.19	99.16
Rb	0	1	0	1	1	0	5	3
Sr	54	125	67	84	101	73	88	88
Y	14	13	11	33	15	10	13	24
Zr	7	7	5	38	24	11	17	16
Nb	0	1	1	1	1	0	1	0
Zn	58	62	66	60	97	52	57	70
Cu	83	3	52	13	58	62	80	0
Ni	112	51	111	41	106	87	81	55
Ba	47	46	38	37	45	32	62	53
V	175	191	167	379	141	151	185	272
Cr	304	131	338	40	402	346	229	75

	79D 150-1	79D 151	79D 152-2	79D 155	79D 156	80D 129-1	80D 130-2	80D 137-1
SiO_2	49.8	50.9	51.7	50.0	50.9	49.1	48.0	49.4
TiO_2	0.55	0.49	0.41	0.44	0.51	0.59	0.41	0.34
Al_2O_3	14.9	16.6	13.6	15.3	15.2	15.4	16.8	15.2
Fe_2O_3	1.48	1.84	1.65	1.43	1.35	2.55	2.64	0.86
FeO	5.88	5.16	6.73	5.48	5.72	5.18	5.45	5.88
MnO	0.16	0.15	0.20	0.16	0.17	0.13	0.16	0.16
MgO	9.72	8.29	9.73	8.96	8.60	9.61	9.39	9.75
CaO	14.6	13.4	11.8	14.5	14.3	13.9	13.0	14.1
Na_2O	1.7	2.2	2.2	1.6	2.3	1.4	1.3	1.5
K_2O	0.06	0.07	0.06	0.06	0.11	0.08	0.10	0.06
P_2O_5	0.06	0.04	0.02	0.02	0.04	0.03	0.04	0.04
L.O.I.	1.25	1.18	1.17	1.28	1.18	1.46	1.91	1.39
Total	100.16	100.32	99.27	99.23	100.38	99.43	99.20	98.68
Rb	2	0	0	2	0	0	3	0
Sr	60	87	57	66	79	101	95	83
Y	20	16	12	20	15	17	11	8
Zr	19	10	7	13	12	20	15	7
Nb	0	0	0	1	0	1	2	0
Zn	59	56	66	60	55	47	59	60
Cu	27	68	52	50	51	0	59	74
Ni	102	64	56	83	54	108	112	80
Ba	35	40	43	34	36	48	44	29
V	208	192	213	192	221	222	149	173
Cr	335	80	46	113	63	240	371	248

0= not detected

variation could be due in large part to differing degrees of plagioclase accumulation.

Fe_2O_3, as measured by the Pratt titration method, varies from 0.86 to 3.36 wt. % and FeO varies from 4.33 to 7.39 wt. %. The ratios of Fe_2O_3 : FeO are probably a function of variable degrees of sea floor alteration as well as modern weathering processes. Therefore no great significance is attached to them. Total Fe, calculated as FeO, has been used in some chemical plots in subsequent sections. Some screens of magnetite rich gabbro occur in the transition zone. These may be the plutonic equivalent of evolved Fe rich basalt, but none were analysed in this study.

CaO is variable (11.8 to 15.4 wt. %) and depends in part on plagioclase chemistry and abundance. It is also subject to leaching by seawater (cf. Mottl, 1983) and as plagioclase is moderately and clinopyroxene completely altered to secondary assemblages in these rocks (Chapter 4) Ca should be considered a mobile element. Na_2O, also a mobile component, is present in low concentrations that range from 1.3 to 2.3 wt. %. K_2O is present in very low concentrations, from 0.06 to 0.16 wt. %, which is typical of rocks with MORB chemistry, in general.

Sr varies between 54 and 125 ppm in the gabbros analysed and Ba varies between 32 and 62 ppm. Their abundances probably vary both as a function of plagiocase content of the rock and degree of seawater interaction, as these are both very mobile elements.

In general, the incompatible trace elements Zr, Y and Nb are present in lower concentrations in the gabbros than in the dykes and lavas of the Annieopsquotch Complex.

5.4 SAMPLES OF DIABASE DYKES

Forty diabase dykes from the Annieopsquotch Complex, eight from the ophiolitic fragments at Shanadithit Brook, four from King George IV Lake and nine dykes from ophiolitic inclusions in the Boogie Lake Intrusion were analysed for major and trace elements in this study (Tables 5.3, 5.4, 5.5). As well, six dykes from the Annieopsquotch Complex were analysed for rare earth elements (Table 5.9).

The diabase dykes from the Annieopsquotch Complex are quite fresh and have raised, aphanitic to glassy chilled margins. The chilled margins, mostly phenocryst-free, are interpreted on the basis of field criteria to represent basaltic liquid compositions. Loss on ignition, a rough measure of the degree of alteration of the rock, ranges from 0.94 to 3.74 wt. % for dykes from the Annieopsquotch Complex (Table 5.3). Dykes from the other ophiolitic fragments have L.O.I. in the same range (Tables 5.4, 5.5).

Fe_2O_3 varies from 1.53 to 6.52 wt. % and FeO from 5.31 to 10.9 wt. % for the Complex and other ophiolitic fragments as well. No Fe rich diabase dykes analagous to compositions at the peak of Fe- enrichment in the Skaergaard trend were found in the sheeted dyke zone.

TABLE 5-3 MAJOR AND TRACE ELEMENT ANALYSES OF DIABASE DYKES

	79D 109-2	79D 148-2	79D 150-2	79D 153-3	79D 237	79D 240	79D 241	80D 081	80D 122	80D 130-1
SiO_2	49.8	47.8	49.4	47.2	48.9	48.6	47.6	49.5	49.8	50.0
TiO_2	1.18	0.74	0.76	0.84	1.05	2.28	1.59	2.17	1.97	1.34
Al_2O_3	14.4	16.8	14.4	15.8	14.5	13.6	14.9	13.6	13.7	15.1
Fe_2O_3	2.04	1.72	1.93	1.84	2.28	6.52	2.16	4.31	3.17	3.25
FeO	8.39	6.67	6.88	6.80	8.78	8.81	10.9	9.36	10.4	6.84
MnO	0.21	0.18	0.17	0.16	0.23	0.20	0.22	0.19	0.27	0.13
MgO	7.70	9.63	10.5	11.6	7.93	5.38	6.89	5.15	6.05	7.36
CaO	12.1	12.5	11.0	11.9	11.5	8.71	9.57	10.3	10.8	12.8
Na_2O	2.4	1.7	1.9	1.8	1.8	3.7	2.5	2.6	2.2	2.3
K_2O	0.07	0.05	0.28	0.10	0.06	0.06	0.06	0.19	0.27	0.09
P_2O_5	0.09	0.03	0.11	0.06	0.08	0.19	0.11	0.19	0.17	0.10
L.O.I.	2.10	2.12	1.9	2.32	1.70	1.36	3.74	1.25	1.57	1.26
Total	100.48	99.94	99.23	100.42	98.81	99.41	100.24	98.81	100.37	100.57
Rb	1	0	7	0	1	0	0	0	2	0
Sr	68	64	221	83	55	80	83	94	78	90
Y	34	22	19	26	36	72	43	61	61	39
Zr	50	30	52	41	42	108	65	108	90	59
Nb	1	0	1	0	0	3	2	5	2	0
Zn	126	67	68	70	92	83	80	72	117	42
Cu	19	33	21	81	61	0	0	0	8	0
Ni	63	167	190	276	67	34	54	21	42	58
Ba	52	38	149	43	51	48	56	81	129	37
V	304	214	269	204	321	493	447	476	443	323
Cr	155	271	518	495	161	55	131	9	71	99

	80D 132-2	80D 193-1	80D 193-2	80D 193-3	80D 193-4	80D 194	80D 196-1	80D 202-2	80D 230	81D 032-1
SiO_2	48.6	48.2	49.3	48.9	48.6	48.5	51.7	49.9	49.6	49.5
TiO_2	0.58	1.45	1.40	0.99	0.57	0.59	0.80	1.30	1.64	1.32
Al_2O_3	16.1	13.8	14.2	15.0	16.2	15.7	15.4	14.2	14.1	15.5
Fe_2O_3	1.85	2.17	2.04	1.84	1.53	2.40	1.92	2.25	1.89	3.2
FeO	6.17	9.61	9.68	7.96	6.48	5.31	7.74	8.53	8.27	8.0
MnO	0.16	0.25	0.23	0.19	0.17	0.16	0.22	0.21	0.20	0.18
MgO	9.22	7.24	7.16	8.41	9.48	8.45	7.63	7.15	7.56	7.43
CaO	13.7	10.5	11.5	12.8	13.4	12.8	6.83	11.5	9.98	11.8
Na_2O	1.3	2.6	2.2	1.8	1.7	2.4	4.8	2.6	3.5	2.3
K_2O	0.04	0.03	0.06	0.06	0.06	0.04	0.07	0.04	0.13	0.10
P_2O_5	0.05	0.09	0.11	0.07	0.04	0.07	0.07	0.11	0.15	0.10
L.O.I.	1.11	2.83	2.20	2.04	2.37	2.86	3.07	2.43	2.82	1.01
Total	98.88	98.77	100.08	100.06	100.60	99.28	100.25	100.22	99.84	100.44
Rb	1	0	1	0	0	2	0	2	5	1
Sr	61	75	61	46	41	60	48	97	151	90
Y	17	42	37	29	22	19	22	39	42	35
Zr	24	61	58	39	18	19	31	61	93	54
Nb	3	2	0	0	2	0	0	1	4	2
Zn	68	112	118	90	77	80	110	95	100	75
Cu	71	29	31	52	73	86	58	34	49	0
Ni	109	61	59	86	151	107	64	65	60	75
Ba	41	41	48	48	48	62	65	49	65	34
V	216	365	344	280	208	201	303	313	325	337
Cr	332	145	123	296	363	287	217	133	117	139

0 = not detected

TABLE 5:3 MAJOR AND TRACE ELEMENT ANALYSES OF DIABASE DYKES

	81D 033-2	81D 033-3	81D 036-1	81D 123-1	81D 124-1	81D 128-1	81D 129	81D 136-1	81D 136-3	81D 137-1
SiO_2	48.9	48.4	48.9	49.3	50.1	49.1	50.5	52.0	50.5	52.1
TiO_2	1.70	1.29	1.39	1.65	1.21	1.70	1.32	0.60	0.61	0.80
Al_2O_3	14.0	15.7	15.2	14.4	15.4	13.9	14.8	14.5	14.1	15.6
Fe_2O_3	4.61	3.16	3.80	3.18	2.38	3.65	2.78	2.22	1.67	2.30
FeO	9.76	8.23	7.79	9.15	8.58	9.65	8.87	7.15	7.65	7.01
MnO	0.24	0.21	0.19	0.23	0.21	0.19	0.21	0.19	0.17	.18
MgO	6.18	6.52	7.16	6.60	6.64	6.18	6.33	8.61	9.44	8.10
CaO	10.6	10.8	11.6	10.1	10.8	10.6	10.6	11.3	11.0	8.02
Na_2O	2.1	2.2	1.9	3.0	2.4	2.2	2.4	2.2	1.5	3.6
K_2O	0.08	0.09	0.09	0.09	0.07	0.07	0.08	0.15	0.26	0.06
P_2O_5	0.10	0.08	0.13	0.13	0.08	0.11	0.08	0.10	0.13	0.06
L.O.I.	1.1	1.72	1.2	2.27	1.82	1.33	1.23	1.38	2.68	2.26
Total	99.37	98.40	99.35	100.10	99.69	98.68	99.20	100.40	99.71	100.09
Rb	0	0	1	0	1	3	3	0	5	4
Sr	95	108	106	66	85	76	86	216	185	89
Y	49	36	32	48	35	48	37	15	18	24
Zr	85	56	64	80	46	74	54	38	46	30
Nb	2	0	1	3	0	3	1	0	3	0
Zn	68	103	59	93	108	49	75	90	76	84
Cu	0	3	12	36	46	0	0	104	36	37
Ni	32	70	55	41	38	31	33	76	130	56
Ba	53	48	52	40	42	46	59	139	171	36
V	407	344	333	401	331	404	353	281	286	311
Cr	24	106	154	86	72	12	63	346	345	204

	81D 137-2	81D 138-1	81D 138-2	81D 140-2	81D 140-3	81D 141-1	81D 141-2	81D 144-3	81D 144-4	81D 145
SiO_2	48.4	48.5	49.3	49.7	50.7	49.3	49.1	49.2	48.8	49.0
TiO_2	1.25	0.85	1.57	1.11	1.48	1.66	1.14	1.35	1.42	1.43
Al_2O_3	16.2	17.0	14.4	15.7	13.9	13.9	15.4	14.4	14.5	13.7
Fe_2O_3	2.54	2.46	2.70	2.6	4.45	3.73	2.62	3.10	2.70	2.46
FeO	8.79	6.01	9.44	8.2	8.22	9.30	8.08	8.15	9.15	9.65
MnO	.21	0.17	0.23	0.18	0.25	0.21	0.17	0.21	0.22	0.27
MgO	7.65	8.75	6.83	7.32	6.39	6.48	8.01	7.14	7.02	6.31
CaO	10.2	13.5	10.7	12.4	10.4	10.9	11.9	10.5	10.6	8.78
Na_2O	2.2	1.5	2.2	1.9	2.4	2.1	1.7	2.8	2.7	3.4
K_2O	0.08	0.09	0.07	0.11	0.09	0.09	0.08	0.08	0.08	0.10
P_2O_5	0.10	0.04	0.12	0.09	0.11	0.12	0.07	0.08	0.12	0.10
L.O.I.	2.73	1.43	1.60	1.14	1.03	0.94	1.34	2.22	2.25	3.19
Total	100.35	100.30	99.16	100.45	99.42	98.73	99.61	99.23	99.56	98.39
Rb	1	0	0	0	0	0	0	4	2	0
Sr	92	55	55	71	71	69	70	97	82	84
Y	33	23	48	32	45	54	30	43	41	43
Zr	58	37	77	44	65	70	50	60	59	66
Nb	1	0	0	2	1	1	1	0	1	1
Zn	73	73	99	64	74	50	52	100	106	197
Cu	0	55	36	5	22	0	0	31	27	25
Ni	68	142	40	66	24	50	83	65	52	29
Ba	50	39	34	40	52	40	36	76	48	61
V	325	219	369	321	377	393	306	344	341	390
Cr	194	345	98	178	22	89	229	151	124	21

0 = not detected

TABLE 5.4 MAJOR AND TRACE ELEMENT ANALYSES OF DIABASE DYKES

KING GEORGE IV LAKE — SHANADITHIT BROOK

	80D 252-1	80D 252-2	81D 210-1	81D 210-3	81D 195-2	81D 195-3	81D 195-4	81D 195-5	81D 196-2	81D 196-3	81D 196-4	81D 196-5
SiO_2	49.3	47.2	48.2	49.5	48.9	48.1	53.9	49.8	50.5	47.4	48.0	50.5
TiO_2	0.80	1.30	0.73	1.63	1.40	1.18	0.13	1.33	1.19	0.82	1.34	0.45
Al_2O_3	16.6	16.4	16.2	14.3	15.3	16.1	14.1	15.9	14.5	16.0	15.0	16.0
Fe_2O_3	1.84	2.07	2.06	3.41	3.09	3.18	2.15	4.37	3.02	2.22	3.34	2.38
FeO	7.66	6.48	6.86	9.51	8.37	7.94	9.01	9.65	7.58	7.01	7.87	6.58
MnO	0.20	0.15	0.18	0.24	0.22	0.20	0.39	0.29	0.20	0.17	0.22	0.17
MgO	7.62	8.28	8.90	6.92	7.75	9.34	5.98	5.29	7.73	9.96	8.03	8.38
CaO	11.2	11.6	13.3	9.81	11.4	10.6	9.78	9.05	12.6	12.4	11.4	11.9
Na_2O	2.8	2.0	1.2	2.1	1.9	1.6	2.1	2.5	1.8	1.1	1.9	1.8
K_2O	0.12	0.09	0.11	0.11	0.12	0.12	0.23	0.16	0.12	0.10	0.24	0.13
P_2O_5	0.13	0.17	0.04	0.10	0.11	0.10	0.03	0.11	0.07	0.05	0.08	0.06
L.O.I.	2.04	3.63	2.0	1.55	1.31	1.83	2.17	1.52	1.01	1.64	1.33	1.28
Total	100.31	99.37	99.78	99.18	99.86	100.29	99.97	99.97	100.32	98.87	98.85	99.63
Rb	2	0	2	2	3	3	4	0	0	0	0	5
Sr	212	264	51	76	85	90	118	124	61	60	97	136
Y	21	29	22	48	39	32	28	29	32	21	36	11
Zr	46	97	26	67	57	48	15	48	49	29	55	13
Nb	2	3	1	0	3	1	0	2	0	0	2	1
Zn	90	80	80	60	98	95	148	92	97	100	107	81
Cu	20	43	49	0	34	31	17	85	39	51	23	55
Ni	29	70	126	77	66	169	20	10	53	166	77	82
Ba	126	130	33	50	47	55	66	56	43	37	61	86
V	269	185	251	377	342	310	99	491	294	244	358	282
Cr	72	106	354	188	158	306	60	1	151	345	181	289

0= not detected

TABLE 5.5 MAJOR AND TRACE ELEMENT ANALYSES OF OPHIOLITIC INCLUSIONS IN THE BOOGIE LAKE INTRUSION

	81D 007	81D 010-3	81D 011-1	81D 012	81D 015-1	81D 015-2	81D 018-1	81D 019	81D 042-2
SiO_2	49.0	49.7	49.5	48.6	50.8	47.8	49.4	46.7	52.9
TiO_2	1.57	1.49	1.37	1.14	1.77	0.82	1.27	1.69	2.06
Al_2O_3	15.0	14.8	14.3	15.3	16.3	16.5	15.5	15.4	15.5
Fe_2O_3	3.56	2.99	2.43	2.43	3.32	1.86	2.10	2.91	3.16
FeO	8.66	8.95	8.74	7.57	6.41	6.92	8.52	8.08	7.43
MnO	0.16	0.22	0.26	0.19	0.18	0.17	0.21	0.21	0.20
MgO	6.74	7.01	7.28	8.05	6.36	9.21	7.47	9.10	4.30
CaO	10.8	11.6	10.5	12.4	8.72	12.1	11.5	10.1	7.12
Na_2O	2.2	2.2	2.3	1.6	3.0	1.3	1.9	2.0	3.4
K_2O	0.21	0.07	0.21	0.12	0.80	0.44	0.15	0.09	0.43
P_2O_5	0.14	0.13	0.10	0.07	0.34	0.03	0.08	0.22	0.35
L.O.I.	1.65	0.82	2.08	1.92	1.94	2.2	1.8	3.17	2.28
Total	99.69	99.98	99.07	99.39	99.94	99.35	99.90	99.67	99.13
Rb	1	0	0	0	15	6	3	5	5
Sr	113	84	91	80	277	96	114	197	297
Y	55	56	42	34	46	25	39	34	41
Zr	65	80	62	53	164	33	50	101	188
Nb	3	2	3	2	7	1	1	4	6
Zn	52	94	77	81	97	63	93	90	107
Cu	0	12	11	67	12	5	13	35	0
Ni	37	52	96	72	65	153	72	192	11
Ba	54	48	84	52	338	129	75	104	239
V	380	348	347	280	216	223	321	240	309
Cr	29	113	227	243	55	296	166	293	0

O= not detected

MgO content of the dykes from the Annieopsquotch Complex varies from 5.2 to 11.6 wt. % with a continuous variation that likely represents differing degrees of fractionation. MgO in the other ophiolitic fragment dykes varies from 4.30 to 9.96 wt. %, a slightly narrower range.

Rb, Sr and Ba are the only 'mobile' trace elements which are reported for the diabase dykes. U, Th and Pb were sought for but all dykes have contents of these elements at the detection limit of the XRF so these elements are not reported in Tables 5.3, 5.4, and 5.5. The distribution of these elements in dykes is modified by the degree of alteration of feldspar in the rocks and the extent of seawater : rock interaction. They are not used on any of the discriminant diagrams.

Ni and Cr contents of diabase dykes co-vary (Figure 5.1) and decrease rapidly with increasing FeO*/MgO of the dykes. Ni varies from 21 to 276 ppm and these extreme values occur in dykes with 5.15 and 11.6 wt. percent MgO respectively. Cr contents vary from 9 to 518 ppm through the suite. In one dyke from Shanadithit Brook and one from an ophiolitic fragment in the Boogie Lake Intrusion only 10 to 11 ppm Ni is present at MgO contents of 5.29 and 4.30 wt. percent. These two dykes have Cr contents below the detection limit of the XRF.

V in diabase dykes of the Complex varies between 185 and 493 ppm. This element co-varies with Ti, increasing with fractionation (Table 5.3). V contents of dykes are higher than those of the gabbros analysed (Table 5.2) and

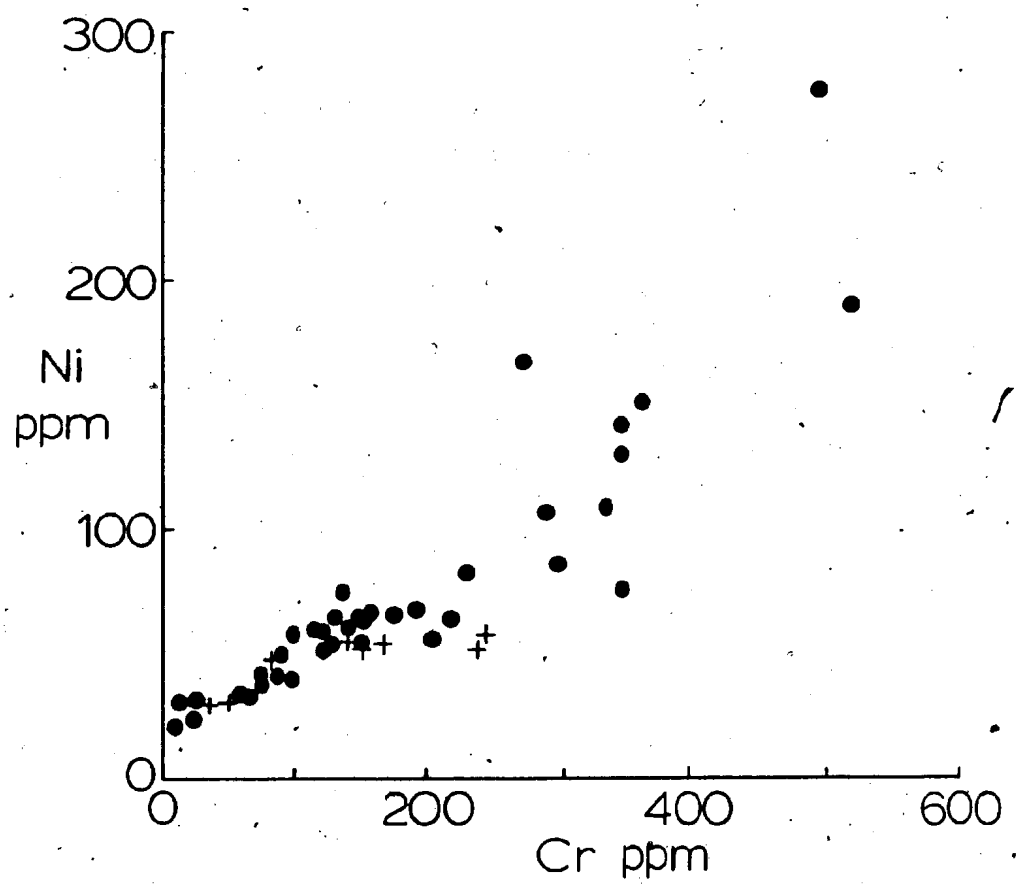

Figure 5.1. Variation of Ni vs. Cr in diabase dykes (dots) and pillow lava (crosses) of the Annieopsquotch Complex.

the highest values are significantly greater than those in the pillow lavas analysed (Table 5.6). This suggests that there likely are more evolved compositions in the pillow lavas than those analysed in this study.

5.5 SAMPLES FROM THE PILLOW LAVA ZONE

Relatively few pillows were analysed in this study, for several reasons; 1. possible repetition of the sequence by faulting (Chapter 3), 2. greater degree of deformation and alteration along faults parallel to the stratigraphy and 3. greater degree of sea floor alteration than affected the diabase dykes of the sheeted dyke zone as reflected in their higher LOI and pervasive albite -epidote veining of pillows and their paler green colour (higher chlorite content). Eight samples were analysed from the Annieopsquotch Complex and six from the ophiolitic fragment at King George IV Lake (Table 5.6).

CaO contents of the pillow lavas vary from 4.93 to 10.6 wt. %, however, this is not thought to be entirely a primary (magmatic) variation. Evidence presented in the next section suggests that Ca has been mobile, and has been lost from the rocks, likely as a result of alteration of plagioclase and clinopyroxene. Na_2O, which varies from 2.2 to 4.9 wt. % in the lavas, is on average higher than in the diabase dykes. This too is likely an alteration effect.

TABLE 5.6 MAJOR AND TRACE ELEMENT ANALYSES OF PILLOW LAVA

	ANNIEOPSQUOTCH COMPLEX								KING GEORGE IV LAKE					
	81D 132-2	81D 132-3	81D 133-1	81D 133-2	80D 196-2	80D 197-3	80D 199	80D 231	81D 208-1	81D 208-2	81D 208-3	81D 208-4	81D 208-5	81D 209-2
SiO_2	54.8	49.0	30.0	51.2	49.1	49.3	54.2	52.0	50.5	51.0	49.6	47.4	50.6	52.6
TiO_2	1.10	1.65	1.21	1.02	1.11	1.67	1.66	1.13	1.56	1.80	1.65	1.71	1.24	1.03
Al_2O_3	13.7	15.3	16.5	14.4	15.70	14.8	13.9	14.0	14.6	14.3	14.2	15.1	15.1	14.1
Fe_2O_3	1.51	4.05	2.06	1.98	2.04	3.04	2.04	2.73	4.29	6.03	3.74	4.37	2.38	2.38
FeO	6.36	8.58	8.01	8.58	7.17	9.97	7.53	6.77	8.29	7.15	8.94	7.51	7.94	6.51
MnO	0.25	0.23	0.41	0.22	0.26	0.31	0.19	0.20	0.21	0.18	0.24	0.19	0.23	0.20
MgO	7.29	7.32	7.06	8.85	7.83	6.36	5.44	7.14	6.50	5.05	7.04	6.25	7.13	6.27
CaO	8.37	4.93	9.53	6.19	7.96	5.99	5.48	9.92	7.00	6.02	7.77	10.6	8.77	9.14
Na_2O	4.6	4.4	2.8	4.1	3.5	4.1	4.9	4.1	4.1	4.5	3.6	2.2	3.2	3.1
K_2O	0.08	0.06	0.09	0.07	0.05	0.04	0.05	0.07	0.10	0.11	0.98	0.11	0.45	0.82
P_2O_5	0.08	0.14	0.09	0.08	0.10	0.15	0.17	0.14	0.13	0.14	0.12	0.15	0.11	0.08
L.O.I.	1.83	3.53	2.24	3.23	3.82	3.28	3.43	2.23	3.31	2.67	2.78	4.30	2.70	3.16
Total	99.97	99.19	100.00	99.92	98.64	99.01	98.99	100.43	100.59	98.95	100.66	99.89	99.85	99.39
Rb	0	0	3	0	1	0	0	0	1	4	9	1	11	11
Sr	48	33	112	85	127	56	37	129	81	57	130	42	191	148
Y	36	53	36	32	35	52	54	29	46	62	56	55	39	32
Zr	47	83	54	49	56	91	93	67	78	84	84	85	59	42
Nb	1	0	3	2	1	1	2	6	2	3	2	1	1	0
Zn	79	215	189	109	149	111	115	111	102	111	109	110	90	83
Cu	0	1	91	0	64	0	0	53	0	0	18	22	43	37
Ni	47	41	50	58	51	25	25	56	49	27	46	57	55	64
Ba	48	55	49	44	42	53	59	48	46	45	118	45	109	134
V	236	423	308	320	319	410	397	285	371	436	384	459	331	295
Cr	234	88	148	243	166	44	33	137	175	43	73	82	194	179

0= not detected

TABLE 5.7

RANGES OF MAJOR AND TRACE ELEMENT CONTENTS
OF ROCKS OF THE ANNIEOPSQUOTCH COMPLEX

	CRITICAL ZONE (6)	GABBRO ZONE (16)	DIABASE DYKES (40)	PILLOW LAVA (8)	TRONDHJEMITE (4)
SiO_2	40.2-46.6	48.0-51.7	47.2-52.1	49.0-54.8	52.6-73.5
TiO_2	0.09-0.21	0.31-1.43	0.57-2.28	1.02-1.67	0.28-0.90
Al_2O_3	7.2-20.1	13.6-20.7	13.6-17.0	13.7-16.5	13.6-26.6
Fe_2O_3	0.88-4.8	0.86-3.36	1.53-6.52	1.51-4.05	0.24-2.08
FeO	4.66-7.17	4.33-7.39	5.31-10.9	6.36-9.97	0.58-3.15
MnO	0.10-0.21	0.11-0.21	0.13-0.27	0.19-0.41	0.01-0.08
MgO	11.8-28.6	7.25-10.5	5.2-11.6	5.44-8.85	0.85-2.54
CaO	6.05-13.5	11.8-15.4	6.18-13.7	4.93-9.92	3.60-13.2
Na_2O	0.2-1.0	1.3-2.3	1.3-4.8	2.8-4.9	3.8-4.6
K_2O	0.1-0.6	0.06-0.16	0.03-0.28	0.04-0.09	0.07-0.81
P_2O_5	0.01-0.03	0.01-0.07	0.03-0.19	0.08-0.17	0.09-0.23
L.O.I.	0.89-5.88	1.0-1.91	1.01-3.74	1.83-3.82	0.30-1.20
Rb	0-11	0-5	0-7	0-3	0-28
Sr	12-52	54-125	41-264	33-129	132-400
Y	1-8	8-33	15-72	29-54	30-131
Zr	2-10	5-38	18-108	47-93	137-610
Nb	0-1	0-2	0-7	0-6	1-7
Zn	52-86	47-97	42-197	79-215	26-50
Cu	39-112	0-83	0-104	0-91	0-8
Ni	276-1246	41-112	21-276	25-58	3-13
Ba	26-38	32-62	34-171	42-59	46-726
V	69-104	141-379	185-493	236-423	24-146
Cr	343-3027	40-402	9-518	33-243	0-9

5.6 DISCUSSION OF MAJOR ELEMENT VARIATION DIAGRAMS

All rocks analysed have been plotted on the standard AFM diagram (Figure 5.2). The samples from the critical zone plot near, or on, the MgO-FeO join reflecting their very low contents of the alkali elements. They plot closest to the MgO apex reflecting their accumulation of ferro-magnesian minerals.

With the exception of one sample, 79HPAD029-1, all the gabbro samples cluster along a tholeiitic trend at higher MgO/FeO than the dyke suite. The two gabbro samples from Star Lake are higher in MgO than most of the Annieopsquotch gabbros analysed. The diabase dykes from the Annieopsquotch Complex and the other ophiolitic fragments show a tholeiitic trend of Fe enrichment over a range of FeO/MgO ratios from .73 to 2.73. Several dykes do overlap the gabbro compositions and the gabbros and dykes together represent a continuum of compositions.

Pillow lava analyses plot to the left of the diabase dykes on the AFM diagram, reflecting the greater Na_2O content of the pillows; an average of 3.8 wt. % vs. 2.4 wt. % in the dykes. This enrichment in Na is interpreted to be a result of albitization of feldspars with the release of Ca.

Trondhjemites plot towards the alkali corner of the diagram but not on a single trend. They fall in the calc-alkaline field of Irvine and Baragar (1971), as expected. The chemistry of these rocks is discussed in

Figure 5.2A. AFM diagram with all analyses plotted of rocks of the Annieopsquotch Complex.

Figure 5.2B. AFM diagram with all analyses plotted of rocks of the ophiolitic fragments of the Annieopsquotch ophiolite belt.

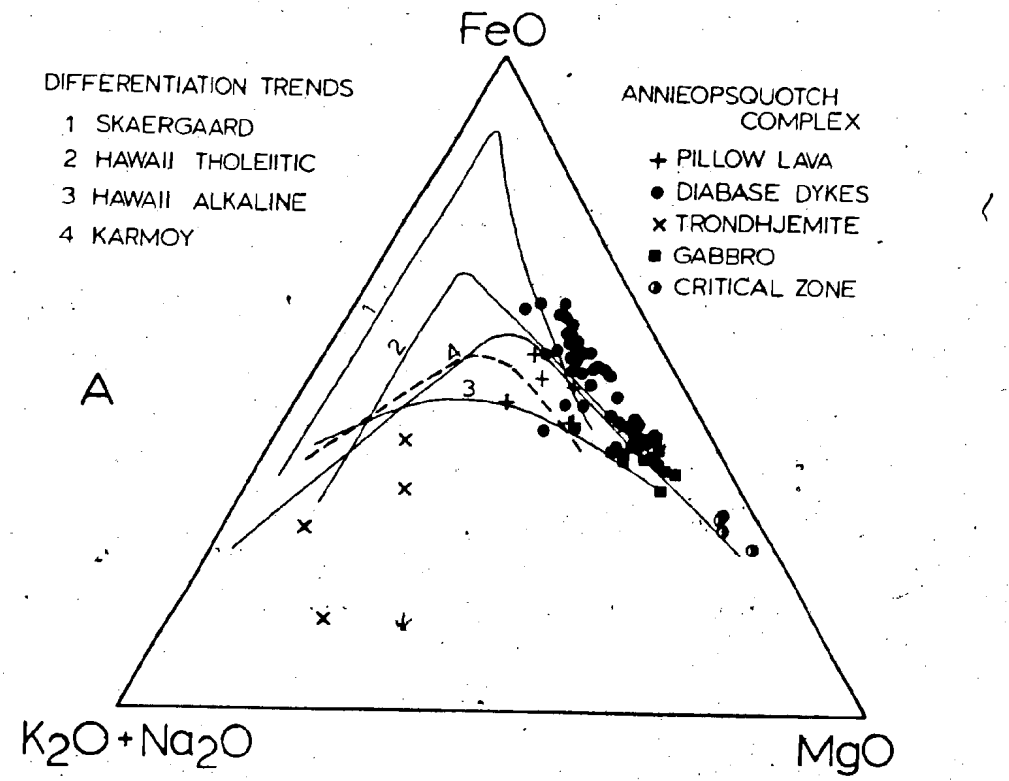
FeO
DIFFERENTIATION TRENDS
1 SKAERGAARD
2 HAWAII THOLEIITIC
3 HAWAII ALKALINE
4 KARMOY
ANNIEOPSQUOTCH COMPLEX
+ PILLOW LAVA
● DIABASE DYKES
× TRONDHJEMITE
■ GABBRO
◐ CRITICAL ZONE
A
1
2
4
3
K2O + Na2O
MgO

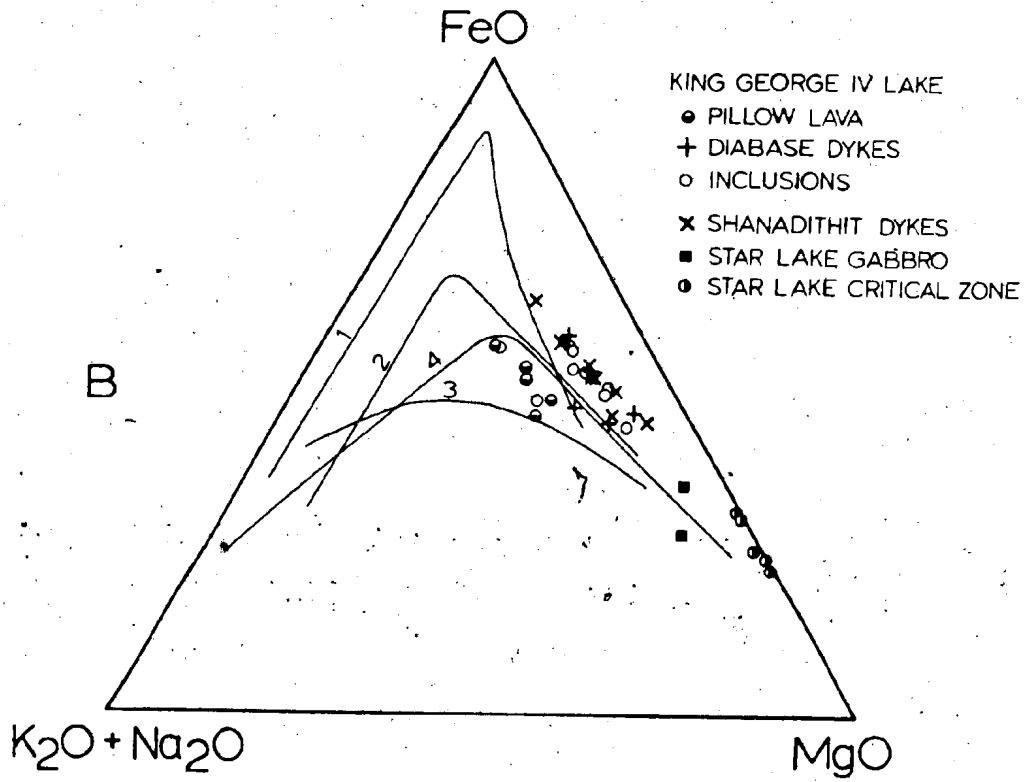
FeO
KING GEORGE IV LAKE
○ PILLOW LAVA
+ DIABASE DYKES
o INCLUSIONS
× SHANADITHIT DYKES
■ STAR LAKE GABBRO
◐ STAR LAKE CRITICAL ZONE
B
1
2
4
3
K2O + Na2O
MgO

more detail below.

On the Na2O + K2O vs. SiO2 diagram of Kushiro (1968), the Annieopsquotch Complex diabase dykes fall well within the field of tholeiitic basalt with total alkali contents in the range 1.34 to 4.87 wt. % (Figure 5.3A). There is a weak positive correlation between total alkalis and silica content of the dykes.

All gabbro, diabase dyke and pillow lava analyses from the Annieopsquotch Complex have been plotted on the TiO2 vs. FeO*/MgO diagram (Figure 5.3B). The gabbros plot off the end of the Skaergaard tholeiitic trend but on the general trend for all Annieopsquotch dyke and lava analyses. The high-Ti gabbro plots on the Skaergaard trend with the dykes.

Serri (1981) used a variant of this plot to distinguish high and low-Ti ophiolites (Figure 5.4). The only difference from Figure 5.3B is the method of normalizing total FeO on the abscissa. On this diagram all Annieopsquotch samples, with the exception of one gabbro, plot in the field of high-Ti ophiolites.

Diagrams employing Al2O3, TiO2, K2O and FeO* plotted against MgO have been used to distinguish major basalt types (Perfit et al., 1980). On these diagrams, the great majority of diabase dykes and pillow lava of the Annieopsquotch Complex fall in the restricted field of MORB glasses (Figure 5.5). This is strong evidence that the rocks are relatively fresh and that they represent true MORB liquid compositions.

Figure 5.3A. Na_2O+K_2O vs. SiO_2 diagram (after Kushiro, 1968), for diabase dykes of the Annieopsquotch Complex.

Figure 5.3B. TiO_2 vs. FeO*/MgO diagram showing Skaergaard tholeiitic trend and analyses from the Annieopsquotch Complex. Symbols as in Figure 5.2A. Skaergaard and Annieopsquotch trends are clearly similar.

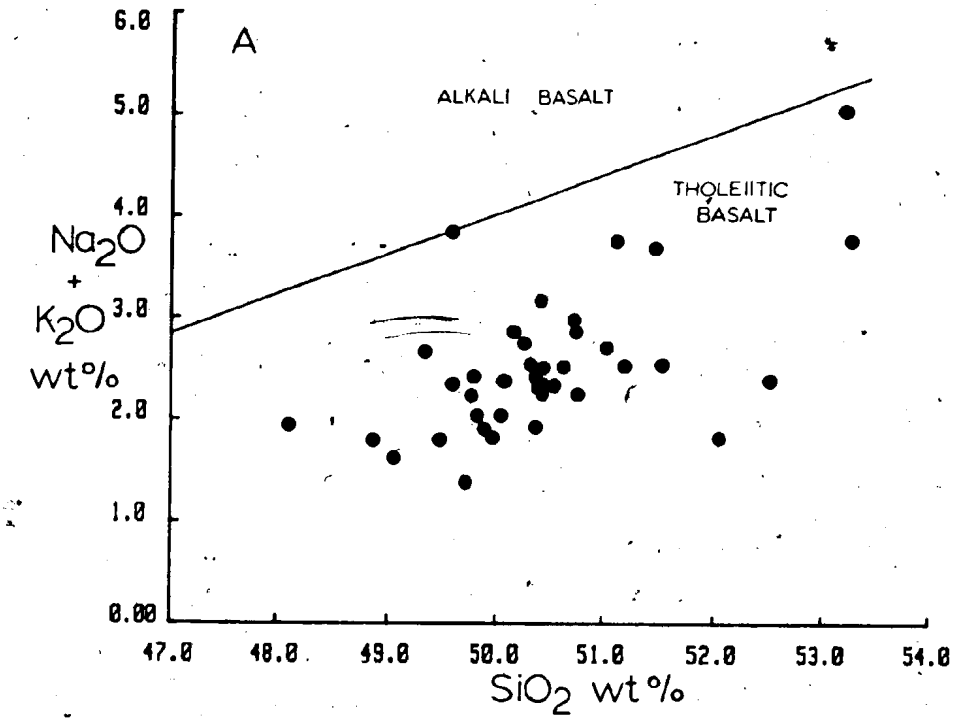
A
ALKALI BASALT
THOLEIITIC BASALT
$Na_2O + K_2O$ wt%
6.0
5.0
4.0
3.0
2.0
1.0
0.00
47.0
48.0
49.0
50.0
51.0
52.0
53.0
54.0
SiO_2 wt %

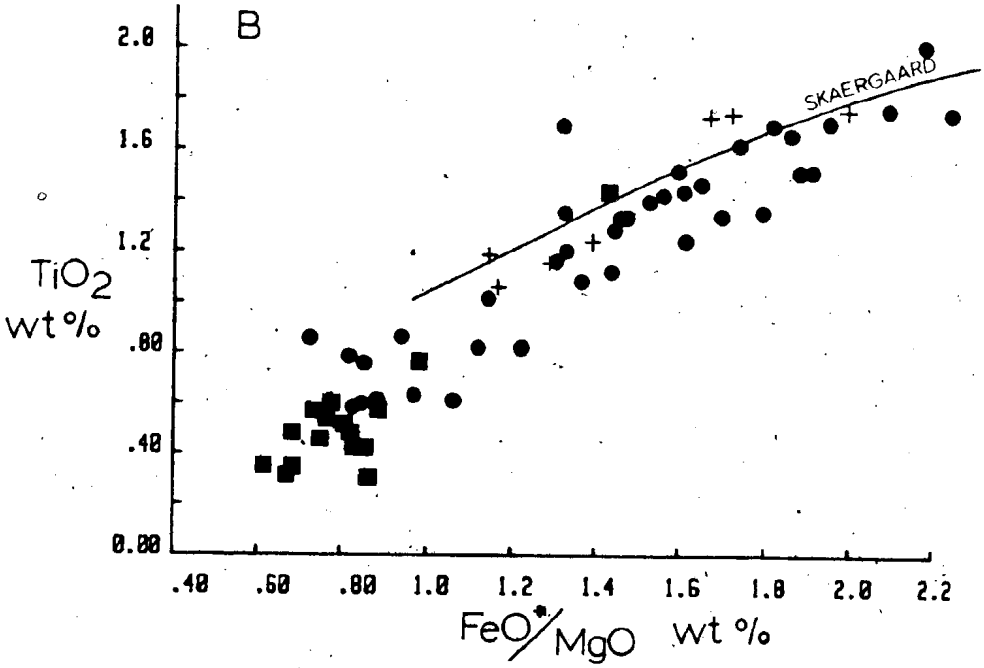
B
SKAERGAARD
TiO_2 wt%
2.0
1.6
1.2
.80
.40
0.00
.40
.60
.80
1.0
1.2
1.4
1.6
1.8
2.0
2.2
FeO^*/MgO wt %

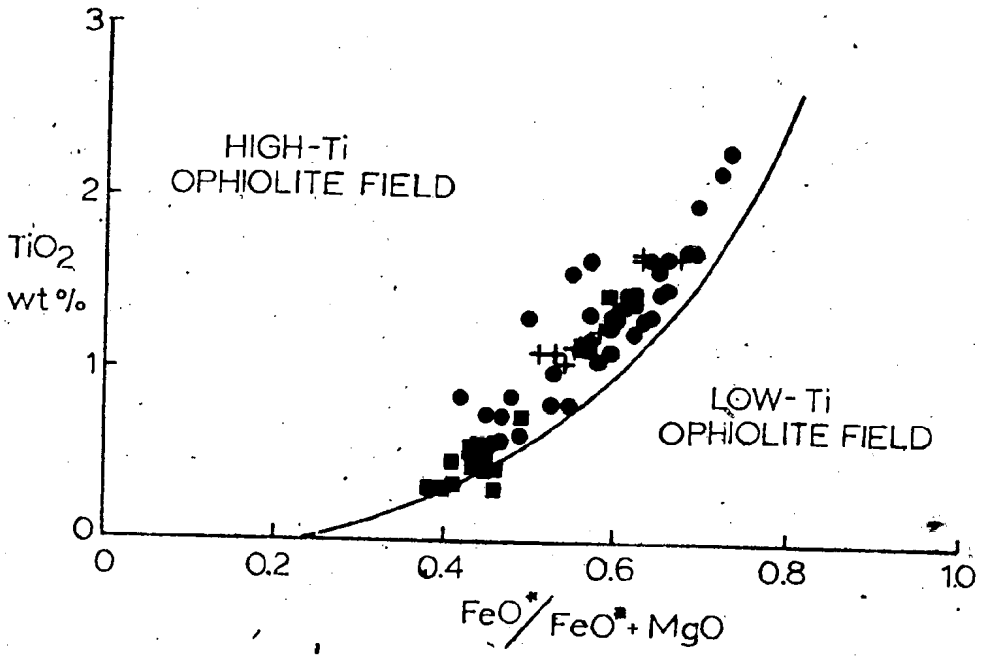

Figure 5.4. TiO2 vs. FeO*/(FeO*+MgO) diagram showing high-Ti and low-Ti ophiolite fields after Serri (1981). Gabbros (squares), diabase dykes (dots) and pillow lava (crosses) of the Annieopsquotch Complex all fall in the high-Ti field, with one exception.

Figure 5.5. Major element variation diagrams (after Perfit et al., 1980). Fields of intraplate basalts, crystalline MORB's and MORB glasses are outlined. Most diabase dykes and pillow lava of the Annieopsquotch Complex fall in the restricted field of MORB glasses in all diagrams.

A. Al_2O_3 vs. MgO
B. TiO_2 vs. MgO
C. K_2O vs. MgO
D. FeO* vs. MgO

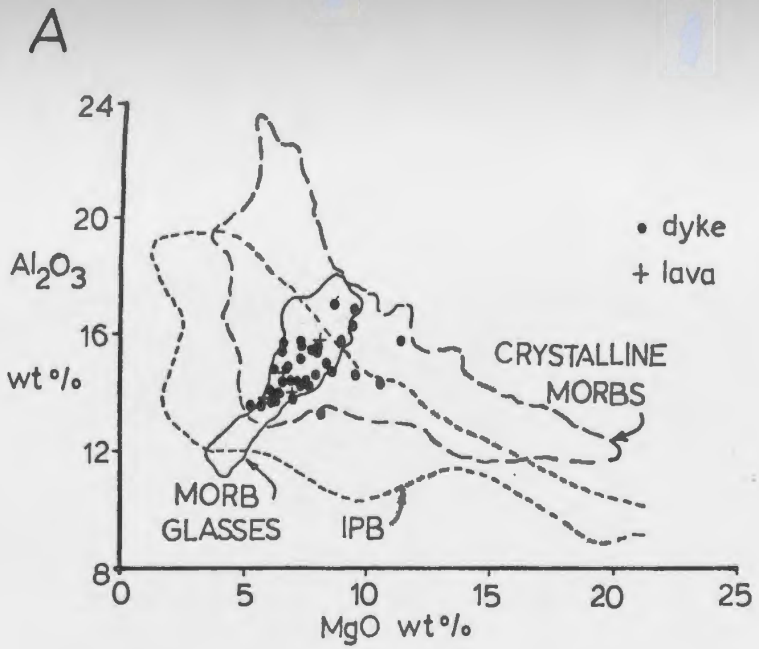
A
24
20
16
12
8
Al_2O_3
wt %
0
5
10
15
20
25
MgO wt %
• dyke
+ lava
CRYSTALLINE
MORBS
MORB
GLASSES
IPB

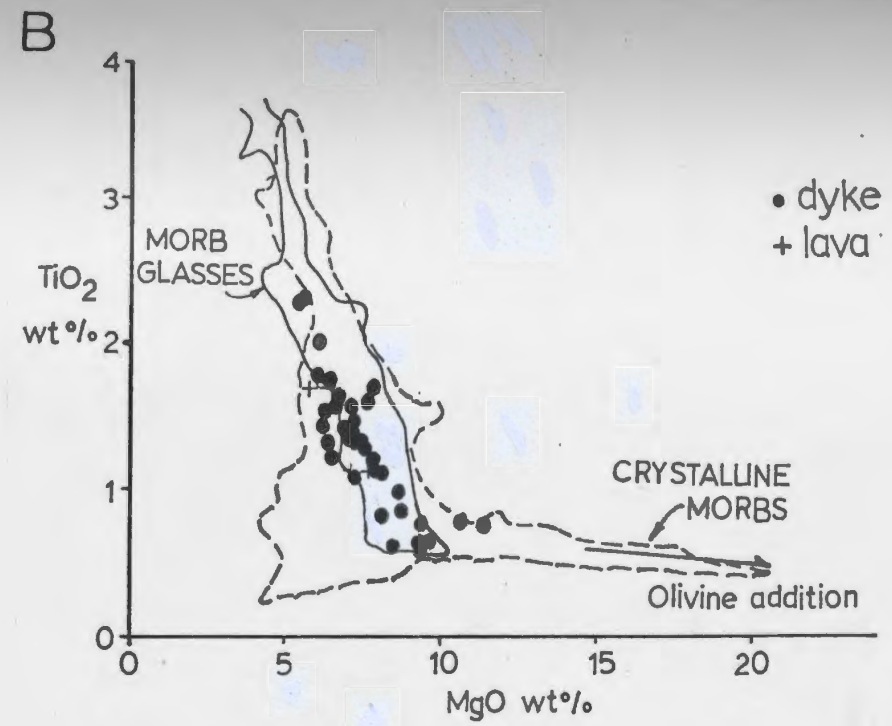
B
4
3
2
1
0
TiO_2
wt %
0
5
10
15
20
MgO wt %
• dyke
+ lava
MORB
GLASSES
CRYSTALLINE
MORBS
Olivine addition

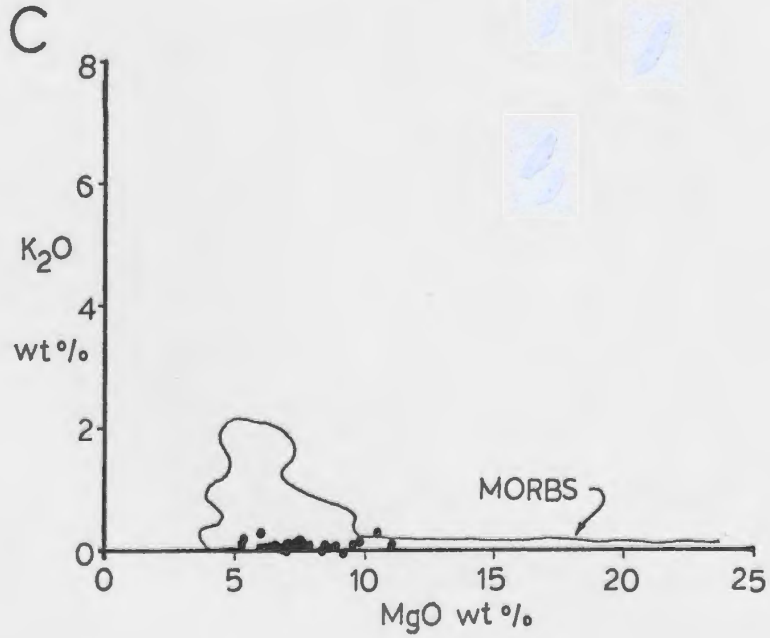
C
8
6
4
2
0
K_2O
wt %
0
5
10
15
20
25
MgO wt %
MORBS

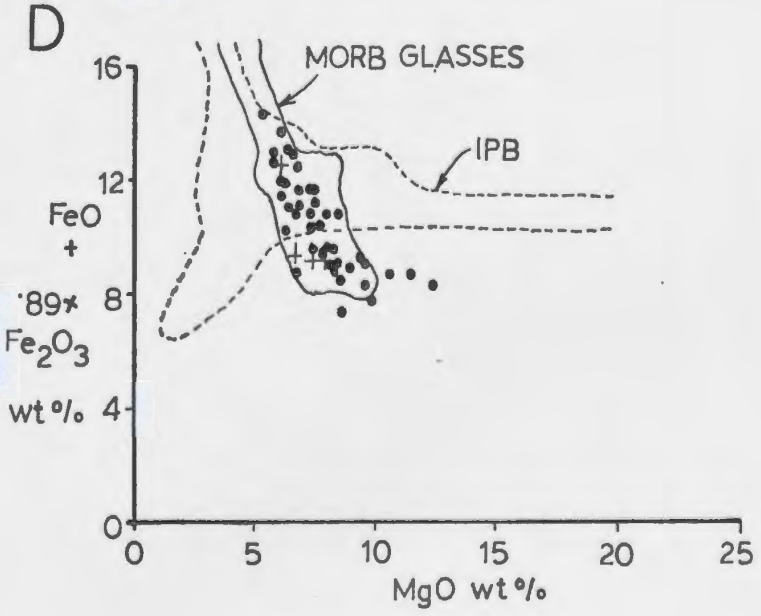
D
16
12
8
4
0
FeO
+
·89×
Fe_2O_3
wt %
0
5
10
15
20
25
MgO wt %
MORB GLASSES
IPB

Many island arc basalts, which cover a wide chemical spectrum would also fall in this field. Perfit et al., (1980) noted that the most important difference in major element contents between MORB and island arc basalts is the very low content of K2O in MORB. They noted that MORB have K2O contents less than 1 wt. % with many less than 0.25 wt. %, while most island arc basalts contain more than 2 wt. % K2O. K2O contents of dykes from the Annieopsquotch Complex vary between 0.03 and 0.28 wt. %. Dykes from the other ophiolitic fragments studied have K2O contents between 0.07 and 0.80 wt. % (Table 5.5). K2O contents of pillow lava analysed vary little and are 0.04 to 0.09 wt. %.

CaO/TiO2 and Al2O3/TiO2 ratios plotted against TiO2 content of dykes and lavas of the Annieopsquotch Complex show a regular variation (Figure 5.6). They fall in the MORB field and in fact extend that field, drawn by Sun and Nesbitt (1978), to higher TiO2 contents. The maximum TiO2 content of a dyke is 2.28 wt. %. One dyke from Shanadithit Brook plots near the field of Betts Cove high-Mg lava, but is in fact, lower in MgO than many of the dykes from the Annieopsquotch Complex (Figure 5.7). This dyke is anomalous. A few analyses that plot below the MORB field in the diagram invoving CaO have likely lost Ca : groundmass plagioclase is strongly altered to mixtures of albite, epidote, chlorite and rare carbonate in many dykes. Most pillow analyses are low in CaO relative to the dykes.

Figure 5.6A,B. CaO/TiO2 and Al2O3/TiO2 vs. TiO2 diagrams (after Sun and Nesbitt, 1978), showing fields of komatiites and Mg basalts, Betts Cove high-Mg lavas (symbol) and MORB. Diabase dykes and pillow lava of the Annieopsquotch Complex fall in the MORB field. Some dykes and all lavas plot to the low-Ca side of the field in Figure 5.6A. This is attributed to loss of Ca as a result of seafloor alteration; see text for discussion.

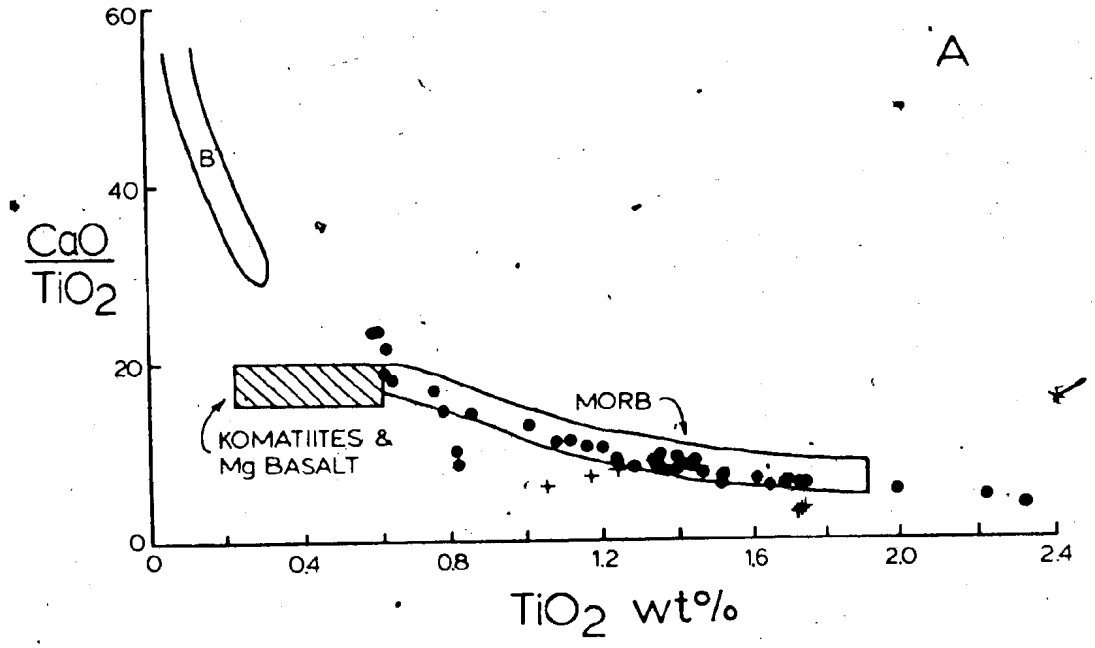
A
60
40
20
0
CaO / TiO2
B
KOMATIITES &
Mg BASALT
MORB
0
0.4
0.8
1.2
1.6
2.0
2.4
TiO2 wt%

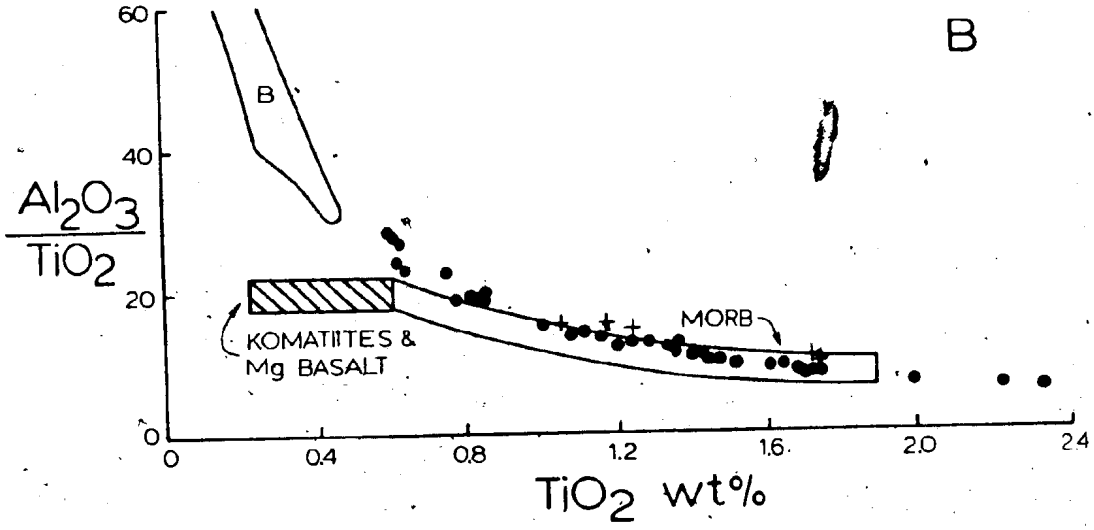
B
60
40
20
0
Al2O3 / TiO2
B
KOMATIITES &
Mg BASALT
MORB
0
0.4
0.8
1.2
1.6
2.0
2.4
TiO2 wt%

Figure 5.7A,B. CaO/TiO2 and Al2O3/TiO2 vs. TiO2 diagrams (after Sun and Nesbitt, 1978), for ophiolitic fragments. Explanation as for Figure 5.6. Analyses of dykes and pillow lavas plotted using the same symbols as Figure 5.2B. The majority of samples fall in the field of MORB.

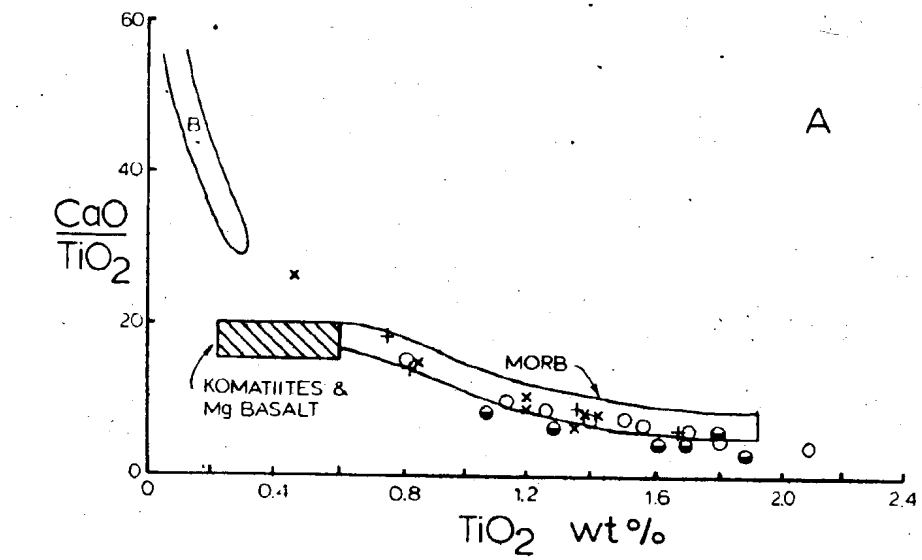
A
B
CaO/TiO2
KOMATIITES &
Mg BASALT
MORB
TiO2 wt %
0
20
40
60
0.4
0.8
1.2
1.6
2.0
2.4

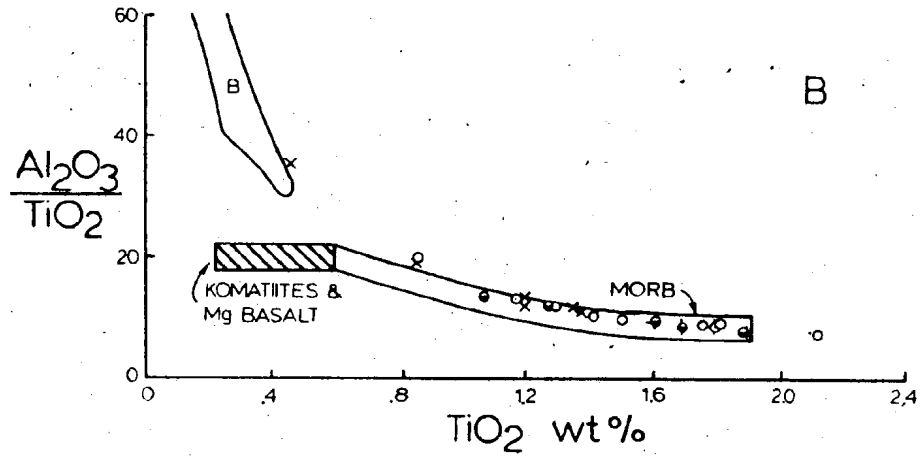
B
Al2O3/TiO2
KOMATIITES &
Mg BASALT
MORB
TiO2 wt %
0
20
40
60
.4
.8
1.2
1.6
2.0
2.4

5.7 DISCUSSION OF TRACE ELEMENT VARIATION DIAGRAMS

Pearce (1975) used a plot of Ti against Cr to separate ocean floor basalts from island arc basalts. Dykes from the Annieopsquotch Complex plot in the field of ocean floor basalt, except for Cr contents undef 30 ppm. These fall in the island arc field (Figure 5.8). Magnetite is present in some pockets of high level gabbro. It is suggested that fractionation of magnetite late in the crystallization history may have reduced Cr contents in some late dykes.

Pearce and Cann (1973) used contents of Sr and the 'immobile' elements; Ti,Zr and Y to distinguish the eruptive setting of basalts of Cenozoic and recent age. The fields shown on these diagrams were empirically derived from analyses of thousands of samples from known tectonic settings (Figure 5.9).

Diagrams involving Sr were not used to discriminate between altered basalts due to evidence for the alteration of feldspar and mobility of Sr with Ca (Pearce and Cann, 1973).

On plots of Ti/100-Zr-Y*3 and Ti vs. Zr (Figure 5.9), after Pearce and Cann (1973) and Pearce (1980), analyses fall partially in the fields of ocean floor basalts and low-K tholeiites but show a trend to low Zr contents. The main concentration of dyke analyses (31 samples) plots to the low- Zr side of all the fields delineated by Pearce and Cann (1973). The trend in the analyses is somewhat regular, away from the Zr corner, suggesting that a mineral

Figure 5.8. Ti vs. Cr diagram (after Pearce, 1975), showing fields of ocean floor basalts and island arc tholeiites. Diabase dykes and pillow lava of the Annieopsquotch Complex fall mainly in the field of ocean floor basalt, except at Cr contents less than 30 ppm.

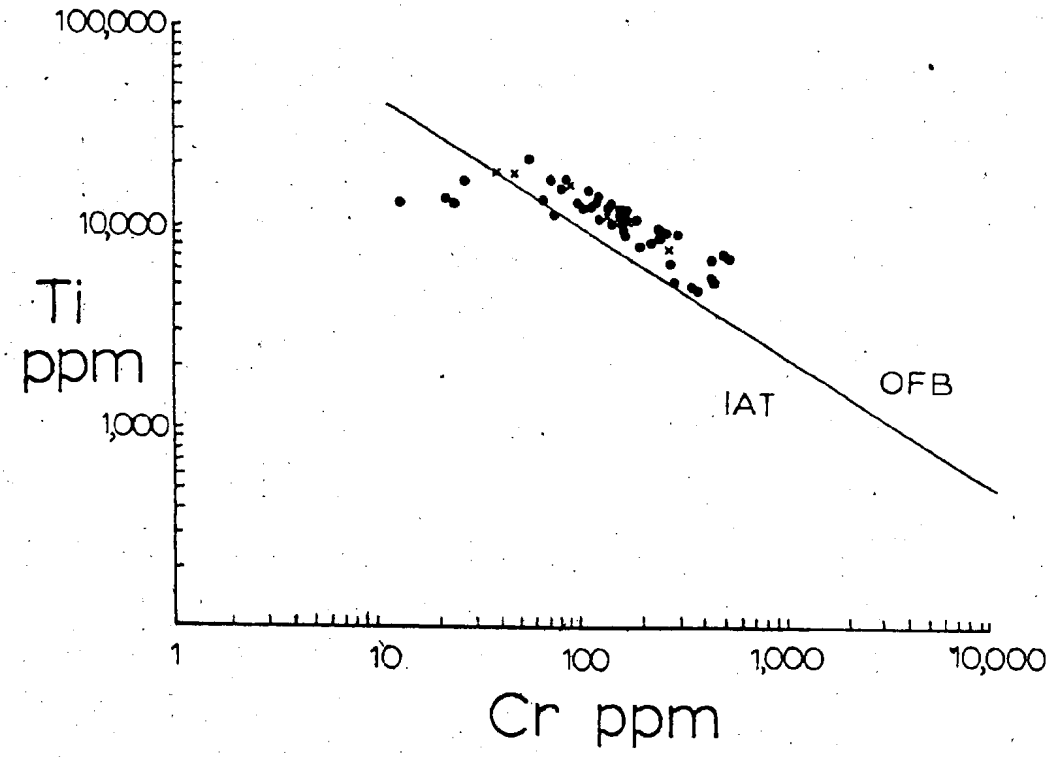
100,000
10,000
1,000
Ti
ppm
IAT
OFB
1
10
100
1,000
10,000
Cr ppm

Figure 5.9A. Ti/100 : Zr : Y*3 diagram (after Pearce and Cann, 1973), showing fields for within plate, calc-alkaline and ocean floor basalts and low-K tholeiites. Diabase dykes of the Annieopsquotch Complex plot in the ocean floor basalt field and to the low-Zr side of all fields.

Figure 5.9B. Ti vs. Zr diagram (after Pearce, 1980), showing the fields of arc and within plate lavas and of MORB. Diabase dykes of the Annieopsquotch Complex fall in all fields. They follow the MORB trend but are displaced to the low-Zr side of the field.

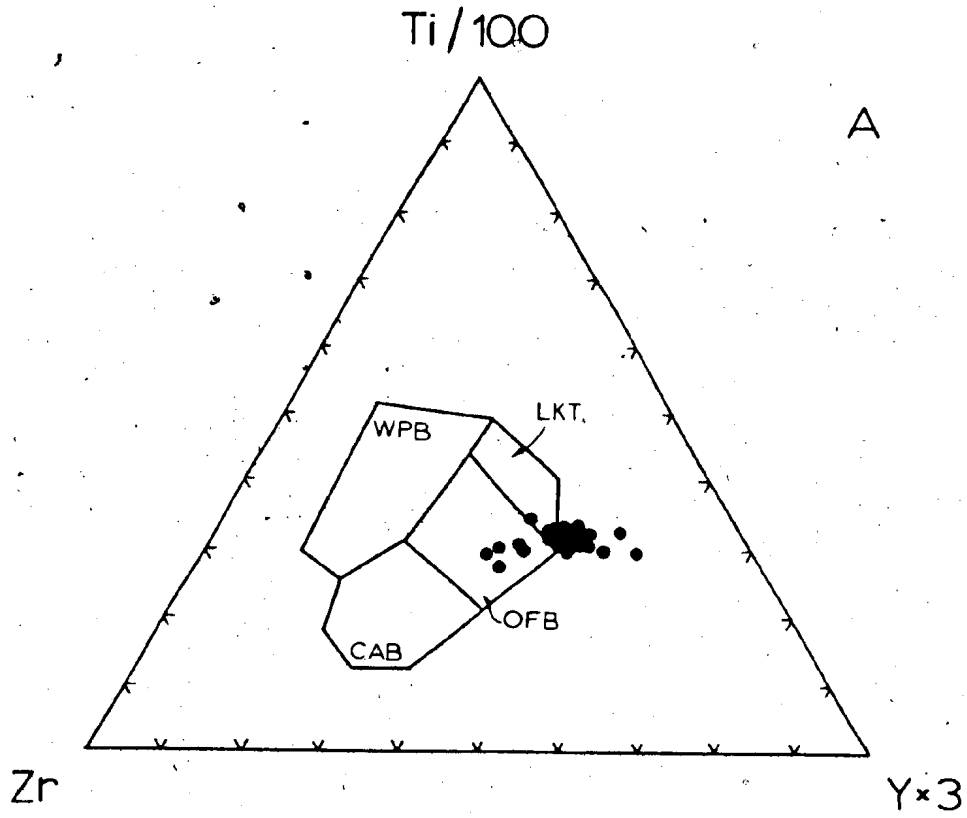
Ti/100
A
WPB
LKT.
OFB
CAB
Zr
Y×3

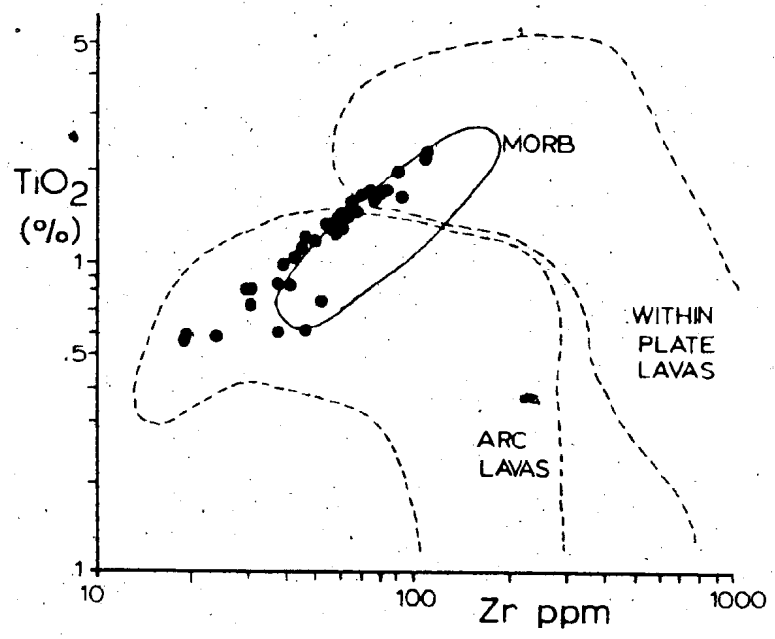
B
5
1
.5
1
TiO2
(%)
MORB
WITHIN
PLATE
LAVAS
ARC
LAVAS
10
100
1000
Zr ppm

which encorporates Zr may have crystallized in the magma chamber that is the source of these dykes.

Zircon has been identified in 'high level' gabbro of the Betts Cove, Bay of Islands and Pipestone Pond Complexes of Newfoundland by crushing large samples (>60 kg.) and performing heavy mineral separations (Chapter 7; Dunning and Krogh, 1983; and unpublished information). It has not been found in gabbros of the Annieopsquotch Complex, but has not been sought in the same manner. If zircon is present in some gabbros, Zr cannot properly be considered to be an incompatible element in some dykes. This would seriously reduce the usefulness of discriminant diagrams employing it.

Pearce (1980) introduced a plot of Cr vs. Y to more easily discriminate between basalts erupted in island arc and MOR settings. There is essentially no overlap between these two groups on this diagram (Figure 5.10). The majority of diabase dykes and pillow lavas analysed from the Annieopsquotch Complex fall in the MORB field but some define weak trends to Cr poor compositions.

The trend of dyke and pillow analyses to low Cr contents, which takes them into the field of within plate basalts, is not interpreted to be of great significance in determining the tectonic setting of these lavas. Rather, it is thought to result from early fractionation of olivine and clinopyroxene which, due to their high partition coefficients for Cr, would have the effect of rapidly depleting this element in the liquid. Pearce (1980)

Figure 5.10A. Cr vs. Y diagram (after Pearce, 1980), showing field of island arc tholeiites and overlapping fields of within plate basalts and MORB. Diabase dykes and pillow lava of the Annieopsquotch Complex fall in all fields. They fall mainly in the area of overlap but extend to very low Cr contents.

Figure 5.10B. Cr vs. Y diagram showing outlines of ranges of analyses of diabase dykes and pillow lavas from Figure 5.9A and best fit lines (fitted by eye) for the data. There appear to be two separate trends but they are not constrained by many analyses. The steeper trend is consistent with olivine and pyroxene (+ spinel?) crystallization. The shallow trend may result from a greater proportion of plagioclase crystallization, as suggested by Pearce (1980).

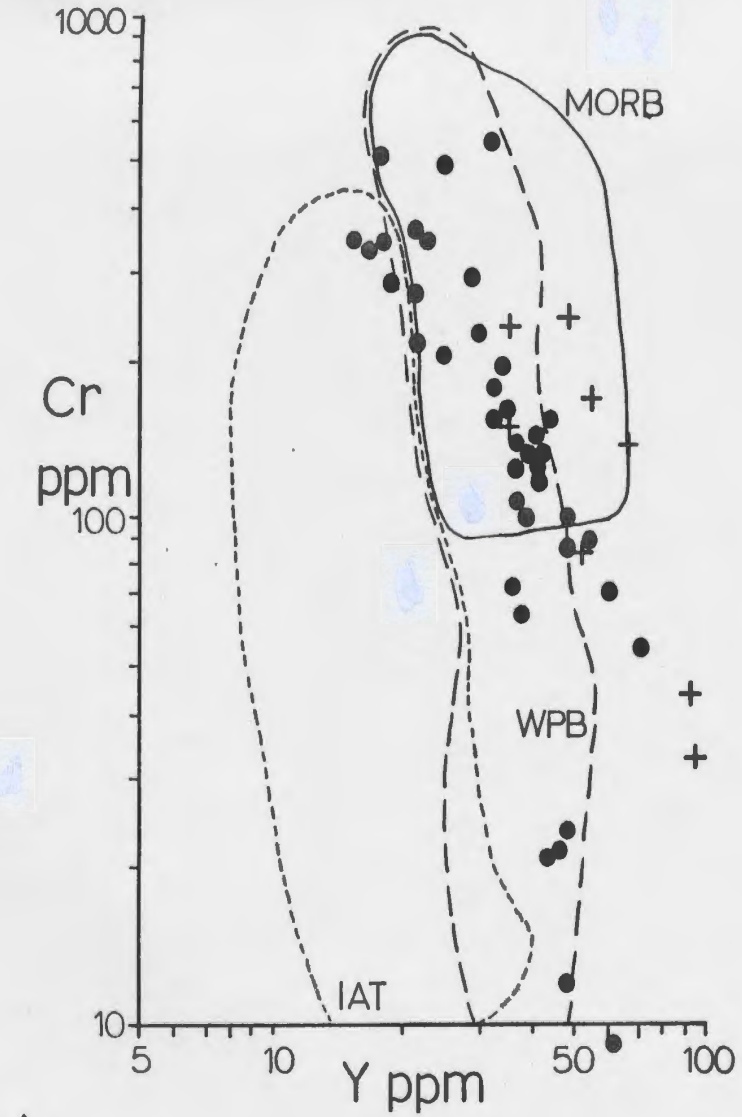
1000
Cr
ppm
100
10
MORB
WPB
IAT
5
10
50
100
Y ppm

A

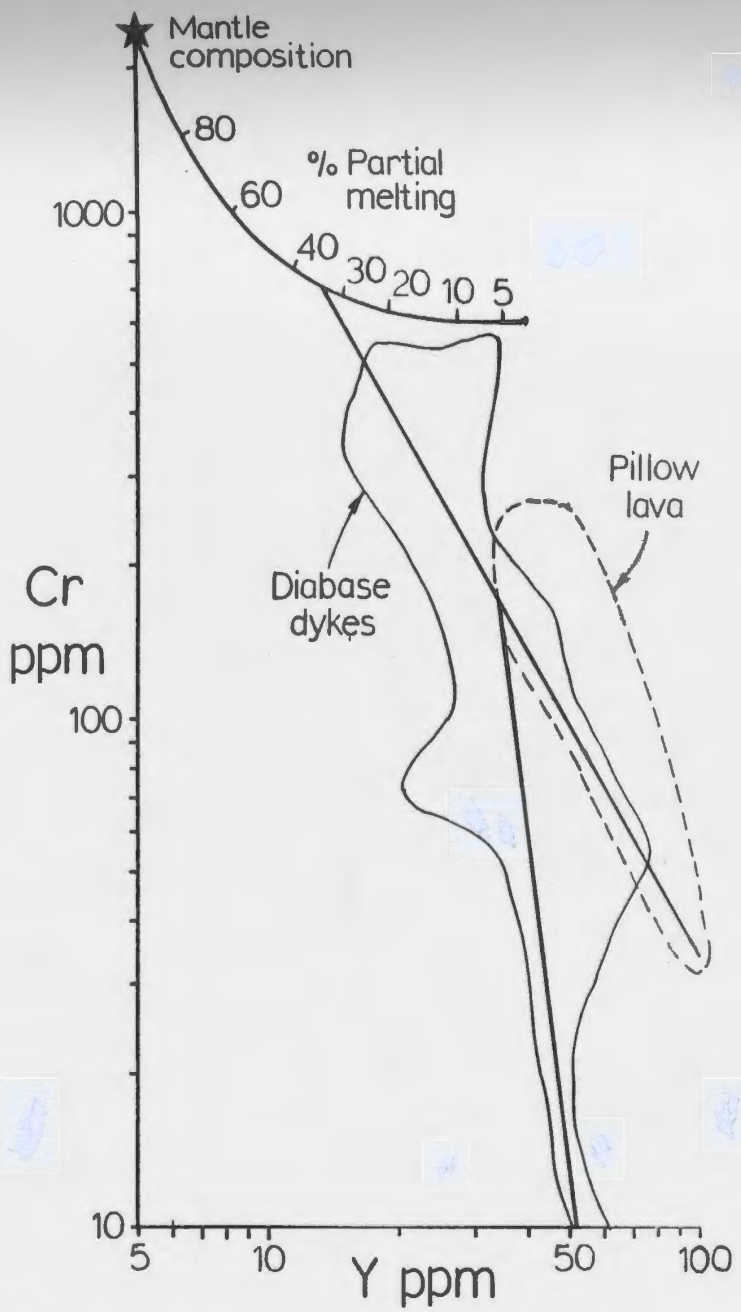
Mantle
composition
80
60
% Partial
melting
40
30
20
10
5
1000
Cr
ppm
100
10
Diabase
dykes
Pillow
lava
5
10
50
100
Y ppm

B

attributed the shallowing of the trend at Cr poor compositions to late fractional crystallization of a mineral assemblage including abundant plagioclase.

TiO2 and Y contents of lavas were used by Perfit et al. (1980) to distinguish tholeiitic basalts from different oceanic tectonic settings (Figure 5.11A). The Ti/Y ratio is lowest for N-Type (normal) MORB. Analyses of gabbros, diabase dykes and pillow lavas of the Annieopsquotch Complex define a linear trend (fitted by eye in Figure 5.11A) which is consistent over a wide range of TiO2 and Y contents. This trend is most similar to that of N-Type MORB but has a slightly lower Ti/Y ratio. The low TiO2 and Y contents of the gabbros could be due to separation of interstitial liquid enriched in these elements.

Various trends on this diagram can be related to fractionation of different mineral assemblages in the source magma chambers. This is shown in the inset in Figure 5.11A. Mineral-liquid partition coefficients were taken from Pearce and Norry (1979). The Annieopsquotch trend is consistent with a combination of clinopyroxene, olivine and plagioclase fractionation. Because all three minerals produce similar changes in the abundances of both elements, it is not possible to say whether or not all three minerals are involved. All three minerals are present in the cumulate and massive gabbros of the plutonic zone of the Complex.

Figure 5.11B shows analyses of diabase dykes and lavas

Figure 5.11A. TiO_2 vs. Y diagram (after Perfit *et al.*, 1980), showing trends for tholeiitic basalts from different oceanic tectonic settings. E-Type MORB and N-Type MORB are from Iceland and surrounding sea floor.

Annieopsquotch data define a linear trend that is most similar to N-Type MORB. Mineral fractionation trends, based on partition coefficients of Pearce and Norry (1979), are shown on inset diagram. Ticks represent increments of 10 wt. % fractional crystallization. Annieopsquotch trend is consistent with a combination of plagioclase, clinopyroxene and olivine fractionation.

Figure 5.11B. Same diagram as in A showing data from ophiolitic fragments of the Annieopsquotch ophiolite belt. Symbols as in Figure 5.2B. The majority of samples fall on the Annieopsquotch trend. One dyke from Shanadithit Brook is clearly anomalous.

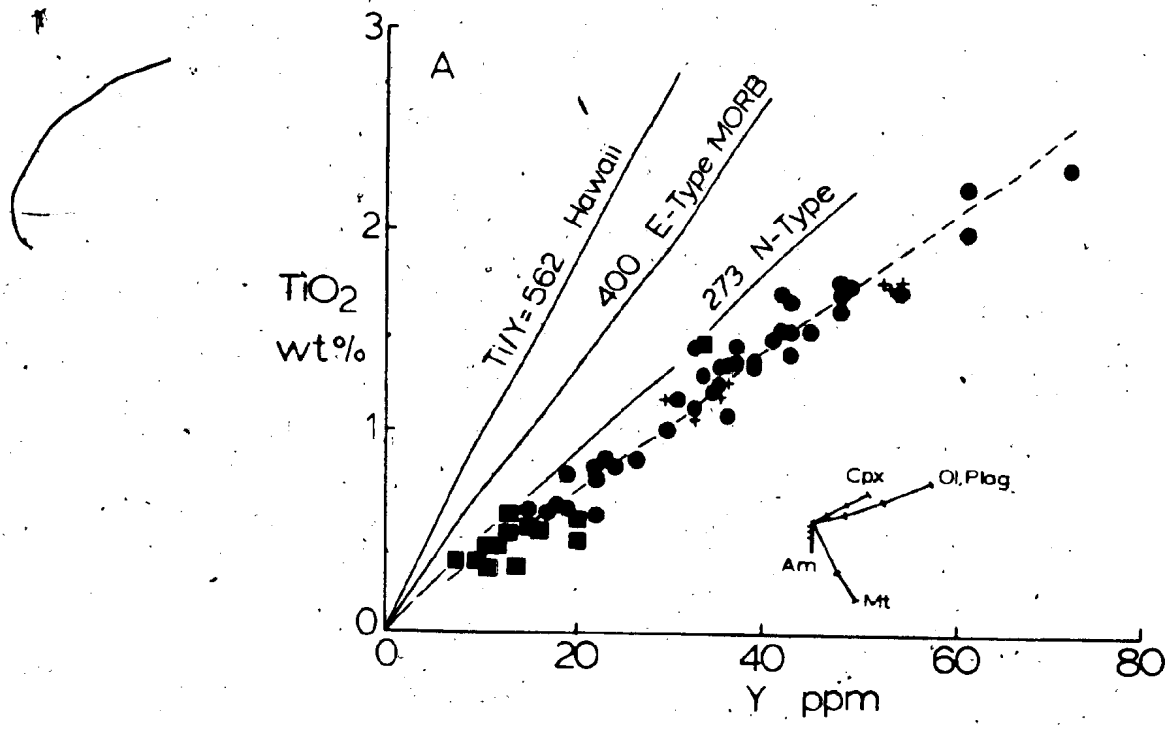
A
Ti/Y=562 Hawaii
400 E-Type MORB
273 N-Type
Cpx
Ol, Plag
Am
Mt
TiO2
wt%
Y ppm
0
1
2
3
0
20
40
60
80

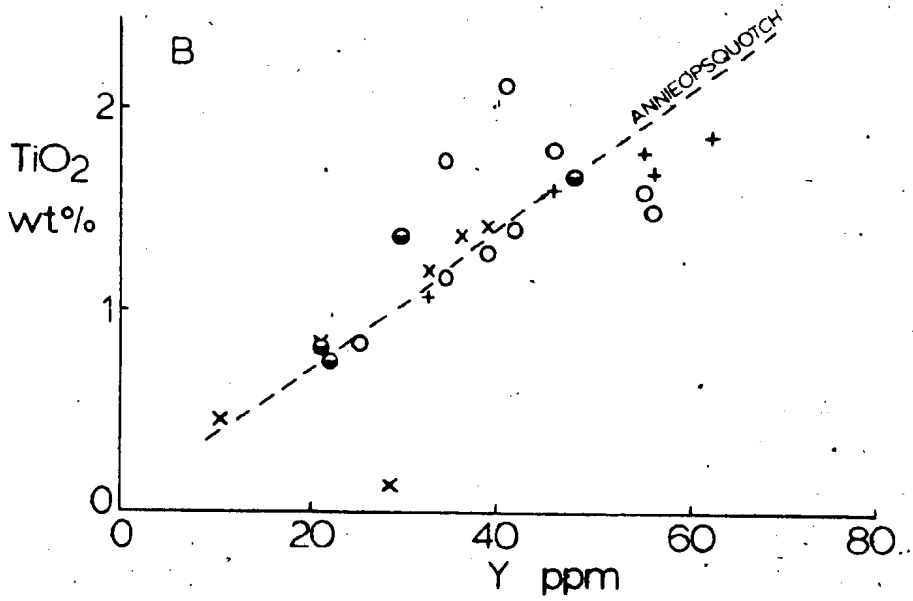
B
ANNIEOPSQUOTCH
TiO2
wt%
Y ppm
0
1
2
0
20
40
60
80

from the ophiolitic fragments of the Annieopsquotch ophiolite belt plotted on the TiO2 vs. Y diagram with the Annieopsquotch Complex trend from Figure 5.11A. The majority of samples plot on the trend but several are off to either side. One dyke, from the fragment containing sheeted dykes at Shanadithit Brook, is clearly anomalous as it is in some of the other plots.

Zr, Nb and Y abundances have been used to characterize MORB's. Ratios of these elements have been shown to vary systematically through the series N-type (normal or depleted) MORB through T-type (transitional) to E or P-type (enriched or plume-generated) MORB (LeRoex et al.,1983). N-type MORB have Zr/Nb ratios (17-64) greater than chondritic and low Zr/Y ratios (1.8-3.6) according to Erlank and Kable (1976). Zr/Nb ratios decrease and Zr/Y ratios increase through T-type to P-type MORB.

Diabase dykes of the Annieopsquotch Complex have anomalously low Zr contents. These are interpreted to be primarily a source characteristic. Nb contents vary from <1 to 5 ppm so precision is poor for this element (+/- 1 ppm, ie; +/- 100 % for many of the measurements). The Nb data may represent minimum estimates and Zr/Nb ratios then may be maximum estimates. Keeping these qualifications in mind, Zr/Nb ratios for the diabase dykes vary from 8 to 70 and only three samples have Zr/Nb ratios less than 20 (Figure 5.12). These are clearly in the range of N-type MORB, as P-type MORB have Zr/Nb ratios of 6 to 7 (LeRoex et al.,1983).

Figure 5.12. Y/Nb and Zr/Y vs. Zr/Nb diagrams, after LeRoex *et al.* (1983), for diabase dykes of the Annieopsquotch Complex. Best fit line (short dashes) to the dyke data drawn by eye. Trend of N-type MORB from the southwest Indian Ridge (LeRoex *et al.*, 1983) shown by long- dashed line.

Annieopsquotch dyke trend is similar to that of N-type MORB but is displaced to lower Zr contents. Note: Accuracy of the Nb analyses is +/- 1 ppm, so at low abundances the uncertainty in the absolute value is large.

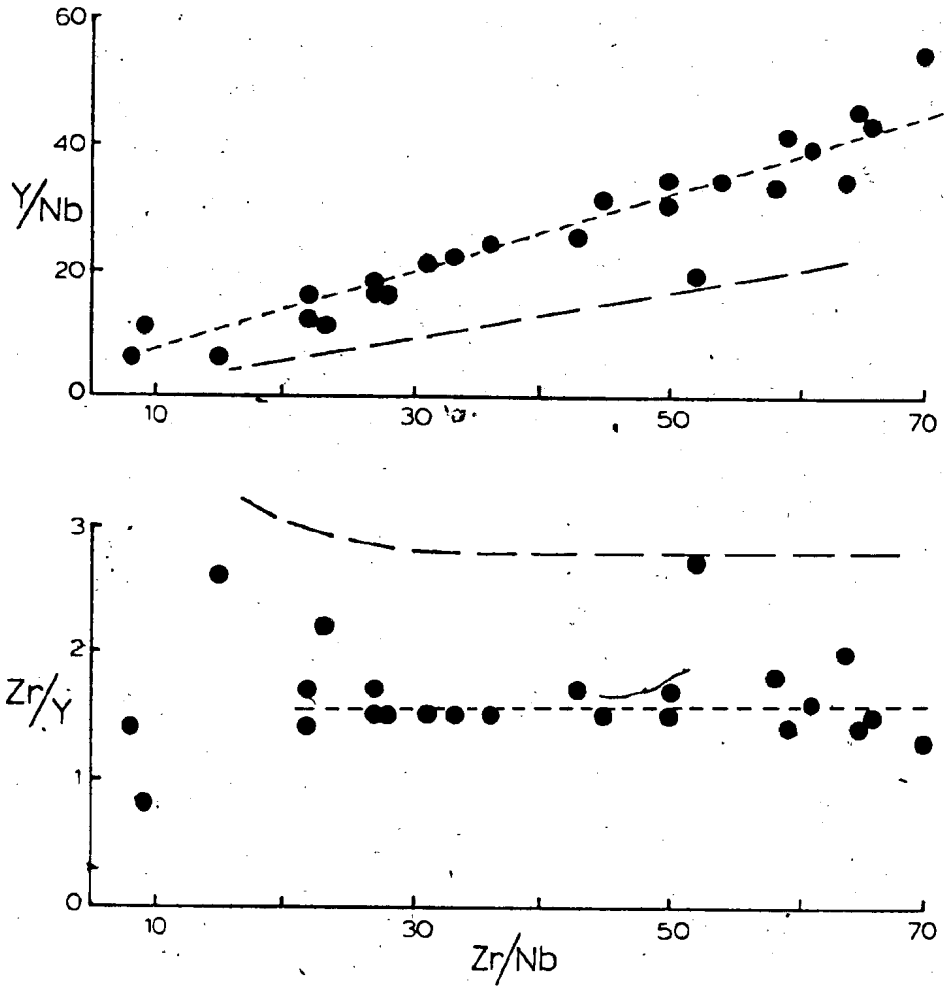
60
40
20
0
Y/Nb
10
30
50
70
3
2
1
0
Zr/Y
10
30
50
70
Zr/Nb

Zr/Y ratios for diabase dykes of the Annieopsquotch Complex vary from 0.8 to 2.7 with most in the range 1.3 to 1.7 (Figure 5.12). These low Zr/Y are expected for N-type MORB (Erlank and Kable, 1976), and are significantly lower than those characteristic of T-type (3.6-6.2) or P-type MORB (6.1-7.9).

Y/Nb ratios are highest for N-type MORB (5-20), intermediate for T-type (1.5-4) and approximately 1 for P-type (LeRoex et al.,1983). Y/Nb ratios for Annieopsquotch diabase dykes are in the range 6 to 54 (Figure 5.12). Some high ratios may be overestimates due to the poor precision of the Nb measurement. Nevertheless, even the lowest values are clearly in the range of N-type MORB.

5.8 CLOSED OR OPEN SYSTEM FRACTIONATION ?

5.8.1 Introduction

Diagrams involving FeO* or FeO*/MgO vs. Zr were used by Stern and de Wit (1980) to distinguish between the Sarmiento Complex, which shows evidence of closed system fractionation, and the Tortuga Complex which underwent open system fractionation. A steeper slope is seen in Figure 5.13 for the Sarmiento Complex because with closed system fractionation the Fe content of the magma increases continuously. In an open system (O'Hara, 1977) new inputs of magma buffer the FeO*/MgO ratio by introducing more

Figure 5.13A,B. FeO* vs. Zr and FeO*/MgO vs. Zr diagrams (after Stern and de Wit, 1980), on which are plotted the differentiation trends for the Tortuga and Sarmiento Complexes of Chile. The former underwent open system fractionation and shows large increases in Zr content of the rocks with small increases in FeO*. The latter underwent closed system fractionation and shows smaller increases in Zr content over the same range of FeO*. The trend defined by gabbros, diabase dykes and pillow lava of the Annieopsquotch Complex (fitted by eye) shows small increases in Zr content with increase in FeO*, suggestive of closed system fractionation.

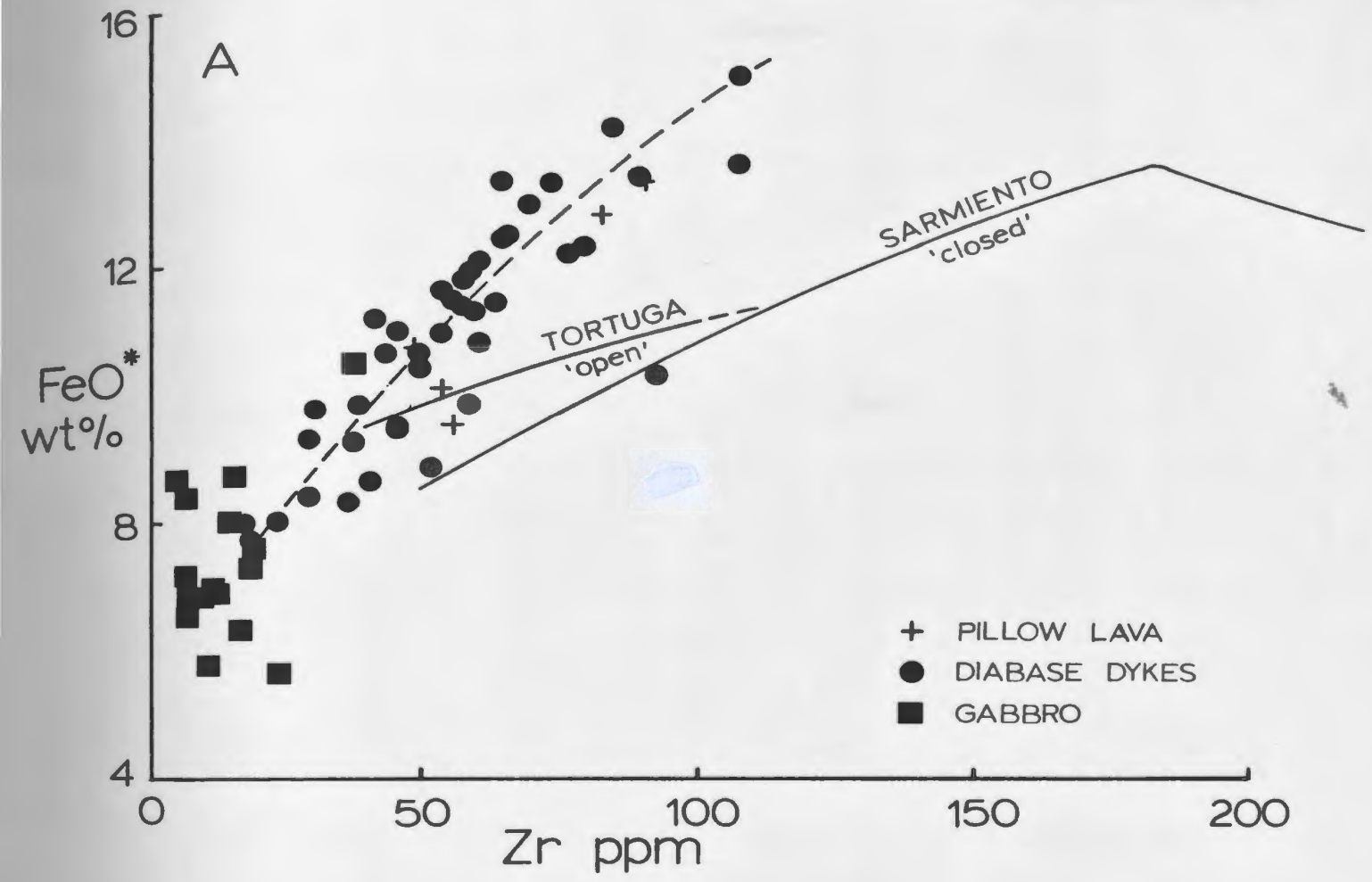
A
16
12
8
4
FeO*
wt%
0
50
100
150
200
Zr ppm
SARMIENTO
'closed'
TORTUGA
'open'
+ PILLOW LAVA
● DIABASE DYKES
■ GABBRO

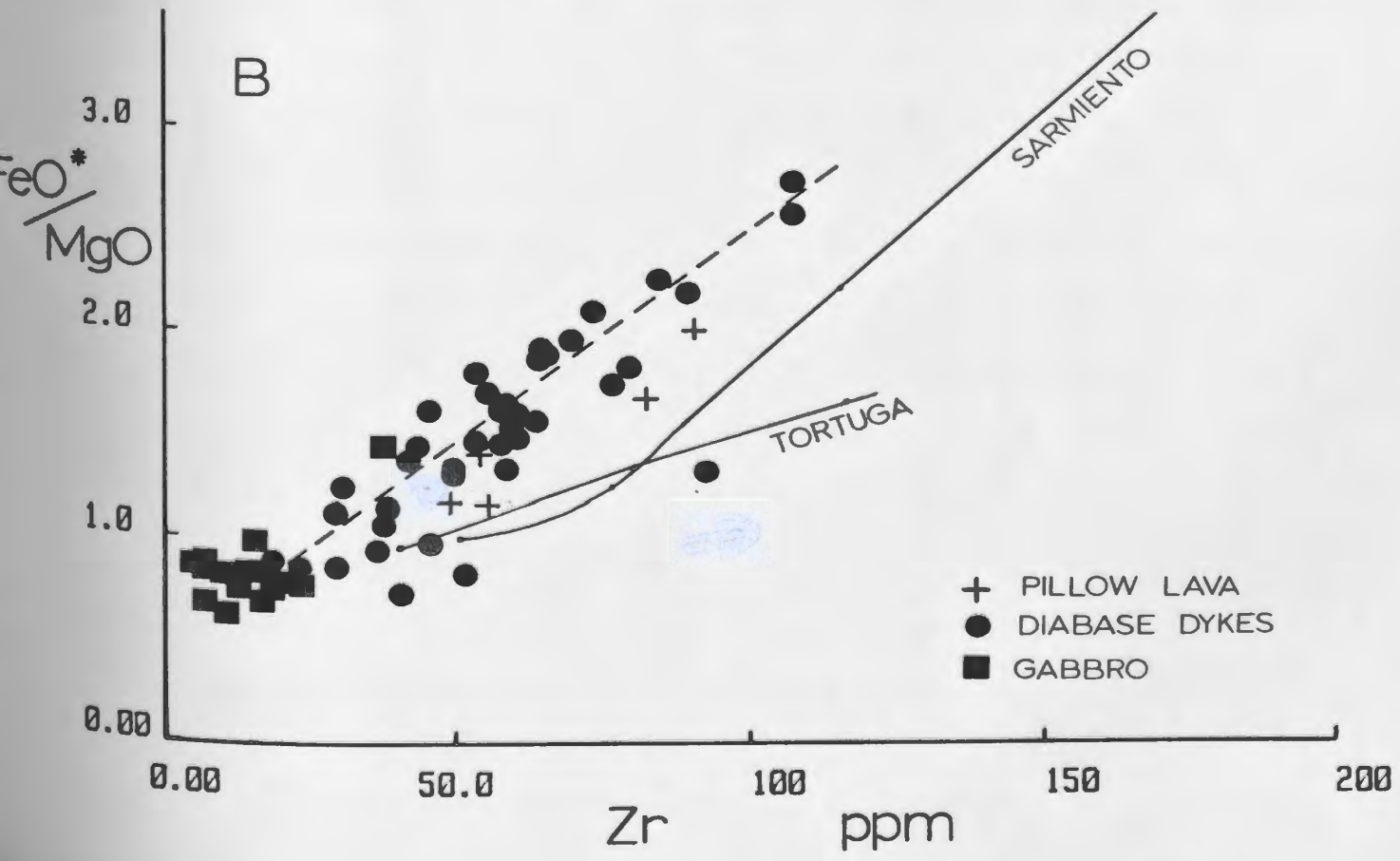
B
3.0
2.0
1.0
0.00
FeO*
MgO
0.00
50.0
100
150
200
Zr ppm
SARMIENTO
TORTUGA
+ PILLOW LAVA
● DIABASE DYKES
■ GABBRO

primitive (higher MgO) magma into the fractionating magma. Zr, however, continues to build up in the magma (if it is not being removed by a fractionating phase).

5.8.2 Annieopsquotch Trend - Size of Magma Chambers

Diabase dykes of the Annieopsquotch Complex define a trend (fitted by eye in Figure 5.13) that is steep, comparable to that of the Sarmiento Complex. It is fixed at its low end by the gabbro analyses, and the pillow lava of the Complex also plot on the trend. The entire trend is shifted to lower Zr contents than that of the Sarmiento Complex.

Closed system fractionation has been related to the size and position of magma chambers beneath a spreading ridge by Stern and de Wit (1980). They suggested that at a slow spreading ridge both open and closed system magma chambers would occur, the former being located below the axial centre of the rift valley and thus most likely to receive new batches of magma from the mantle. Closed system magma chambers would occur peripherally. The result, as observed within the Mid-Atlantic rift valley by Bryan and Moore (1977), would be a greater abundance of more fractionated lavas erupted along the flanks of the rift valley.

Stern and de Wit (1980) suggested that an open system magma chamber generally occurs beneath a fast spreading ridge where magma supply is sufficiently frequent. This is consistent with the geophysical evidence for a large magma

chamber beneath the fast spreading East Pacific Rise (Orcutt et al.,1975).

The evidence from the major and trace element geochemistry of diabase dykes of the Annieopsquotch Complex is compatible with closed system fractionation, as noted above, and therefore with the presence of small, discrete magma chambers in the plutonic zone.

5.9 GEOCHEMICAL INDICATORS OF SPREADING RATE

The TiO2 content of lavas has been used as an indicator of spreading rate by Nisbet and Pearce (1977) and Gale and Pearce (1982). The latter showed that different ophiolites in the Norwegian Caledonides have different mean TiO2 contents that increase from north to south.

TiO2 contents of diabase dykes and pillow lavas from the Annieopsquotch Complex and the other ophiolitic fragments are plotted with those of Norwegian ophiolite lavas from Gale and Pearce (1982) in Figure 5.14A. While the Annieopsquotch data show a wide distribution, the mean is 1.26 wt. %, lower than that of Spitzbergen or Lokken; the slow spreading centre ophiolites of Norway.

A diagram using Zr/Y vs. Zr has been used to estimate spreading rate by Pearce (1980) and Gale and Pearce (1982). The contours (Figure 5.14B) represent mean analyses from present day MORB localities. On these the higher Zr contents reflect greater spreading rates and the Norwegian

Figure 5.14A. Histogram of basalt TiO2 contents (after Gale and Pearce, 1982). TiO2 contents of Norwegian ophiolitic lavas are shown on the lower five plots, and those of diabase dykes (white) and pillow lavas (black) of the Annieopsquotch Complex and other ophiolitic fragments (diagonal lines) are shown at the top. Mean TiO2 contents and the number of analyses (in brackets) are shown at the right. The mean TiO2 content is the lowest for the Annieopsquotch Complex and, by the correlation of Nisbet and Pearce (1977), would imply that it formed at a slow spreading ridge.

Figure 5.14B. Zr/Y vs. Zr diagram (after Pearce, 1980), contoured according to spreading rate based on present day MORB localities. Fields of Norwegian ophiolites shown indicate the same relative spreading rate as do their TiO2 contents. Diabase dykes and pillow lava of the Annieopsquotch Complex are widely scattered on this plot and have lower Zr contents than the Norwegian lavas. The star represents the average of the Annieopsquotch diabase dyke data (Zr/Y= 1.6, Zr= 57 ppm)

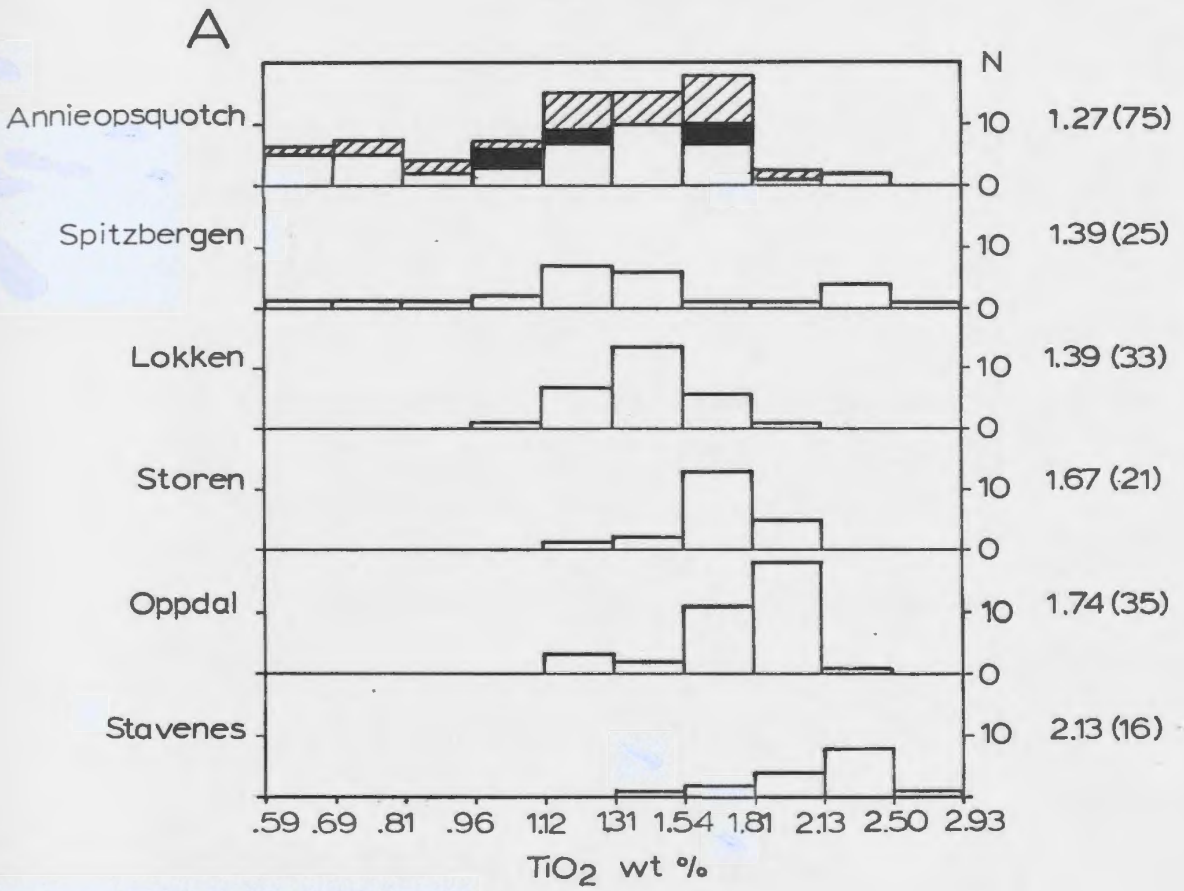
A
N
Annieopsquotch
10
0
1.27(75)
Spitzbergen
10
0
1.39(25)
Lokken
10
0
1.39 (33)
Storen
10
0
1.67 (21)
Oppdal
10
0
1.74 (35)
Stavenes
10
2.13 (16)
.59 .69 .81 .96 1.12 1.31 1.54 1.81 2.13 2.50 2.93
TiO2 wt %

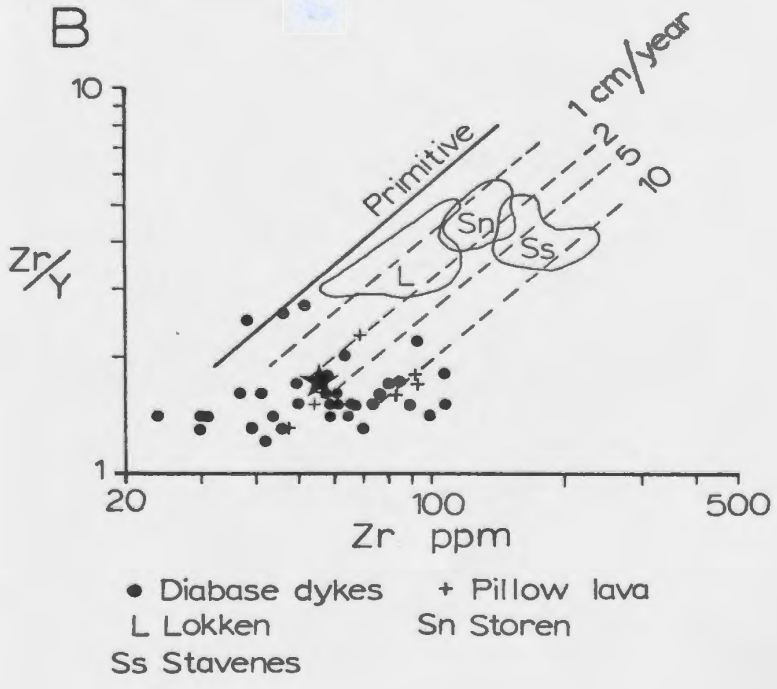
B
10
1
Zr/Y
20
100
500
Zr ppm
1 cm/year
2
5
10
Primitive
Sn
Ss
L
• Diabase dykes
+ Pillow lava
L Lokken
Sn Storen
Ss Stavenes

ophiolite lavas plotted on this diagram have the same relative spreading rates as were determined by their TiO2 contents.

Analyses of diabase dykes and pillow lava from the Annieopsquotch Complex, plotted on Figure 5.14B, show a wide scatter and have lower Zr contents than any of the Norwegian ophiolites. A mean value for all dykes and lavas is shown by the star, however it is not considered to be of great significance in identifying the spreading rate.

In summary, the author is skeptical of the validity of using TiO2 or Zr contents of basalts to infer relative (or even worse; absolute!) spreading rates. The former does show some regularity, however some of the Norwegian plots contain only a small number of analyses. Zr contents certainly do not give a meaningful result in the case of the Annieopsquotch Complex.

5.10 GEOCHEMISTRY OF TRONDHJEMITES

5.10.1 Major Elements

The major element chemistry of trondhjemites of the Annieopsquotch Complex is quite variable (Table 5.8). SiO2 contents vary from 52.6 to 73.5 wt. %, a very large range which is partly matched inversely by Al2O3 contents; 13.6 to 26.6 wt. %. The total SiO2 + Al2O3 range is thus more limited, varying from 76.6 to 87.1 wt. %.

The Al2O3 contents of three of the four samples from

TABLE 5.8. MAJOR AND TRACE ELEMENT ANALYSES OF TRONDHJEMITE AND DIORITE FROM THE ANNIEOPSQUOTCH COMPLEX AND TRONDHJEMITE DATED FROM BAY OF ISLANDS COMPLEX

	79D 163-2	79D 250	80D[1] 222	80D[1] 223-1	80D 223-2	80D[1] 257
SiO_2	73.5	52.6	53.7	63.6	49.9	76.6
TiO_2	0.28	0.41	0.90	0.63	1.15	0.15
Al_2O_3	13.6	26.6	22.9	16.3	15.5	12.6
Fe_2O_3	0.88	0.24	2.08	1.44	3.03	1.36
FeO	1.30	0.58	2.09	3.15	7.58	0.89
MnO	0.01	0.02	0.05	0.08	0.21	0.01
MgO	0.85	1.22	2.54	1.85	6.73	0.13
CaO	3.60	13.2	9.14	6.25	11.7	0.49
Na_2O	4.1	3.8	4.6	4.2	2.3	6.6
K_2O	0.64	0.07	0.81	0.17	0.18	0.11
P_2O_5	0.09	0.10	0.23	0.11	0.09	0.04
L.O.I.	0.51	0.30	1.20	0.65	0.88	0.43
Total	99.36	99.14	100.24	98.43	99.25	99.41
Rb	15	0	28	2	3	0
Sr	230	319	400	132	112	31
Y	30	95	131	63	65	143
Zr	137	610	449	468	38	264
Nb	1	7	3	4	1	7
Zn	29	26	34	50	93	22
Cu	8	3	0	0	74	4
Ni	3	8	13	9	83	2
Ba	726	46	240	106	69	81
V	24	44	98	146	343	3
Cr	0	0	9	0	51	0

[1] Samples for which U/Pb (zircon) ages determined (Chapter 7).

0= not detected

the Annieopsquotch Complex fall in the field of high-Al2O3 trondhjemites (>16 wt. % Al2O3) of Barker et al. (1976). Malpas (1979a) suggested that high Al2O3 contents of trondhjemites from the Bay of Islands Complex might result from accumulation of plagioclase.

CaO varies with Al2O3, as both are components of the major rock forming mineral; plagioclase.

Na2O and K2O contents have been used to distinguish between continental and oceanic silicic rocks since the early work of Coleman and Peterman (1976). On a plot of K2O vs. SiO2 they outlined a field of oceanic plagiogranite with lower contents of K2O than continental trondhjemites and granophyres. Malpas (1979a) found that Bay of Islands trondhjemites plotted in two distinct groups, one at lower K contents than the oceanic plagiogranite field and the other straddling the oceanic-continental boundary. He suggested that plagioclase accumulation might have effected this separation. The four Annieopsquotch samples are widely scattered on the K2O vs. SiO2 diagram (Figure 5.15); only one sample, 80HPAD223-1, plots squarely in the oceanic plagiogranite field. Two of these samples are dyke material which do not appear to have accumulated plagioclase crystals.

Na, K and Si are mobile elements during hydrothermal processes and it is unlikely that their concentrations in oceanic plagiogranites will serve to elucidate their relationship to the gabbroic rocks. More likely, differing Na and K contents are due in part to interaction with a

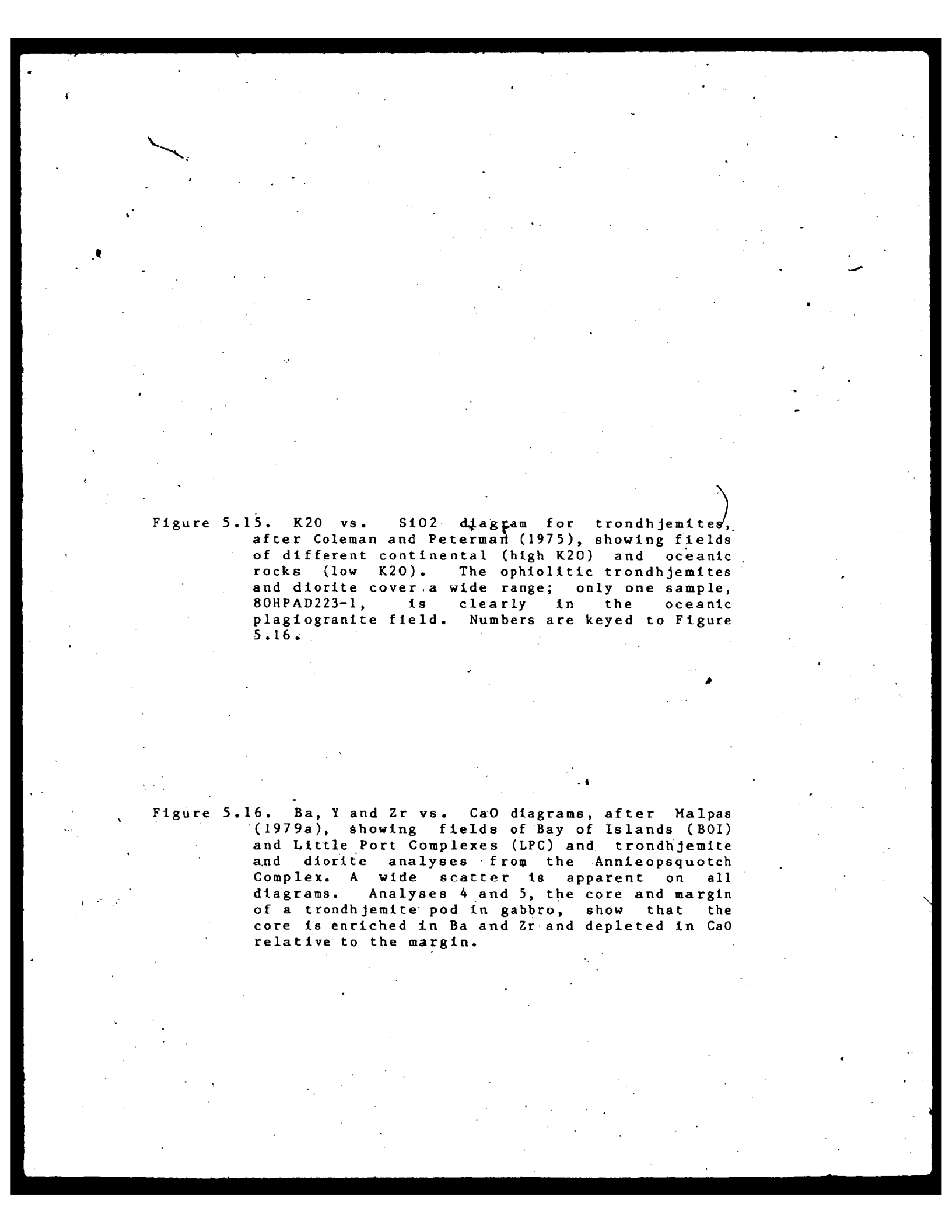

Figure 5.15. K_2O vs. SiO_2 diagram for trondhjemites, after Coleman and Peterman (1975), showing fields of different continental (high K_2O) and oceanic rocks (low K_2O). The ophiolitic trondhjemites and diorite cover a wide range; only one sample, 80HPAD223-1, is clearly in the oceanic plagiogranite field. Numbers are keyed to Figure 5.16.

Figure 5.16. Ba, Y and Zr vs. CaO diagrams, after Malpas (1979a), showing fields of Bay of Islands (BOI) and Little Port Complexes (LPC) and trondhjemite and diorite analyses from the Annieopsquotch Complex. A wide scatter is apparent on all diagrams. Analyses 4 and 5, the core and margin of a trondhjemite pod in gabbro, show that the core is enriched in Ba and Zr and depleted in CaO relative to the margin.

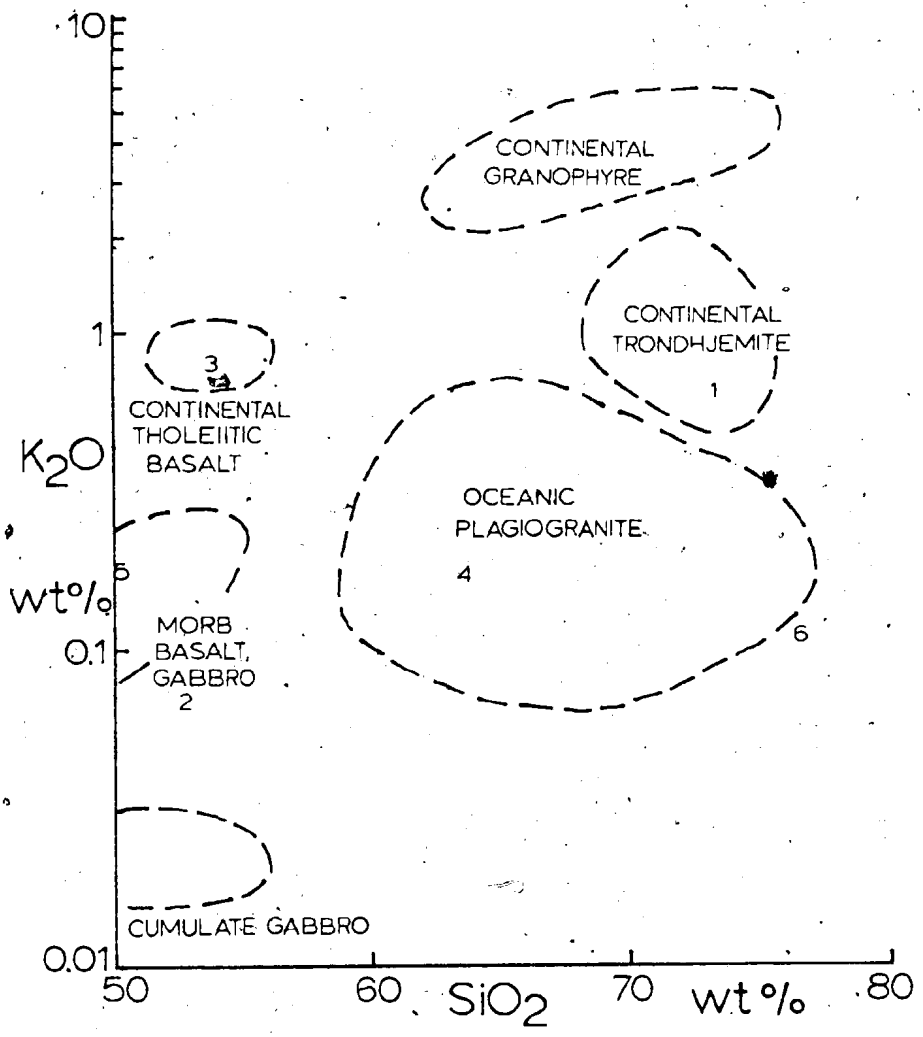
10
1
0.1
0.01
K_2O
wt%
CONTINENTAL GRANOPHYRE
CONTINENTAL TRONDHJEMITE
1
3
CONTINENTAL THOLEIITIC BASALT
OCEANIC PLAGIOGRANITE
4
5
MORB BASALT, GABBRO
2
6
CUMULATE GABBRO
50
60
SiO_2
70
wt%
80

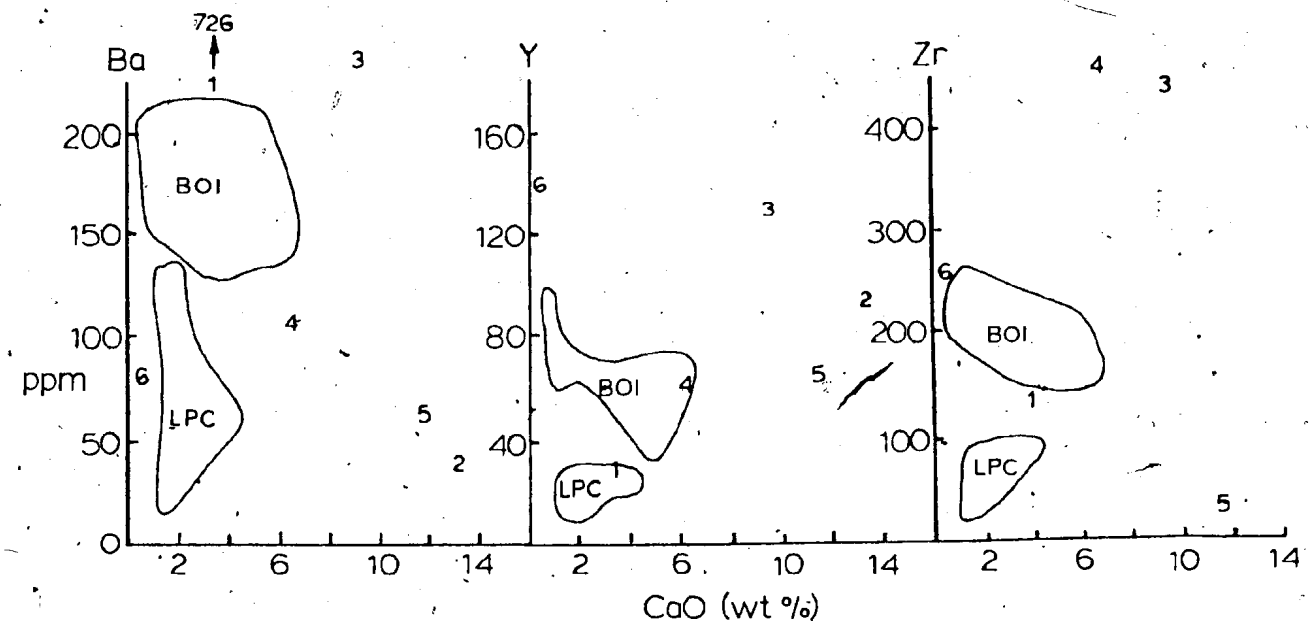

1 79D163-2
2 79D250
3 80D222
4 80D223-1
5 80D223-2
6 80D257

volatile phase. Na/K ratios in the four samples are variable; 5.6, 46.7, 5.0 and 22.9.

5.10.2 Trace Elements

Trace element contents of the four trondhjemite samples are also quite variable. Rb contents, 0 to 28 ppm, are proportional to K2O content and are likely redistributed.

Sr, also a 'mobile' element, is enriched in trondhjemite relative to the gabbros analysed (Table 5.2, maximum Sr in gabbro; 125 ppm) despite extensive plagioclase fractionation to form the gabbroic rocks. Sr is presumably contained in the feldspar in the trondhjemites but its high concentration, especially in samples 79HPAD250 and 80HPAD222, may be due to either hydrothermal effects or plagioclase accumulation.

Y and Zr, both 'immobile' incompatible trace elements are enriched in trondhjemite relative to gabbro (Table 5.2, maximum Y; 33 ppm, Zr; 38 ppm), as expected. It would appear from the high contents of these elements that samples 79HPAD250 and 80HPAD222 are the most highly differentiated. However they are lowest in SiO2 and highest in Al2O3 and CaO. This is a reflection of the near monomineralic nature of the rock, but might reflect leaching of Si with K and retention of 'immobile' Al, Zr and addition of Na and Ca by a volatile phase.

Ba is variable and 'mobile'. Malpas (1979a) used Ba, Y and Zr, each plotted against CaO to separate

trondhjemites from the Bay Islands Complex and the Little Port Complex. The former were found to have higher contents of all three trace elements, however Ba contents show the most overlap between suites. Sample 80HPAD257 plots with the Little Port Complex on the Ba vs. CaO diagram but with the Bay of Islands Complex samples on all other diagrams (Figure 5.16). Likewise, two Annieopsquotch trondhjemites, 79HPAD250 and 80HPAD223-1, plot with the Little Port Complex samples on the diagram involving Ba, but with Bay of Islands samples on the Y and Zr plots, however at higher CaO contents than either of the latter.

5.10.3 Generation of Ophiolitic Trondhjemites

Dixon and Rutherford (1979) demonstrated by experiment that plagiogranite could form as an immiscible liquid from basalt of MORB chemistry. They suggested that late stage Fe-rich basaltic magma would be the host from which the silicic liquid separated, so that one might expect the two to be associated in the field. In the Annieopsquotch Complex, obvious Fe-rich gabbros (not analysed) with abundant magnetite clots occur locally at the top (southeast) of the gabbro zone and as screens within the sheeted dykes. However, these are not associated with trondhjemite bodies as far as is known. The trondhjemite breccias, full of mafic blocks, occur in average coarse grained gabbro. Therefore an origin by separation of an immiscible liquid is not thought likely for these bodies.

Sinton and Byerly (1980) described granophyric patches

in three thick basalt flows (or sills) from the western Atlantic in DSDP hole 417D. They noted that these patches have Na/K ratios greater than 10 whereas fresh silicic glasses in MORB have ratios less than 10 and higher K2O contents. The crystalline granophyre patches have far lower K contents than could be explained by crystal fractionation of basaltic magma, according to the modelling of Sinton and Byerly (1980). As the patches are essentially anhydrous, they invoked late magmatic vapour phase transport of K to explain the low K contents relative to ocean floor silicic glasses. The problem of the source of the vapour phase was not addressed by Sinton and Byerly (1980).

Gregory and Taylor (1979) suggested that the absence of K in plagiogranites may be related to exchange with seawater. Based on O isotope data, they suggested that plagiogranite in the Oman ophiolite, which has a border phase rich in xenoliths (>75%) of altered diabase, gabbro and hornfels, formed by assimilation of hydrated roof rock. They observed a ratio of 'border facies' material, which is mainly xenoliths, to plagiogranite of 2.5:1 and noted that they sit in coarse grained cumulate and hornblende gabbros.

Gregory and Taylor (1979) further suggested that the crystallization of hornblende from magma made hydrous by assimilation of hydrated roof rock makes the remaining melt become oversaturated with silica and forces it to a plagiogranite end member.

The association of hornblende-rich diorite with

trondhjemite at sample location 80HPAD223 is noted in Chapter 3 as is the occurrence of pegmatitic hornblende in the gabbro and trondhjemite itself. This mechanism, involving assimilation of hydrated diabase and gabbro blocks, therefore seems reasonable to explain the presence of some trondhjemite pods in the Annieopsquotch Complex.

Because of the effects of fluids in the generation of ophiolitic trondhjemites it is unlikely that their chemistry will show regular trends on X-Y plots. Rather they will vary with degree of assimilation of mafic blocks and interaction with and element transport by a volatile phase. Note (Table 5.8) that Na2O contents are relatively constant but K2O contents vary by an order of magnitude. The vast range of Na/K ratios recorded in the four trondhjemites analysed from the Annieopsquotch Complex therefore likely result from fluid interaction, likely superimposed on differing original K2O contents, perhaps in the range for fresh silicic glasses analysed by Sinton and Byerly (1980).

5.11 RARE EARTH ELEMENT CHEMISTRY

Rare earth element contents (REE) were determined for four gabbro, six diabase dyke, five pillow lava and two trondhjemite samples from the Annieopsquotch Complex. They are reported in Table 5.9 and plotted, normalized to the chondritic values of Taylor and Gorton (1977), in Figure

5.17.

An increase in REE content occurs through the sequence; gabbro,diabase dykes and pillow lava to trondhjemite. Lava and dyke patterns largely overlap. The trondhjemite samples analysed are those used to determine U/Pb (zircon) dates for the Complex (Chapter 7).

5.11.1 Diabase Dykes and Pillow Lava

Eleven samples were analysed that can reasonably be interpreted to represent basaltic liquid compositions of the ophiolite. The dykes analysed cover the spectrum of MgO contents determined for the sheeted dyke zone (Figure 5.18). The pillow lava samples are more altered than the dykes and therefore results from them should be interpreted with some caution (Figure 5.19).

One diabase dyke and two pillow lava samples have REE patterns and abundances similar to that of the most REE enriched gabbro. Four diabase dykes have patterns that are essentially identical and they plot together in Figure 5.18. One diabase dyke, 80HPAD122, has a flat REE pattern with abundances approximately 30 times chondritic. This is the most LREE enriched sample of the dykes or lavas. Two lava samples, 80HPAD197-3 and 80HPAD231 have similar La contents but their HREE contents are slightly depleted like the other dykes. Four pillow lava samples have REE patterns that generally match those of the four similar dykes. This is to be expected because, in general, the dykes are their feeders.

TABLE 5.9 . RARE EARTH ELEMENT CONTENTS OF ROCKS OF THE ANNIEOPSQUOTCH COMPLEX

	GABBRO				DIABASE DYKES					
	79D 143	79D 144-1	79D 153-1	80D 129-1	79D 109-2	79D 237	79D 240	79D 241	80D 081	80D 122
La	3.10	.64	.37	1.23	2.89	2.20	3.50	3.43	4.21	8.21
Ce	4.82	1.04	--	3.75	11.19	5.54	11.61	11.91	13.43	21.70
Pr	.70	.52	--	.67	2.40	--	1.79	2.06	2.28	3.24
Nd	5.44	2.56	3.10	3.91	12.92	6.12	12.01	11.46	13.06	15.80
Sm	2.47	1.01	1.93	1.87	5.72	2.43	4.88	4.79	5.33	5.35
Eu	1.25	1.03	.73	1.08	2.53	1.32	2.31	2.53	1.59	1.93
Gd	1.95	2.25	2.60	2.14	6.99	3.88	6.67	6.17	6.83	6.88
Dy	1.91	1.77	3.18	2.69	7.06	4.04	7.02	7.10	7.63	8.16
Er	1.14	1.26	1.68	1.62	3.36	2.36	3.98	3.43	4.98	4.79
Yb	1.56	1.76	1.20	1.06	2.26	1.84	2.59	2.14	4.82	4.31

	PILLOW LAVA					TRONDHJEMITE	
	80D 197-3	80D 231	80D 246	81D 132-2	81D 133-1	80D 222	80D 223-2
La	5.06	7.73	3.24	.86	1.00	19.45	9.46
Ce	16.27	18.31	12.03	4.08	4.00	66.70	32.79
Pr	2.24	2.57	1.88	.73	.82	9.81	6.08
Nd	15.45	11.87	11.59	5.38	5.77	52.12	30.49
Sm	5.60	3.45	4.39	2.25	2.52	15.88	11.35
Eu	2.44	1.88	2.36	1.15	.73	4.16	4.37
Gd	6.94	4.76	5.70	3.58	3.28	17.85	12.90
Dy	6.61	4.43	5.53	4.37	4.03	17.46	9.77
Er	3.62	2.35	3.09	2.33	2.84	8.65	5.07
Yb	1.96	2.13	2.48	2.63	2.89	5.39	2.82

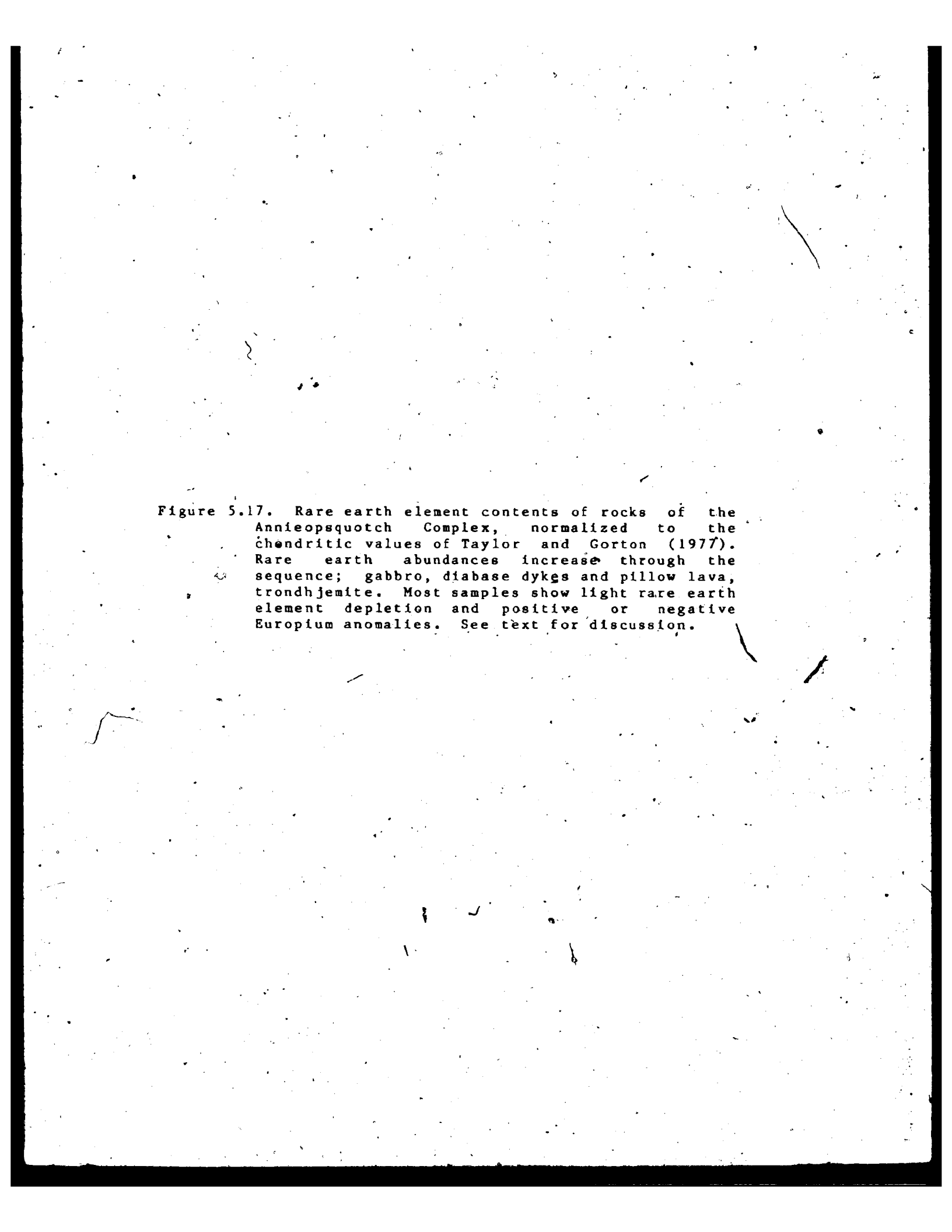

Figure 5.17. Rare earth element contents of rocks of the Annieopsquotch Complex, normalized to the chondritic values of Taylor and Gorton (1977). Rare earth abundances increase through the sequence; gabbro, diabase dykes and pillow lava, trondhjemite. Most samples show light rare earth element depletion and positive or negative Europium anomalies. See text for discussion.

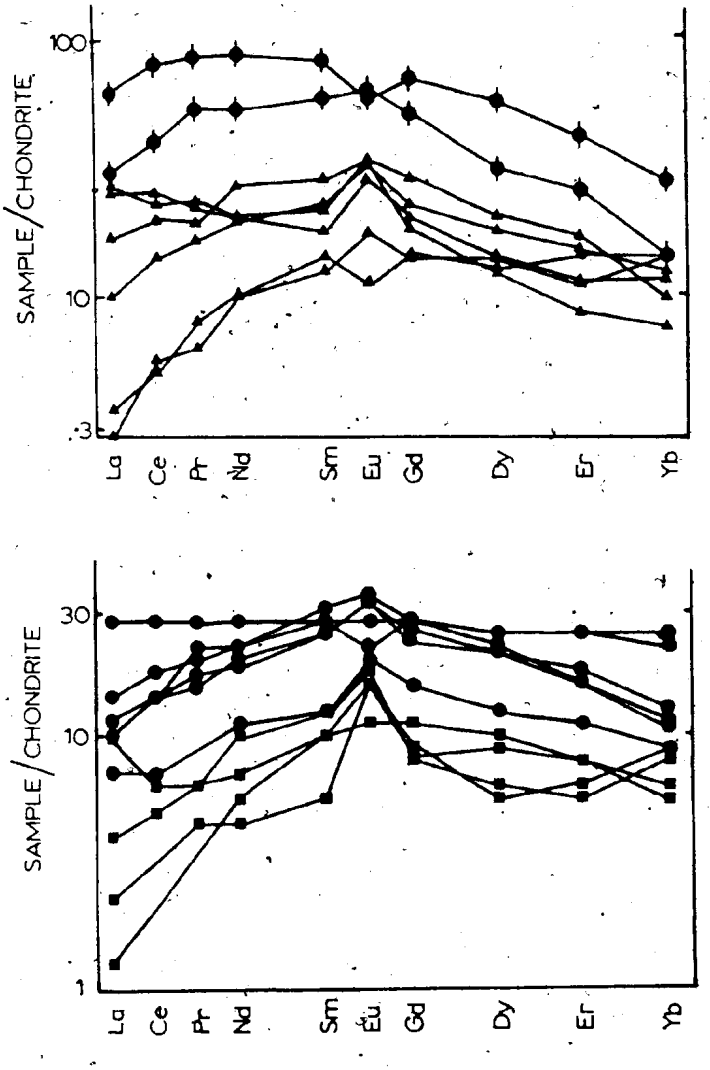
SAMPLE/CHONDRITE
100
10
.3
La
Ce
Pr
Nd
Sm
Eu
Gd
Dy
Er
Yb
SAMPLE/CHONDRITE
30
10
1
La
Ce
Pr
Nd
Sm
Eu
Gd
Dy
Er
Yb
TRONDHJEMITE
DIABASE DYKES
PILLOW LAVA
GABBRO

Figure 5.18. Rare earth element contents of six diabase dykes of the Annieopsquotch Complex, and the field for dykes and lavas of the Bay of Islands Complex (Suen et al., 1979). Patterns are similar for both, but three Annieopsquotch dykes show greater depletion of the heavy rare earth elements. Average rare earth abundances are greater in the Annieopsquotch Complex dykes. Dashed lines outline the field of MORB after Saunders and Tarney (1979).

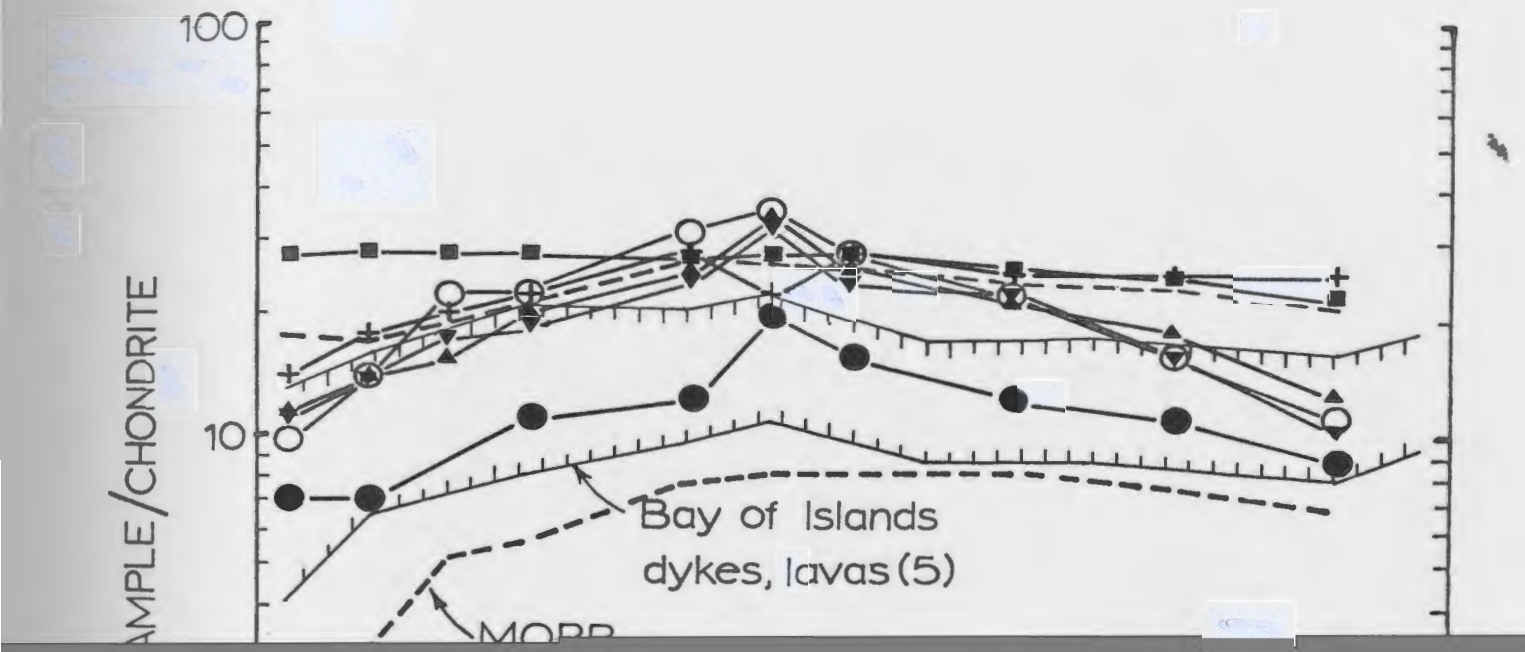
100
10
AMPLE/CHONDRITE
Bay of Islands
dykes, lavas (5)
MORB

Figure 5.19. Rare earth element contents of five samples of pillow lava of the Annieopsquotch Complex, with the field for dykes and lava of the Bay of Islands Complex (Suen et al., 1979). Patterns are similar; some samples fall above or below the field for some elements. Dashed lines outline the MORB field (Saunders and Tarney, 1979).

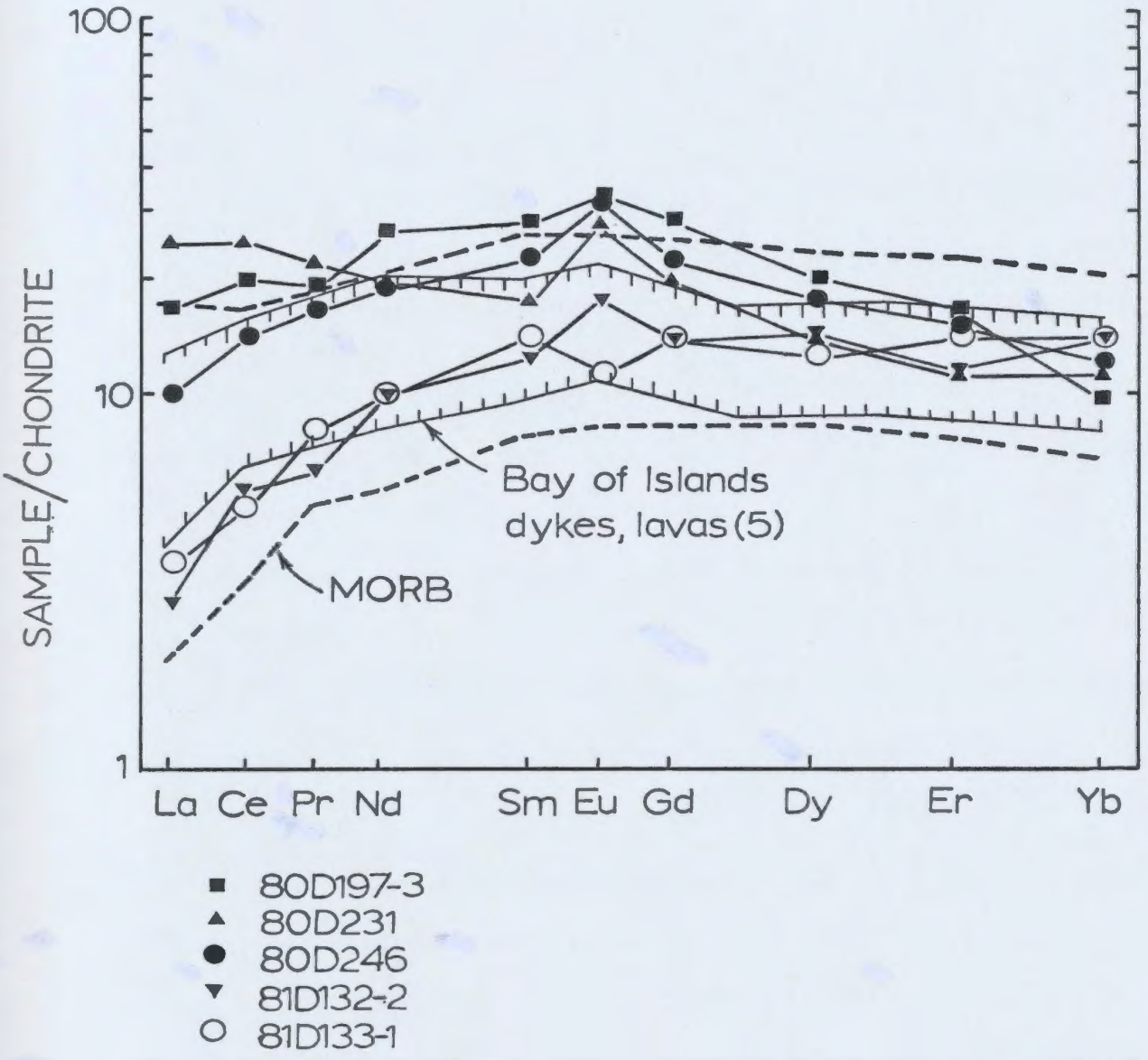
100
10
1
SAMPLE/CHONDRITE
La Ce Pr Nd Sm Eu Gd Dy Er Yb
Bay of Islands
dykes, lavas (5)
MORB
80D197-3
80D231
80D246
81D132-2
81D133-1

5.11.1.1 Light Rare Earth Element Depletion

Light rare earth element (LREE) depletion is a characteristic feature of MORB as well as the Troodos (Kay and Senechal,1976), Bay of Islands Complex (Suen et al.,1979) and other ophiolites. All but one diabase dyke and two pillow lava samples from the Annieopsquotch Complex exhibit significant LREE depletion.

The cause of this LREE depletion is a matter of controversy. Some have attributed it to seafloor alteration or metamorphism (Kay and Senechal,1976; Robertson and Fleet,1975; Herrmann et al.,1974 and Helmann et al.,1977) however, Suen et al.(1979) suggested that LREE enrichment, not depletion, should occur as a result of these processes. This was suggested by the studies of seafloor alteration by Frey et al. (1974), Ludden and Thompson (1979) and others.

To quantify the degree of alteration of rinds of pillow lava samples dredged from 23 degrees N in the Atlantic, Ludden and Thompson (1979) normalized REE contents to a constant HREE (Yb) composition; that of the pillow interior. They then calculated enrichment of the LREE in the pillow rinds over the interiors. They found that all the LREE were enriched in the rind, with no anomalous behavior of Eu. The HREE remained unaffected. These, however, were surface MORB samples; they noted that some deeper DSDP drilled samples show no such LREE enrichment and suggested that an important factor in LREE enrichment was the greater seawater: rock ratio affecting

the pillow lavas on the surface of the seafloor.

Variations are likely more radical than this however, as adjacent sections of the oceanic crust may undergo different styles of alteration dependent upon whether they are zones of influx or outflow of hydrothermal circulation (cf. Mottl, 1983 and others).

As samples from the Annieopsquotch Complex likely had different original REE concentrations and degrees of LREE enrichment, it is not resonable to normalize their Yb contents to some value and try to identify secondary enrichment of the LREE. It is impossible to know the magmatic LREE pattern and thus define the effects of alteration by seawater. It is possible that the pillow lava LREE patterns, which show the widest range of concentration and would have had greater exposure to seawater than the dykes, were affected by interaction with seawater.

La/Sm ratios can be increased by clinopyroxene fractionation (Blanchard et al.,1976) while olivine or plagioclase fractionation will simply increase the REE concentration of the magma, without enriching LREE, as these minerals exclude REE (except Eu).

Annieopsquotch dykes and lavas cluster at La/Sm ratios between 0.5 and 1.0 (Figure 5.18, 19) and at Yb contents of 1.7 to 3.0 ppm, except for two dykes, 80HPAD122 and 80HPAD081 which have higher La/Sm and Yb and higher Yb respectively. One lava, 80HPAD231 has a high La/Sm ratio. Frey et al.(1974) have demonstrated that La/Sm can be

increased by seafloor alteration. Such a process might account for the higher ratio of the two samples. Of the samples analysed by Blanchard et al.(1976), the Annieopsquotch Complex suite have La/Sm and Yb contents most similar to Type 1 basalts of DSDP Leg 37, site 335. These DSDP basalts are plagioclase - phyric and comprise all of the samples at the site and most at nearby site 332. Relatively, they have higher TiO2 and lower Mg/Mg + Fe (0.51-0.66) than other DSDP basalts studied by these authors. They rarely contain olivine phenocrysts, never clinopyroxene phenocrysts and many contain glomerocrysts of plagioclase interpreted to have been derived from the magma chamber.

Annieopsquotch dykes are likewise predominantly plagioclase- phyric and some contain glomerocrysts of plagioclase or plagioclase + clinopyroxene, often with resorbed edges. These are interpreted (Chapter 3) to be derived from the gabbro zone. In general, no certain clinopyroxene phenocrysts are present, although some subhedral grains may be. One clinopyroxene- rich dyke was observed in the Complex. It was not analysed because it is so charged with crystals it would not represent a liquid composition.

5.11.1.2 Eu Anomalies and HREE Contents

Small positive Eu anomalies occur in five pillow lava and three diabase dyke samples of the Annieopsquotch Complex. Eu anomalies have generally been interpreted to be the result of plagioclase fractionation or as a source characteristic of the melt (Ludden and Thompson, 1979). Plagioclase is the predominant phenocryst phase in the dykes but samples were chosen which had few or no phenocrysts so it is not clear if plagioclase is the cause of these anomalies.

One dyke and one pillow lava sample have small negative Eu anomalies. These could be due to depletion by plagioclase fractionation in the gabbro magma chamber that was the source of these rocks. However, these anomalies might result from seawater interaction and transport of Eu in its +2 oxidation state (cf. Sun and Nesbitt, 1978).

Some lavas and diabase dykes, as well as both trondhjemites, display a distinct heavy rare earth element (HREE) depletion in addition to the LREE depletion typical of MORBs. It is possible that this is a result of fractionation of a minor phase in the magma chamber that was the source of these liquids although no such phase was identified during the petrographic study. Because of the low abundances of REE in these rocks and possible problems with the Fryer method (1977) these patterns may be an artifact of the chemical separation (I. Gibson, pers. comm., 1984).

5.11.2 Gabbros

Gabbros have the lowest REE contents of any rocks analysed from the Annieopsquotch suite (Table 5.9) and three of the gabbro samples show LREE depleted patterns. Two gabbro samples show positive Er/Yb and two are negative, but all four Er (1.14- 1.68 ppm) and Yb values (1.06- 1.76 ppm) are tightly clustered.

Three of the gabbro samples have pronounced positive Eu anomalies. This is consistent with the field evidence for plagioclase accumulation, to varying degrees, in many of the gabbros (Chapter 3). Similar patterns, of LREE depletion with positive Eu anomalies, are reported for gabbro of the Bay of Islands Complex (Suen et al.,1979), the Troodos ophiolite (Kay and Senechal,1976) and the Point Sal ophiolite (Menzies et al.,1977) as well as others. REE contents of gabbro sampled at DSDP site 334 (Dostal and Mueke,1978) show the same pattern.

The overall higher abundances of REE in gabbros of the Annieopsquotch Complex compared to those from the Atlantic sea floor reported by Dostal and Mueke (1978) might be due to the presence of a greater proportion of trapped REE-enriched interstitial liquid in the former. Kay and Senechal (1976) first suggested this possibility for ophiolitic gabbros and further suggested that the range of original basalt chemistries from which the gabbros formed could account for the wide range of REE contents in ophiolitic gabbros.

Varying plagioclase contents of ophiolitic gabbros and

Figure 5.20. Rare earth element contents of three samples of 'high level' gabbro and one mafic granulite of the Annieopsquotch Complex. All samples contain greater rare earth abundances than Bay of Islands (Suen et al., 1979) or DSDP Leg 37 gabbros (Dostal and Mueke, 1978). The latter contain cumulate textures and orthopyroxene. The Annieopsquotch gabbros, in part, overlap the field of Bay of Islands dykes and lavas.

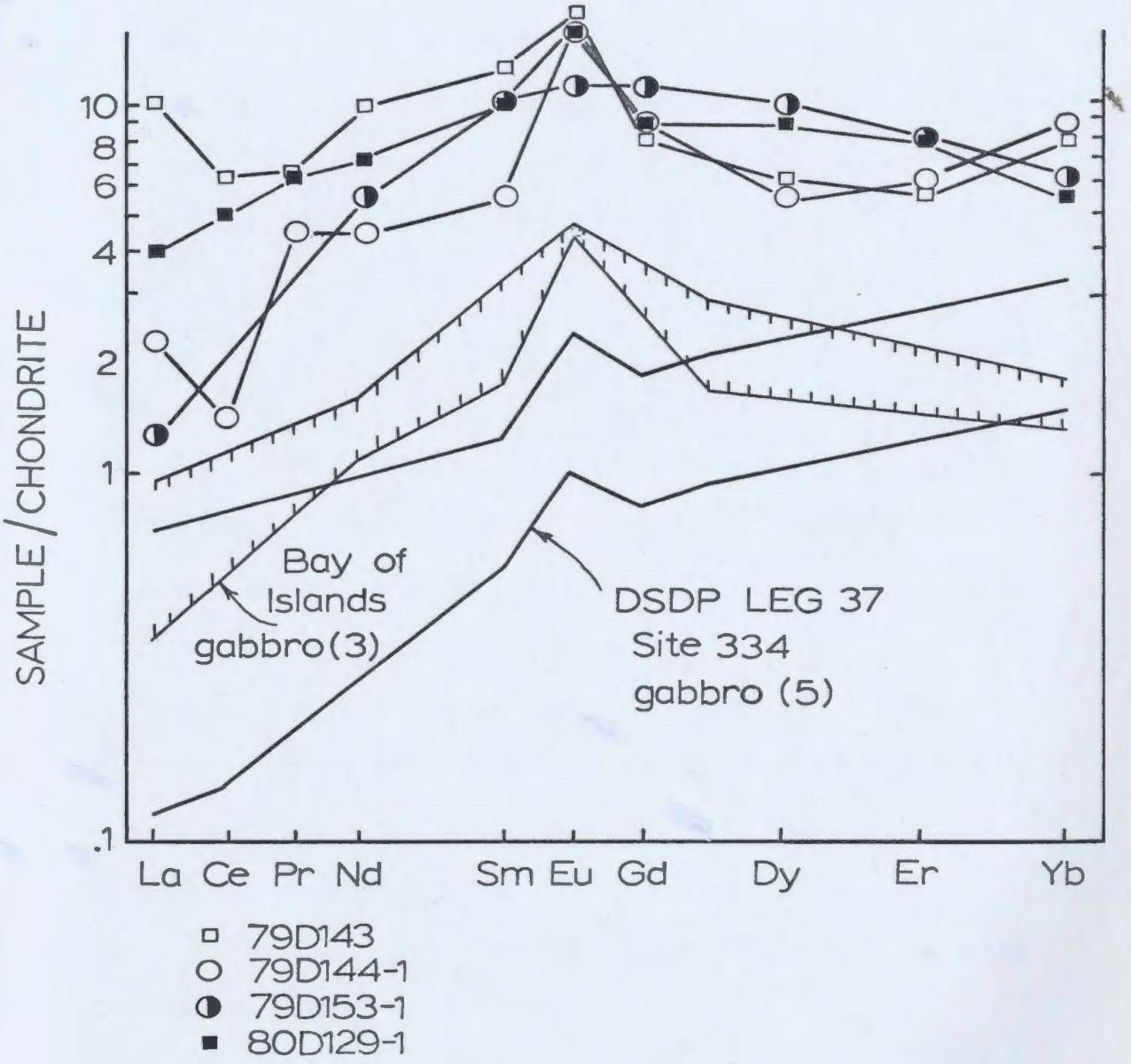
SAMPLE/CHONDRITE
10
8
6
4
2
1
.1
La Ce Pr Nd Sm Eu Gd Dy Er Yb
Bay of Islands gabbro(3)
DSDP LEG 37 Site 334 gabbro (5)
79D143
79D144-1
79D153-1
80D129-1

their relative times of crystallization within the magma chamber could account for the range of Eu anomalies observed. Suen et al. (1979) correlated the pronounced Eu anomalies in the gabbros of the Bay of Islands Complex with high Al203 contents, which are a reflection of high modal plagioclase. In the Annieopsquotch Complex, the highest Eu content likewise occurs in the gabbro with the highest Al203 content (20.7 wt. %). However the greatest Eu anomaly, relative to Sm and Gd contents, occurs in sample 79HPAD144-1 which has 17.1 wt. % Al203.

5.11.3 Equigranular Rock

Sample 79HPAD153-1, from the gabbro zone, is a medium grained rock, cut by amphibole alteration veinlets. As described in Chapter 3, it occurs in a zone which grades into average coarse grained gabbro. These areas of equigranular rock are interpreted to be either stoped blocks from the roof of the magma chamber or earlier crystallized parts of the intrusion, dehydrated and metamorphosed at temperatures in the stability range of coexisting clinopyroxene and orthopyroxene.

The REE pattern of this rock is a smooth convex upward curve with HREE contents comparable to those of the gabbros. There is no Eu anomaly and the Eu content is lower than that of the gabbros (Figure 5.20). The La content is the lowest of any sample analysed from the Annieopsquotch Complex. It is not possible to determine the protolith of this rock for certain. It was suggested

in Chapter 3 that it represents a stoped block or part of the gabbro intrusion itself. Its 'immobile' HREE contents are consistent with either suggestion as they are lower than those of any diabase dyke analysed and are in the range of the gabbros.

5.11.4 Trondhjemite

REE abundances are highest in the two trondhjemites analysed (Table 5.9). This is presumably due to concentration of these incompatible elements in the residual liquid from which these rocks crystallized. The REE pattern of the trondhjemites is similar in shape to that of the gabbros but with a larger La/Eu ratio. This could be due to greater seawater interaction. There is abundant evidence for the presence of fluids related to the trondhjemites; partially assimilated blocks of hydrated gabbro and diabase and crosscutting prehnite veins in 80HPAD222, and the occurrence of primary hornblende and biotite in 80HPAD223-1. The latter sample has a small positive Eu anomaly that could be due to minor plagioclase accumulation; euhedral plagioclase is present in the rock. Sample 80HPAD222 has a minor negative Eu anomaly that might be due to depletion by earlier plagioclase fractionation in the gabbro or due to leaching by fluids. The rock is locally strongly epidotized, presumably by fluid interaction.

Sample 80HPAD223-1 is from a pod that contains coarse grained zircon in great abundance in its core. It has the lower REE content of the two trondhjemites and shows significant HREE depletion. It is suggested that this might be due to the effect of early crystallizing hornblende and zircon taking up the HREE.

5.12 CHEMISTRY OF CLINOPYROXENES OF THE ANNIEOPSQUOTCH COMPLEX

5.12.1 Occurrences

Fresh clinopyroxene occurs in rocks of the critical zone and sheeted dyke zone of the Annieopsquotch Complex. Those samples analysed are shown on Map 1. Clinopyroxene in most samples from the gabbro zone is completely uralitized. In some cases, near the base of the zone, coarse green hornblende has formed apparently at the expense of the early fibrous amphibole of the tremolite-actinolite series.

5.12.1.1 The Critical Zone

Clinopyroxenes from the lower layered cumulate section show compositional variation with stratigraphic height (cryptic layering) in ophiolite complexes such as the Oman ophiolite (Smewing, 1981). This variation has been attributed to fractional crystallization and to influxes of new primitive picritic magma into the magma chamber at the spreading centre which replenish the elements depleted by fractional crystallization.

In the Annieopsquotch Complex the critical zone rocks are disrupted, locally metamorphosed and intruded by coarse grained gabbro. It has been suggested (Chapter 3) that only the top of the critical zone is now preserved in the Complex. No detailed sampling was done across the thin cumulate section and it is not possible to plot a section

through which clinopyroxenes display cryptic layering. However, the analyses (Table 5.10) are plotted on various major and trace element discrimination diagrams and compared to ocean floor basalts and the Bay of Islands Complex in the following sections. Analyses of co-existing orthopyroxene, olivine and plagioclase are reported in Tables 5.11, 12 and 13.

5.12.1.2 The Sheeted Dyke Zone

Clinopyroxene occurs as irregular equant grains which, in many cases, enclose plagioclase feldspar in the groundmass of diabase dykes. It is usually altered to fine grained fibrous pale green, colourless or pale brown amphibole. Many thin sections examined contain no fresh pyroxene.

Large subhedral crystals of clinopyroxene, rarely bright green chromian augite, occur in some dykes in association with clots or individual plagioclase phenocrysts. Some are interpreted to be xenocrysts from the underlying magma chambers. Analyses are reported in Table 5.14.

5.12.2 Pyroxene Quadrilateral

Pyroxenes from the critical zone plot in a restricted area of the pyroxene quadrilateral (Figure 5.21A). The Fe/Mg ratios vary between 0.12 and 0.25. All analyses are sub-calcic augites with some having a calcium content as low as $Wo_{34}En_{55}Fs_{11}$. Irregular exsolved blebs of clear

TABLE 5.10 ELECTRON MICROPROBE ANALYSES OF CLINOPYROXENES FROM THE CRITICAL ZONE

	1.	2. core	2.rim	3.	4.	5.c	5.r	6.	7.	8.	9.
SiO_2	53.70	52.82	52.05	53.34	53.21	53.14	53.28	52.93	53.00	53.16	52.33
TiO_2	0.24	0.15	0.26	0.35	0.21	0.21	0.26	0.20	0.40	0.25	0.28
Al_2O_3	2.84	3.05	2.63	2.81	2.48	3.82	2.51	3.11	2.83	2.89	3.14
Cr_2O_3	0.65	0.95	0.59	0.59	0.59	0.59	0.54	0.77	0.67	0.56	0.95
FeO*	4.16	7.13	4.68	5.36	4.31	5.30	4.23	4.43	3.60	4.11	4.00
MnO	0.09	0.05	0.09	0.11	0.09	0.11	0.09	0.07	0.08	0.07	0.09
MgO	16.42	19.27	16.90	16.59	16.69	17.88	16.30	16.48	17.26	17.05	16.99
CaO	21.77	16.47	21.43	20.86	21.66	18.88	21.66	21.38	22.30	21.53	21.73
Na_2O	0.37	0.38	0.32	0.34	0.29	0.31	0.26	0.35	0.45	0.45	0.53
Total	100.24	100.28	98.95	100.35	99.53	100.24	99.13	99.73	100.59	100.07	100.04
Si	1.949	1.919	1.924	1.942	1.946	1.922	1.956	1.933	1.921	1.933	1.910
Al^{iv}	.051	.081	.076	.058	.054	.078	.044	.067	.079	.067	.090
Al^{vi}	.069	.049	.038	.062	.052	.084	.064	.067	.041	.056	.044
Ti	.006	.003	.006	.008	.005	.005	.006	.005	.010	.006	.006
Cr	.018	.026	.017	.016	.016	.016	.016	.021	.019	.016	.027
Fe^{+2}	.125	.216	.144	.162	.131	.159	.129	.135	.108	.125	.121
Mn	.002	.001	.002	.003	.002	.003	.002	.001	.002	.002	.002
Mg	.888	1.042	.930	.899	.910	.963	.892	.897	.932	.926	.924
Ca	.847	.641	.848	.813	.849	.731	.852	.836	.866	.840	.849
Na	.025	.025	.022	.023	.020	.021	.017	.023	.031	.031	.036
Total (O_6)	3.981	4.004	4.007	3.986	3.985	3.982	3.978	3.984	4.009	3.999	4.009

	10.	11.	12.	13.	14.	15.	16.	17.	18.	19.	20.
SiO_2	52.48	52.05	53.32	53.13	53.50	52.81	52.04	51.04	54.23	50.90	52.61
TiO_2	0.38	0.21	0.18	0.16	0.14	0.16	0.53	0.20	0.09	0.28	0.20
Al_2O_3	3.07	2.95	3.41	2.59	2.93	2.67	2.78	4.30	1.60	4.70	4.04
Cr_2O_3	0.67	0.60	0.71	0.30	0.41	0.31	0.66	0.61	0.23	0.93	0.64
FeO*	3.71	4.73	4.37	4.79	4.54	3.86	5.18	6.02	10.11	4.82	5.52
MnO	0.12	0.11	0.08	0.13	0.08	0.10	0.12	0.11	0.23	0.13	0.12
MgO	17.07	18.87	17.79	19.87	18.16	17.33	17.19	18.15	23.15	17.16	18.76
CaO	22.39	19.71	20.57	18.79	19.94	22.03	20.53	18.00	10.93	19.84	18.37
Na_2O	0.46	0.30	0.29	0.16	0.21	0.19	0.37	0.16	0.17	0.21	0.16
Total	100.35	99.53	100.72	99.92	99.91	99.46	99.40	98.59	100.74	98.97	100.42
Si	1.909	1.905	1.923	1.925	1.939	1.934	1.914	1.884	1.951	1.875	1.900
Al^{iv}	.091	.095	.077	.075	.061	.066	.086	.116	.049	.125	.100
Al^{vi}	.040	.031	.067	.034	.063	.049	.034	.070	.018	.078	.072
Ti	.009	.005	.004	.004	.003	.004	.014	.005	.002	.007	.005
Cr	.019	.017	.020	.008	.011	.008	.018	.017	.006	.026	.018
Fe	.112	.144	.131	.145	.137	.118	.158	.185	.304	.148	.166
Mn	.003	.003	.002	.003	.002	.002	.003	.003	.006	.003	.003
Mg	.925	1.029	.956	1.073	.980	.945	.942	.999	1.241	.941	1.010
Ca	.872	.772	.794	.729	.774	.864	.808	.712	.421	.782	.710
Na	.032	.021	.019	.010	.014	.013	.026	.011	.011	.014	.011
Total (O_6)	4.012	4.022	3.993	4.006	3.984	4.003	4.003	4.002	4.009	3.999	3.995

Analyses 1-6: 79D032-3, 7-10: 79D039-2, 11-12: 79D263-4, 13-15: 79D269-3, 16: 79D265-5, 17-18: 79D272-2; two spots on zoned grain, 19-20: 79D272-2; two spots on zoned grain.

* Total Fe as FeO

TABLE 5.10 ELECTRON MICROPROBE ANALYSES OF CLINOPYROXENES FROM THE CRITICAL ZONE

	21.	22.	23.	24.	25.	26.	27.	28.	29.	30.	31.
SiO_2	51.00	52.14	52.12	52.02	51.46	52.25	50.95	51.48	51.58	52.16	50.21
TiO_2	0.20	0.23	0.20	0.21	0.19	0.22	0.79	0.47	0.55	0.65	0.58
Al_2O_3	4.36	3.76	3.68	3.52	3.50	3.87	2.64	2.58	2.83	3.03	2.50
Cr_2O_3	0.66	0.66	0.56	0.55	0.54	0.79	0.42	0.39	0.49	0.61	0.39
FeO*	4.98	6.49	6.54	6.98	6.38	6.16	7.38	6.30	6.34	6.21	7.45
MnO	0.10	0.18	0.14	0.14	0.14	0.11	0.14	0.14	0.12	0.16	0.16
MgO	17.92	18.63	18.46	18.83	18.54	18.64	16.81	16.44	16.01	16.21	17.32
CaO	19.66	17.73	17.68	17.46	18.19	17.89	19.93	20.98	20.95	21.69	19.69
Na_2O	0.16	0.16	0.18	0.17	0.19	0.21	0.30	0.28	0.28	0.28	0.28
Total	99.04	99.98	99.56	99.88	99.13	100.14	99.36	99.06	99.15	101.00	98.58
Si	1.876	1.898	1.906	1.901	1.897	1.897	1.897	1.913	1.915	1.902	1.886
Al^{iv}	.124	.102	.094	.099	.103	.103	.103	.087	.085	.098	.110
Al^{vi}	.065	.059	.064	.052	.048	.062	.012	.025	.038	.031	----
Ti	.005	.005	.005	.005	.004	.005	.021	.013	.015	.017	.015
Cr	.018	.018	.016	.015	.015	.022	.012	.011	.014	.017	.011
Fe	.153	.197	.199	.212	.196	.186	.229	.195	.196	.189	.233
Mn	.002	.005	.004	.004	.004	.003	.004	.003	.003	.004	.004
Mg	.982	1.010	1.005	1.025	1.019	1.009	.932	.911	.886	.881	.969
Ca	.774	.691	.692	.683	.718	.696	.794	.835	.832	.848	.792
Na	.011	.010	.013	.012	.013	.014	.022	.020	.020	.019	.020
Total (O_6)	4.010	3.991	3.998	4.008	4.017	3.997	4.026	4.013	4.004	4.006	4.040

	32.	33.	34.	35.	36.	37.	38.	39.	40.	41.	42.
SiO_2	51.41	50.91	53.24	52.71	52.52	51.59	51.72	52.41	51.79	52.67	51.79
TiO_2	0.62	0.52	0.26	0.23	0.21	0.24	0.23	0.50	0.21	0.51	0.55
Al_2O_3	2.68	2.54	3.12	3.17	3.12	3.27	3.00	2.43	3.34	2.13	2.02
Cr_2O_3	0.49	0.39	0.78	0.81	0.75	0.84	0.82	0.39	1.09	0.21	0.27
FeO*	6.54	6.36	4.70	5.35	5.20	4.93	4.79	5.31	4.33	5.67	5.71
MnO	0.13	0.14	0.07	0.11	0.08	0.09	0.09	0.10	0.11	0.09	0.12
MgO	16.46	16.58	17.20	17.70	18.54	16.29	17.43	17.02	16.46	16.64	16.06
CaO	21.23	21.00	20.52	19.41	18.62	21.34	20.43	21.30	21.69	20.96	22.18
Na_2O	0.27	0.27	0.28	0.32	0.21	0.31	0.31	0.31	0.34	0.28	0.40
Total	99.83	98.71	100.17	99.81	99.25	98.90	98.82	99.77	99.36	99.16	99.10
Si	1.900	1.902	1.933	1.923	1.921	1.911	1.912	1.926	1.905	1.943	1.926
Al^{iv}	.100	.098	.067	.077	.079	.089	.088	.074	.095	.057	.074
Al^{vi}	.016	.012	.066	.059	.055	.053	.042	.030	.050	.035	.013
Ti	.016	.014	.006	.005	.005	.006	.006	.013	.005	.014	.015
Cr	.014	.011	.022	.022	.021	.023	.023	.011	.031	.005	.007
Fe	.202	.198	.142	.163	.159	.152	.147	.163	.132	.174	.177
Mn	.003	.003	.001	.003	.002	.002	.002	.002	.003	.002	.003
Mg	.906	.923	.930	.962	1.010	.899	.960	.932	.902	.915	.889
Ca	.840	.840	.798	.758	.729	.847	.809	.837	.855	.828	.883
Na	.018	.019	.019	.022	.014	.021	.021	.021	.023	.019	.028
Total (O_6)	4.015	4.020	3.984	3.994	3.995	4.003	4.010	4.009	4.001	3.992	4.015

Analyses 21-26: 79D272-2, 27-33: 80D143-5, 34-39: 79D263-3 bright green grains, 39 encloses orthopyroxene blebs. 40-42: 80D133-5.

* Total Fe as FeO

TABLE 5.10 ELECTRON MICROPROBE ANALYSES OF CLINOPYROXENES FROM THE CRITICAL ZONE

	43.	44.	45.	46.	47.	48.	49.	50.	51.	52.	53.
SiO_2	52.60	52.32	50.73	50.12	51.71	51.31	51.33	50.94	51.34	51.16	52.95
TiO_2	0.32	0.88	0.44	0.51	0.44	0.70	0.47	0.59	0.58	0.71	0.29
Al_2O_3	1.91	2.55	3.30	3.63	2.58	3.12	3.34	2.86	2.78	3.10	3.17
Cr_2O_3	0.16	0.13	0.82	0.93	0.71	0.79	0.81	0.63	0.58	0.70	0.73
FeO*	5.04	5.30	5.80	5.73	6.21	6.39	6.64	6.75	6.30	6.24	5.42
MnO	0.06	0.16	0.11	0.07	0.10	0.10	0.13	0.14	0.13	0.07	0.07
MgO	16.32	15.96	15.54	15.36	16.03	15.95	16.50	16.20	16.12	15.77	17.86
CaO	22.09	21.95	21.59	22.09	21.14	20.57	20.09	20.26	20.77	21.33	19.92
Na_2O	0.25	0.41	0.33	0.33	0.30	0.33	0.30	0.27	0.29	0.31	0.32
Total	98.75	99.66	98.66	98.77	99.22	99.26	99.61	98.64	98.89	99.39	100.73
Si	1.951	1.927	1.894	1.875	1.918	1.902	1.896	1.905	1.911	1.899	1.916
Al^{iv}	.049	.073	.106	.125	.082	.098	.104	.095	.089	.101	.084
Al^{vi}	.034	.037	.039	.034	.030	.038	.041	.030	.032	.034	.051
Ti	.008	.023	.012	.014	.012	.020	.013	.016	.015	.020	.007
Cr	.004	.003	.024	.027	.021	.022	.022	.017	.016	.020	.020
Fe	.155	.162	.181	.179	.192	.198	.205	.210	.195	.192	.163
Mn	.001	.004	.003	.002	.002	.002	.003	.004	.003	.002	.002
Mg	.902	.875	.864	.856	.886	.881	.908	.902	.895	.873	.963
Ca	.877	.866	.863	.885	.839	.816	.794	.811	.828	.847	.772
Na	.017	.028	.023	.023	.021	.022	.021	.019	.021	.021	.022
Total (O_6)	3.998	3.998	4.009	4.020	4.002	3.999	4.007	4.009	4.005	4.009	4.000

	54.	55.	56.	57.	58.	59.	60.	61.	62.	63.	64.
SiO_2	52.20	51.42	51.51	52.10	52.14	52.00	51.36	52.27	51.51	51.57	51.41
TiO_2	0.66	0.62	0.37	0.37	0.37	0.25	0.27	0.54	0.21	0.23	0.29
Al_2O_3	2.99	3.09	3.33	3.16	3.25	3.42	3.52	2.86	3.59	3.36	3.30
Cr_2O_3	0.71	0.83	0.79	0.87	0.67	0.82	0.82	0.54	1.06	1.20	0.95
FeO*	4.70	4.44	4.53	5.36	4.79	5.77	4.50	4.66	3.92	4.74	3.90
MnO	0.10	0.10	0.12	0.09	0.09	0.07	0.10	0.10	0.05	0.09	0.06
MgO	16.38	16.48	16.25	17.42	16.72	17.77	16.42	16.58	16.24	16.30	16.06
CaO	21.45	21.77	21.61	19.92	20.94	19.29	21.45	21.48	22.28	21.59	22.45
Na_2O	0.32	0.31	0.26	0.28	0.27	0.21	0.29	0.19	0.50	0.27	0.26
Total	99.51	99.06	98.77	99.57	99.24	99.60	98.73	99.22	99.36	99.35	98.68
Si	1.918	1.902	1.908	1.910	1.917	1.907	1.903	1.925	1.896	1.903	1.905
Al^{iv}	.082	.098	.092	.090	.083	.093	.097	.075	.104	.097	.095
Al^{vi}	.047	.036	.052	.045	.057	.054	.056	.048	.051	.048	.048
Ti	.017	.016	.010	.009	.009	.006	.006	.014	.005	.005	.007
Cr	.020	.023	.023	.024	.019	.023	.023	.015	.030	.034	.027
Fe	.143	.137	.140	.163	.146	.176	.139	.143	.120	.146	.121
Mn	.002	.002	.003	.002	.002	.002	.002	.002	.001	.002	.001
Mg	.897	.908	.896	.952	.916	.971	.907	.910	.891	.896	.886
Ca	.844	.863	.857	.782	.824	.757	.851	.847	.878	.853	.890
Na	.022	.021	.018	.019	.018	.014	.021	.013	.036	.018	.018
Total (O_6)	3.992	4.006	3.999	3.996	3.991	4.003	4.005	3.992	4.012	4.002	3.998

Analyses 43-44: 80D133-5, 45-52: 80D140-2, 53-61: 79D036, 62-64: 79D032-4.

* Total Fe as FeO

TABLE 5.10 ELECTRON MICROPROBE ANALYSES OF CLINOPYROXENES FROM THE CRITICAL ZONE

	65.	66.	67.	68.	69.
SiO_2	51.50	52.03	51.73	50.36	51.71
TiO_2	0.27	0.25	0.20	0.20	0.26
Al_2O_3	3.07	3.05	3.17	5.89	3.16
Cr_2O_3	0.78	0.94	0.65	0.72	0.95
FeO*	4.52	4.82	4.63	5.05	4.16
MnO	0.09	0.12	0.09	0.06	0.13
MgO	16.61	16.68	16.53	17.30	15.82
CaO	22.00	21.67	21.60	20.06	21.82
Na_2O	0.28	0.29	0.35	0.23	0.45
Total	99.12	99.85	98.95	99.87	98.46
Si	1.904	1.911	1.911	1.840	1.921
Al^{iv}	.096	.089	.089	.060	.079
Al^{vi}	.037	.042	.048	.192	.058
Ti	.006	.006	.005	.005	.006
Cr	.022	.027	.018	.020	.027
Fe	.139	.147	.143	.154	.128
Mn	.002	.003	.002	.002	.003
Mg	.915	.912	.909	.942	.875
Ca	.871	.852	.854	.784	.869
Na	.019	.020	.023	.015	.031
Total (O_6)	4.011	4.009	4.002	4.014	3.997

Analyses 65-69: 79D032-4

* Total Fe as FeO

TABLE 5.11. ELECTRON MICROPROBE ANALYSES OF ORTHOPYROXENES FROM THE CRITICAL ZONE

	1.	2.	3.	4.	5.	6.	7.	8.
SiO_2	56.02	55.02	54.27	55.25	56.11	55.68	54.24	54.67
TiO_2	0.22	0.17	0.17	0.19	0.25	0.24	0.31	0.36
Al_2O_3	1.60	1.28	1.50	1.53	0.98	1.02	1.34	1.66
Cr_2O_3	0.24	0.25	0.30	0.27	----	----	0.05	----
FeO*	11.65	12.20	11.69	11.16	12.49	12.87	12.96	12.65
MnO	0.18	0.20	0.17	0.12	0.23	0.22	0.19	0.20
MgO	30.16	30.21	30.57	30.31	30.33	30.13	29.77	29.14
CaO	0.88	0.66	1.11	1.07	0.58	0.57	0.61	0.94
Na_2O	0.04	-----	----	0.02	----	0.03	0.02	0.04
Total	100.99	99.99	99.78	99.92	100.97	100.76	99.49	99.66
Si	1.961	1.953	1.931	1.952	1.970	1.965	1.942	1.951
Al^{iv}	.039	.047	.063	.048	.030	.035	.056	.049
Al^{vi}	.026	.006	----	.015	.010	.006	----	.020
Ti	.005	.004	.004	.004	.006	.006	.008	.009
Cr	.006	.006	.008	.007	----	----	.001	----
Fe	.341	.361	.348	.330	.367	.379	.388	.377
Mn	.005	.005	.004	.003	.006	.006	.005	.005
Mg	1.574	1.598	1.622	1.597	1.587	1.585	1.589	1.550
Ca	.033	.024	.042	.040	.021	.021	.023	.035
Na	.022	----	----	.001	----	.002	.001	.002
Total (O_6)	3.992	4.004	4.022	3.997	3.997	4.005	4.013	3.998
En	82.0	81.4	82.2	82.7	81.0	80.5	80.2	80.2

	9.	10.	11.	12.	13.	14.	15.	16.
SiO_2	53.45	54.06	53.61	54.33	54.43	53.81	55.07	55.14
TiO_2	0.42	0.41	0.46	0.27	0.37	0.09	0.09	0.07
Al_2O_3	1.44	1.38	1.51	2.61	1.20	1.46	1.54	1.76
Cr_2O_3	----	----	----	----	0.04	0.21	0.22	0.24
FeO*	12.88	12.94	12.48	12.43	12.75	10.04	10.21	10.02
MnO	0.23	0.20	0.11	0.21	0.25	0.17	0.14	0.14
MgO	29.12	29.43	29.04	29.09	28.66	31.84	31.45	31.89
CaO	0.91	0.80	1.46	0.48	1.07	0.84	0.90	0.90
Na_2O	0.02	0.03	0.07	0.02	0.05	0.02	-----	----
Total	98.47	99.25	98.74	99.44	98.82	98.48	99.62	100.16
Si	1.937	1.942	1.936	1.938	1.960	1.929	1.945	1.937
Al^{iv}	.061	.058	.063	.062	.040	.061	.055	.063
Al^{vi}	----	----	----	.047	.010	----	.008	.009
Ti	.010	.010	.011	.006	.009	.002	.002	.001
Cr	----	----	----	----	.001	.005	.006	.006
Fe	.390	.388	.376	.371	.383	.301	.301	.293
Mn	.006	.005	.003	.005	.007	.004	.004	.003
Mg	1.573	1.575	1.563	1.548	1.539	1.606	1.655	1.670
Ca	.035	.030	.056	.018	.040	.032	.033	.033
Na	.001	.002	.004	.001	.003	.001	----	----
Total (O_6)	4.013	4.010	4.012	3.996	3.992	3.941	4.009	4.015
En	79.9	80.0	80.5	80.5	79.8	84.0	84.4	84.9

Analyses 1-4: 79D263-3, blebs in cpx 39, 5-13: 80D133-5, 14-16: 79D032-4.

*Total Fe as FeO.

TABLE 5.12. ELECTRON MICROPROBE ANALYSES OF OLIVINES FROM THE CRITICAL ZONE

	1.	2.	3.	4.	5.	6.	7.	8.	9.	10.
SiO_2	38.91	41.00	39.95	39.64	39.71	39.56	39.14	38.47	38.73	39.31
FeO*	14.06	14.51	15.39	15.82	15.41	15.51	15.52	20.54	22.25	17.36
MnO	0.16	0.06	0.19	0.14	0.16	0.14	0.21	0.19	0.27	0.22
MgO	46.68	46.14	46.08	45.68	45.85	45.96	45.17	41.79	40.18	44.68
NiO	0.14	0.12	0.16	0.13	0.11	0.15	0.13	0.10	0.19	0.15
Total	100.85	101.83	101.77	101.41	101.24	101.32	100.17	101.09	101.62	101.72
Si	.972	1.005	.987	.984	.986	.983	.985	.981	.990	.981
Fe	.312	0.297	.317	.328	.320	.322	.326	.438	.476	.362
Mn	.003	.001	.003	.002	.002	.002	.003	.003	.005	.004
Mg	1.737	1.686	1.698	1.690	1.698	1.704	1.694	1.589	1.531	1.664
Ni	.002	.002	.002	.002	.001	.002	.002	.001	.003	.003
Total (O_4)	3.026	2.991	3.007	3.006	3.007	3.013	3.010	3.012	3.005	3.014

	11.	12.	13.	14.	15.	16.	17.	18.	19.	20.
SiO_2	39.19	38.61	38.88	39.34	39.68	39.25	39.79	39.55	38.63	40.59
FeO*	17.19	17.55	17.81	17.23	16.94	16.91	13.32	11.06	13.82	12.86
MnO	0.20	0.22	0.19	0.23	0.19	0.22	0.14	0.10	0.17	0.13
MgO	44.41	44.12	44.29	44.68	44.16	44.48	46.64	48.97	45.39	46.51
NiO	0.14	0.14	0.17	0.09	0.15	0.12	0.30	0.31	0.25	0.25
Total	101.13	100.64	101.34	101.57	101.12	100.98	100.19	99.99	98.26	100.34
Si	.983	.977	.978	.983	.994	.985	.989	.976	.974	1.001
Fe	.360	.371	.374	.360	.354	.355	.276	.228	.292	.265
Mn	.003	.004	.003	.004	.004	.004	.002	.002	.003	.002
Mg	1.662	1.664	1.659	1.664	1.649	1.665	1.728	1.802	1.707	1.710
Ni	.002	.002	.003	.001	.003	.002	.005	.006	.004	.004
Total (O_4)	3.010	3.018	3.017	3.012	3.004	3.011	3.000	3.014	2.980	2.982

Analyses 1-3: 79D039-2, 4-7: 79D263-4, 8: 79D269-3, 9: 795L-4, 10-16: 79D265-5
17-20: 79D272-2.

*Total Fe as FeO

TABLE 5.12. ELECTRON MICROPROBE ANALYSES ON OLIVINES FROM THE CRITICAL ZONE

	21.	22.	23.	24.	25.	26.	27.	28.	29.	30.
SiO_2	39.55	39.50	37.95	38.27	37.81	38.01	38.77	38.60	39.41	39.66
FeO*	13.79	14.20	21.71	21.22	20.98	20.83	20.99	21.74	19.73	19.39
MnO	0.16	0.13	0.25	0.27	0.20	0.21	0.17	0.24	0.17	0.14
MgO	46.02	46.61	40.78	40.82	41.70	41.16	40.66	40.54	42.41	42.07
NiO	0.29	0.28	0.11	0.10	0.12	0.16	0.09	0.08	0.14	0.14
Total	99.81	100.72	100.81	100.68	100.81	100.37	100.81	101.20	101.86	101.70
Si	.986	.980	.977	.979	.971	.979	.992	.988	.992	.997
Fe	.287	.294	.467	.454	.450	.448	.449	.465	.415	.407
Mn	.002	.002	.005	.005	.003	.004	.003	.004	.003	.003
Mg	1.710	1.725	1.564	1.558	1.597	1.581	1.551	1.547	1.592	1.577
Ni	.005	.005	.001	.001	.002	.003	.001	.001	.002	.002
Total (O_4)	2.990	3.006	3.014	2.997	3.023	3.015	2.999	3.005	3.004	2.994

	31.	32.	33.	34.	35.	36.	37.	38.	39.	40.
SiO_2	38.82	39.09	37.98	38.34	38.05	38.55	38.67	37.43	39.72	38.82
FeO*	19.04	18.91	19.59	18.68	20.22	20.26	19.84	19.97	19.68	19.27
MnO	0.21	0.22	0.19	0.18	0.20	0.20	0.23	0.13	0.23	0.18
MgO	42.61	43.02	41.75	43.13	41.41	41.52	41.50	41.26	41.92	41.55
NiO	----	0.13	0.12	0.11	0.11	0.14	0.18	0.14	0.14	0.08
Total	100.68	101.37	99.63	100.44	99.99	100.67	100.42	98.93	101.69	99.90
Si	.987	.987	.979	.978	.981	.985	.991	.975	1.000	.995
Fe	.404	.398	.422	.398	.436	.433	.425	.435	.414	.413
Mn	.004	.004	.003	.003	.003	.003	.004	.002	.004	.003
Mg	1.614	1.619	1.606	1.640	1.593	1.582	1.584	1.603	1.574	1.587
Ni	-----	.002	.002	.001	.001	.002	.003	.002	.002	.001
Total (O_4)	3.009	3.010	3.012	3.020	3.014	3.005	3.007	3.017	2.994	2.999

Analyses 21-22: 79D272-2, 23-28: 80D143-5, 29-34: 79D263-3, 35-40: 80D133-5.

*Total Fe as FeO

TABLE 5.12. ELECTRON MICROPROBE ANALYSES OF OLIVINES FROM THE CRITICAL ZONE

	41.	42.	43.	44.	45.	46.	47.	48.	49.	50.
SiO_2	37.95	37.71	38.58	38.57	38.47	37.87	38.75	37.87	38.43	38.95
FeO	19.26	20.41	20.35	20.19	19.80	20.11	20.63	20.44	20.10	17.50
MnO	0.18	0.21	0.23	0.20	0.22	0.19	0.20	0.21	0.22	0.18
MgO	42.39	41.47	41.57	41.38	41.53	41.46	41.48	41.13	41.96	44.69
NiO	0.16	0.12	0.10	----	0.14	0.09	0.08	0.07	0.13	0.14
Total	99.94	99.92	100.83	100.34	100.16	99.72	101.14	99.72	100.84	101.46
Si	.975	.975	.985	.989	.988	.979	.988	.981	.982	.977
Fe	.414	.440	.434	.433	.425	.435	.439	.442	.429	.366
Mn	.003	.004	.004	.003	.004	.003	.003	.004	.004	.003
Mg	1.624	1.598	1.583	1.582	1.589	1.599	1.577	1.588	1.599	1.671
Ni	.003	.002	.001	----	.002	.001	.001	.001	.002	.002
Total (O_4)	3.019	3.019	3.007	3.007	3.008	3.017	3.008	3.016	3.016	3.019

	51.	52.	53.	54.	55.	56.	57.	58.	59.	60.
SiO_2	38.85	38.77	39.96	39.68	39.69	40.46	39.42	39.48	39.26	40.04
FeO	17.11	17.71	17.10	17.15	15.86	14.50	15.77	15.70	15.63	15.18
MnO	0.14	0.19	0.21	0.20	0.14	0.14	0.16	0.15	0.15	0.19
MgO	44.14	44.52	44.17	44.22	45.66	45.18	45.41	45.40	46.18	45.74
NiO	0.12	0.15	0.11	0.14	0.12	0.14	0.16	0.18	0.18	0.20
Total	100.36	101.34	101.55	101.39	101.47	100.42	100.92	100.91	101.40	101.35
Si	.983	.975	.996	.992	.986	1.004	.984	.984	.977	.992
Fe	.361	.372	.356	.358	.330	.301	.329	.327	.325	.314
Mn	.003	.003	.004	.003	.002	.002	.003	.002	.002	.003
Mg	1.665	1.668	1.642	1.649	1.691	1.672	1.691	1.688	1.712	1.690
Ni	.002	.003	.001	.002	.002	.002	.003	.002	.002	.003
Total (O_4)	3.014	3.021	2.999	3.004	3.011	2.981	3.010	3.003	3.018	3.002

Analyses 41: 80D133-5, 42-49: 80D140-2, 50-54: 79D036, 55-60: 79D032-4.

*Total Fe as FeO.

TABLE 5.13. ELECTRON MICROPROBE ANALYSES OF PLAGIOCLASE FROM THE CRITICAL ZONE

	1.	2.	3.	4.	5.	6.	7.	8.
SiO_2	46.76	48.30	47.41	47.88	48.05	47.92	47.97	48.07
Al_2O_3	33.00	32.37	32.75	32.13	32.36	32.16	31.90	32.07
FeO*	0.14	0.07	0.08	0.14	0.06	0.18	0.29	0.16
CaO	17.22	16.86	17.46	17.20	17.01	16.60	16.61	16.33
Na_2O	1.09	1.83	1.80	1.63	1.84	1.72	1.91	1.80
Total	98.21	99.43	99.50	98.98	99.32	98.58	98.68	98.43
Si	2.180	2.223	2.188	2.215	2.212	2.224	2.227	2.233
Al	1.813	1.756	1.780	1.752	1.755	1.758	1.745	1.756
Fe	.004	.001	.002	.005	.001	.006	.011	.005
Ca	.859	.831	.862	.852	.839	.825	.825	.813
Na	.097	.163	.162	.145	.163	.154	.171	.162
Total (O_8)	4.953	4.974	4.994	4.969	4.970	4.967	4.979	4.969
An	89.9	83.6	84.2	85.5	83.7	84.3	83.0	83.5

	9.	10.	11.	12.	13.	14.	15.	16.
SiO_2	48.48	47.83	48.62	47.30	47.72	47.45	48.27	46.64
Al_2O_3	31.97	31.86	31.70	32.44	32.38	33.51	31.91	33.43
FeO*	0.09	0.06	0.19	0.26	0.22	0.10	0.12	0.10
CaO	16.14	16.49	16.17	16.82	16.86	16.52	16.24	17.48
Na_2O	2.16	2.02	1.89	1.66	1.70	1.43	2.09	1.43
Total	98.84	98.26	98.57	98.48	98.88	99.01	98.63	99.08
Si	2.242	2.227	2.247	2.201	2.210	2.189	2.235	2.162
Al	1.742	1.747	1.726	1.779	1.767	1.822	1.740	1.826
Fe	.002	.001	.006	.009	.008	.002	.004	.002
Ca	.799	.822	.800	.838	.836	.816	.806	.868
Na	.192	.182	.169	.148	.152	.127	.186	.127
Total (O_8)	4.977	4.979	4.948	4.975	4.973	4.956	4.971	4.985
An	80.7	81.9	82.1	85.1	84.7	86.6	81.3	87.2

Analyses 1: 79D032-3, 2-5: 79D039-2, 6-7: 79D263-4, 8: 79D269-3,
9: 795L-4, 10: 79D265-5, 11: 79D272-2, 12-13: 79D263-3, 14: 79D036.

*Total Fe as FeO.

TABLE 5.14 ELECTRON MICROPROBE ANALYSES OF CLINOPYROXENES FROM DIABASE DYKES

	1.	2.	3.	4.	5.	6.	7.	8.	9.	10.	11.
SiO_2	51.77	50.73	52.12	51.93	51.44	52.05	52.12	51.76	52.50	52.68	52.78
TiO_2	0.59	0.77	0.47	0.64	0.84	0.59	0.62	0.48	0.67	0.55	0.31
Al_2O_3	3.09	2.87	3.32	2.89	2.83	2.99	3.06	3.48	2.82	2.95	2.54
Cr_2O_3	----	----	0.58	0.06	----	0.25	0.11	0.52	----	0.36	0.55
FeO*	7.77	10.58	6.20	7.88	9.19	6.91	8.04	6.30	8.28	6.53	5.41
MnO	0.16	0.16	0.09	0.16	0.16	0.13	0.13	0.12	0.17	0.14	0.11
MgO	17.01	15.27	16.94	16.42	15.86	17.02	17.58	16.79	16.73	17.14	18.17
CaO	19.15	18.64	19.55	19.04	19.02	19.16	17.72	19.24	19.40	19.70	19.46
Na_2O	0.20	0.24	0.21	0.11	0.32	0.26	0.30	0.10	0.38	0.25	0.24
Total	99.74	99.26	99.48	99.13	99.66	99.36	99.68	98.79	100.95	100.30	99.61
Si	1.909	1.905	1.917	1.927	1.912	1.919	1.917	1.915	1.917	1.922	1.931
Al^{IV}	.091	.095	.083	.073	.088	.081	.083	.085	.083	.078	.069
Al^{VI}	.042	.031	.060	.053	.035	.048	.048	.066	.038	.048	.039
Ti	.016	.021	.013	.017	.022	.016	.016	.013	.018	.015	.008
Cr	----	----	.016	.001	----	.006	.002	.015	----	.009	.015
Fe	.239	.332	.189	.244	.285	.213	.247	.194	.252	.199	.165
Mn	.004	.004	.002	.004	.004	.003	.003	.003	.004	.004	.003
Mg	.935	.854	.928	.908	.878	.935	.964	.926	.911	.933	.991
Ca	.756	.749	.769	.756	.757	.756	.698	.762	.758	.770	.762
Na	.014	.018	.015	.007	.022	.018	.021	.006	.026	.017	.017
Total (O_6)	4.006	3.989	3.992	3.990	4.003	3.995	3.999	3.985	4.007	3.995	4.000

	12.	13.	14.	15.	16.	17.	18.	19.	20.	21.	22.
SiO_2	52.64	53.14	52.21	50.09	50.55	49.91	49.32	50.95	51.91	49.44	50.78
TiO_2	0.50	0.53	0.38	1.28	1.10	1.16	1.35	1.42	0.43	1.22	1.02
Al_2O_3	2.80	2.59	3.46	3.83	3.81	4.11	3.59	3.20	2.59	5.15	3.74
Cr_2O_3	0.25	0.13	0.82	----	----	0.10	----	0.10	0.33	0.23	0.10
FeO*	7.22	7.41	4.72	9.59	10.21	8.84	12.54	10.64	5.50	8.43	9.70
MnO	0.14	0.11	0.10	0.17	0.16	0.16	0.21	0.24	0.08	0.11	0.11
MgO	18.02	17.70	17.72	15.07	15.20	15.30	13.73	14.18	17.96	15.48	15.22
CaO	18.21	18.84	20.13	19.18	18.59	19.85	18.04	19.28	20.11	19.21	18.86
Na_2O	0.27	0.24	0.27	0.29	0.30	0.25	0.36	0.31	0.21	0.30	0.21
Total	100.05	100.69	99.81	99.50	99.92	99.68	99.14	100.32	99.12	99.57	99.74
Si	1.926	1.931	1.904	1.874	1.882	1.861	1.875	1.899	1.914	1.839	1.891
Al^{IV}	.074	.069	.096	.126	.118	.139	.125	.101	.086	.161	.109
Al^{VI}	.046	.040	.052	.042	.049	.041	.036	.039	.026	.064	.055
Ti	.013	.014	.009	.035	.030	.032	.038	.039	.012	.034	.028
Cr	.006	.003	.023	----	----	.002	----	.002	.008	.006	.002
Fe	.220	.225	.143	.299	.318	.274	.398	.331	.168	.262	.301
Mn	.004	.003	.002	.004	.004	.004	.005	.006	.002	.003	.003
Mg	.982	.958	.963	.840	.842	.850	.778	.788	.987	.858	.845
Ca	.713	.733	.787	.768	.741	.792	.734	.770	.794	.765	.752
Na	.018	.016	.018	.021	.021	.017	.026	.021	.014	.021	.015
Total (O_6)	4.002	3.992	3.997	4.009	4.005	4.012	4.015	3.996	4.011	4.013	4.001

Analyses 1-10 79D109-2, 11 79D109-2 Phenocryst
12-14 80D204-2 Phenocryst, 15-23 80D204-2

* Total Fe as FeO

TABLE 5.14 ELECTRON MICROPROBE ANALYSES OF CLINOPYROXENES FROM DIABASE DYKES

	23.	24.	25.	26.	27.	28.	29.	30.	31.	32.	33.
SiO_2	51.06	49.99	50.82	50.84	50.77	49.84	50.28	50.82	50.01	51.21	50.95
TiO_2	1.19	1.74	1.68	1.76	1.74	1.96	1.82	1.63	1.96	1.61	1.63
Al_2O_3	3.88	3.44	3.11	3.84	2.82	3.64	3.93	2.98	3.79	2.65	2.89
Cr_2O_3	0.06	----	----	0.05	----	----	0.07	----	----	----	----
FeO*	9.31	10.27	11.35	10.00	10.98	10.27	9.95	10.69	11.46	11.62	10.98
MnO	0.16	0.16	0.26	0.10	0.27	0.20	0.16	0.20	0.24	0.28	0.22
MgO	14.79	14.79	15.67	14.68	15.22	14.14	14.65	14.82	14.60	15.29	14.55
CaO	20.00	18.89	16.93	19.38	18.18	19.35	19.33	19.20	17.70	16.77	18.62
Na_2O	0.38	0.48	0.30	0.38	0.35	0.37	0.43	0.41	0.39	0.44	0.34
Total	100.83	99.76	100.12	101.03	100.33	99.77	100.62	100.75	100.15	99.87	100.18
Si	1.883	1.874	1.891	1.875	1.891	1.869	1.864	1.887	1.869	1.912	1.900
Al^{iv}	.117	.126	.109	.125	.109	.131	.136	.113	.131	.088	.100
Al^{vi}	.050	.025	.026	.042	.014	.030	.035	.016	.036	.028	.027
Ti	.032	.048	.047	.048	.048	.055	.050	.044	.055	.044	.044
Cr	.001	----	----	.001	----	----	.001	----	----	----	----
Fe	.287	.321	.353	.307	.341	.321	.308	.331	.357	.362	.342
Mn	.004	.004	.007	.002	.007	.005	.004	.005	.006	.008	.006
Mg	.813	.826	.869	.806	.845	.790	.810	.819	.813	.850	.809
Ca	.790	.757	.675	.765	.726	.777	.767	.764	.708	.670	.743
Na	.027	.035	.021	.026	.025	.026	.030	.029	.028	.030	.024
Total (O_6)	4.004	4.016	3.998	3.997	4.006	4.004	4.005	4.008	4.003	3.992	3.995

	34.	35.	36.	37.	38.	39.	40.	41.	42.	43.	44.
SiO_2	54.51	53.09	51.73	54.62	52.92	55.05	54.04	52.25	52.97	52.58	53.30
TiO_2	0.25	0.50	0.86	0.31	0.50	0.35	0.24	0.74	0.48	0.40	0.43
Al_2O_3	1.98	3.09	2.96	1.71	3.70	1.62	1.95	2.84	2.84	3.05	2.70
Cr_2O_3	0.41	0.15	----	0.07	0.30	0.05	0.33	----	0.12	0.10	----
FeO*	5.79	6.30	11.29	7.32	5.97	7.67	5.67	9.75	6.79	7.22	8.51
MnO	0.13	0.10	0.23	0.18	0.12	0.13	0.14	0.17	0.11	0.14	0.16
MgO	18.93	16.93	15.45	18.43	16.98	18.54	18.88	16.25	17.34	17.40	17.17
CaO	17.96	19.71	17.45	17.92	19.72	17.81	18.23	18.36	18.85	18.79	18.31
Na_2O	0.13	0.23	0.19	0.18	0.19	0.12	0.17	0.24	0.12	0.18	0.19
Total	100.09	100.10	100.16	100.74	100.40	101.34	99.65	100.60	99.62	99.86	100.77
Si	1.971	1.936	1.921	1.974	1.921	1.979	1.963	1.922	1.939	1.928	1.941
Al^{iv}	.029	.064	.079	.026	.079	.021	.037	.078	.061	.072	.059
Al^{vi}	.054	.068	.049	.046	.079	.047	.046	.044	.061	.059	.056
Ti	.006	.013	.022	.007	.013	.008	.006	.019	.013	.011	.012
Cr	.011	.004	----	.001	.008	.001	.008	----	.003	.002	----
Fe	.174	.191	.350	.220	.181	.229	.171	.300	.207	.220	.258
Mn	.003	.002	.006	.005	.003	.003	.003	.004	.003	.003	.004
Mg	1.019	.920	.854	.993	.918	.992	1.022	.891	.946	.951	.932
Ca	.695	.769	.694	.694	.767	.686	.709	.724	.739	.738	.714
Na	.008	.016	.013	.011	.013	.007	.012	.016	.008	.013	.013
Total (O_6)	3.970	3.983	3.988	3.977	3.984	3.973	3.977	3.998	3.980	3.997	3.989

Analyses 24-33 81D114-2
34-42 79D108-3,

* Total Fe as FeO

TABLE 5.14 ELECTRON MICROPROBE ANALYSES OF CLINOPYROXENES FROM DIABASE DYKES

	45.	46.	47.	48.	49.	50.	51.	52.	53.	54.	55.
SiO_2	51.70	51.33	52.36	52.21	52.77	52.59	52.66	52.77	49.87	50.67	50.41
TiO_2	0.46	0.47	0.38	0.44	0.43	0.36	0.43	0.44	1.06	1.24	1.08
Al_2O_3	3.85	3.95	3.59	3.19	3.46	3.13	4.09	3.65	3.23	4.39	4.61
Cr_2O_3	0.25	0.40	0.21	0.13	0.15	0.18	0.27	0.30	----	0.14	0.19
FeO*	5.95	6.07	6.74	7.10	6.40	6.79	5.50	6.46	15.08	10.13	8.94
MnO	0.11	0.11	0.07	0.14	0.13	0.13	0.08	0.09	0.26	0.21	0.18
MgO	16.29	16.73	17.41	16.97	16.96	16.74	16.41	17.02	13.79	15.29	15.93
CaO	20.43	20.06	19.15	19.46	19.52	19.62	20.88	19.95	16.68	18.58	18.73
Na_2O	0.12	0.21	0.27	0.18	0.22	0.23	0.16	0.23	0.29	0.27	0.35
Total	99.16	99.33	100.18	99.82	100.04	99.77	100.49	100.91	100.26	100.92	100.42
Si	1.907	1.892	1.911	1.917	1.925	1.930	1.912	1.913	1.884	1.868	1.858
Al^{iv}	.093	.108	.089	.083	.075	.070	.088	.087	.116	.132	.142
Al^{vi}	.074	.063	.065	.055	.073	.064	.087	.068	.027	.058	.058
Ti	.012	.013	.009	.012	.012	.009	.012	.011	.030	.033	.029
Cr	.006	.011	.005	.003	.004	.004	.007	.008	----	.003	.005
Fe	.183	.187	.206	.217	.195	.208	.166	.195	.476	.311	.274
Mn	.003	.003	.002	.004	.003	.003	.002	.002	.007	.005	.005
Mg	.895	.918	.947	.929	.922	.915	.888	.919	.776	.839	.875
Ca	.808	.792	.749	.765	.762	.771	.812	.774	.675	.733	.739
Na	.008	.014	.018	.013	.015	.016	.010	.016	.021	.019	.024
Total (O_6)	3.989	4.001	4.001	3.998	3.986	3.990	3.984	3.993	4.012	4.001	4.009

	56.	57.	58.	59.	60.	61.	62.	63.	64.	65.	66.
SiO_2	50.79	50.92	50.68	51.14	49.47	48.65	50.29	50.73	50.59	50.77	50.48
TiO_2	1.09	1.04	1.14	1.20	1.22	1.01	0.71	0.98	1.02	0.96	1.22
Al_2O_3	4.43	3.95	4.07	4.76	2.87	3.07	3.23	4.49	4.43	4.13	3.91
Cr_2O_3	0.19	0.06	0.14	0.15	----	----	0.10	0.19	0.13	0.22	0.09
FeO*	9.25	10.82	10.47	9.35	15.07	13.85	11.43	7.94	9.41	8.84	11.94
MnO	0.16	0.18	0.16	0.16	0.32	0.26	0.27	0.17	0.21	0.13	0.18
MgO	15.97	15.10	15.32	15.67	13.23	14.48	15.11	16.67	16.00	16.13	15.10
CaO	18.48	18.75	18.48	18.64	17.07	17.16	17.67	18.56	18.07	18.80	17.70
Na_2O	0.34	0.28	0.30	0.31	0.24	0.29	0.23	0.28	0.18	0.21	0.28
Total	100.70	101.10	100.76	101.38	99.49	98.77	99.04	100.01	100.04	100.19	100.90
Si	1.867	1.878	1.872	1.868	1.889	1.867	1.897	1.866	1.872	1.875	1.873
Al^{iv}	.133	.122	.128	.132	.111	.133	.103	.134	.128	.125	.127
Al^{vi}	.057	.049	.048	.073	.017	.005	.040	.060	.065	.055	.042
Ti	.030	.028	.031	.032	.035	.028	.020	.027	.028	.026	.034
Cr	.005	.001	.003	.004	----	----	.002	.005	.003	.005	.002
Fe	.283	[illegible]	.323	.285	.480	.443	.359	.244	.291	.272	.370
Mn	.004	[illegible]	.004	.004	.010	.008	.007	.004	.006	.003	.005
Mg	.875	[illegible]	.843	.853	.753	.828	.849	.914	.881	.888	.835
Ca	.728	.740	.730	.729	.698	.705	.714	.730	.716	.743	.703
Na	.023	.019	.021	.021	.018	.021	.017	.019	.012	.014	.020
Total (O_6)	4.005	4.005	4.003	4.001	4.011	4.038	4.008	4.003	4.002	4.006	4.011

Analyses 43-52 80D193-4
53-66 81D144-4.

* Total Fe as FeO

TABLE 5.14.

ELECTRON MICROPROBE ANALYSES OF CLINOPYROXENES FROM DIABASE DYKES

	67.	68.	69.	70.	71.	72.
SiO_2	49.65	50.79	49.29	49.10	51.35	49.82
TiO_2	1.06	1.15	1.23	0.90	0.96	1.12
Al_2O_3	3.66	2.83	4.43	4.13	3.69	3.93
Cr_2O_3	0.05	-----	0.18	0.11	0.14	0.13
FeO*	11.52	14.74	9.73	9.91	9.82	9.70
MnO	0.26	0.26	0.14	0.18	0.11	0.18
MgO	14.33	13.17	15.11	15.96	16.17	15.71
CaO	18.69	18.10	19.17	18.37	17.74	18.97
Na_2O	0.41	0.39	0.21	0.25	0.32	0.37
Total	99.63	101.43	99.49	98.91	100.30	99.93
Si	1.871	1.900	1.848	1.850	1.895	1.859
Al^{iv}	.129	.100	.152	.150	.105	.141
Al^{vi}	.033	.024	.042	.032	.055	.031
Ti	.030	.032	.034	.025	.026	.031
Cr	.001	----	.004	.003	.003	.003
Fe	.362	.461	.305	.312	.302	.302
Mn	.007	.007	.004	.005	.003	.005
Mg	.804	.734	.844	.896	.889	.873
Ca	.754	.724	.770	.741	.700	.758
Na	.028	.027	.015	.018	.022	.026
Total (O_6)	1.019	4.009	4.018	4.032	4.000	4.029

Analyses 67-72 81D144-4

* Total Fe as FeO

Figure 5.21A. Portion of the pyroxene quadrilateral showing all analyses of clinopyroxenes (dots), orthopyroxenes (crosses) and tie lines connecting co-existing clinopyroxene grains and enclosed orthopyroxene blebs, from cumulates of the critical zone. The range of olivine compositions (Table 5.12) is shown by the black bar. Dashed lines show the limits of pyroxene and olivine Fe/Mg. Curved line is the Skaergaard trend and straight solid and dashed line is orthopyroxene - inverted pigeonite trend. Small area enclosed by dashed line includes clinopyroxenes from the critical zone of the Bay of Islands Complex from Malpas (1976).

Figure 5.21B. Portion of the pyroxene quadrilateral showing analyses of clinopyroxene (dots) from diabase dykes of the sheeted dyke zone. Dashed outline is field of critical zone clinopyroxenes from A. Analyses show scatter but extend along the Skaergaard trend to higher Fe/Mg ratios than those of the critical zone.

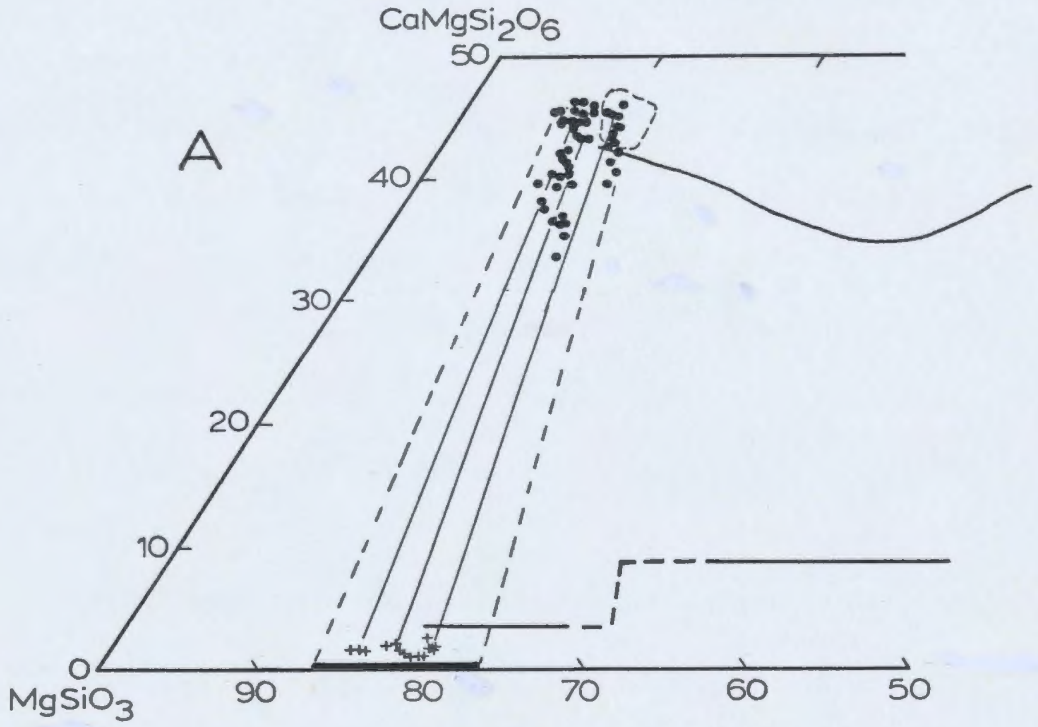
CaMgSi2O6
50
40
30
20
10
0
A
MgSiO3
90
80
70
60
50

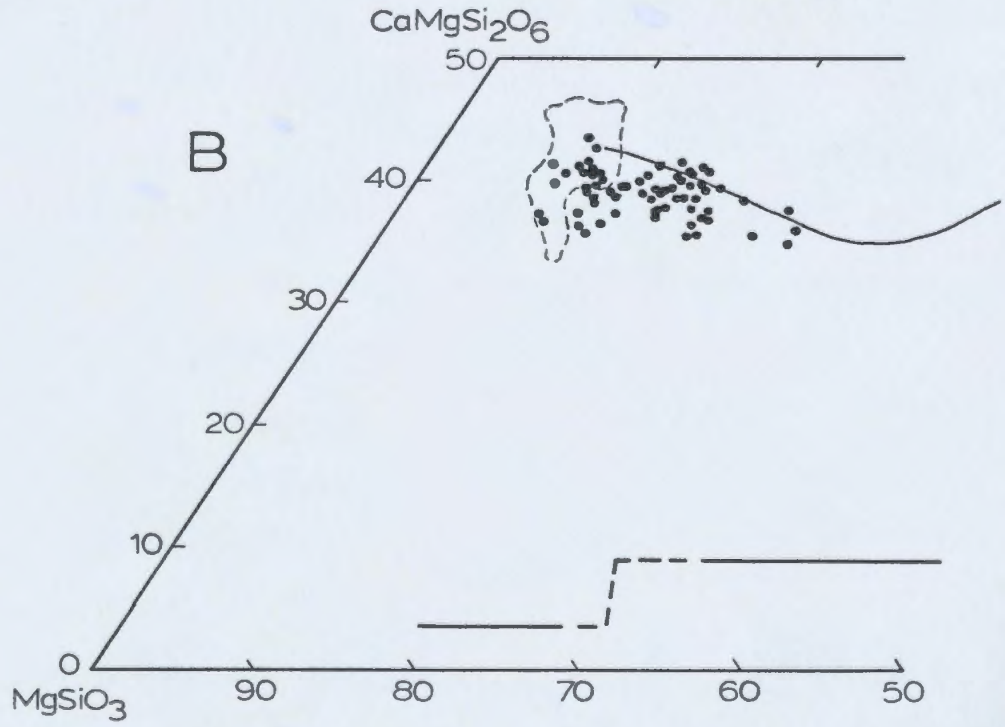
CaMgSi2O6
50
40
30
20
10
0
B
MgSiO3
90
80
70
60
50

non-pleochroic orthopyroxene vary between En80 and En86 (Table 5.11). Tie lines between three coexisting clinopyroxene hosts and orthopyroxene blebs indicate by their parallelism that local equilibrium was attained.

Olivine compositions in the suite of critical zone rocks (Table 5.12) are shown by the black bar in Figure 5.21A and have Fe/Mg ratios comparable to those of the orthopyroxenes. The greater range for olivine is likely due to a greater number of analyses from more rock samples.

Plagioclase from the critical zone varies from An80.7 to An89.9 (bytownite, Table 5.13).

Clinopyroxenes from the sheeted dyke zone extend from the field of critical zone pyroxenes (dashed area in Figure 5.21B) to more Fe-rich compositions in the pyroxene quadrilateral. The most Fe-rich analysis is Wo35En40Fs25. In general they follow the Skaergaard tholeiitic trend shown in Figure 5.21B, but with considerable scatter. It is clear from this diagram that the clinopyroxenes from the sheeted dyke zone represent a more chemically evolved population than those of the critical zone.

5.12.3 Pyroxenes as Indicators of Basalt Type

5.12.3.1 Introduction

Clinopyroxene chemistry has been used by many workers to identify the affinity of basalts as a check on trace element diagrams used to discriminate between tectonic settings of eruption. In the case of altered basalts, the

chemistry of fresh clinopyroxenes may be the only evidence remaining of their chemical affinities. Kushiro (1960) and LeBas (1962) first demonstrated that pyroxene composition varies with the chemistry of the lava and designed plots to distinguish different types of basalts based on their pyroxene chemistry. Since then many plots employing the elements Cr, Ti, Al, Si, Na and Ca have been constructed to discriminate between tectonic settings (Pearce et al.,1975; Pearce and Norry,1979; Nisbet and Pearce,1977). A recent review of the limitations of most of these classifications has been presented by Leterrier et al. (1982). These limitations include; 1.coupled substitutions, 2.crystallization sequence, 3.quenching of lava, 4.variation of KD with temperature and pressure, 5.the small number of analyses used to define fields, 6.errors in measurement of small amounts of some elements by microprobe, and 7.inability to separate all basalt types on any one diagram.

In the following sections, the classic diagrams of Kushiro (1960) and LeBas (1962), as well as the newly published diagrams of Leterrier et al. (1982), are used to determine the chemical affinities of the clinopyroxenes of the Annieopsquotch Complex and to infer the tectonic setting. For each figure, pyroxenes from the critical zone and sheeted dyke zone are plotted on diagrams A and B respectively to facilitate comparison of the two groups.

5.12.3.2 Chemical Variation Diagrams

On plots of TiO2 and Al2O3 versus SiO2 (Figure 5.22, LeBas,1962) clinopyroxenes of the critical zone fall mainly in the field of ocean floor basalts. The range of SiO2 contents is from 50.12 wt. % to 54.23 wt. % (Table 5.10). TiO2 contents are in the range 0.14 wt. % to 0.88 wt. %, and Al2O3 varies from 1.60 wt. % to 5.89 wt. %. The analyses with lowest SiO2 contents fall below the field of ocean floor basalts in Figure 5.22A. The error in the SiO2 measurement is approximately +/- 2% and within this error most analyses could be within the ocean floor field.

Most pyroxene analyses from the sheeted dyke zone fall in the field of ocean floor basalts in Figure 5.22B. They extend to more TiO2-rich compositions. Pyroxenes from one dyke, 81HPAD114-2, have the highest TiO2 content measured (Table 5.14, average 1.75 wt. %) and fall outside the field of ocean floor basalts (Figure 5.22B). These pyroxenes are quite fresh, show sector zoning in the manner of titanaugites, but do not have the distinctive violet colour. The dyke is noticeably different in the field, containing thousands of lithic fragments and crystals. It was not analysed. The higher TiO2 content of the pyroxenes may indicate non- equilibrium crystallization or, if the dyke has a high TiO2 content, a different source.

About fifteen pyroxenes analysed from the sheeted dyke zone fall in the alkaline field on the Al2O3 vs. SiO2 plot (Figure 5.22B) as compared to none from the critical zone.

Al is plotted against Fe/Mg ratio in Figure 5.23. The

Figure 5.22A,B. SiO_2 vs. TiO_2 and Al_2O_3 diagrams (after LeBas, 1962) for clinopyroxenes of the critical zone and sheeted dyke zone respectively. Dashed lines outline field of ocean floor basalts in each diagram. Pyroxenes from the sheeted dyke zone show a wider range in composition, especially higher TiO_2 contents, and cross into the alkaline field. Points plotting to the high TiO_2 side of the OFB field in diagram B are from sample 81HPAD114-2, which contains sector zoned augite.

A

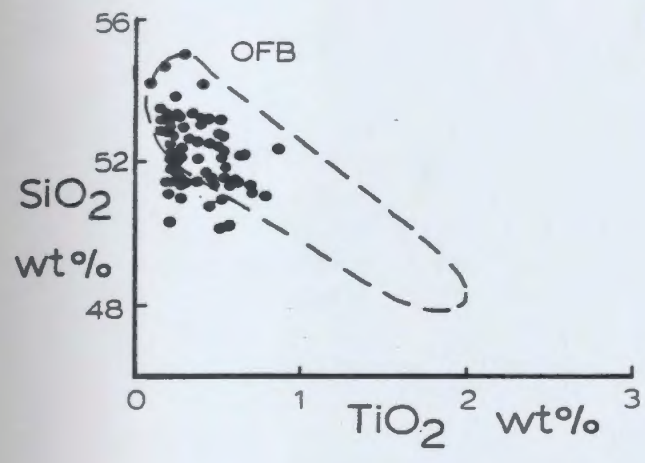
56
52
48
OFB
SiO2
wt%
0
1
2
3
TiO2 wt%

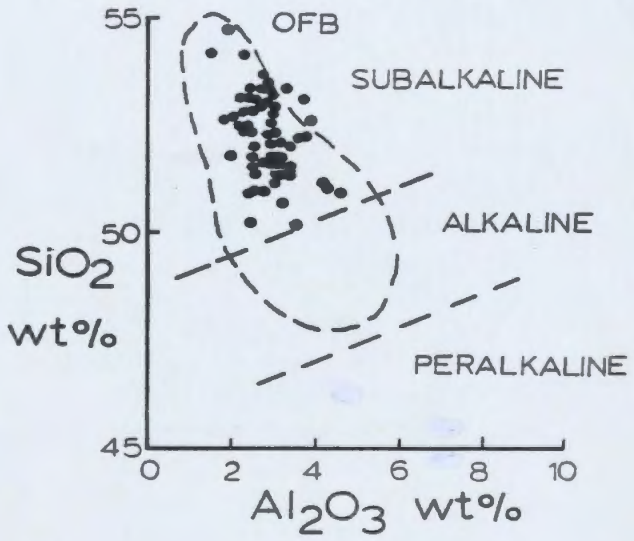
55
50
45
OFB
SUBALKALINE
ALKALINE
PERALKALINE
SiO2
wt%
0
2
4
6
8
10
Al2O3 wt%

B

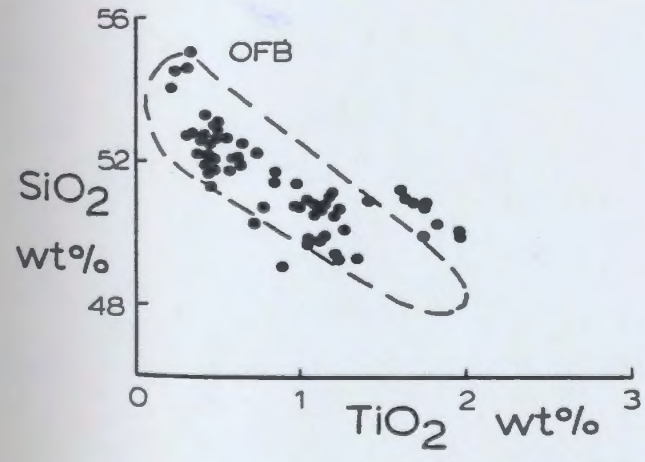
56
52
48
OFB
SiO2
wt%
0
1
2
3
TiO2 wt%

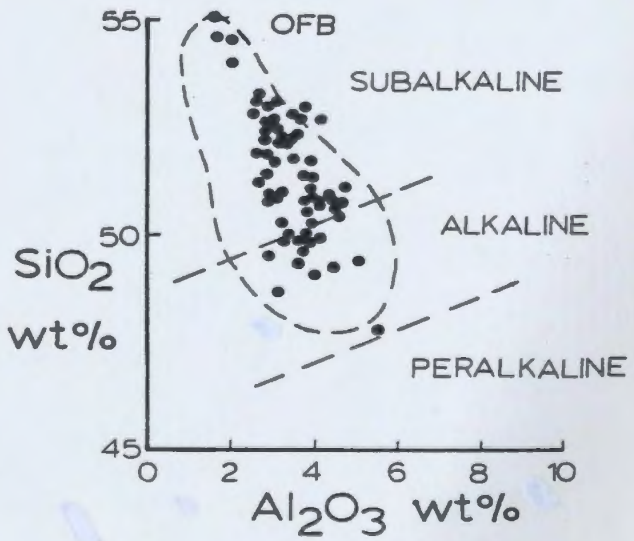
55
50
45
OFB
SUBALKALINE
ALKALINE
PERALKALINE
SiO2
wt%
0
2
4
6
8
10
Al2O3 wt%

Figure 5.23. Al (atomic, based on six O atoms) plotted against Fe/Mg ratio for clinopyroxenes of the Annieopsquotch Complex. Curved line is the trend determined for clinopyroxene from the critical zone of the Bay of Islands Complex by Riccio (1976) and field of crosses enclosed by dashed line presents clinopyroxenes from the critical zone of the Bay of Islands Complex analysed by Malpas (1976). The two trends are a right angles. Near vertical tie-line connects core-rim pair of analyses for one clinopyroxene from the Annieopsquotch Complex.

A. Clinopyroxenes from the critical zone show a steep trend at low Fe/Mg ratios.

B. Clinopyroxenes from diabase dykes of the sheeted dyke zone show a wide scatter and no clear trend.

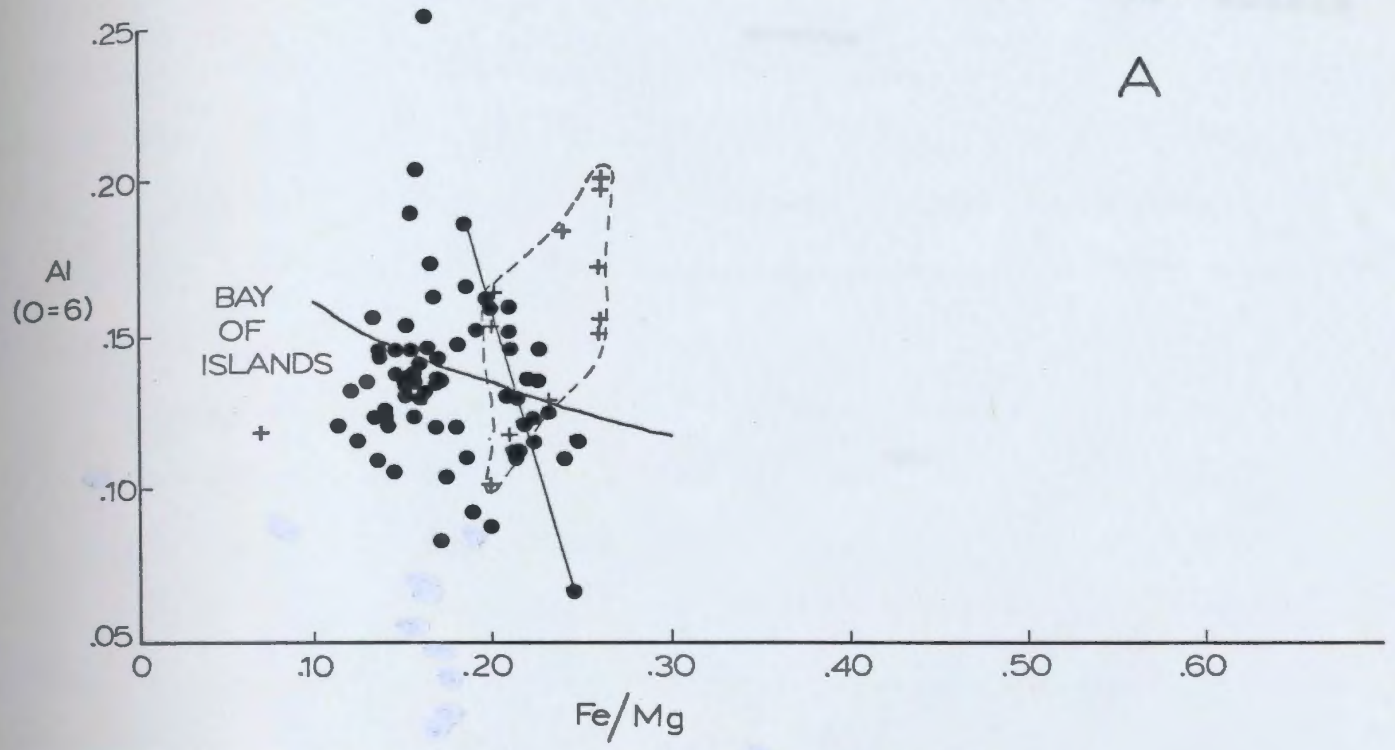

● CRITICAL ZONE

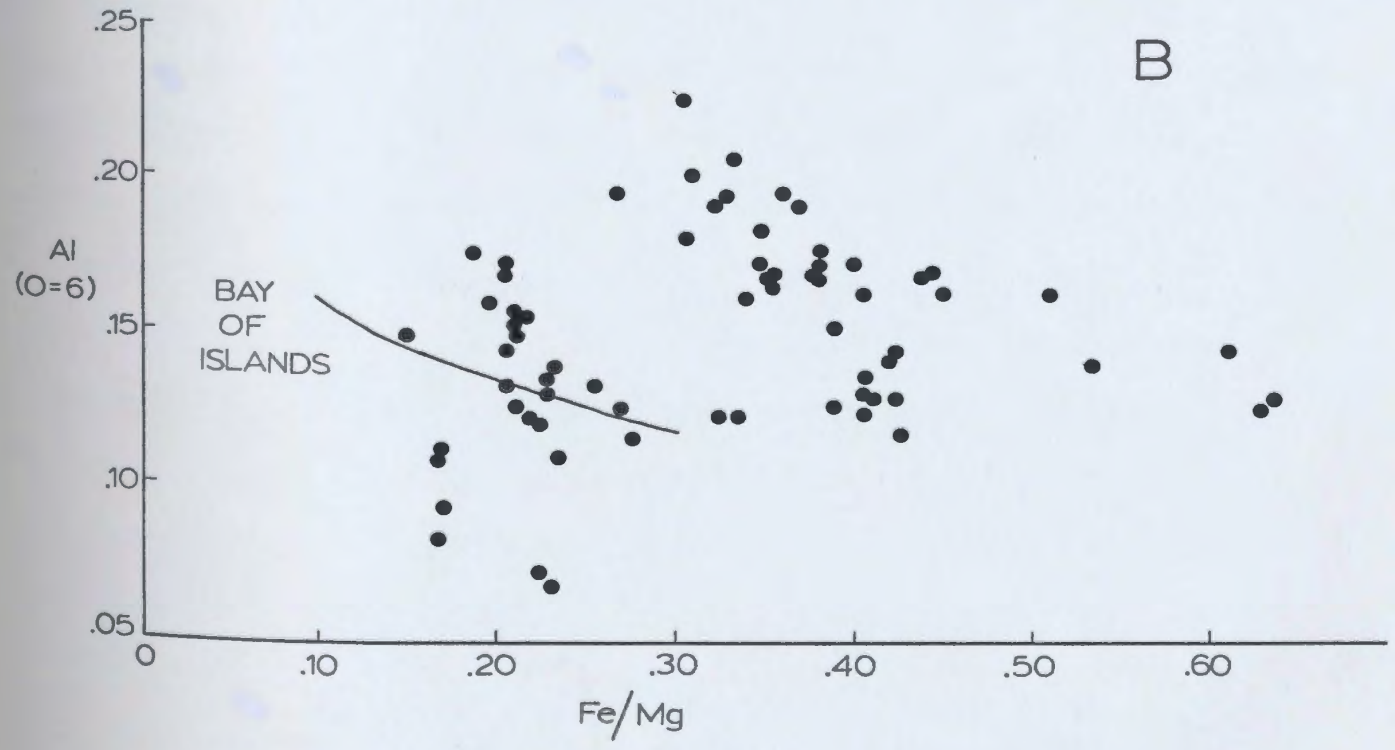

curve shown is the trend determined for clinopyroxenes of the critical zone of the Bay of Islands Complex by Riccio (1976). It is controlled by only six points. In contrast, the trend defined by thirteen clinopyroxenes from the critical zone of the Bay of Islands Complex analysed by Malpas (1976) is nearly at right angles to that of Riccio (1976).

Al contents (atomic) of clinopyroxenes from the critical zone of the Annieopsquotch Complex show some scatter when plotted against Fe/Mg ratio (Figure 5.23A), but there is an overall steep trend which is at a high angle to that defined by Riccio (1976). The range of Al content is likely due to; 1.cryptic variation within the layered sequence and 2.small scale variations within one layer due to the presence of zoned crystals. The latter would result from equilibration of grain edges with late, more differentiated, pockets of liquid. Some modification of the original chemistry may have resulted from metamorphic recrystallization, however an attempt was made to analyse the freshest samples with the best preserved igneous textures. A core-rim pair for one pyroxene is connected by a tie line in Figure 5.23A. This line is approximately parallel to the trend for all analyses.

Al contents of clinopyroxenes from diabase dykes of the sheeted dyke zone show a wide scatter over a wide range of Fe/Mg ratios(Figure 5.23B). No trend can be discerned.

Ti contents (atomic) show considerable scatter, plotted against Fe/Mg ratio, but show a rough positive

correlation. They cluster along the line defined by clinopyroxenes from the critical zone of the Bay of Islands and Lewis Hills (Riccio,1976). No clinopyroxenes were found in the critical zone of the Annieopsquotch Complex with Fe/Mg ratios greater than 0.25, in contrast to those of the Bay of Islands Complex, so only the lower part of the B.O.I. trend is represented by data from the Annieopsquotch Complex (Figure 5.24A). This is hard to reconcile with the suggestion from the field observations that only the top of the critical zone is preserved in the Annieopsquotch Complex.

Compared to critical zone clinopyroxenes, those of the sheeted dyke zone have higher Ti contents consistent with their more evolved nature (Figure 5.24B). The scatter of points at high Ti contents defies any attempt to fit a line. Low Ti pyroxenes from the sheeted dyke zone cluster on the Bay of Islands and Lewis Hills best-fit lines. Analyses of phenocrysts (symbol P), which may have been transported from the magma chamber, are no different than some pyroxenes which occur as groundmass grains. This is consistent with the whole rock chemistry, which indicates that dyke compositions overlap those of the gabbros.

Cr content (atomic) of critical zone clinopyroxenes is plotted against Fe/Mg in Figure 5.25A. A near vertical trend is seen which is roughly the same as that determined for samples from the Bay of Islands and Lewis Hills (Riccio,1976). This pattern corresponds to that shown by the suite of MORB samples of Papike (1980), outlined by the

Figure 5.24. Ti (atomic, based on six O atoms) vs. Fe/Mg ratio for clinopyroxenes of the Annieopsquotch Complex. Curved trend is that for clinopyroxenes of the critical zone of the Bay of Islands Complex and the straight trend is for the Lewis Hills, both from Riccio (1976). Crosses are clinopyroxenes from Malpas (1976), again showing a far different trend than those analysed by Riccio (1976).

A. Clinopyroxenes from the critical zone cluster along the low Fe/Mg end of both trends, but show considerable scatter, probably in part due to analytical uncertainty at low Ti contents.

B. Clinopyroxenes from the sheeted dyke zone range from values on the Bay of Islands trend to high Fe/Mg values with variable Ti contents. No single trend is apparent.

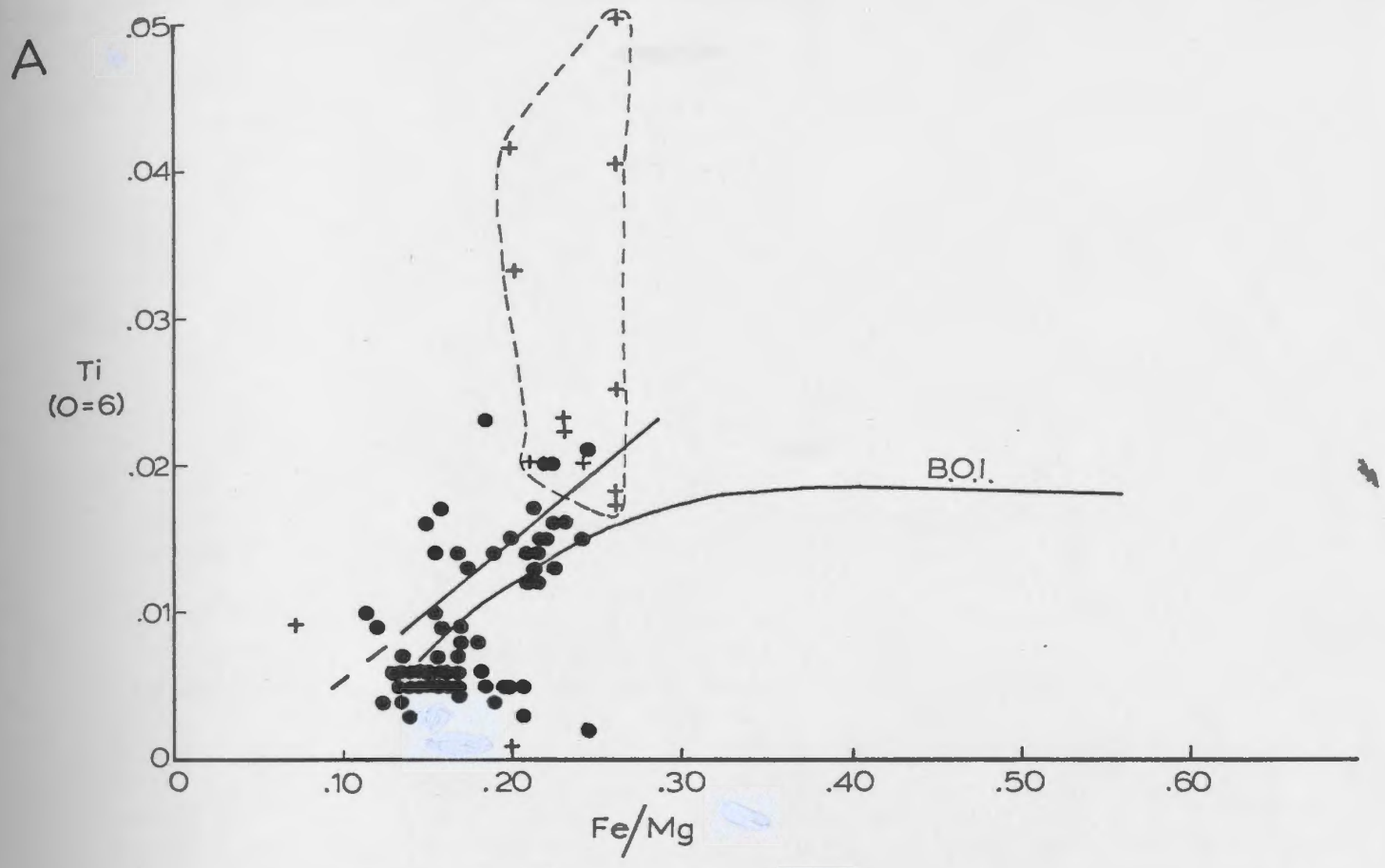
A
.05
.04
.03
.02
.01
0
Ti
(O=6)
B.O.I.
0
.10
.20
.30
.40
.50
.60
Fe/Mg

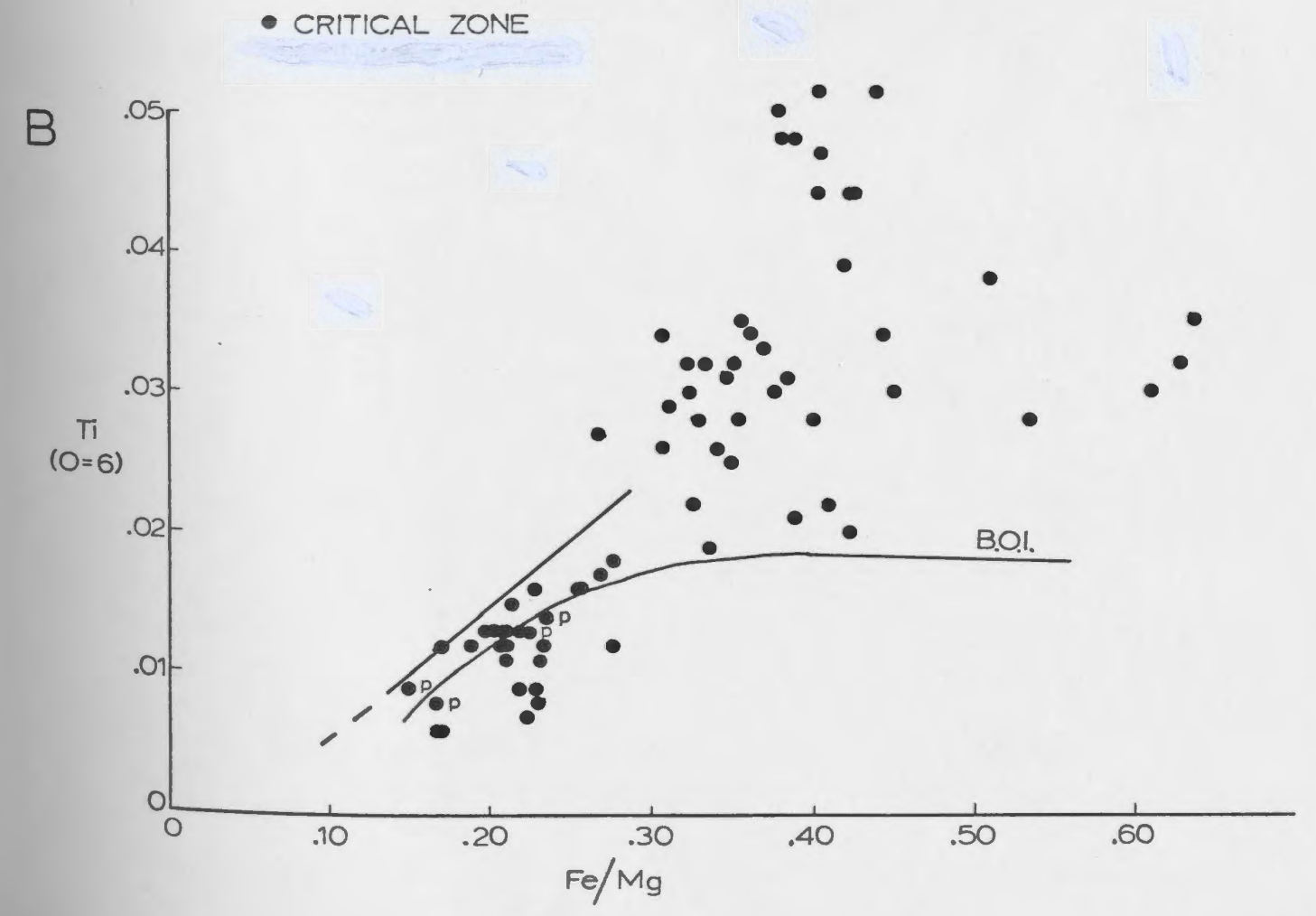
● CRITICAL ZONE
B
.05
.04
.03
.02
.01
0
Ti
(O=6)
B.O.I.
p
p
p
p
0
.10
.20
.30
.40
.50
.60
Fe/Mg

Figure 5.25. Cr (atomic, based on six O atoms) plotted against Fe/Mg ratio for clinopyroxenes of the Annieopsquotch Complex. Curved line is the trend for clinopyroxenes from the critical zone of the Bay of Islands Complex and the straight line is for clinopyroxene from the Lewis Hills, both from Riccio (1976). Crosses enclosed in long- dashed line are from Malpas (1976). Area enclosed by dashed lines is the field of ocean floor tholeiites, also called deep sea basalts, from Papike (1980). The two groups of clinopyroxenes from the Annieopsquotch Complex cover most of the field.

A. Clinopyroxenes from the critical zone plot generally along the Bay of Islands trend at Cr contents from .003 to .036 atomic. All fall in the field outlined by Papike (1980).

B. Clinopyroxene from the sheeted dyke zone trend to low Cr contents and high Fe/Mg. There is little overlap with the pyroxenes from the critical zone; even less if phenocrysts (symbol P) are excluded.

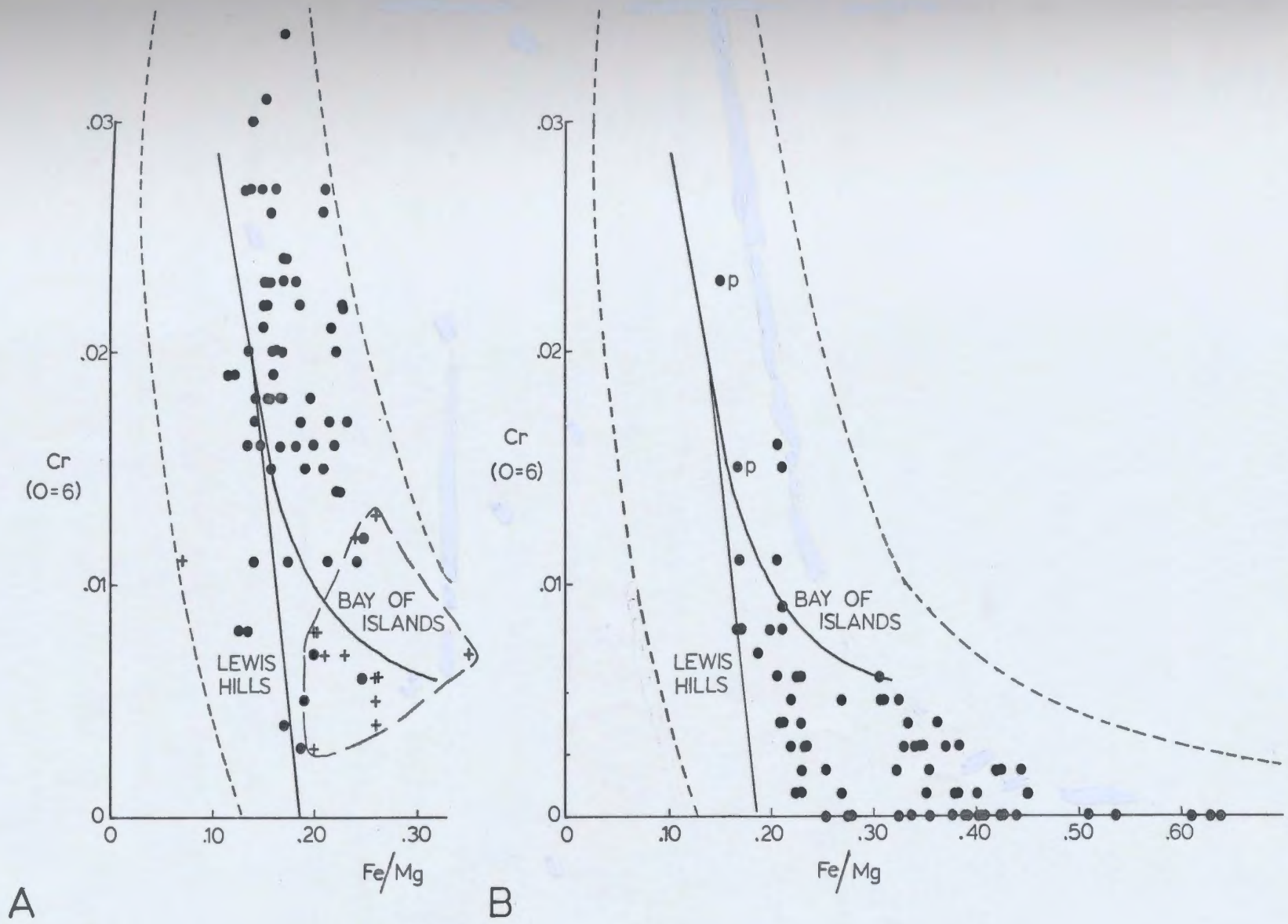
.03
.02
.01
0
Cr
(O=6)
LEWIS
HILLS
BAY OF
ISLANDS
0
.10
.20
.30
Fe/Mg
A
.03
.02
.01
0
Cr
(O=6)
p
p
LEWIS
HILLS
BAY OF
ISLANDS
0
.10
.20
.30
.40
.50
.60
Fe/Mg
B

dashed lines in Figure 5.25. This pattern reflects the early removal of Cr from the basaltic liquid by precipitation of chromite and chromian augite. These minerals co-exist in some rocks of the critical zone of the Annieopsquotch Complex. Bright green chromian augite (Cr approximately 0.7 to 1.2 wt %) grains plot at the top of the range. In contrast to the trend of critical zone clinopyroxenes defined by the analyses of Riccio (1976), those analysed by Malpas (1976) cluster at low Cr contents and overlap the range of diabase dykes of the Annieopsquotch Complex.

Cr plotted against Fe/Mg ratio for the dyke samples is shown in Figure 5.25B. There is a clear trend to low Cr values with increasing Fe/Mg. There is little overlap with the near vertical trend to high Cr values shown by clinopyroxenes of the critical zone. Magma which was the source of the diabase dykes presumably had undergone chromite and pyroxene fractionation, which depleted it in chrome before emplacement. All analyses plot between the trends for the Bay of Islands Complex and Lewis Hills, from Riccio (1976) and fall in the field of MORB (Papike, 1980).

In Figure 5.26 Cr, a compatible element which is removed from the basaltic magma early in the crystallization history, is plotted against Ti, which is incompatible and increases in concentration during fractionation. A large amount of scatter is present but, when data from both the critical zone (Figure5.26A) and sheeted dyke zone (Figure 5.26B) are considered together,

Figure 5.26. Cr plotted against Ti (both atomic, based on six O atoms) for clinopyroxenes of the Annieopsquotch Complex.

A. Clinopyroxenes of the critical zone plot at high Cr and low Ti contents. Crosses are clinopyroxenes from Malpas (1976).

B. Clinopyroxenes of the sheeted dyke zone are more chemically evolved and plot at lower Cr contents at Ti contents from <.01 to .055. A trend of decreasing Cr with increasing Ti content is evident.

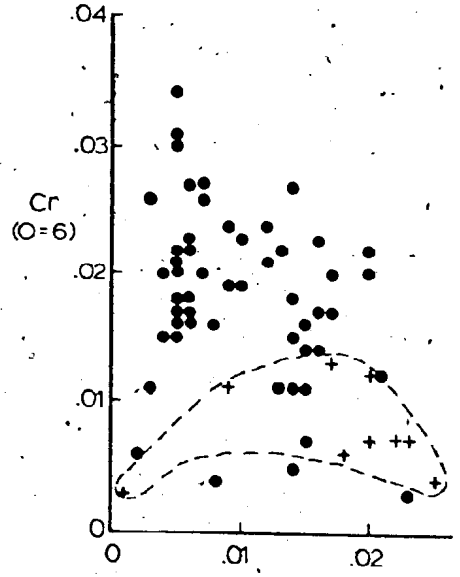

A

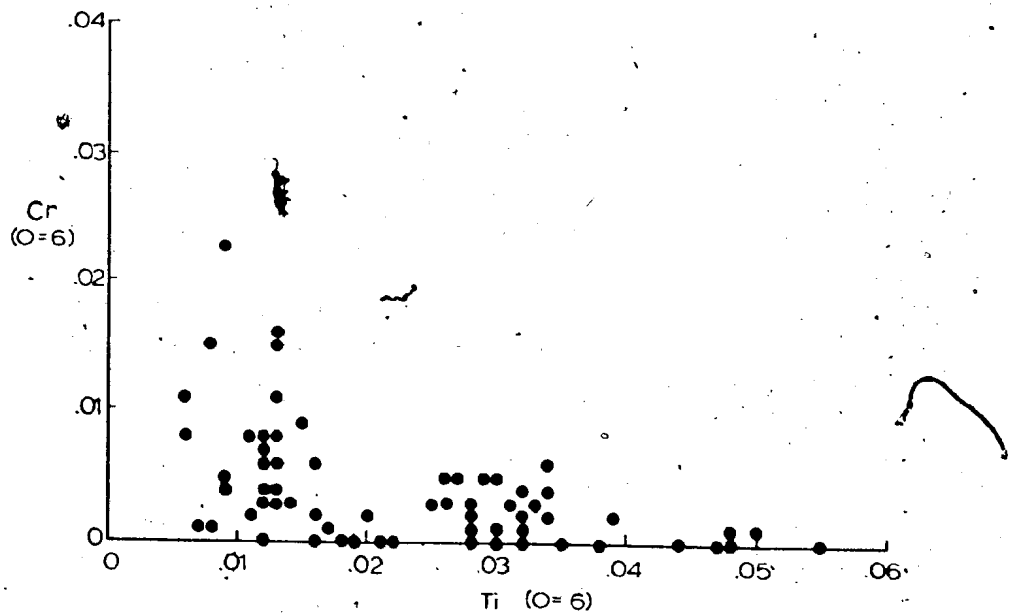

B

it is clear that Cr contents of clinopyroxenes fall rapidly with increasing Ti content and are below 0.01 (atomic) at Ti contents greater than 0.02 (atomic).

Si and Ti have been plotted against Al (atomic proportions to six oxygen) for pyroxenes of the critical zone in Figure 5.27 after Kushiro (1960). The fields of clinopyroxenes from tholeiitic, feldspathoidal-free and feldspathoidal-bearing alkalic rocks (Kushiro, 1960) are shown along with the field of clinopyroxenes from the critical zone of the Bay of Islands Complex (vertical stripes) from Riccio (1976). Clinopyroxenes from the critical zone of the Annieopsquotch Complex fall in the tholeiitic field and overlap the Bay of Islands field at its low Al end on each diagram. A negative correlation between Si and Al (atomic) indicates substitution between these elements in the crystal structure. Calculations indicate that the majority of Al determined in each analysis is required to be Al+4 to fill the tetrahedral site. This calculation can be subject to high errors however, as a result of uncertainty in the determination of Si content.

Leterrier et al. (1982) used a series of plots of various elements in turn to distinguish clinopyroxenes of basalts erupted in different tectonic settings. Firstly they used a plot of Ti vs. Ca+Na to distinguish calk-alkali and tholeiitic basalts from alkali basalts. Next they used a plot of Ti+Cr vs. Ca to distinguish non-orogenic basalts from orogenic basalts. The orogenic

Figure 5.27A,B. Si and Ti vs. Al (atomic, based on six O atoms), after Kushiro (1960). The fields of clinopyroxenes from tholeiitic (A), feldspathoidal - free (B) and feldspathoidal - bearing alkalic rocks (C) are shown. The field of clinopyroxenes from the critical zone of the Bay of Islands Complex (vertical lines) is from Riccio (1976). Clinopyroxenes from the critical zone of the Annieopsquotch Complex (dots and black field) fall in the tholeiitic field and overlap the Bay of Islands field at its low-Al end on each diagram.

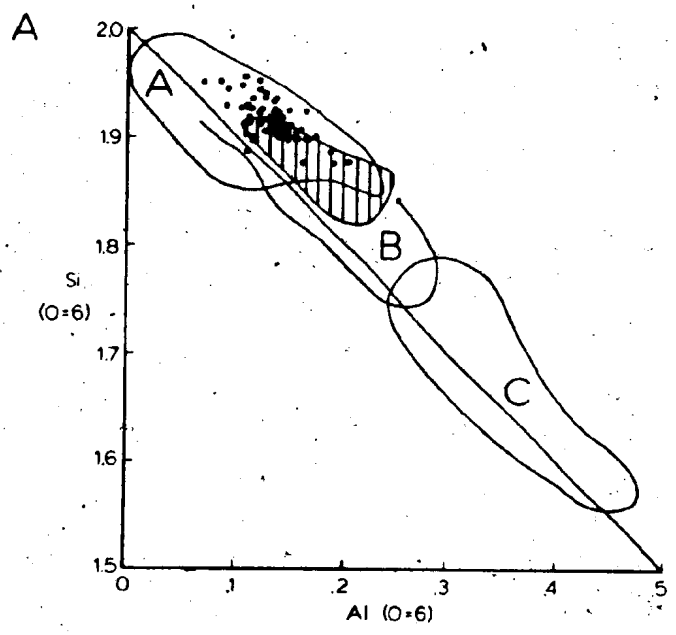
A
2.0
1.9
1.8
1.7
1.6
1.5
Si
(O=6)
A
B
C
0
.1
.2
.3
.4
.5
Al (O=6)

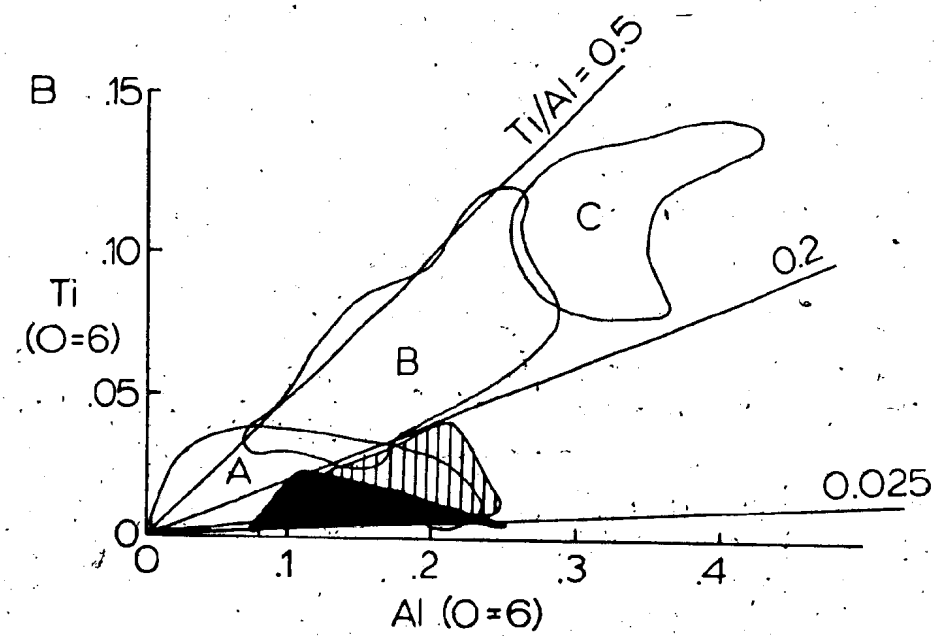
B
.15
.10
.05
0
Ti
(O=6)
Ti/Al=0.5
C
0.2
B
A
0.025
0
.1
.2
.3
.4
Al (O=6)

basalts are then subdivided on a third plot of Ti vs. Al (total) into calk-alkali and tholeiitic basalts.

As it has already been established above that the basalts and the pyroxenes of the Annieopsquotch Complex are tholeiitic, the pyroxenes are only plotted on the second diagram, which separates non-orogenic basalts, including MORB, from orogenic basalts (Figure 5.28). About eighty percent of the pyroxenes from each basalt type were found to fall on the appropriate side of the line on this diagram. Leterrier et al. (1982) emphasized that phenocrysts were more useful than groundmass clinopyroxene for determining the tectonic setting. However, few phenocrysts are present in diabase dykes of the Annieopsquotch Complex, so groundmass grains were plotted (Figure 5.28B). In addition, clinopyroxenes from the critical zone are plotted in Figure 5.28A.

Clinopyroxenes from the critical zone show a wide scatter, likely related to evolution of the liquid in the magma chamber. Most plot in the field of non-orogenic tholeiites and some that overlap do so in the same area that suites do that were used to define the fields.

Clinopyroxenes from the sheeted dyke zone cover a wide range of Ti+Cr contents. Most plot in the field of non-orogenic tholeiites, but some fall in the orogenic field in or near the area of overlap of the fields (Figure 5.28B).

Figure 5.28. Ti+Cr vs. Ca diagram for discriminating clinopyroxenes from non orogenic tholeiitic basalt (chiefly MORB) and orogenic basalt (after Leterrier et al.,1982). The two fields overlap but the dividing line has eighty-one percent of clinopyroxenes from non orogenic basalt above and eighty percent of clinopyroxenes from orogenic basalt below.

A. Clinopyroxenes from the critical zone show a wide scatter with many analyses plotting on each side of the line.

B. Clinopyroxenes from the groundmass of six diabase dykes of the sheeted dyke zone. Pyroxenes from each dyke have a limited compositional range within the area of all analyses. Most analyses plot in the field of non orogenic tholeiites and those that are across the line fall mainly in the area of overlap of the two fields.

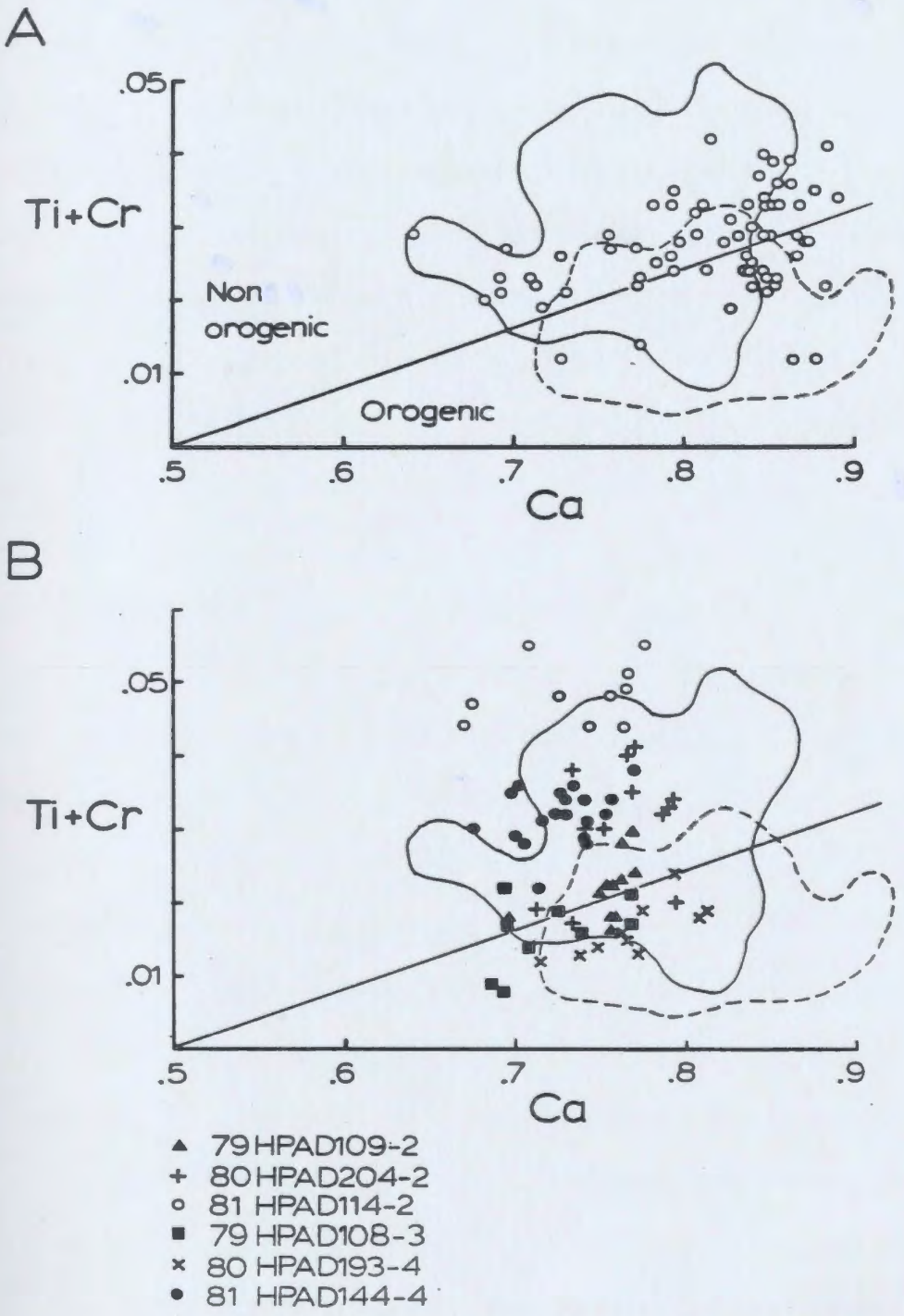
A
.05
Ti+Cr
.01
Non
orogenic
Orogenic
.5
.6
.7
.8
.9
Ca
B
.05
Ti+Cr
.01
.5
.6
.7
.8
.9
Ca
▲ 79 HPAD109-2
+ 80 HPAD204-2
○ 81 HPAD114-2
■ 79 HPAD108-3
× 80 HPAD193-4
● 81 HPAD144-4

5.13 SUMMARY

The chemistry of diabase dykes of the sheeted dyke zone of the Annieopsquotch Complex is little affected by seafloor alteration and the suite of forty dykes define clear magmatic trends on chemical variation diagrams. They are tholeiitic and closely match the Skaergaard differentiation path and the trends of MORB glasses on major element plots. The dykes have a wide range of TiO2 contents but all fall in the field of MORB on the diagrams of CaO/TiO2 and Al2O3/TiO2 vs. TiO2 of Sun and Nesbitt (1978) and are high-Ti ophiolites by the criteria of Serri (1981).

Trace element contents, with the exception of Zr, fall in the range of MORB and on most diagrams used to discriminate tectonic setting the dykes plot in the MORB field. On the classic Ti/1000:Zr:Y*3 diagram of Pearce and Cann (1973) dykes plot to the low Zr side of all fields and define a weak trend away from the Zr apex. This low Zr content of the suite could result from a low initial content in the source region in the mantle or from minor fractionation of zircon in the magma chamber. Five of six 'high level' gabbros sampled for geochronology were found to contain zircon.

On the TiO2 vs. Y diagram all dyke analyses clearly define a linear trend that is most similar to that of N-Type (Normal) MORB and is consistent with a combination of olivine, plagioclase and clinopyroxene fractionation.

These are the three minerals present in the the critical zone cumulates and the high level gabbro.

On diagrams of FeO*/MgO vs. Zr the dyke analyses define a steep trend, similar to that of the Sarmiento Complex of Chile, that is indicative of closed system fractionation. This is consistent with the suggestion, from the mapping, of the presence of several magma chambers in the Annieopsquotch Complex. The steep trend parallels that of the Sarmiento Complex but is offset to lower Zr contents. This, together with the trend mentioned above suggests that the lower Zr contents of the suite result from a lower initial Zr content in the source region.

Diagrams used to determine the spreading rate at which the ophiolite formed, based on the content of Zr, Y or TiO2 in its lavas are not very satisfactory. Zr contents are too low and variable; an average would be meaningless. TiO2 contents of the dykes and lavas of the Annieopsquotch Complex and other ophiolitic fragments in the belt do suggest a slow spreading rate, by analogy with modern ridge basalts and those of Caledonian ophiolites in Norway.

The few pillow lavas analysed are more altered than the diabase dykes. On most diagrams they plot with the diabase dykes, but on the diagram involving CaO/TiO2 they fall to lower Ca contents indicating loss of this element by seawater alteration.

The high level gabbros analysed are depleted in most trace elements compared to the dyke suite. They show evidence of plagioclase accumulation; a mineral that

excludes trace elements, except Sr and Eu. Accumulation of plagioclase has likely lowered most trace element contents relative to the basalt from which they crystallized. In addition, removal of the interstitial liquid by filter pressing has probably depleted the gabbro in incompatible trace elements.

REE contents of the suite of rocks analysed are increasingly enriched through the sequence gabbro, diabase dykes and pillow lava to trondhjemite. This reflects increasing differentiation. Most rocks of the suite show LREE depletion and some also have a HREE depletion which results in a slight convex-upwards pattern. Diabase dykes and pillow lavas of the Annieopsquotch Complex have REE patterns which largely overlap the field of MORB, but are slightly enriched relative to basalts of the Bay of Islands Complex. This may be a true difference or reflect the limited number of analyses from the latter. Most rocks of the Annieopsquotch Complex show Eu anomalies. These are interpreted to result from plagioclase accumulation, in gabbros, and fractionation removing Eu from the liquid to account for some negative anomalies in dykes and lavas.

Analyses of diabase dykes from sheeted dyke zones of ophiolitic fragments at Shanadithit Brook and King George IV Lake and pillow lava from King George IV Lake are plotted on many of the chemical variation diagrams. In general, they plot along the trends defined by diabase

dykes of the Annieopsquotch Complex, confirming their chemical association with the Complex. They were mapped as lithic equivalents of the Annieopsquotch Complex in the field.

Pyroxenes of the critical zone and sheeted dyke zone are tholeiitic. Those of the critical zone are more primitive, ie; higher in Cr and lower in Ti and Fe/Mg, than those of the dykes. They are comparable to those of the critical zone of the Bay of Islands Complex analysed by Riccio (1976) but cluster at lower Ti and Al contents, despite a larger number of analyses. Pyroxenes analysed by Malpas (1976) have higher Ti and lower Cr contents than those analysed by Riccio or in the present study and may be from more chemically evolved layers in the critical zone. Pyroxenes of the sheeted dyke zone cover a wide compositional range. The most evolved contain nil Cr and high, though variable, Ti contents. Overall, the pyroxene chemistry indicates that the basalts are of the non-orogenic or MORB type.

5.14 CONCLUSION

All evidence from major, trace and rare earth elements and clinopyroxene chemistry indicates that the rocks of the Annieopsquotch Complex are tholeiitic and are most similar to Normal-type mid ocean ridge basalts. This is compatible with formation of the Complex at a major ocean spreading

centre or perhaps in a back-arc basin. Only the Zr contents are anomalous and this could be due to low Zr content of the source region.

All ophiolitic fragments analysed from the Annieopsquotch ophiolite belt are closely comparable in chemistry to the Annieopsquotch Complex itself and it appears reasonable to assume that all were formed in the same setting.

5.15 PETROGENESIS OF THE MORB SUITE

5.15.1 Introduction

The petrogenesis of MORB's is a subject that is still controversial despite fifteen years of detailed study and thousands of analyses since the pioneering work of Gast (1968), Engel et al. (1965), Kushiro (1968), Green and Ringwood (1967), O'Hara (1965) and many others.

The early ideas that the generation of MORB's involves a high degree of partial melting of a once depleted mantle (Gast, 1968) and that the liquids so produced are modified en route to the surface by fractionation of olivine, plagioclase and clinopyroxene (O'Hara, 1965) are still valid. Numerous workers since have reached essentially the same conclusions and these two basic processes are still intepreted to be the major controls on MORB petrogenesis.

A major controversy surrounds the composition of the 'primitive' melt, whether picritic as suggested by O'Hara (1968), Clarke (1970), Malpas (1978), Elthon (1979), Duncan and Green (1980) and Stolper (1980) and others or

olivine-porphyritic basalt as suggested by Presnall (1979), Sen (1982), Bryan (1983), LeRoex et al. (1983) and Takahashi and Kushiro (1983).

Both arguments are persuasive and in fact Duncan and Green (1980) argue for the existence of two primary melts, one picritic generated at a depth greater than forty-five km. and a second of tholeiitic composition generated at a depth of approximately 25 km.

Bryan (1983) sums up the current dilemma when he points out that MORB's could equally well be derived from 1. an olivine-rich picritic primary liquid, those MORB's 'oversaturated in olivine representing the last stages of evolution to low pressure equilibrium resulting from olivine fractionation' or 2. 'partial melting and separation at different pressures over a range of depths in the mantle or by polybaric crystallization'.

Variable mantle compositions and degrees of partial melting would complicate the picture further.

The debate may be irresolvable with present data as both types of 'primitive' lavas are observed in ophiolites and in oceanic crust whilst experimental data also supports both views.

The relative scarcity of erupted picritic liquids is sometimes taken to indicate that they are rarely generated, but this has been explained by Sparks et al. (1980) and Stolper and Walker (1980) as a function of their greater density. Sparks et al. suggest that picritic magmas are trapped at the bottom of the crustal magma chambers where

they precipitate olivine. When their density is lowered they convectively mix with the overlying tholeiitic liquid in the magma chamber and are assimilated. This would explain the presence of thick dunite layers at the base of the crustal section of many ophiolites (eg. Bay of Islands Complex; Leka, Norway) and such a model has been applied to the Oman ophiolite by Smewing (1981).

Stolper and Walker (1980) suggested that picritic lavas are rarely seen because the dense magma is trapped under the less dense oceanic crust and only fractionates that reach a density minimum, corresponding to the appearance of clinopyroxene, are less dense than the crust and so erupt. A histogram of Fe/(Fe+Mg) ratios of MORB's presented by them has its maximum at the point of the minimum density liquids.

Increased emphasis in recent work on the petrogenesis of MORB's has been placed on processes operative in magma chambers that modify basalt compositions independent of olivine-plagioclase- clinopyroxene fractionation. These include assimilation of hydrated roof rock (Gregory and Taylor, 1979), Soret separation (Walker and DeLong, 1982), liquid immiscibilty (Dixon and Rutherford, 1979) and chemical diffusion and zonation within magma chambers.

Magma mixing is, in addition, likely in ocean ridge magma chambers (O'Hara, 1977; Stern, 1979; Alabaster et al., 1982) and could mix magmas that were already affected to varying degrees by these other processes. Indeed, considering the number of processes likely operative within

magma chambers, it may be impossible to detect a primary liquid among modern MORB's (O'Hara, 1982). It may be that no pristine partial melts exist in ophiolite sections either, except possibly for veins cutting the mantle sequence.

5.15.2 The Annieopsquotch Suite

Diabase dykes of the Annieopsquotch Complex define clear trends on most major and trace element diagrams. However, this does not mean that they are all co-magmatic. Indeed, considering the distribution of the samples this is practically impossible.

No modelling of the generation of Annieopsquotch diabase dyke compositions has been undertaken in this study. It appears reasonable however, since they are so similar to N-type MORB, that they were generated by the same process. The one enigmatic feature of the suite, which may be inherited from its mantle source, is the low Zr content. All Annieopsquotch dykes were likely generated by similar degrees of partial melting of a homogeneous mantle source.

The suite can, in general, be explained by either partial melting of a depleted mantle source at 9- 10 kbar. (30 km. depth) or by fractionation of olivine, plagioclase and clinopyroxene from a picritic melt. These contrasting models are discussed below. Much of the variation in trace element contents can be simply explained by depletion by fractionation of olivine (Ni), spinel and clinopyroxene

(Cr), and plagioclase (Sr, Eu) or by enrichment in the evolving basaltic magma (Ti, V, Zr, Y and Nb).

As mentioned above, other processes operative in magma chambers may affect basaltic liquid compositions.. The fractionation of small amounts of zircon, or other minor phases, may affect the trace element contents of derivative liquids. While not commonly observed in ophiolitic high level gabbros which are the source of the diabase dykes, and usually thought not to crystallize in rocks of low silica content (<52 wt. %), zircon has been found in gabbros in layered intrusions and ophiolites. It likely crystallizes from interstitial liquid that has evolved slightly relative to the primitive basalt.

The assimilation of roof rock from magma chambers is thought to occur commonly and often evidence is preserved in outcrop in the form of stoped blocks, hybrid zones etc. In ophiolites, stoping of hydrated gabbro and diabase from the roof has been suggested as a mechanism to account for the input of water into the magma chambers, as recorded by H and O isotopic ratios of the gabbros. This assimilation would also increase O fugacity sufficiently to stabilize Fe-Ti oxides, which upon crystallization would rapidly deplete the magma in Ti. This could explain the low Ti content of several diabase dykes of the suite.

Magnetite gabbros are present locally in pegmatitic pods in the high level gabbro and near the top of the gabbro zone. Crystallization in both these areas would likely occur from an evolved, volatile- enriched basalt

liquid.

5.15.3 Primary Magma, Primitive Partial Melt

The most magnesian diabase dykes, with the highest Ni contents, are samples 79HPAD150-2 and 79HPAD153-3 with 10.5 and 11.6 wt. % MgO respectively (Ni 190, 276 ppm). These dykes cut the gabbro zone and are similar to experimental melts produced from plagioclase and spinel lherzolite at 9 kbar by Sen (1982) and at 10 kbar by Takahashi and Kushiro (1983).This is approximately the pressure and source composition assumed by Bryan (1983) to be characteristic for the generation of MORB's. The resultant melts would be Type 1 (olivine- phyric) basalts and plot in his field A.

The experiments of Takahashi and Kushiro (1983) convincingly demonstrated that a wide range of compositions of primary partial melts of spinel lherzolite can be generated over a range of temperatures, pressures and degrees of partial melting. Those generated at a single pressure fall along curves at near constant normative olivine content (Figure 5.29). Melts generated at higher pressures plot at progressively higher normative olivine contents, a relationship first predicted by O'Hara (1965). Takahashi and Kushiro (1983) suggested as a result of their work that basalts parental to MORB can be generated at 10 kbar and 1275 degrees C (point A, Figure 5.29, Table 5.15) and that fractional crystallization of olivine, plagioclase and clinopyroxene can produce the more evolved MORB compositions.

Figure 5.29. Normative olivine- clinopyroxene- silica diagram, projected from plagioclase, with analyses of diabase dykes of the Annieopsquotch Complex plotted by the method of Walker et al. (1979). Shown are the 1, 10 and 15 kbar cotectics and the liquid line of descent determined by analyses of glasses from the Oceanographer Fracture Zone from Walker et al. (1979). Field of MORB's is shown by solid outline and the area of greatest concentration of MORB's by the dashed line.

Concentric curves represent isobaric liquid compositional trends at the pressures noted and point A represents an experimental melt formed at 10 kbar and 1275 degrees C (Table 5.15) from Takahashi and Kushiro (1983).

Open and solid stars are samples 79HPAD150-2 and 153-3, the most primitive from the Annieopsquotch suite, not normalized to 100 percent. Normalizing the data shifts these points towards the silica apex by approximately 10 percent.

Striped arrows are inferred crystallization paths from 15 and 10 kbar cotectics and the continuation along the path of low pressure fractionation of olivine + plagioclase + clinopyroxene.

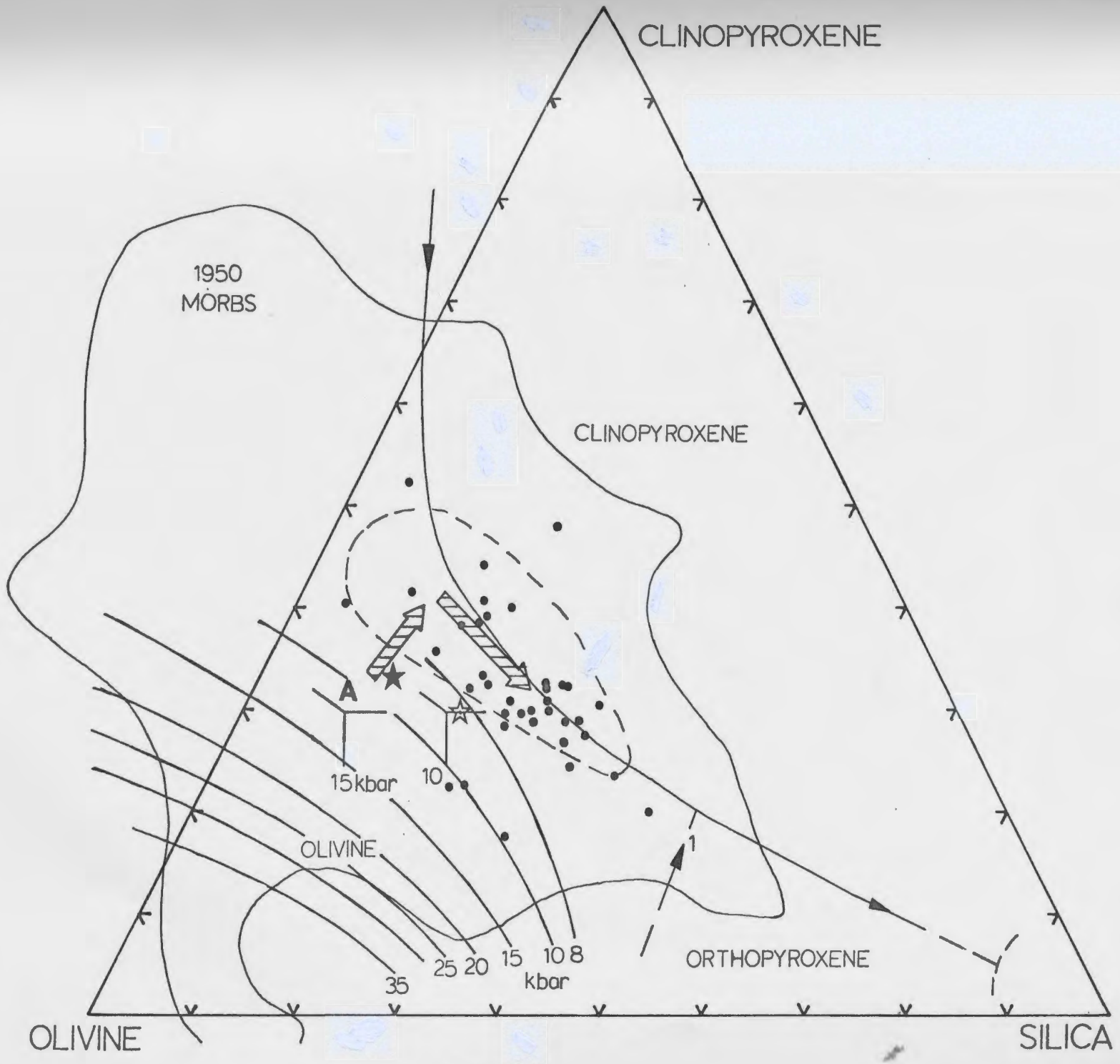
CLINOPYROXENE
1950
MORBS
CLINOPYROXENE
A
15kbar
10
OLIVINE
1
35
25
20
15
10
8
kbar
ORTHOPYROXENE
OLIVINE
SILICA

TABLE 5.15 MAGMAS POSTULATED TO BE 'PRIMARY' 'PRIMITIVE' OR 'PARENTAL' TO MORB**

	1.	2.	3.	4.	5.	6.	7.	8.	9.	10.	11.
SiO_2	49.7	49.1	50.06	47.25	48.53	51.20	54.20	51.64	50.7	48.10	49.25
TiO_2	0.72	0.62	0.82	0.79	0.62	0.87	0.40	0.34	0.78	0.86	1.60
Al_2O_3	16.4	16.5	15.84	13.64	16.65	15.03	15.40	15.53	14.79	16.10	14.54
FeO*	7.89	8.78	7.53	9.77	8.41	8.39	7.90	7.84	8.85	8.61	9.82
MnO	0.12	0.15	0.15	0.14	-	-	-	-	0.17	0.16	0.18
MgO	10.1	10.3	10.14	17.61	10.25	9.21	8.70	10.6	10.78	11.82	10.26
CaO	13.0	12.4	13.09	9.58	12.68	12.73	11.50	13.51	11.30	12.13	10.84
Na_2O	1.98	1.92	1.97	0.89	2.26	1.87	1.60	0.48	1.95	1.83	2.44
K_2O	0.01	0.07	0.17	0.06	0.06	0.10	0.10	0.07	0.29	0.10	0.26
P_2O_5	-	0.06	0.08	0.07	-	-	-	-	0.11	0.06	0.16
Mg'	.72	.70	.73	.78	.70	.68	.68	.73	.71	.73	.65
Ni	200	232	249	-	-	-	-	-	190	276	-
Cr_2O_3	.07	.06	.14	.20	.03	.07	-	.03	.05	.05	.07

*Total Fe as FeO

$Mg' = Mg/(Mg + Fe^{2+})$ where $Fe^{2+} = 0.9 \times (Fe^{2+} + Fe^{3+})$

**Normalized to 100 percent, volatile-free.

1. Most 'primitive' ocean floor basaltic glass, DSDP leg 3 (Frey et al., 1974)
2. 'Primitive' ocean floor basaltic glass, FAMOUS area (Langmuir et al., 1977)
3. Aphyric ocean floor basalt, N. Atlantic 45° (Rhodes, unpub. data in Basaltic Volcanism Study Project, 1981)
4. High magnesium dyke from Tortuga Complex (Elthon, 1979)
5. High-olivine parental liquid to FAMOUS basalt glasses (Bryan, 1979)
6. Low-olivine parental liquid to FAMOUS basalt glasses (Bryan, 1979)
7. Second stage melt (Duncan and Green, 1980)
8. Experimental 9 kbar partial melt of plagioclase-spinel lherzolite (Sen, 1982)
9. Diabase dyke 79HPAD150-2, Annieopsquotch Complex
10. Diabase dyke 79HPAD153-3, Annieopsquotch Complex
11. Experimental 10 kbar liquid equilibrated with spinel lherzolite (Takahashi and Kushiro, 1983)

Table 5.15 lists nine analyses postulated by various workers to be 'primitive' or 'parental' to MORB and samples 79HPAD150-2 and 79HPAD153-3 (anal. 9,10), all volatile-free and normalized to 100 %. It is apparent that the samples from the Annieopsquotch Complex are very similar to primitive glasses from the present ocean floor and analysis 9 is especially similar to the 'high- olivine' parental liquid (Table 5.15, anal.5) of Bryan (1979). In addition sample 80HPAD150-2 is very similar to the experimental melt produced by Takahashi and Kushiro (1983) at 10 kbar (Table 5.15, anal. 11). Notably, the MgO and Ni contents of sample 79HPAD153-3 are higher than those of any of the modern MORB's postulated to be primitive. However, the Ni content of sample 79HPAD150-2 is somewhat lower than that expected for a primary melt formed by a high degree of partial melting of mantle material.

Both dyke compositions are significantly different than the postulated 'primary' picritic dyke from the Tortuga Complex (Table 5.15, anal. 4) of Elthon (1979). If picritic melts are parental to MORB, from inspection of Figure 5.30, it is apparent that (provided that the lines of inferred constant partial melting of Hart and Davis (1978) are correct) the composition of sample 79HPAD153-3 could result from about 5 % of olivine fractionation of a primary melt. While this sample is the most 'primitive' member of the dyke suite analysed, it is not a 'primary' magma by this criteria.

The suite of Annieopsquotch dykes appear to outline a

Figure 5.30. Ni vs. MgO diagram, after Hart and Davis (1978), showing;

1. lines of inferred constant partial melting of a mantle source (10, 20 and 30 %),
2. curves for fractional crystallization of olivine from liquids with original MgO contents of 12, 16 or 20 wt. %,
3. field of basalts with high pressure xenoliths (vertical ruled) and field of basalts and differentiates from five volcanic series (horizontal ruled),
4. three postulated 'primary' basalts, parental to MORB (labelled 1 -3 corresponding to analyses in Table 5.15),
5. analyses of diabase dykes from the Annieopsquotch Complex, showing the most primitive samples (79HPAD150-2, 153-3) and the inferred liquid line of descent for the suite (heavy dashed line),
6. star, representing postulated 'primary' partial melt parental to the Annieopsquotch suite.

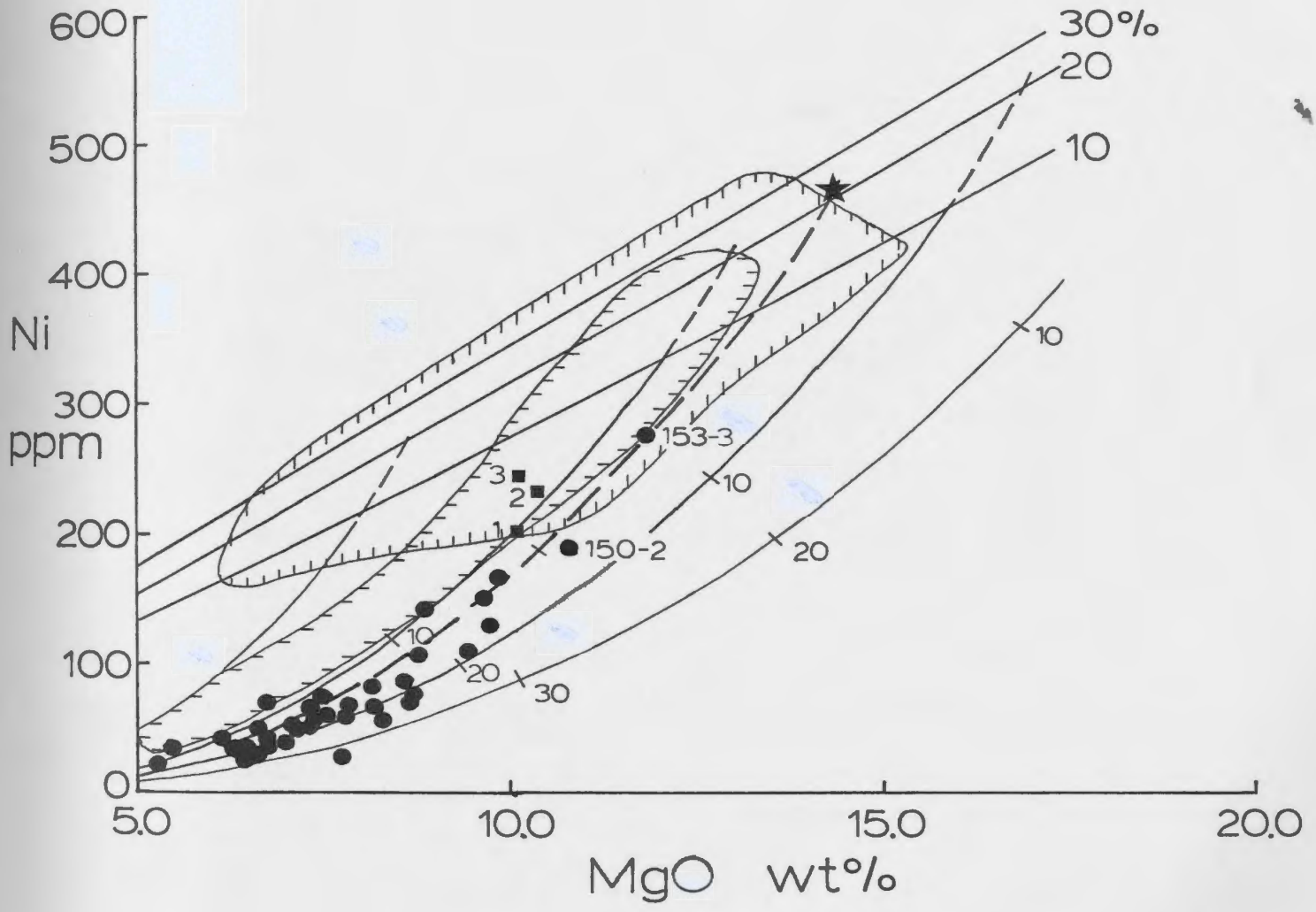
600
500
400
Ni
300
ppm
200
100
0
5.0
10.0
15.0
20.0
MgO wt%
30%
20
10
10
153-3
10
3
2
1
150-2
20
10
20
30

trend consistent with the fractional crystallization of olivine as shown by the solid lines on Figure 5.30. Projecting this trend (admittedly roughly) to intersect the line of 20 (or 30) % partial melting one determines an initial MgO content for the primary melt of approximately 14 wt. %, with a corresponding Ni content of approximately 470 ppm.

5.15.4 Summary

The Annieopsquotch dyke suite, like most MORB's offer no conclusive evidence as to the composition of 'primary' partial melts of depleted upper mantle. The most 'primitive' dykes have compositions consistent with primary melts and are directly comparable to experimentally produced liquids at 9- 10 kbar. The present writer favours the idea that basalts with MgO contents of approximately 10 wt. % are primary, based on recent work by Sen (1982) and Takahashi and Kushiro (1983). However, sample 80HPAD153-3 is also compatible with a model involving approximately 5% of olivine fractionation from a primary picritic melt. Olivine fractionation (+/- spinel) would have increased the Fe/(Fe+Mg) ratio and rapidly depleted the liquid of Ni (+/- Cr).

The compositions of the more differentiated members of the dyke suite could have been derived by a combination of olivine + plagioclase + clinopyroxene fractionation. This is reflected in the composition of the critical zone cumulates which include troctolite, olivine gabbro and

minor anorthosite. The major fractionating minerals in the high level crustal magma chambers were plagioclase and clinopyroxene. As recorded by their variable Fe/(Fe+Mg) ratios, emplacement of diabase dykes to form the sheeted dyke zone proceeded throughout much of the crystallization history of the magma chambers.

CHAPTER 6 GEOLOGY AND GEOCHEMISTRY OF THE VICTORIA LAKE GROUP

6.1 INTRODUCTION

The Victoria Lake Group (Kean,1977) is a series of isoclinally folded and faulted mafic, intermediate and felsic flows, tuffs and tuffaceous sedimentary rocks and associated plutonic rocks which underlies a large V-shaped area of central Newfoundland. The folds have northeast trending axes and are cut by northeast striking faults. The Group is poorly exposed with less than one percent outcrop in general.

The only known age for the Victoria Lake Group comes from conodonts in limestone interbedded with tuffs near Red Indian Lake. The Llanvirnian- Llandeilian age determined by Stouge (reported in Kean and Jayasinghe, 1980) is from an uncertain height within the sequence and consequently the time span represented by deposition of the Victoria Lake Group is unknown.

The contact between the Victoria Lake Group and the Annieopsquotch Complex is interpreted to be a fault on the northwest side of Victoria Lake. There has been post Ordovician movement on this fault involving intrusion of granite (Map 1) and disruption and steepening of terrestrial sedimentary rocks in Silurian or later time. However, this structure may have been a thrust fault in Ordovician time. In Wigwam Brook, dark and light grey

cm-scale bedded cherts (Map 1) form folds overturned towards the ophiolite. They have northeast striking axial planes that dip 60 to 70 degrees southeast. These cherts may represent the original sedimentary cover to the ophiolite and are in apparent conformity with mafic and intermediate tuffs of the Victoria Lake Group. However, no continuous section can be demonstrated through the sequence ophiolite - bedded cherts - tuffs.

Dacitic dykes, which are lithologically and chemically similar to rocks of the Victoria Lake Group, cut the Annieopsquotch Complex. This indicates, as does the fossil evidence, that magmatic activity in the Victoria Lake Group in part postdated formation of the ophiolite. It also suggests that the ophiolite and Victoria Lake Group were adjacent in Ordovician time and not brought together later by transcurrent movement along the fault now separating them. The fact that the dacitic sills are only found cutting the top of the ophiolite, the part closest to the Victoria Lake Group now, suggests that the oceanic crust was disrupted before or during dacitic volcanism. Otherwise one would expect to observe similar dykes in other parts of the ophiolite.

Felsic flows, tuffs and sedimentary rocks have a penetrative cleavage with a northeast trend and generally steep dips. Some mafic rocks and small diorite intrusions, which are common in the Victoria Lake area, have massive interiors and cleaved margins. Strain was heterogeneous in dacitic agglomerates. The cores of large bombs are

essentially undeformed but the margins of the blocks and the tuffaceous sedimentary matrix are strongly cleaved and the cleavage wraps around the blocks.

Alteration and silicification of the volcanic rocks is widespread. The tuffs of intermediate and felsic composition are now predominantly chlorite - sericite - quartz - feldspar schists with the latter two minerals as phenocrysts that appear as clasts in the schist. Carbonate is abundant in the matrix and as thin seams and fracture fillings in these rocks. This accounts, in part, for the high losses on ignition reported for some samples. Dacitic bombs in the agglomerate have grey-green 'fresh' cores and buff to white silicified margins, often as much as five cm thick. Analyses reported in this work are of the least altered cores of the bombs.

6.2 AREAS SAMPLED

During this study rocks of the Victoria Lake Group were examined in the Victoria Lake area (Map 3) and in quarries and roadcuts along the Burgeo road (Map 2). These areas were not remapped because recent geological maps of the Victoria Lake and King George IV Lake map areas (Kean, 1977,1983) are sufficiently detailed, considering the poor exposure.

Most tuffaceous rocks were waterlain and show mineral grading, crystal- rich beds and argillaceous interbeds. Crossbeds and scoured bases of beds are locally present.

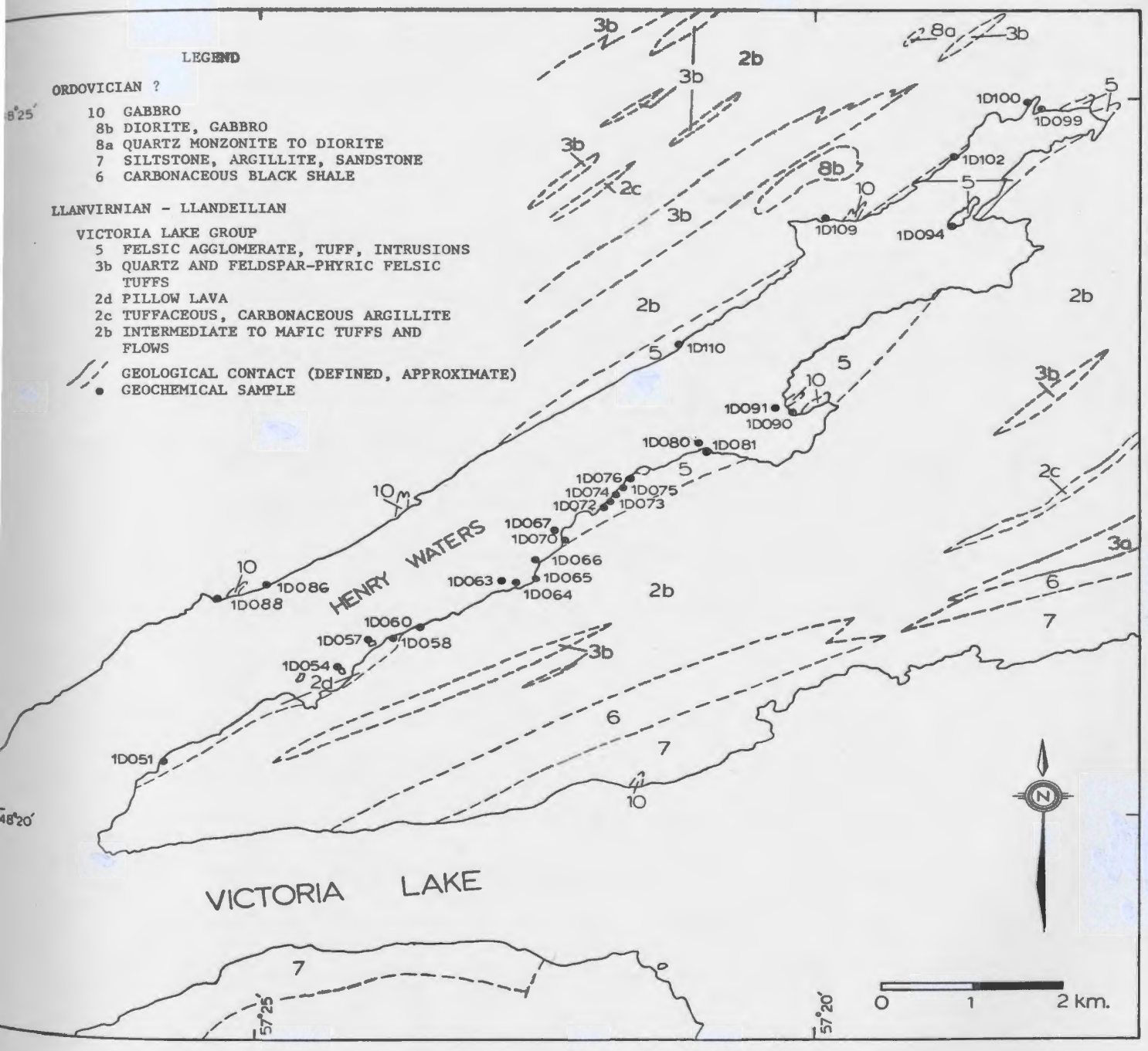

Map 3. Geology of a portion of the Victoria Lake map area (NTS 12A/6), after Kean (1977), showing location of geochemical samples.

None of these rocks were analysed as any sample would constitute a mixture of sorted volcanic and sedimentary materials. Only pillowed and massive flows, sills, dykes and diorite plugs were analysed as these could reasonably be interpreted to represent liquid compositions.

6.3 OCCURRENCES OF MAFIC ROCKS

Mafic rocks of the Victoria Lake Group occur as massive and pillowed flows, tuffs, diabase dykes and sills, and gabbro. On the east shore of Henry Waters (Map 3) gabbro is present, cut by diabase dykes. Farther south, on the same shore, pillow lavas are present. To the south of these, bedded tuffaceous sedimentary rocks are cut by a dacitic porphyry intrusion. The contact between the pillow lava and the sedimentary rocks and porphyry was not seen.

Mafic flows and pillow lava also occur in roadcuts on the Burgeo road and in a quarry east of the road (Map 2). Flows in the roadcuts just south of the Annieopsquotch Mountains are quite fresh but pillows in the quarry are strongly epidotized and sheared and contain carbonate in fractures. Pillow lava, interpreted by Kean and Jayasinghe (1981) to be part of the Victoria Lake Group, occurs in a fault-bounded block east of Boogie Lake in the King George IV Lake map area (Map 2).

Mafic dykes, interpreted to be part of the Group, cut dacitic agglomerate at the north end of Henry Waters and

tuffaceous rocks west of the Burgeo road. Mafic tuffs, cut by a diabase sill, outcrop at the south end of Victoria Lake. The tuffs appear quite massive and may contain little detrital sedimentary material. Similar tuffs were also observed in Wigwam Brook at its mouth at Victoria Lake. They may be part of the same horizon.

6.4 CHEMISTRY OF THE MAFIC ROCKS

These rocks are weakly to moderately cleaved and have undergone variable amounts of hydrothermal alteration. This is reflected in their losses on ignition, reported in Tables 6.1,2, which vary from 1.30 to 7.16 wt. %. This alteration is also reflected in the variation in some major as well as 'mobile' trace element contents. Nevertheless, an attempt is made to characterize the Group by relying mainly on its 'immobile' trace element contents. Twenty-nine samples of basalt were analysed although four were rejected due to high losses on ignition. The major and trace element contents of twenty- five are reported in Table 6.1. In addition, thirteen samples of mafic dykes and sills were analysed (Table 6.2). REE contents of seven of these rocks are reported in Table 6.3.

SiO_2 contents vary from 45.3 to 58.8 wt. % in rocks that were mapped in the field as basalt. Two samples, 81HPAD014-1 and 2 with 58.6 and 58.8 wt. % SiO_2 are strongly altered. Secondary silicification is thought to

TABLE 6.1. MAJOR AND TRACE ELEMENT ANALYSES OF MAFIC VOLCANIC ROCKS OF THE VICTORIA LAKE GROUP

	81D 014-1	81D 014-2	81D 016	81D 017-1	81D 043-1	81D 046-1	81D 047	81D 051-2	81D 051-3	81D 051-4	81D 054-1	81D 057	81D 058
SiO_2	58.6	58.8	48.0	49.6	50.5	49.1	47.9	56.0	50.8	52.6	52.0	46.7	51.2
TiO_2	1.54	1.50	2.20	2.75	1.59	1.31	1.06	1.47	1.47	1.48	2.43	0.77	1.32
Al_2O_3	16.2	15.9	13.8	15.5	14.0	15.1	15.7	18.9	18.8	19.2	15.8	18.1	16.1
Fe_2O_3	1.45	1.62	4.21	4.20	3.48	2.80	3.77	2.94	4.61	3.34	4.53	4.76	1.35
FeO	5.53	5.53	10.4	8.74	8.30	7.21	6.04	4.29	5.51	5.01	5.58	5.86	5.79
MnO	0.15	0.15	0.20	0.37	0.21	0.20	0.19	0.12	0.17	0.14	0.20	0.20	0.14
MgO	3.14	3.40	6.95	2.89	6.62	7.95	7.91	3.68	5.20	4.53	4.42	7.03	4.93
CaO	6.21	5.69	11.4	8.04	9.44	8.78	10.0	2.49	2.25	2.32	3.09	7.07	6.19
Na_2O	3.5	4.1	2.1	4.1	3.9	3.2	2.8	7.4	6.0	5.9	5.4	2.6	4.0
K_2O	1.18	1.06	0.14	0.21	0.14	0.14	0.29	0.33	0.39	1.24	0.59	2.27	1.07
P_2O_5	0.28	0.26	0.15	1.17	0.12	0.12	0.06	0.31	0.34	0.35	0.33	0.45	0.31
L.O.I.	2.32	2.59	1.30	2.72	1.31	4.23	3.70	2.71	3.61	3.41	4.8	4.0	7.16
Total	100.10	100.50	100.85	100.29	99.31	100.14	99.42	100.64	99.75	99.52	99.17	99.81	99.56
Rb	22	25	3	3	1	1	3	5	5	27	23	69	21
Sr	309	244	108	183	66	140	203	142	180	155	57	767	288
Y	41	45	57	115	55	40	33	42	44	44	60	23	28
Zr	189	182	39	517	73	70	53	134	136	137	199	77	141
Nb	9	9	3	44	1	4	1	4	3	3	5	3	7
Zn	56	60	72	162	106	69	86	122	140	134	148	103	82
Cu	1	1	0	0	2	5	70	0	0	0	54	74	6
Ni	10	12	47	0	34	80	88	14	15	11	20	17	39
Ba	486	423	89	219	80	124	61	100	129	266	233	1319	536
V	200	216	431	103	420	326	279	243	320	276	516	339	195
Cr	0	0	68	0	62	232	319	18	14	16	17	0	100

0= not detected

TABLE 6.1. MAJOR AND TRACE ELEMENT ANALYSES OF MAFIC VOLCANIC ROCKS OF THE VICTORIA LAKE GROUP

	81D 063-1	81D 063-2	81D 65	81D 113-4	81D 186-1	81D 186-3	81D 188-1	81D 295-1	81D 295-2	81D 298	81D 299-3	80D 246
SiO_2	49.8	48.9	49.7	50.6	50.2	50.9	49.0	48.5	47.7	50.6	45.3	52.6
TiO_2	1.13	1.60	2.38	0.89	1.43	1.47	1.38	2.07	2.06	0.52	0.76	1.53
Al_2O_3	14.8	14.7	16.0	19.1	15.7	16.2	15.5	13.2	13.3	15.8	18.8	13.1
Fe_2O_3	2.14	3.50	4.05	1.43	3.73	3.18	2.06	3.73	2.70	2.38	4.05	2.71
FeO	7.22	7.79	7.87	7.87	6.51	6.58	8.37	9.80	10.58	7.65	3.29	8.45
MnO	0.22	0.25	0.21	0.09	0.18	0.17	0.26	0.25	0.26	0.22	0.16	0.27
MgO	7.60	5.42	5.07	5.61	5.95	5.75	7.90	6.64	6.52	7.02	6.75	6.09
CaO	7.50	6.69	5.43	3.27	9.17	7.43	8.08	10.1	10.5	9.57	11.4	6.99
Na_2O	4.6	4.4	4.5	5.0	4.0	4.4	3.7	2.4	2.3	2.8	2.2	4.3
K_2O	0.21	0.86	0.88	0.20	0.28	0.22	0.15	0.11	0.10	0.43	0.08	0.12
P_2O_5	0.11	0.17	0.43	0.05	0.13	0.11	0.11	0.15	0.17	0.10	0.04	0.12
L.O.I.	5.32	5.25	3.13	6.13	2.80	2.87	3.64	3.38	3.23	2.86	6.95	2.71
Total	100.65	99.53	99.65	100.24	100.08	98.47	100.15	100.33	99.42	99.95	99.78	98.99
Rb	5	33	29	4	2	1	0	0	0	9	0	2
Sr	156	170	214	182	159	151	132	100	106	219	220	73
Y	30	44	55	27	45	42	39	57	54	15	21	49
Zr	69	125	179	43	76	81	66	110	117	27	37	79
Nb	3	3	4	1	4	3	4	4	5	0	0	2
Zn	87	110	121	96	88	99	131	121	114	104	69	113
Cu	51	53	5	4	58	60	101	45	38	0	89	60
Ni	33	17	9	2	97	93	82	43	38	44	141	27
Ba	94	249	356	74	97	100	79	65	84	149	55	77
V	299	393	461	377	329	369	305	419	424	346	183	379
Cr	121	27	21	11	234	262	194	54	45	86	355	35

O= not detected

TABLE 6.2. MAJOR AND TRACE ELEMENT ANALYSES OF MAFIC DYKES AND SILLS OF THE VICTORIA LAKE GROUP

	81D 013-2	81D 054-2	81D 070-1	81D 070-2	81D 070-3	81D 070-4	81D 074
SiO_2	46.6	48.3	45.8	49.1	48.7	48.4	48.0
TiO_2	1.32	2.25	2.90	1.53	1.81	1.88	1.68
Al_2O_3	16.9	14.5	13.3	17.0	14.5	14.8	15.1
Fe_2O_3	1.69	12.6	5.56	4.28	3.57	4.21	4.84
FeO	6.84	7.01	9.80	6.01	8.44	8.22	7.08
MnO	0.21	0.15	0.28	0.18	0.23	0.23	0.22
MgO	8.51	2.73	5.87	5.43	5.84	6.30	6.07
CaO	10.8	1.72	9.17	10.4	8.66	8.30	9.54
Na_2O	1.6	5.4	2.4	2.6	3.4	3.0	2.9
K_2O	0.15	1.03	1.25	0.44	0.55	0.22	0.41
P_2O_5	0.17	0.34	0.23	0.19	0.18	0.19	0.17
L.O.I.	5.35	2.7	2.54	3.27	3.80	3.25	3.00
Total	100.14	98.73	99.10	100.43	99.68	99.00	99.01
Rb	0	31	53	14	23	3	12
Sr	217	66	231	249	160	248	236
Y	32	62	45	41	48	43	37
Zr	91	186	132	97	106	112	90
Nb	2	6	1	0	4	4	3
Zn	105	132	139	103	116	128	112
Cu	44	11	177	14	11	0	52
Ni	129	20	41	19	19	16	26
Ba	96	568	369	299	179	126	162
V	179	697	629	300	377	384	312
Cr	166	17	39	33	23	18	33

	81D 075-1	81D 086-3	81D 091	81D 094-3	81D 099	81D 102-2
SiO_2	49.2	52.3	48.6	44.3	48.6	45.4
TiO_2	2.05	0.88	2.17	0.48	1.95	2.28
Al_2O_3	14.9	19.8	14.3	15.3	15.2	14.4
Fe_2O_3	5.09	2.62	4.36	1.75	4.93	5.72
FeO	8.87	7.08	8.51	6.08	7.65	8.15
MnO	0.27	0.24	0.25	0.20	0.20	0.40
MgO	5.26	4.73	5.18	8.56	5.14	6.92
CaO	7.55	1.97	8.90	9.06	6.07	9.46
Na_2O	3.4	4.6	3.1	0.2	3.2	0.0
K_2O	0.81	0.95	1.25	6.14	0.27	0.09
P_2O_5	0.23	0.10	0.27	0.03	0.22	0.34
L.O.I.	2.81	4.43	2.25	7.9	5.46	6.15
Total	100.44	99.70	99.14	100.00	98.89	99.31
Rb	32	23	60	235	10	0
Sr	312	147	240	60	215	479
Y	56	37	58	20	41	39
Zr	150	5	13	1	126	139
Nb	4	1	3	0	3	20
Zn	134	127	128	95	121	187
Cu	34	0	85	0	38	21
Ni	8	11	27	120	20	88
Ba	252	408	290	670	133	66
V	371	339	408	219	398	377
Cr	0	35	36	588	33	142

0 = not detected

be the reason for the high silica content of some of these rocks. All rock samples reported in Tables 6.1,2 were identified as basalts according to the scheme of Irvine and Baragar (1971). TiO_2 contents of the basalts vary from 0.52 to 2.75 wt. %; a wider range than that determined for diabase dykes of the Annieopsquotch Complex (Chapter 5). Al_2O_3 contents vary from 13.1 to 19.2 wt. % in the basalts, likely due to plagioclase fractionation, as this mineral is the commonly observed phenocryst phase.

Fe_2O_3 content of the basalts, certainly affected by alteration, varies from 1.35 to 4.76 wt. %. FeO varies from 3.29 to 10.6 wt. %. MnO contents range between 0.09 and 0.37 wt. %. MgO varies from 2.89 to 7.95 wt. %, probably due to both primary fractionation and secondary enrichment by seafloor alteration (cf. Mottl, 1983).

Ca, Na and K contents were certainly modified by alteration processes.

Pb, Th and U were sought for but were not detected in mafic volcanic rocks of the Victoria Lake Group. Rb and Sr are both considered 'mobile' elements in rocks of the Group. The high Rb and Sr values of 69 and 767 ppm both occur in sample 81HPAD057 which contains the highest K_2O, P_2O_5 and Ba contents as well (Table 6.1).

Nb, Y and Zr are anomalously high at 115, 44 and 517 ppm, in sample 81HPAD017-1. This sample is an altered plagioclase - porphyritic pillow lava from an outcrop on the Burgeo road.

6.5 DISCUSSION OF VARIATION DIAGRAMS

Mafic volcanic rocks and dykes and sills plot over a large area on the standard AFM diagram (Figure 6.1). Twenty - four analyses plot on the tholeiitic side of the tholeiitic - calc-alkaline dividing line of Irvine and Baragar (1971) and fourteen plot on the calc-alkaline side. This is likely a result of enrichment of alkalis, especially Na. The same effect is noted, to a lesser extent, in the Annieopsquotch Complex where pillow lavas plot to the alkali - rich side of the Fe enrichment trend defined by fresh diabase dykes of the sheeted dyke zone (Figure 5.2).

TiO_2 contents of mafic rocks of the Victoria Lake Group increase with increasing FeO*/MgO and, in general, display a tholeiitic trend similar to that of the Skaergaard Intrusion (Figure 6.2).

Sr, K, Rb and Ba have been used by Pearce (1980) to discriminate between fresh basalts erupted in different tectonic settings. Basalts in island arc and oceanic island settings have higher concentrations of these elements and, when normalized to the average MORB of Pearce (1980), they plot above 1 on the trace element variation diagram (Figure 6.4,5). Pearce cautioned against using these elements when studying 'metabasalts' however as they are demonstrably mobile. These elements are enriched in basalts of the Victoria Lake Group (Figure 6.4,5) but it is not possible to say what proportion of this enrichment is a

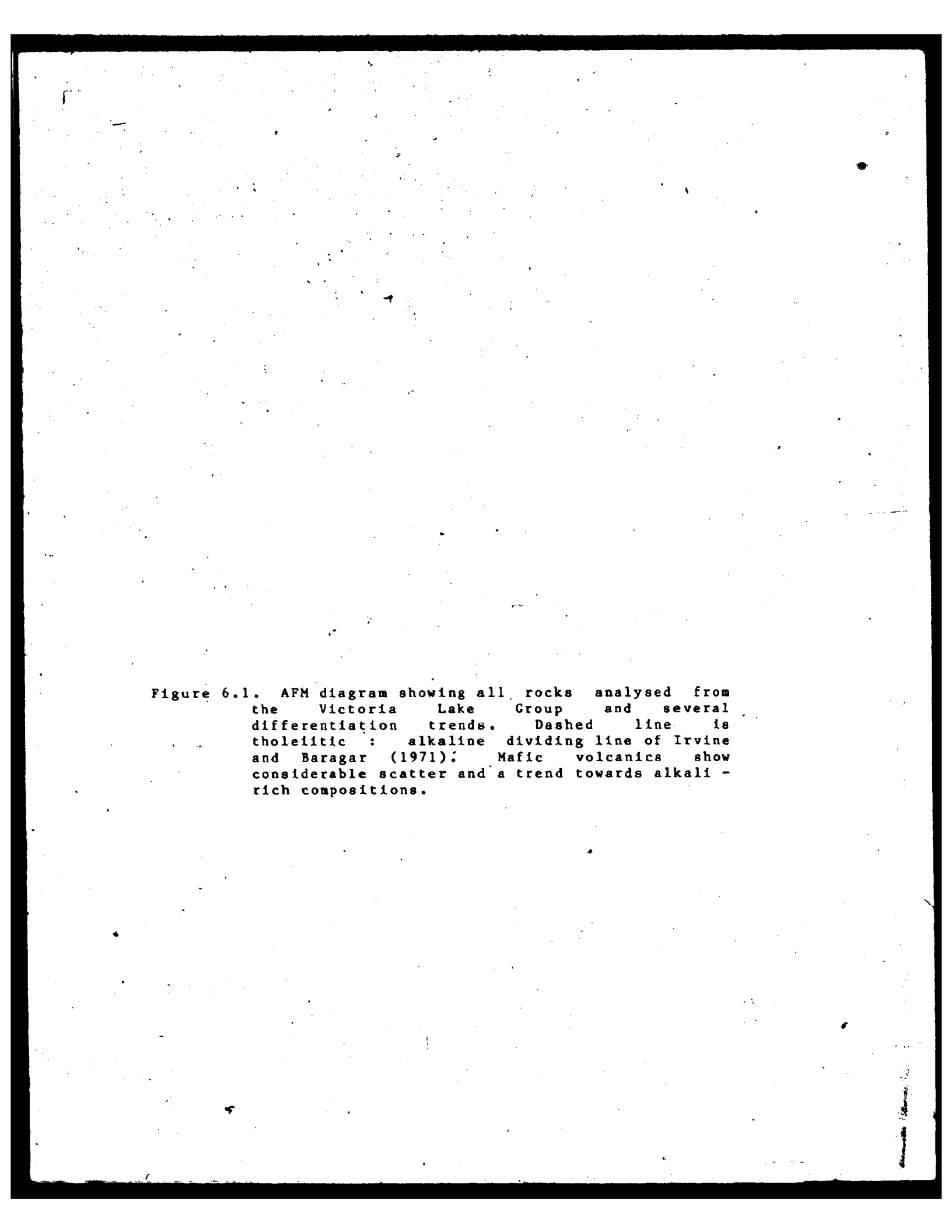

Figure 6.1. AFM diagram showing all rocks analysed from the Victoria Lake Group and several differentiation trends. Dashed line is tholeiitic : alkaline dividing line of Irvine and Baragar (1971). Mafic volcanics show considerable scatter and a trend towards alkali - rich compositions.

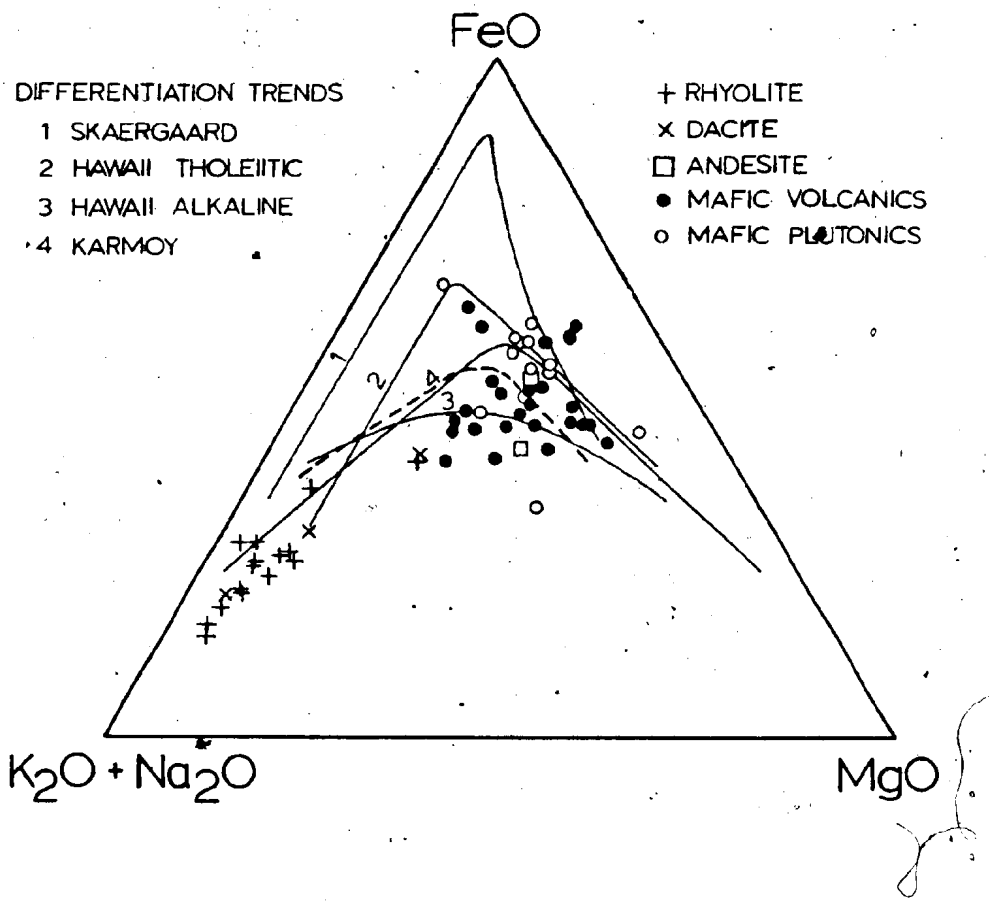
FeO
DIFFERENTIATION TRENDS
1 SKAERGAARD
2 HAWAII THOLEIITIC
3 HAWAII ALKALINE
4 KARMOY
+ RHYOLITE
× DACITE
□ ANDESITE
● MAFIC VOLCANICS
o MAFIC PLUTONICS
K2O + Na2O
MgO

Figure 6.2. TiO2 vs. FeO*/MgO diagram with mafic volcanic and plutonic samples plotted, and the Skaergaard trend. Symbols are as in Figure 6.1. Despite some scatter, especially at low TiO2 contents, most points fall along the trend.

Figure 6.3. Al2O3/TiO2 vs. TiO2 diagram (after Sun and Nesbitt, 1978) showing fields of komatiites and Mg basalt, Betts Cove high - Mg lava and MORB. Mafic volcanic and plutonic rocks show a wide range of TiO2 contents. Most samples fall in the MORB field or along its projection to higher TiO2 contents. Samples with low TiO2 contents plot above MORB on a trend towards the Betts Cove field.

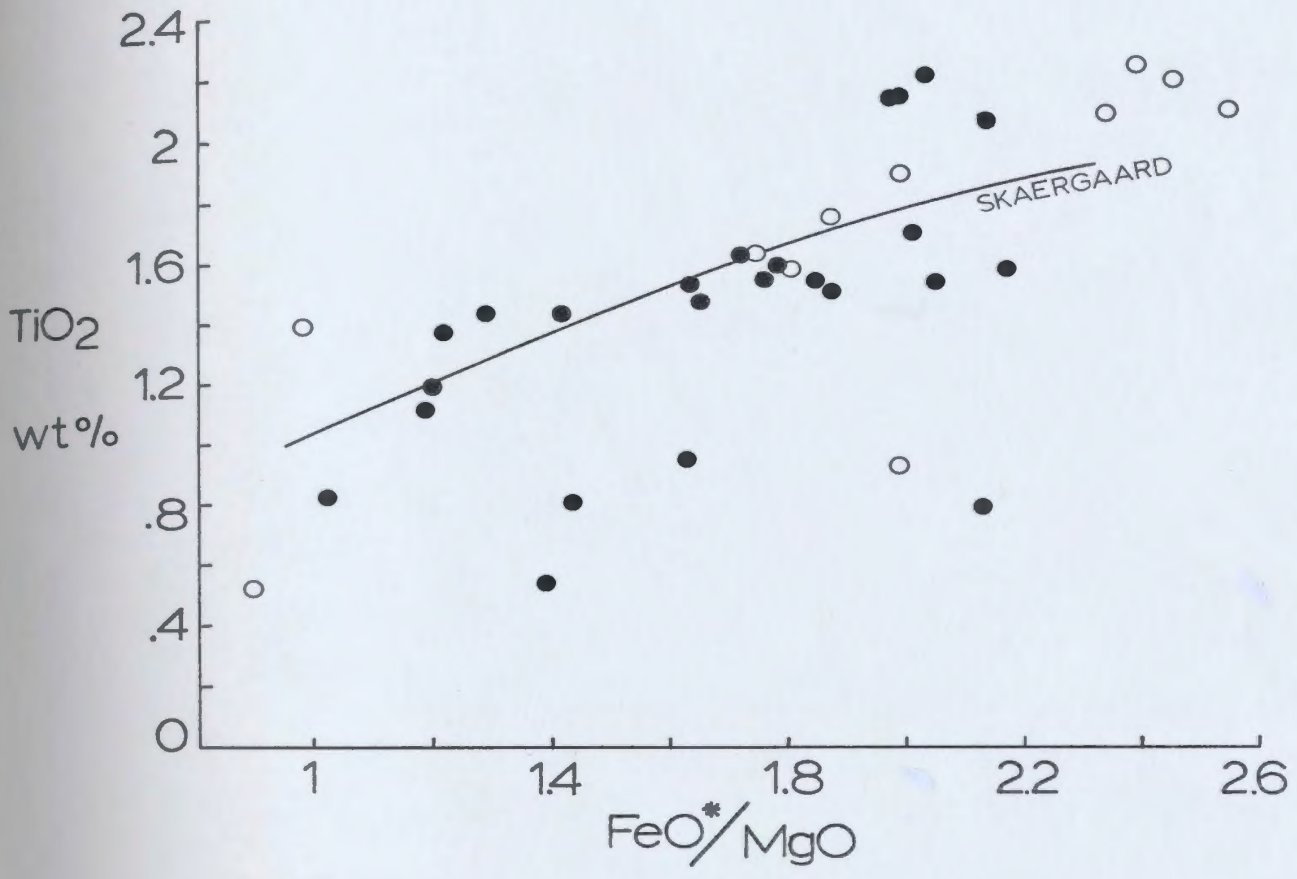
2.4
2
1.6
1.2
.8
.4
0
TiO2
wt%
SKAERGAARD
1
1.4
1.8
2.2
2.6
FeO*/MgO

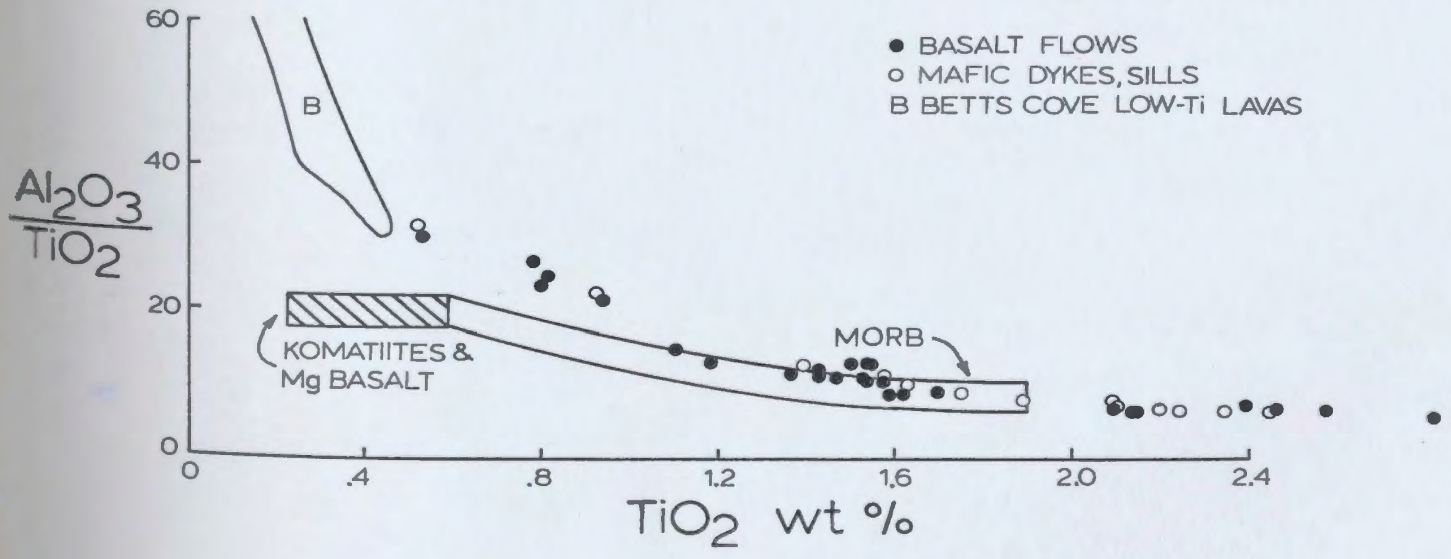
60
40
20
0
Al2O3/TiO2
B
KOMATIITES &
Mg BASALT
MORB
BASALT FLOWS
MAFIC DYKES, SILLS
B BETTS COVE LOW-Ti LAVAS
0
.4
.8
1.2
1.6
2.0
2.4
TiO2 wt %

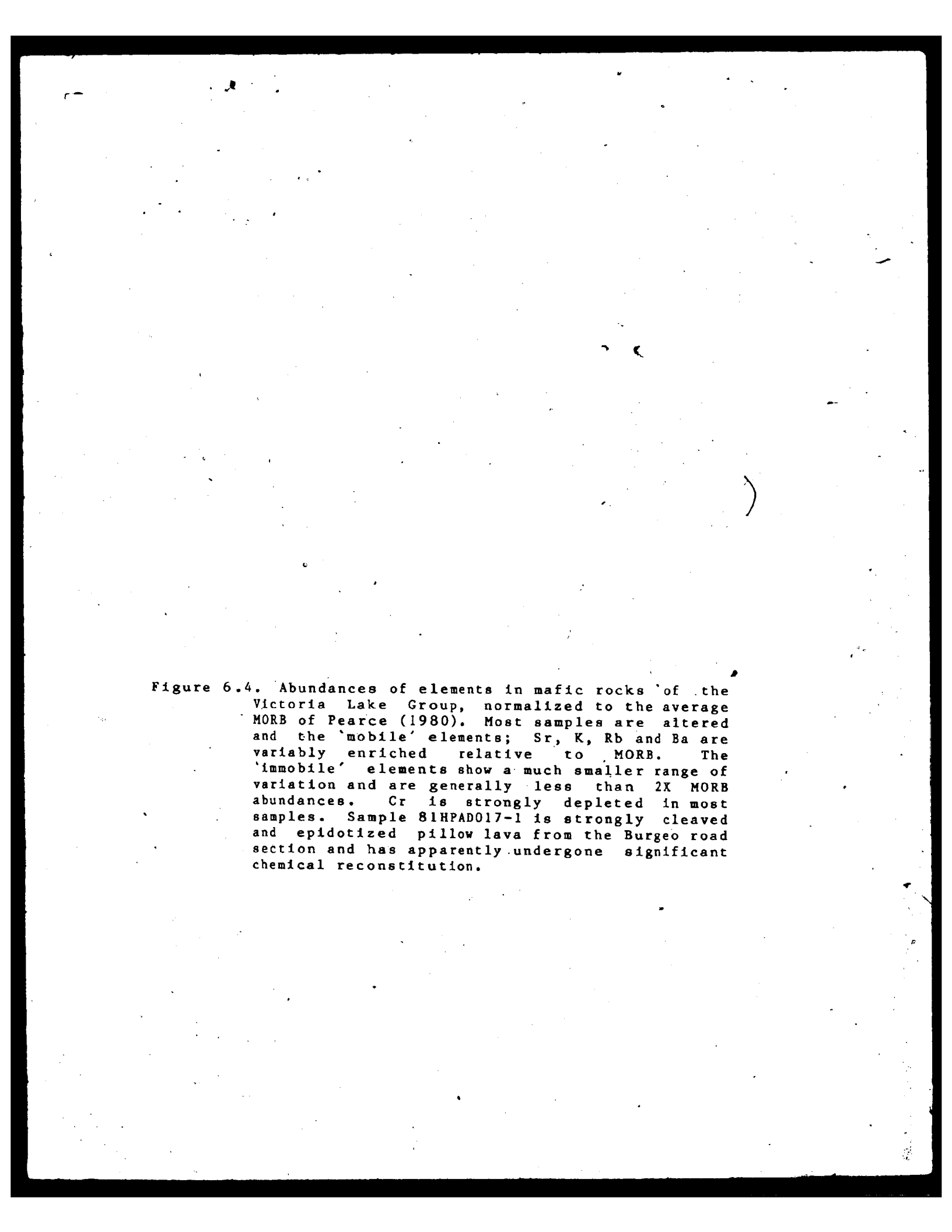

Figure 6.4. Abundances of elements in mafic rocks of the Victoria Lake Group, normalized to the average MORB of Pearce (1980). Most samples are altered and the 'mobile' elements; Sr, K, Rb and Ba are variably enriched relative to MORB. The 'immobile' elements show a much smaller range of variation and are generally less than 2X MORB abundances. Cr is strongly depleted in most samples. Sample 81HPAD017-1 is strongly cleaved and epidotized pillow lava from the Burgeo road section and has apparently undergone significant chemical reconstitution.

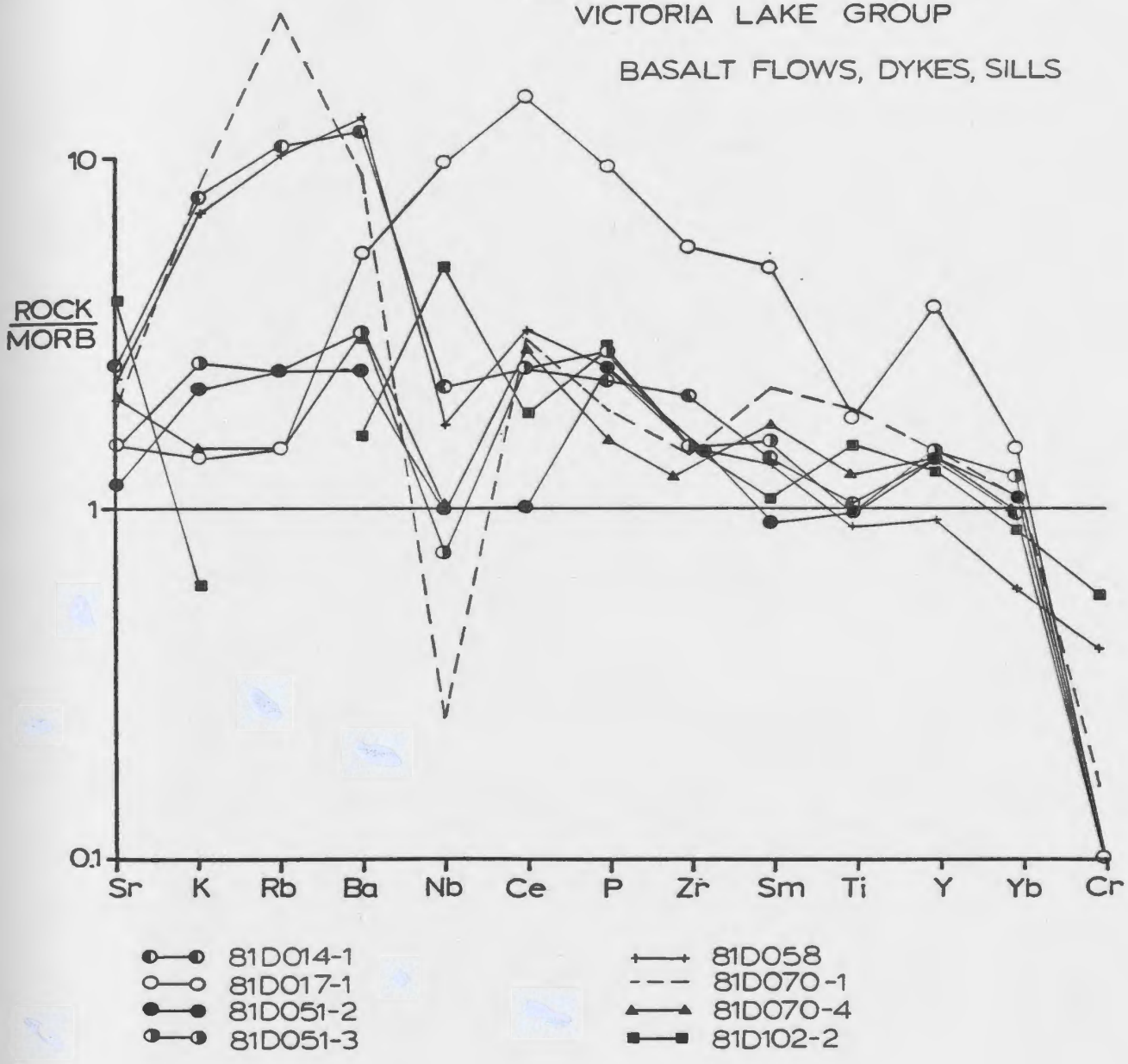
VICTORIA LAKE GROUP
BASALT FLOWS, DYKES, SILLS
ROCK / MORB
10
1
0.1
Sr
K
Rb
Ba
Nb
Ce
P
Zr
Sm
Ti
Y
Yb
Cr
81D014-1
81D017-1
81D051-2
81D051-3
81D058
81D070-1
81D070-4
81D102-2

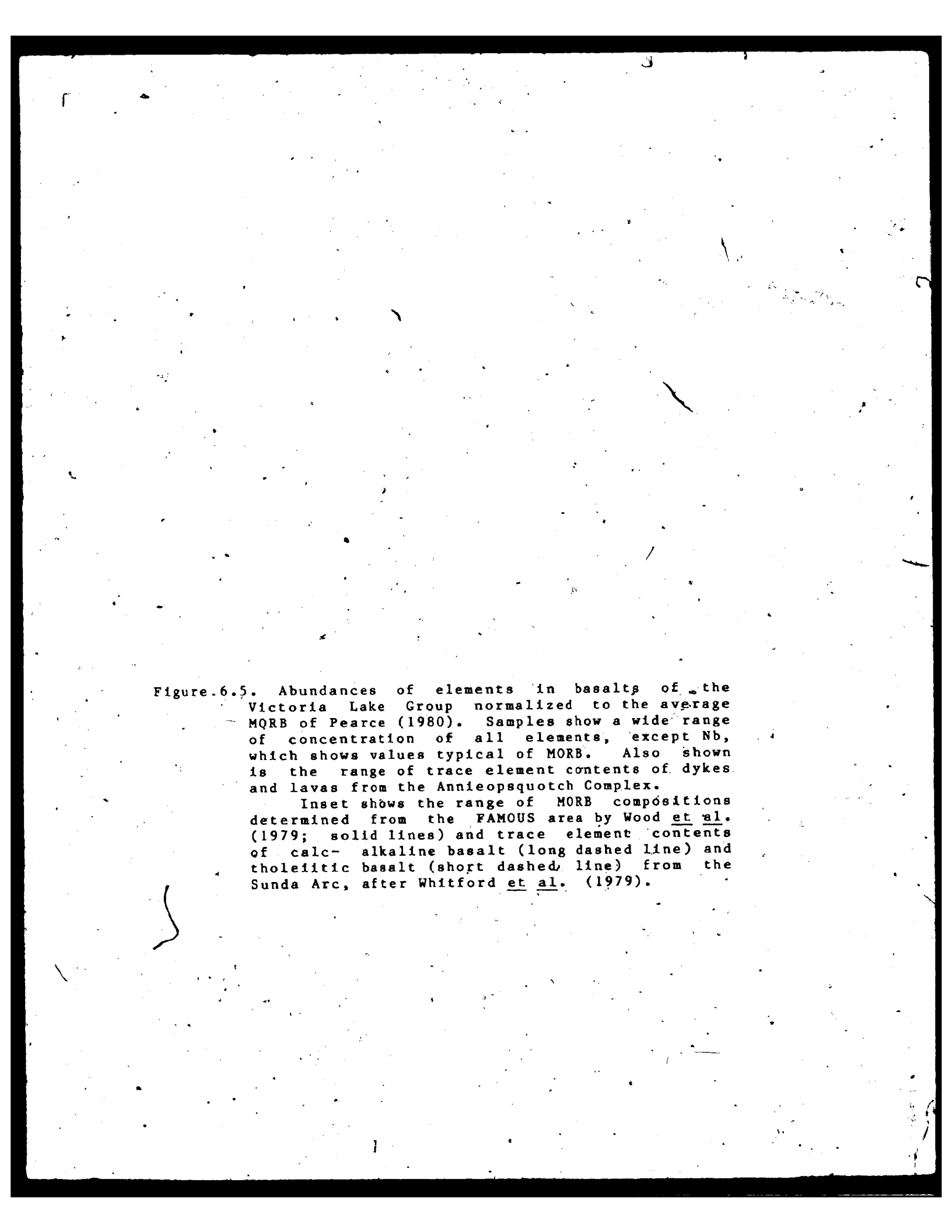

Figure.6.5. Abundances of elements in basalts of the Victoria Lake Group normalized to the average MQRB of Pearce (1980). Samples show a wide range of concentration of all elements, except Nb, which shows values typical of MORB. Also shown is the range of trace element contents of dykes and lavas from the Annieopsquotch Complex.

Inset shows the range of MORB compositions determined from the FAMOUS area by Wood et al. (1979; solid lines) and trace element contents of calc- alkaline basalt (long dashed line) and tholeiitic basalt (short dashed line) from the Sunda Arc, after Whitford et al. (1979).

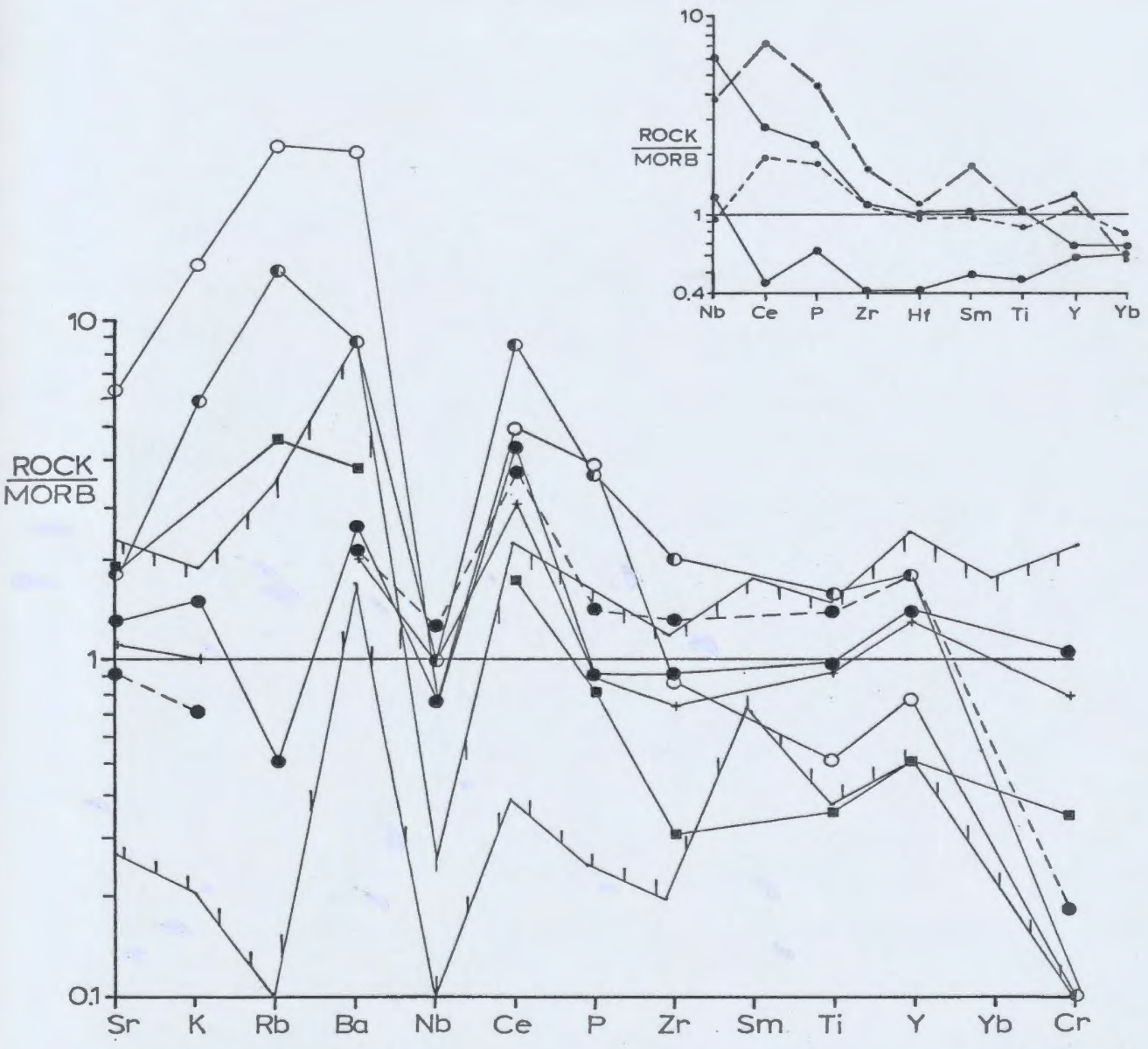
10
ROCK
MORB
1
0.4
Nb Ce P Zr Hf Sm Ti Y Yb
10
ROCK
MORB
1
0.1
Sr K Rb Ba Nb Ce P Zr Sm Ti Y Yb Cr
81D057
81D065
81D186-3
81D188-1
81D295-2
81D298
ANNIEOPSQUOTCH DYKES, PILLOWS (48)

primary feature of the lavas and what is due to alteration.

The incompatible elements P, Zr, Ti and Cr were shown by Pearce (1980) to be depleted in island arc basalts relative to MORB. However, other studies have demonstrated that both island arc basalts and mid - ocean ridge basalts have a broad spectrum of contents of these elements (Whitford et al.,1979; Dixon and Batiza,1979; Wood et al.,1979 and others), and a significant overlap exists.

Some samples from the Group (81HPAD057, 186-3, 188-1 and 298) show depletion of Zr, Ti and Y relative to the standard MORB, similar to that shown by basalt from the Sunda Arc (Whitford et al., 1979) or MORB from the FAMOUS area (Wood et al., 1979; Figure 6.5). However, the majority of samples are not depleted in these elements relative to MORB and, except for Sr, K, Rb and Ba, they overlap the range of basalt compositions from the Annieopsquotch Complex (Figure 6.5).

On the Ni vs. Cr diagram (Figure 6.6), samples cluster at low Ni and Cr contents with some samples showing a positive correlation to Ni and Cr contents as high as 141 and 588 ppm respectively.

On the Ti vs. Cr diagram of Pearce (1975), used to separate ocean floor basalts from island arc basalts, most mafic rocks of the Victoria Lake Group plot in the island arc field (Figure 6.7). These rocks have TiO2 contents in the range typical of MORB but Cr contents vary through the full MORB and island arc tholeiite range.

On the Cr vs. Y diagram, the mafic volcanics, dykes

Figure 6.6. Ni vs. Cr diagram for mafic rocks of the Victoria Lake Group; symbols as in Figure 6.1. These elements co-vary but most samples have Cr contents under 100 ppm. Compare to the equivalent diagram for diabase dykes of the Annieopsquotch Complex (Figure 5.1).

Figure 6.7. Ti vs. Cr diagram (after Pearce, 1975) for mafic volcanic rocks of the Victoria Lake Group. Most samples fall in the low-Cr field of island arc tholeiites at roughly similar Ti contents.

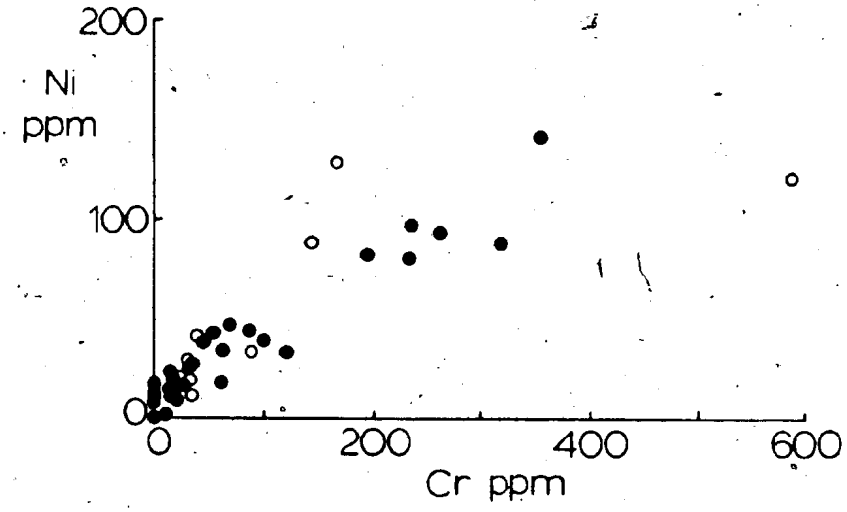
200
Ni
ppm
100
0
0
200
400
600
Cr ppm

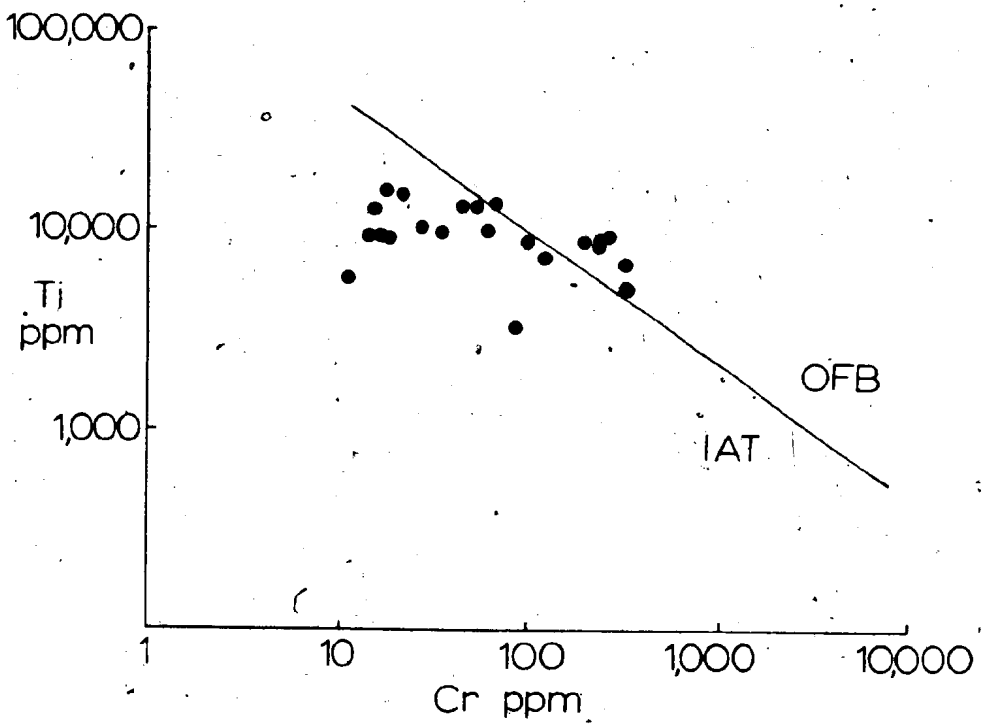
100,000
10,000
Ti
ppm
1,000
OFB
IAT
1
10
100
1,000
10,000
Cr ppm

and sills of the Victoria Lake Group plot in the within-plate basalt field, which overlaps the field of MORB at Cr contents between 100 and 900 ppm (Figure 6.8).

There is a strong positive correlation between TiO2 and Zr and TiO2 and Y contents of these mafic rocks (Figure 6.9, 10,). Furthermore, on the TiO2 vs. Y diagram they cluster along the line defined by diabase dykes of the sheeted dyke zone of the Annieopsquotch Complex, which represent MORB liquid compositions (Chapter 5).

6.6 RARE EARTH ELEMENT CONTENTS

Gabbro and a diabase dyke from the east side of Henry Waters were analysed for REE, as were five basalts from the Victoria Lake Group (Table 6.3). All samples, except basalt 81HPAD017-1, have flat patterns with concentrations between 15 and 40X chondritic (Figure 6.11). They are very similar to dykes and pillow lavas from the Annieopsquotch Complex (Figure 6.12), except for some enrichment of the LREE, and most also fall within the field of island arc tholeiites of Jakes and Gill (1970). As they have abundances that largely fall in the area of overlap of MORB, island arc tholeiites and Annieopsquotch basalt fields, the REE patterns of these rocks are of little help in determining the eruptive setting.

The concentrations of REE in the gabbro and diabase dyke° are significantly higher than those of the gabbros in

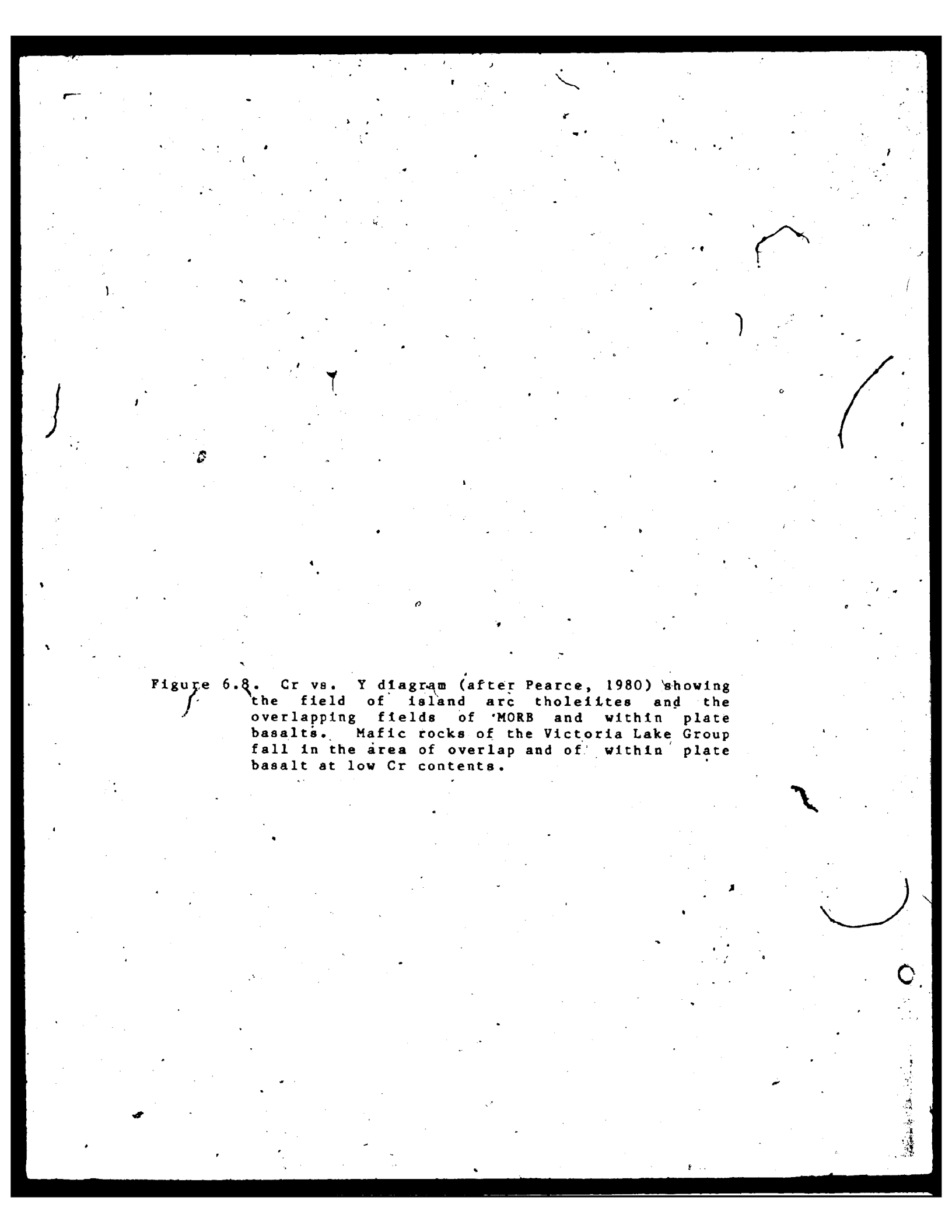

Figure 6.8. Cr vs. Y diagram (after Pearce, 1980) showing the field of island arc tholeiites and the overlapping fields of MORB and within plate basalts. Mafic rocks of the Victoria Lake Group fall in the area of overlap and of within plate basalt at low Cr contents.

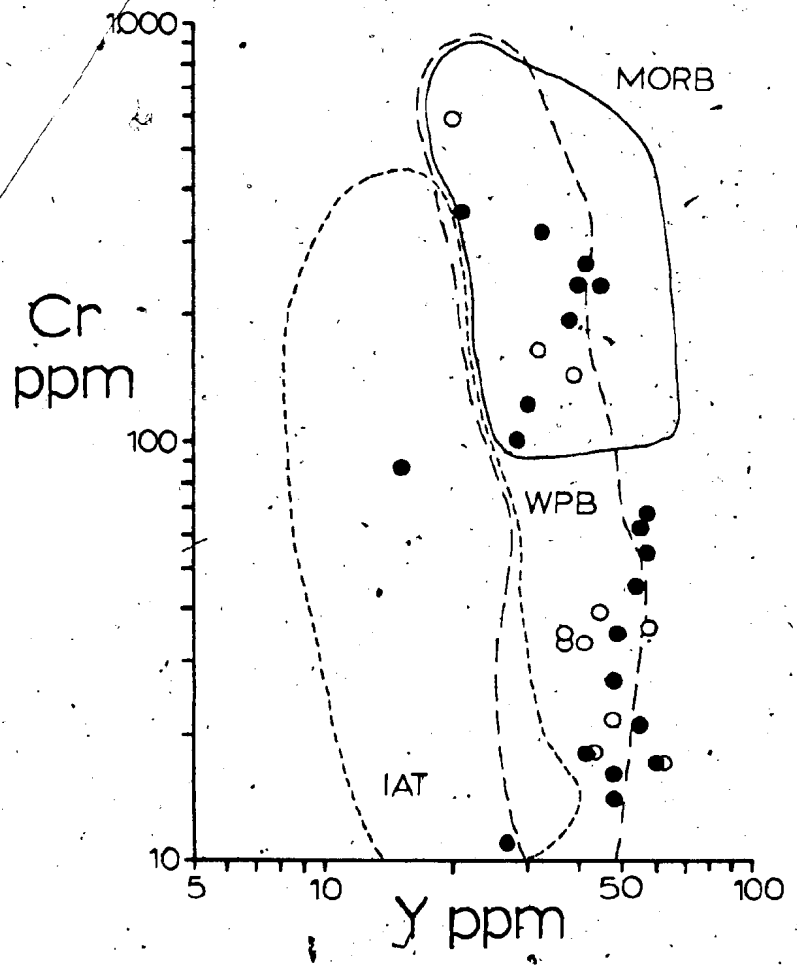
1000
100
10
Cr
ppm
MORB
WPB
IAT
8o
5
10
50
100
Y ppm

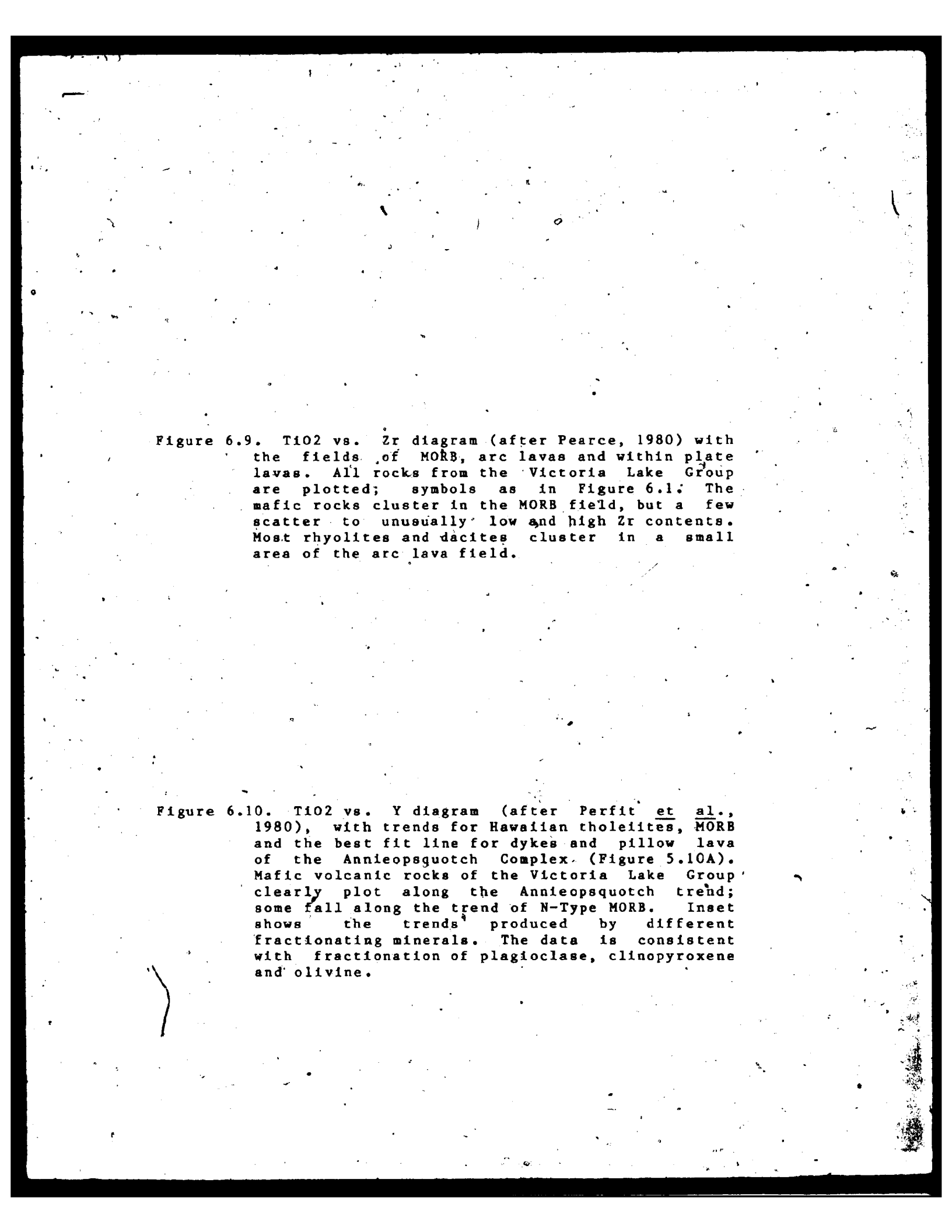

Figure 6.9. TiO2 vs. Zr diagram (after Pearce, 1980) with the fields of MORB, arc lavas and within plate lavas. All rocks from the Victoria Lake Group are plotted; symbols as in Figure 6.1. The mafic rocks cluster in the MORB field, but a few scatter to unusually low and high Zr contents. Most rhyolites and dacites cluster in a small area of the arc lava field.

Figure 6.10. TiO2 vs. Y diagram (after Perfit et al., 1980), with trends for Hawaiian tholeiites, MORB and the best fit line for dykes and pillow lava of the Annieopsquotch Complex (Figure 5.10A). Mafic volcanic rocks of the Victoria Lake Group clearly plot along the Annieopsquotch trend; some fall along the trend of N-Type MORB. Inset shows the trends produced by different fractionating minerals. The data is consistent with fractionation of plagioclase, clinopyroxene and olivine.

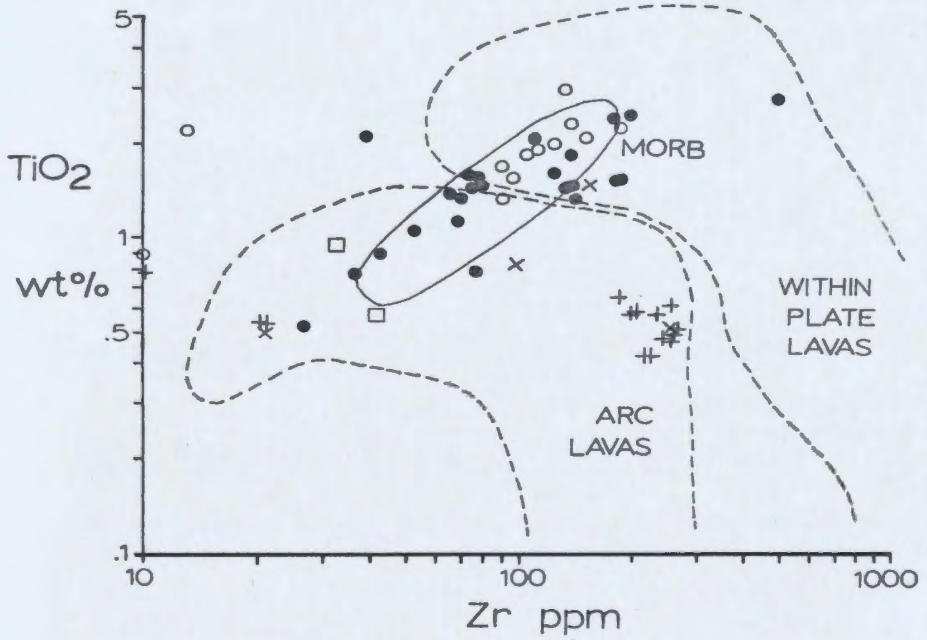
TiO2
wt%
5
1
.5
.1
10
100
1000
Zr ppm
MORB
WITHIN
PLATE
LAVAS
ARC
LAVAS

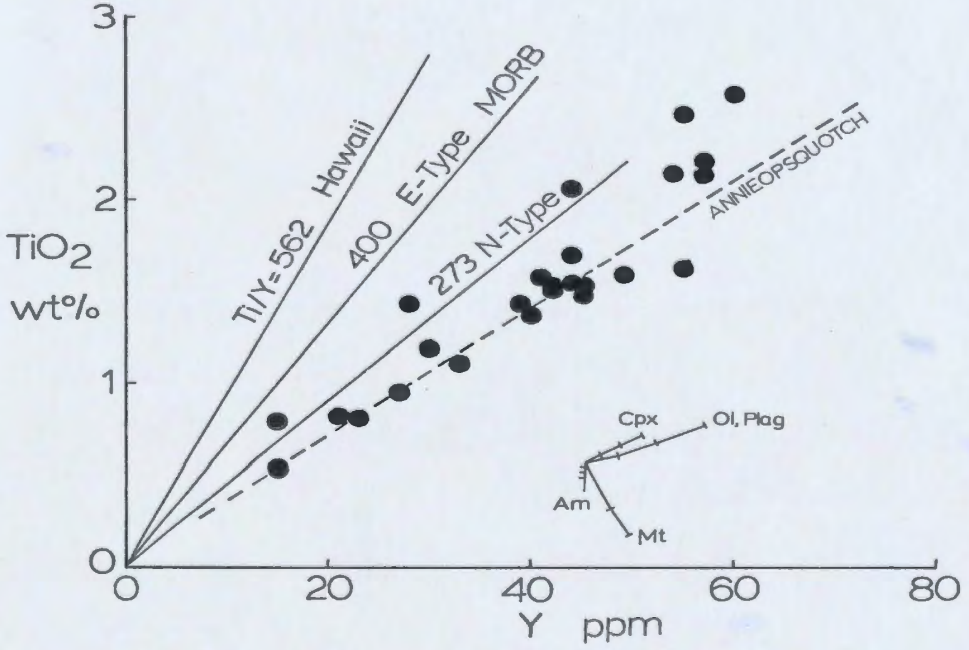
TiO2
wt%
3
2
1
0
0
20
40
60
80
Y ppm
Ti/Y=562 Hawaii
400 E-Type MORB
273 N-Type
ANNIEOPSQUOTCH
Cpx
Ol, Plag
Am
Mt

TABLE 6.3

RARE EARTH ELEMENT ANALYSES OF ROCKS
FROM THE VICTORIA LAKE GROUP

	GABBRO	DIABASE DYKE	BASALT					DIORITE	DACITE			RHYOLITE
	81D 070-1	81D 070-4	81D 014-1	81D 017-1	81D 051-2	81D 051-3	81D 102-2	81D 075-2	81D 067	81D 081-2	81D 088-1	81D 073
La	10.99	9.72	13.11	64.48	2.98	8.56	6.34	17.57	20.49	17.40	11.74	5.16
Ce	30.73	28.47	25.64	154.34	10.26	25.59	18.87	41.70	43.73	35.20	31.63	15.54
Pr	4.28	3.92	4.20	20.18	1.97	3.89	2.76	5.05	6.31	5.25	4.05	1.88
Nd	23.35	20.29	17.29	80.16	8.80	16.72	12.93	19.18	25.08	20.44	16.45	9.73
Sm	7.38	5.81	4.57	16.52	2.98	5.22	3.59	3.70	5.00	4.17	3.98	3.08
Eu	2.57	2.14	1.38	2.88	1.05	1.57	1.83	0.19	0.75	0.84	0.20	1.17
Gd	7.24	6.62	4.63	15.83	3.78	5.94	5.13	3.93	4.03	4.57	4.94	3.37
Dy	7.98	6.83	4.77	16.76	4.64	7.47	9.58	4.31	3.63	5.78	7.27	5.05
Er	4.96	3.95	3.31	7.34	3.73	4.30	4.80	2.84	2.42	3.75	5.37	4.10
Yb	3.82	3.27	3.34	5.11	3.65	4.18	3.02	3.03	3.14	4.19	6.36	4.39

Figure 6.11. Rare earth element contents of mafic rocks of the Victoria Lake Group, normalized to the chondritic values of Taylor and Gorton (1977). Approximately flat patterns, at concentrations of 10X to 45X chondrite predominate. Field of island arc tholeiites (Jakes and Gill, 1970) covers a wide range of concentrations and includes most sample data, except for some LREE and sample 81HPAD017-1.

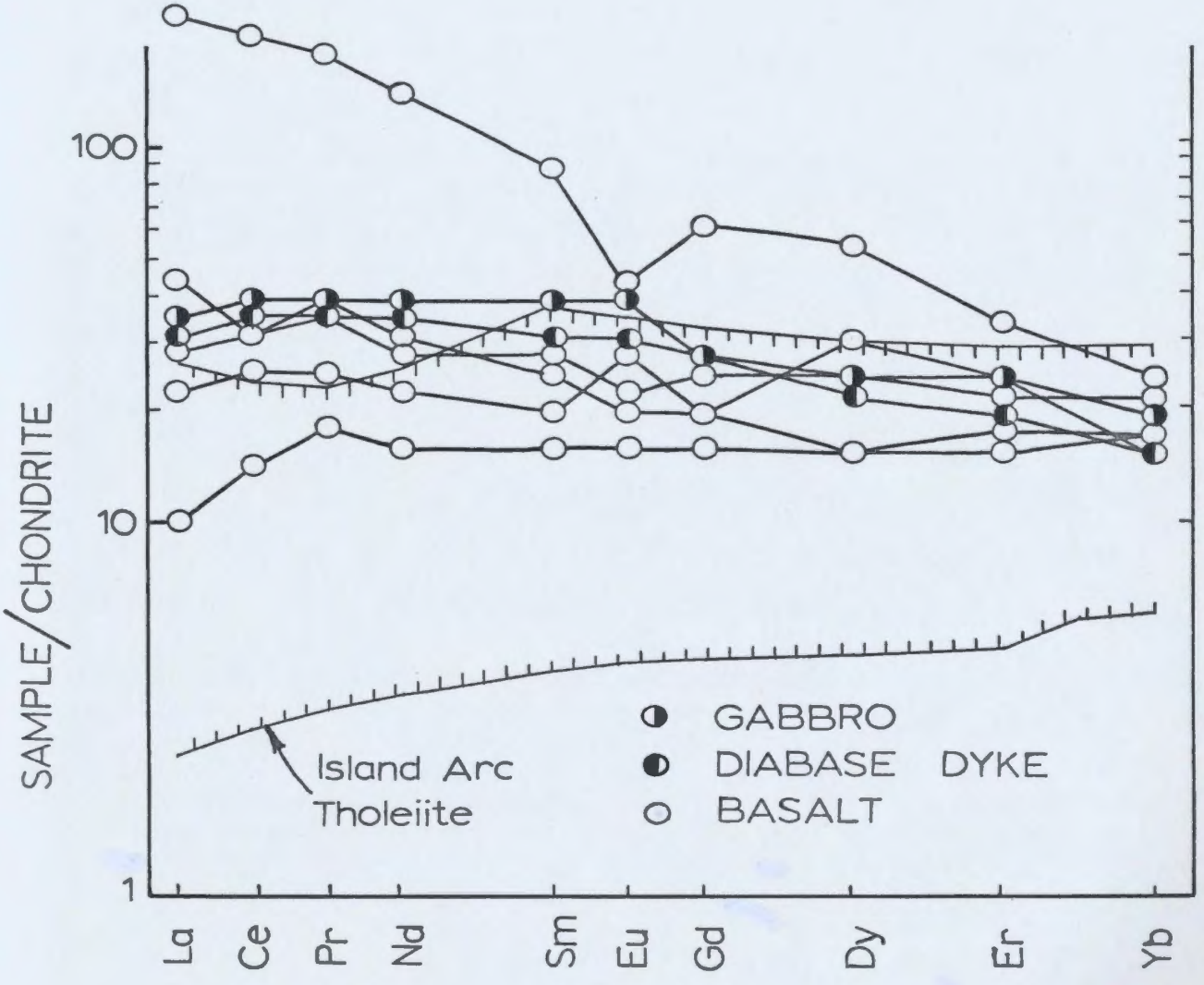
100
10
1
SAMPLE/CHONDRITE
La
Ce
Pr
Nd
Sm
Eu
Gd
Dy
Er
Yb
Island Arc
Tholeiite
GABBRO
DIABASE DYKE
BASALT

Figure 6.12. Field of rare earth element contents of the six clustered samples from the Victoria Lake Group compared to the eleven dykes and pillow lava from the Annieopsquotch Complex. The fields overlap; however, some samples from the Victoria Lake Group are enriched in the 'mobile' LREE.

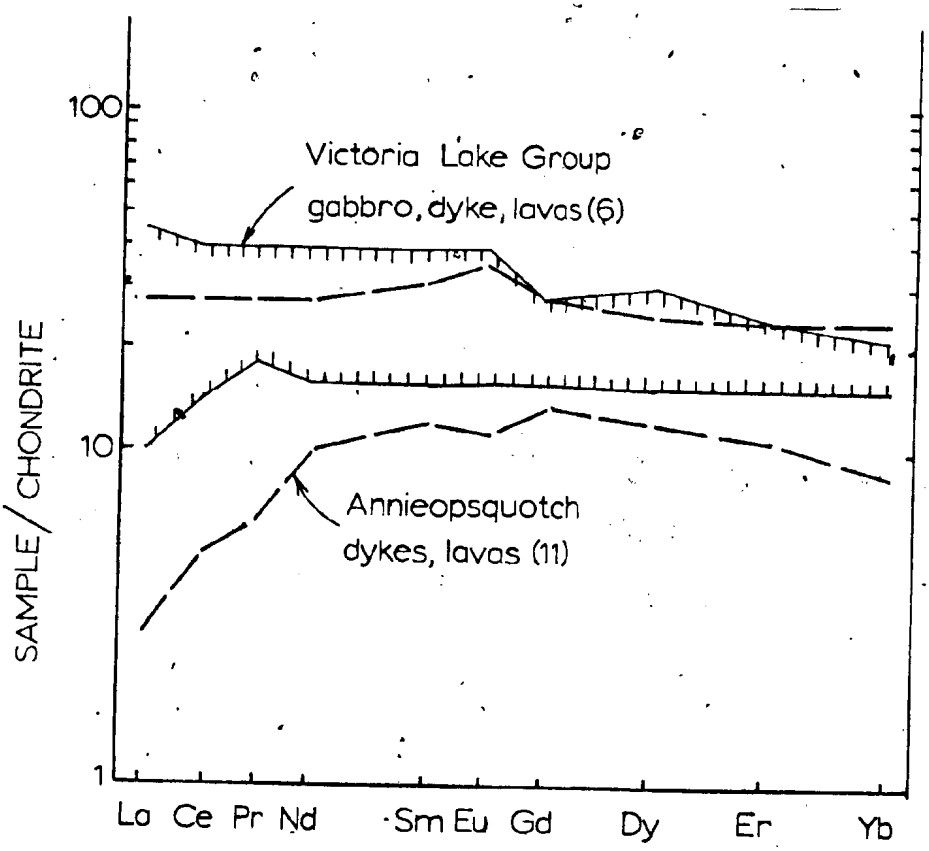
100
10
1
SAMPLE / CHONDRITE
Victoria Lake Group
gabbro, dyke, lavas (6)
Annieopsquotch
dykes, lavas (11)
La Ce Pr Nd Sm Eu Gd Dy Er Yb

the Annieopsquotch Complex (40X chondrite vs. 12X chondrite, Figure 6.12). This suggests, but does not prove, that the gabbro is related to the volcanics rather than part of a 'high level' gabbro magma chamber.

6.7 DISCUSSION - SETTING OF BASALT FORMATION

The basalts of the Victoria Lake Group in the area studied show a range of variation from those with chemical signatures similar to MORB to those with significant enrichment of Sr, K, Rb, Ba and LREE similar to island arc tholeiites.

The chemistry of the basaltic rocks is suggestive of MORB but their trace element contents are variable, with some rocks markedly enriched in the mobile large ion lithophile elements. However, this suite of rocks is much more altered than lavas and dykes of the adjacent Annieopsquotch Complex and therefore, little confidence is placed in classification schemes which use these elements.

Cr contents are lower and Zr contents higher for basalts of the Victoria Lake Group than those of the Annieopsquotch Complex. This results the suite plotting predominantly in the IAT field on the Ti vs. Cr diagram but squarely in the MORB field on the Ti vs. Zr diagram. Ti contents are in the MORB range, and on the Ti vs. Y plot analyses plot on the Annieopsquotch trend.

The trace element data (except for Cr contents, which

are in some cases very low in basalts of the Annieopsquotch Complex too) indicate that the suite has MORB geochemical affinities. Rare earth element data are compatible with such an interpretation.

It has been previously suggested that basalts outcropping along the Burgeo road are ophiolitic and that they differ from those of the King George IV Lake ophiolitic fragment mainly as a result of deformation and alteration (J. Fenton, pers. comm.,1979). The trace element chemistry supports this suggestion; only mobile LIL and LREE elements are enriched in these rocks relative to MORB.

It is likely that the basalts in the area studied are related to the King George IV Lake ophiolitic fragment. However, it is uncertain whether or not they are representative of basalts throughout the Victoria Lake Group.

6.8 ROCKS OF INTERMEDIATE COMPOSITION

Andesitic rocks are relatively uncommon in the Victoria Lake Group in the areas examined; a maximum of five percent by area. A few hornblende and plagioclase porphyritic sills were observed, which are interpreted to be andesites, however these were not analysed. Several dark green rocks, interpreted in the field to be basalts were found, on analysis, to be andesitic. Two are reported

in Table 6.4, however, they are very close in composition to the basalts and may be silicified equivalents.

6.9 FELSIC ROCKS

6.9.1 Dacites

Dacites were identified in the field by their grey-green to buff colour, presence of quartz and feldspar phenocrysts and lack of mafic phenocrysts. Thick, bleached silicified zones are common.

Dacitic volcanic rocks and their presumed plutonic equivalents, diorite and dacitic porphyry intrusions, are common in the Stanley Waters area. Field relationships indicate that the three rock types are consanguineous. Dacitic porphyry locally intrudes and engulfs tuffaceous sedimentary rocks that show evidence of being soft during intrusion. Diorite bodies intrude agglomerates containing dacitic blocks. The large size of these blocks, up to three metres by two metres, in Stanley Waters suggests proximity to a volcanic vent. This supposed proximity may explain the abundance of small subvolcanic and coarse-grained plutonic bodies.

Dacitic agglomerate on the west side of Stanley Waters displays a grading of block sizes in a bed several metres thick. It is interbedded with tuffaceous sedimentary rocks which also show graded beds. Al most of these tuffaceous rocks show features characteristic of subaqueous

TABLE 6.4. MAJOR AND TRACE ELEMENT ANALYSES OF INTERMEDIATE AND FELSIC ROCKS OF THE VICTORIA LAKE GROUP

	81D 060-1	81D 060-2	81D 076	81D 086-2	81D 064	81D 066	81D 067	81D 072-1	81D 073	81D 080-2
SiO_2	50.7	51.6	60.3	60.0	62.2	60.9	66.6	57.8	59.8	60.5
TiO_2	0.57	0.95	0.51	0.82	0.49	0.48	0.42	0.65	0.48	0,58
Al_2O_3	18.6	16.9	18.3	17.0	19.0	18.3	15.3	17.6	17.9	17.5
Fe_2O_3	3.02	2.86	2.06	2.54	0.16	1.51	1.12	1.51	1.91	1.73
FeO	6.22	9.01	3.00	4.29	3.86	2.79	0.86	2.93	2.79	2.15
MnO	0.18	0.26	0.11	0.21	0.10	0.11	0.07	0.15	0.13	0.09
MgO	6.64	6.13	1.79	3.05	1.76	1.07	0.70	1.59	1.54	1.21
CaO	4.41	2.27	2.28	2.26	0.72	1.51	1.75	2.52	2.12	1.36
Na_2O	4.6	3.6	5.8	5.9	6.6	5.5	1.4	5.3	4.5	0.8
K_2O	0.82	0.67	3.58	0.25	3.09	5.76	8.61	4.52	6.35	11.8
P_2O_5	0.12	0:05	0.26	0.16	0.20	0.20	0.16	0.38	0.26	0.33
L.O.I.	3.89	4.23	1.12	3.53	1.18	1.45	2.12	3.35	2.32	1.74
Total	99.77	98.53	99.11	100.01	99.36	99.58	99.11	98.30	100.10	99.81
Pb	0	0	21	4	38	33	23	33	12	28
Th	0	5	35	1	44	47	35	31	35	36
U	2	0	10	8	11	20	9	0	13	11
Rb	11	13	83	5	75	186	174	109	192	235
Sr	267	129	298	124	63	120	69	166	118	85
Y	20	29	46	44	46	49	39	44	44	42
Zr	42	33	253	98	260	256	224	187	246	204
Nb	1	1	10	2	13	13	10	11	11	15
Zn	83	125	78	108	78	159	61	81	61	81
Cu	70	0	2	0	12	4	0	1	0	0
Ni	32	24	0	0	0	2	0	0	0	0
Ba	420	263	1317	118	621	1048	1530	1505	1872	3741
V	293	334	75	195	66	67	24	131	72	90
Cr	34	109	0	0	0	0	0	0	0	0

	81D 081-2	81D 081-3	81D 086-4	81D 088-1	81D 090	81D 094-1	81D 094-2	81D 100	81D 109	81D 110
SiO_2	65.6	69.0	60.7	81.6	64.9	64.5	63.3	62.4	55.5	61.4
TiO_2	0.51	0.42	0.79	0.15	0.53	0.51	0.54	0.57	0.61	0.57
Al_2O_3	17.2	14.5	17.0	10.1	16.6	15.1	16.8	17.8	18.1	18.4
Fe_2O_3	0.63	0.8	2.38	0.6	1.43	1.43	1.43	3.02	3.89	2.06
FeO	1.57	1.6	4.29	1.1	1.57	1.86	2.50	1.64	3.29	1.93
MnO	0.09	0.09	0.19	0.06	0.10	0.12	0.16	0.09	0.19	0.13
MgO	0.62	0.64	3.09	0.64	0.84	0.74	0.68	0.45	1.53	0.94
CaO	1.80	1.71	2.03	0.42	2.08	2.07	2.99	1.72	2.86	1.81
Na_2O	5.6	2.9	6.0	4.3	5.1	0.7	7.0	7.4	4.0	3.9
K_2O	4.53	6,30	0.32	0.35	4.35	10.4	1.75	3.03	6.24	6.01
P_2O_5	0.14	0.15	0.15	0.01	0.20	0.19	0.20	0.23	0.33	0.25
L.O.I.	1.54	1.41	3.64	0.64	1.24	1.14	1.82	1.22	2.84	2.72
Total	99.83	99.52	100.58	99.95	98.94	98.76	99.17	99.57	99.38	100.12
Pb	9	62	0	7	21	36	20	49	3	27
Th	36	35	4	11	43	50	46	34	40	41
U	13	5	0	5	13	17	10	4	7	8
Rb	122	141	7	7	82	144	61	56	186	188
Sr	110	101	114	134	98	107	138	163	116	55
Y	48	39	46	85	47	42	45	41	50	45
Zr	267	219	8	28	22	21	21	200	257	232
Nb	17	12	2	7	14	15	14	11	14	11
Zn	77	70	107	44	72	107	70	66	145	114
Cu	9	26	0	0	3	0	0	0	0	0
Ni	0	0	2	0	0	0	0	0	0	0
Ba	990	1011	134	159	894	1976	406	765	2094	1432
V	37	40	175	1	51	44	49	63	120	63
Cr	0	0	0	0	0	0	0	0	0	0

0 = not detected

deposition, only blocks in the agglomerate and the intrusive rocks were analysed.

6.9.2 Rhyolites

Rhyolitic rocks are more abundant in the Victoria Lake Group than in the Ordovician 'early arc' volcanic sequences to the north in Notre Dame Bay (Swinden and Thorpe, in press). Rhyolite occurs as flows and sills in the area examined. Buff to purple flows, which contain quartz and feldspar phenocrysts, occur in a quarry on the east side of the Burgeo road (Route 480). They are vertically dipping and fairly massive. Rhyolite also occurs in a roadcut west of the road, immediately northwest of the quarry.

The other area of rhyolite examined is the west shore of Henry Waters, Victoria Lake. There, rhyolite dykes and sills cut tuffaceous and tuffaceous - sedimentary rocks. Tuffs of probable rhyolitic composition were observed but because they are waterlain and have sorted crystal - rich beds, none were analysed.

6.10 CHEMISTRY OF THE FELSIC ROCKS

Sixteen samples that were classified as rhyolites according to the criteria of Irvine and Baragar (1971) and two dacites were analysed. They are discussed together in the following sections. All element concentrations are discussed uncorrected for losses on ignition. Losses on

ignition are relatively low for these rocks, varying from 1.12 to 3.64 wt. %.

SiO2 contents of the dacites and rhyolites range from 55.5 wt. % (with a loss on ignition of 2.84 wt. %) to 69.0 wt. % with one exception, a silicified dacite with 81 wt. % SiO2.

CaO, K2O and Na2O contents cover a wide range, likely as a result of alteration of the rocks, although some primary variation is likely, due to both fractionation and variable amounts of feldspar phenocrysts.

Pb varies from 0 to 62 ppm in the dacites and rhyolites analysed. Th contents likewise vary considerably, from 0 to 47 ppm however, all but three samples fall in the range 30 to 40 ppm. U varies from 0 to 20 ppm and shows a weak correlation with Th.

Rb contents vary widely, from 5 to 235 ppm and have likely been strongly modified by hydrothermal alteration. Sr, likewise, varies from 55 to 298 ppm. Ba , a 'mobile' element, is enriched in rocks of the Victoria Lake Group in general (Thurlow, 1981). Samples analysed in this study have extremely variable, including very high, Ba contents. Dacites and rhyolites have Ba contents in the range 118 to 3741 ppm. This highest value occurs in sample 81HPAD080-2, which has the highest Rb (235 ppm) and K (11.8 wt. %) contents as well.

Zr contents are quite variable (8 to 267 ppm) however, in these felsic rocks, Zr contents may be related to variations in zircon content.

Zn contents are remarkably low; 61 to 159 ppm, considering that minor sphalerite mineralization occurs near rhyolites sampled in the quarry on the Burgeo road.

On the standard AFM diagram (Figure 6.1) the rhyolites cluster at the alkali corner of the diagram, along the projection of the tholeiitic trends. One sample is anomalous, plotting near the centre of the diagram.

On the Ti vs Zr diagram of Pearce (1980) the rhyolites fall in a restricted area of the arc lava field (Figure 6.9), suggesting that they might represent one magma batch.

6.11 RARE EARTH ELEMENT CONTENTS

Rare earth element patterns of two dacite porphyries, one dacite bomb from the agglomerate in Henry Waters and one diorite intrusion are very similar (Figure 6.13) and have similar degrees of enrichment vs. chondritic values. They are LREE enriched relative to Sm suggesting fractionation of minerals such as olivine, clinopyroxene or hornblende. Negative Eu anomalies are probably due to various degrees of feldspar fractionation; those of samples 81HPAD067 and 81HPAD081-2 being relatively insignificant. The pattern of HREE is flat to slightly enriched.

One rhyolite sample (81HPAD073) has a flat REE pattern with abundances approximately 15X chondritic abundances (Figure 6.13). This pattern is significantly different

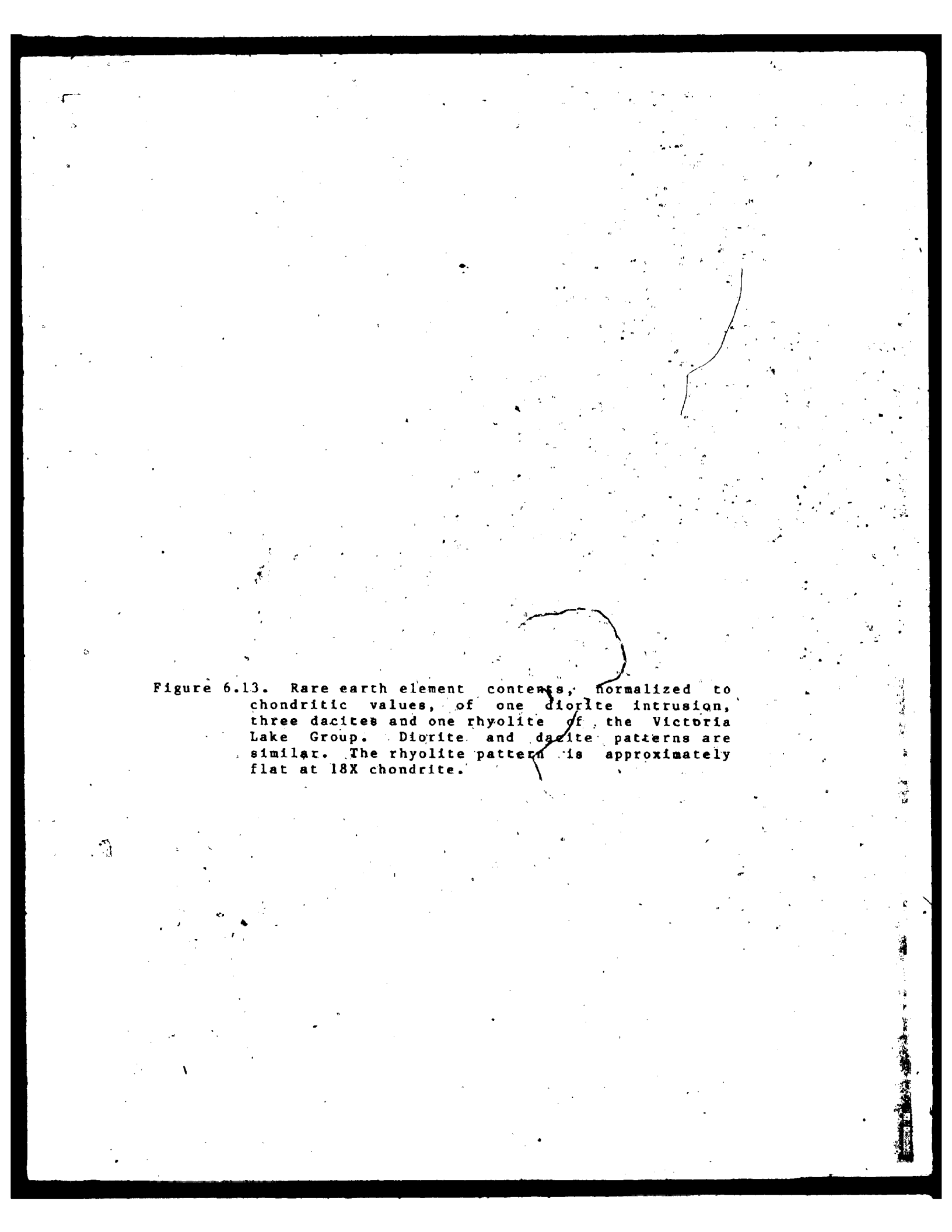

Figure 6.13. Rare earth element contents, normalized to chondritic values, of one diorite intrusion, three dacites and one rhyolite of the Victoria Lake Group. Diorite and dacite patterns are similar. The rhyolite pattern is approximately flat at 18X chondrite.

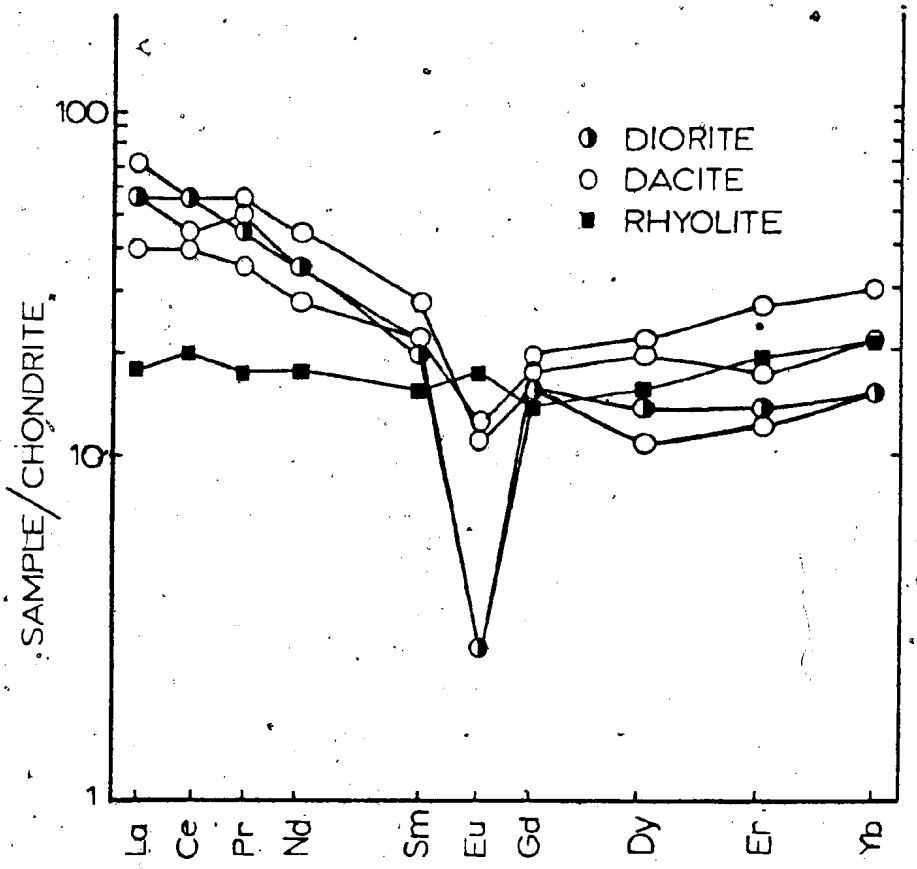
100
10
1
SAMPLE/CHONDRITE
DIORITE
DACITE
RHYOLITE
La
Ce
Pr
Nd
Sm
Eu
Gd
Dy
Er
Yb

than those of the dacites and may represent a different magma batch, possibly from a different source, despite their close proximity. However, the LREE enrichment in the dacites may result from enrichment by hydrothermal fluids. The samples come from the centres of large bombs in agglomerate and although obvious alteration rinds were removed, the cores contain secondary albite and chlorite. Plots of alkali elements (not presented) show a wide scatter which likely is an alteration feature.

Therefore, the present writer is unwilling to use the chemistry of the felsic volcanic rocks to characterize the Victoria Lake Group.

6.12 DISCUSSION

Many of the volcanic formations of the Dunnage Zone exposed in Notre Dame Bay have been interpreted to be the products of intra- oceanic island arc volcanism (Upadhyay, 1973; Kean and Strong, 1975). This interpretation was extended to the Victoria Lake Group by Kean et al.. (1981).

Felsic rocks are abundant in the Victoria Lake Group and if some basalts, suggested to be ophiolitic, are excluded from the Group its bimodal nature is more pronounced. This relative abundance of rhyolite and dacite, compared to the volcanic groups of Notre Dame Bay, suggests that the rocks of the Victoria Lake Group were generated in a somewhat different way.

Apparently coeveal volcanic groups to the south and southwest, the Bay du Nord and La Poile Groups, are composed of over fifty percent of felsic volcanic rocks. Based on this preponderance of felsic volcanic rocks and the presence of more radiogenic Pb in galenas in these Groups, Swinden and Thorpe (in press) suggest that these two groups were derived in part from melting of continental crust. In their model they suggest that the volcanic arc, as represented by rocks of the Dunnage Zone, was built on oceanic crust in the north but transgressed a continental margin and was built on continental crust in the south.

The bimodal nature of the volcanic rocks of the Victoria Lake Group may indicate that it formed in an environment transitional between the oceanic and continental realm. This sort of paleogeographic assessment is risky though, because there is no paleomagnetic or faunal control on the relative positions of volcanic groups in the Iapetus Ocean. Furthermore, as a result of the geochemical study it is uncertain that, within the Victoria Lake Group, the basalts are directly related to the felsic rocks. They may be the products of separate volcanic events taking place in a transitional tectonic environment.

CHAPTER 7 GEOCHRONOLOGY OF OPHIOLITES OF THE NEWFOUNDLAND APPALACHIANS

7.1 INTRODUCTION AND PREVIOUS WORK

The age of origin and time of emplacement of ophiolites in Newfoundland is of fundamental importance in deciphering the history of formation and destruction of the Iapetus Ocean.

In this chapter new U/Pb (zircon) age determinations are presented for the Bay of Islands Complex, Betts Cove Complex and the Annieopsquotch Complex (two samples). These are discussed in relation to local stratigraphy and compared to ages determined for ophiolites elsewhere in the Appalachian- Caledonian Mountain Belt.

7.1.1 Bay of Islands Complex

The Bay of Islands Complex of west Newfoundland is the largest and most studied ophiolite in the Appalachians. It occurs as the highest of at least five structural slices, separated by melanges, in the Humber Arm Allochthon (Stevens, 1970).

Early models for the emplacement of the allochthon (Rodgers,1965; Stevens, 1970; Church and Stevens, 1971) were constrained in time by fossil data. The first occurrence of ophiolitic detritus in sandstones of the Blow Me Down Brook Formation derived from the east was

interpreted by Stevens (1970) to indicate initiation of ophiolite obduction. Evidence from the graptolite fauna indicates that this formation is late Arenigian in age. The final emplacement of the assembled Humber Arm Allochthon is dated by fossils in the unconformably overlying (neoautochthonous) sediments of the Long Point Formation (Rodgers,1965; Stevens,1970). Conodonts indicate a Caradocian age for this formation (Fahraeus,1973). Correlations between these ages and the absolute time scale are very uncertain. The many Ordovician time scales now in use attest to the problem (van Eysinga,1975; Armstrong, 1978; McKerrow, Lambert and Chamberlain, 1980; and others).

The Bay of Islands Complex (Figure 7.1) has been the subject of four previous radiometric age studies. Two of these were directed at the metamorphic aureole, interpreted to have formed during initial displacement of the ophiolite from its oceanic setting (Williams and Smyth,1973; Malpas,1979b) and two attempted to determine the primary age of crystallization of the plutonic sequence within the ophiolite suite. In addition Mattinson (1975) determined an age for the 'Trout River ophiolite' which he grouped with the Bay of Islands Complex.

Dallmeyer and Williams (1975) analysed hornblende from three samples of amphibolite from the aureole at North Arm Mountain. The three 40Ar/39Ar ages produced overlap between 462 and 457 Ma to give a best estimate of the age of the aureole of 460+/-5 Ma. This they took to be the

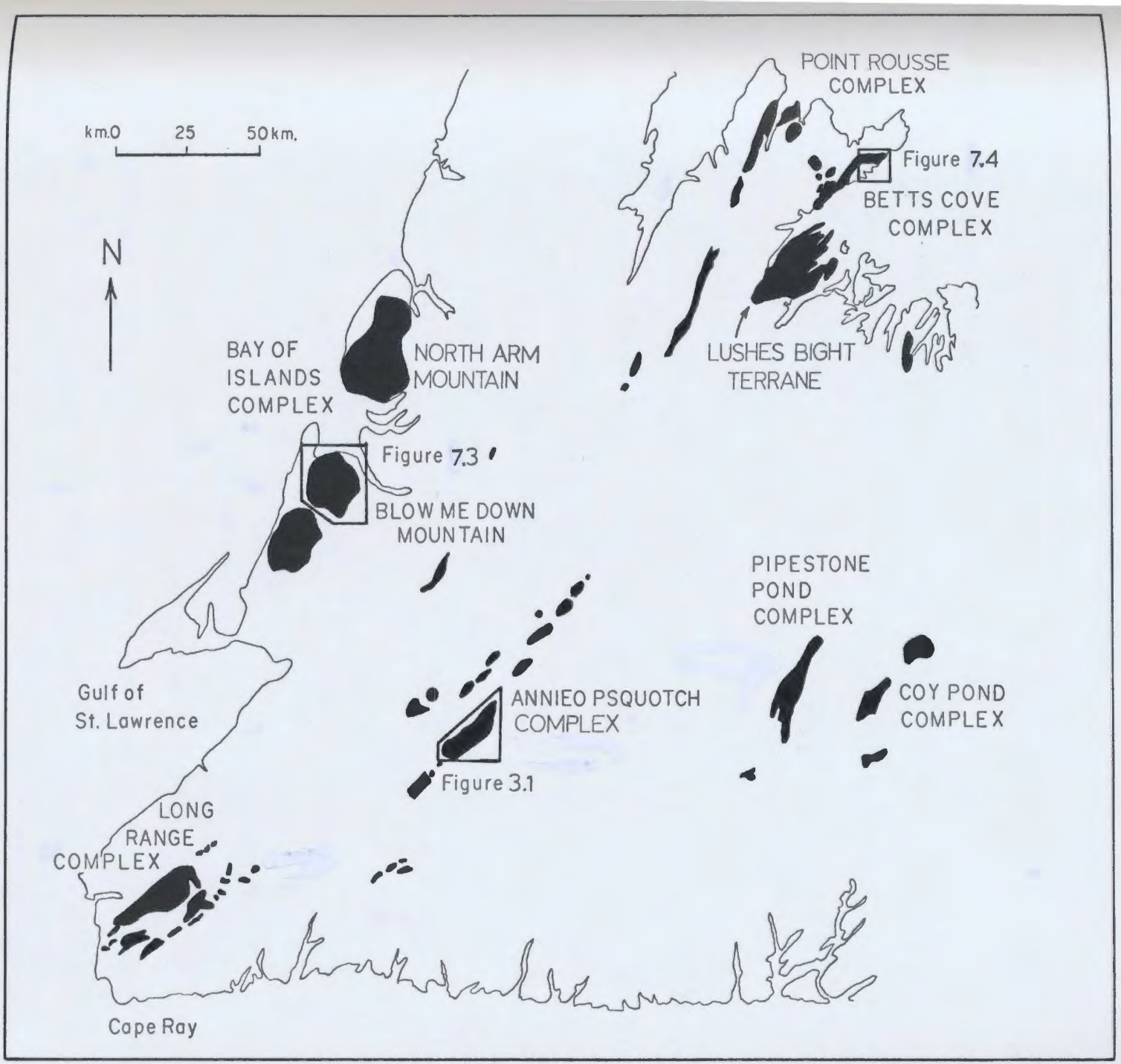

Figure 7.1. Ophiolite complexes of western and central Newfoundland after Williams (1978), Dunning (1981), Chorlton (1983), Colman-Sadd (1981) and Swinden and Collins (1982).

synchronous metamorphic age of the three samples. With the new K decay constant (Steiger and Jager,1977), this age recalculates to 469+/-5 Ma (Dallmeyer, pers. comm.,1983).

Archibald and Farrar (1976) dated seven samples of hornblende from the metamorphic aureole of North Arm Mountain and Table Mountain by the K/Ar method. They determined an age of 454+/-9 Ma, on the assumption that all samples incorporated equal amounts of initial argon of uniform composition. With the new decay constant this age recalculates to approximately 464+/-9 Ma.

Mattinson (1975) determined a U/Pb (zircon) age of 508+/-8 Ma for trondhjemite of the 'Trout River ophiolite'. He considered this to be the age of the Bay of Islands Complex as well. However, the rocks at Trout River are part of the Little Port Complex (Williams, 1973) and are thought not to be directly correlative with the Bay of Islands Complex. Mattinson (1976) sampled the trondhjemites of Blow Me Down Mountain and determined a U/Pb (zircon) age of 504+/-10 Ma. The 207Pb/206Pb ages for individual points are 480+/-7, 485+/-7 and 494+/-5 Ma. All three points are concordant within the limits of uncertainty and a line through them is nearly parallel to concordia. To fit a line to the points Mattinson (1976) assumed a Pb-loss event occurred at 460 Ma; the age of the metamorphic aureole as determined by Dallmeyer and Williams (1975). He fixed the lower intercept at 460 such that the assumed discordia line projected to a significantly older age than that suggested by the concordant points.

Jacobsen and Wasserburg (1979) determined two Sm/Nd internal isochrons for pyroxene-gabbros of the Bay of Islands Complex as part of a larger study of the petrogenesis of the Complex. The first isochron based on three points, one each for a plagioclase mineral separate, clinopyroxene mineral separate and the total rock gives an age of 508+/-6 Ma. The points for the total rock and clinopyroxene separate lie very close together. The second isochron, based on one point each for plagioclase and clinopyroxene mineral separates gives an age of 501+/-13 Ma. They therefore quote an average age for the Bay of Islands Complex of 505 Ma. No error is stated for this age.

7.1.2 Betts Cove Complex

The Betts Cove Complex, mapped in detail by Upadhyay (1973), is located on the east coast of the Burlington Peninsula (Figure 7.1). It is the largest of several ophiolite complexes underlying the northern part of the Peninsula. Recent work by Hibbard (in press) has led to the suggestion that the ophiolites, which are progressively more deformed and metamorphosed westwards, are imbricate slabs of oceanic crust (s.l.) of essentially the same age. In this model, the Betts Cove Complex is the least deformed, uppermost slab.

The stratigraphic units of the ophiolite dip and face southeast. The Complex is broken by faults parallel to strike which locally thin or remove some zones and locally

juxtapose gabbro and pillow lava.

The Betts Cove Complex is conformably overlain by a pile of volcanic flows, tuffs and volcanogenic sediments dated as Arenigian by graptolites (Snelgrove,1931). The volcanic sequence, the Snooks Arm Group, has been interpreted to represent deposition in an island arc (Upadhyay,1973) or oceanic island environment (Jenner and Fryer,1980).

Mattinson (1975) determined a U/Pb (zircon) age of 463+/-6 Ma for a trondhjemite dyke cutting the Nippers Harbour Ophiolite. This ophiolite is believed to be part of the Betts Cove Complex but the dyke itself has been the subject of controversy. Church (1976) suggested, on the basis of its geochemistry, that it is not directly related to the ophiolite and thus provides only a minimum age for the Betts Cove Complex. Mattinson (1977) conceded this possibility. Ross, Naessar and Lambert (1978) found it "difficult to reconcile" this age with the presence of Arenigian fossils in the overlying sediments. It has been suggested (D.F. Strong, pers. comm.,1980) that the dyke is an offshoot of the Burlington Granodiorite, a nearby subvolcanic intrusion dated at 464+/-5 Ma by the 40Ar/39Ar method (J. Hibbard and D. Dallmeyer, pers. comm.,1982). On the basis of the trace element geochemistry of the dyke Epstein (1983) suggested that it is related to the Stocking Harbour Intrusive Suite, a part of the Burlington Granodiorite.

7.1.3 Annieopsquotch Complex

The Annieopsquotch Complex (Figures 7.1) is in fault contact with volcanic rocks of the Victoria Lake Group (Dunning and Herd,1980) which are of Llanvirnian-Llandeilian age (Kean and Jayasinghe, 1980). Dykes, thought to be related to the Victoria Lake Group lavas, cut the pillow lava zone of the ophiolite providing a minimum age for the latter. In addition, the Annieopsquotch Complex is unconformably overlain by terrestrial sedimentary rocks with interbedded volcanic rocks. A preliminary U/Pb (zircon) age of 431+/-5 Ma for a rhyolite flow in this sequence places an upper limit on the time of emplacement of the ophiolite (Chandler and Dunning, 1983).

7.2 NEW DATA

Sample preparation, analytical techniques and method of age calculation are discussed in Appendix 5.

7.2.1 Bay of Islands Complex

A sample of trondhjemite (80HPAD257) was collected from Blow Me Down Mountain by the author, guided by J. Malpas, within one hundred metres of Mattinson's (1976) sample location (Figure 7.3). Abundant small yellow (euhedral to subhedral) zircons were separated from the sample. They contain tiny needle inclusions of an unknown mineral (Figure 7.2).

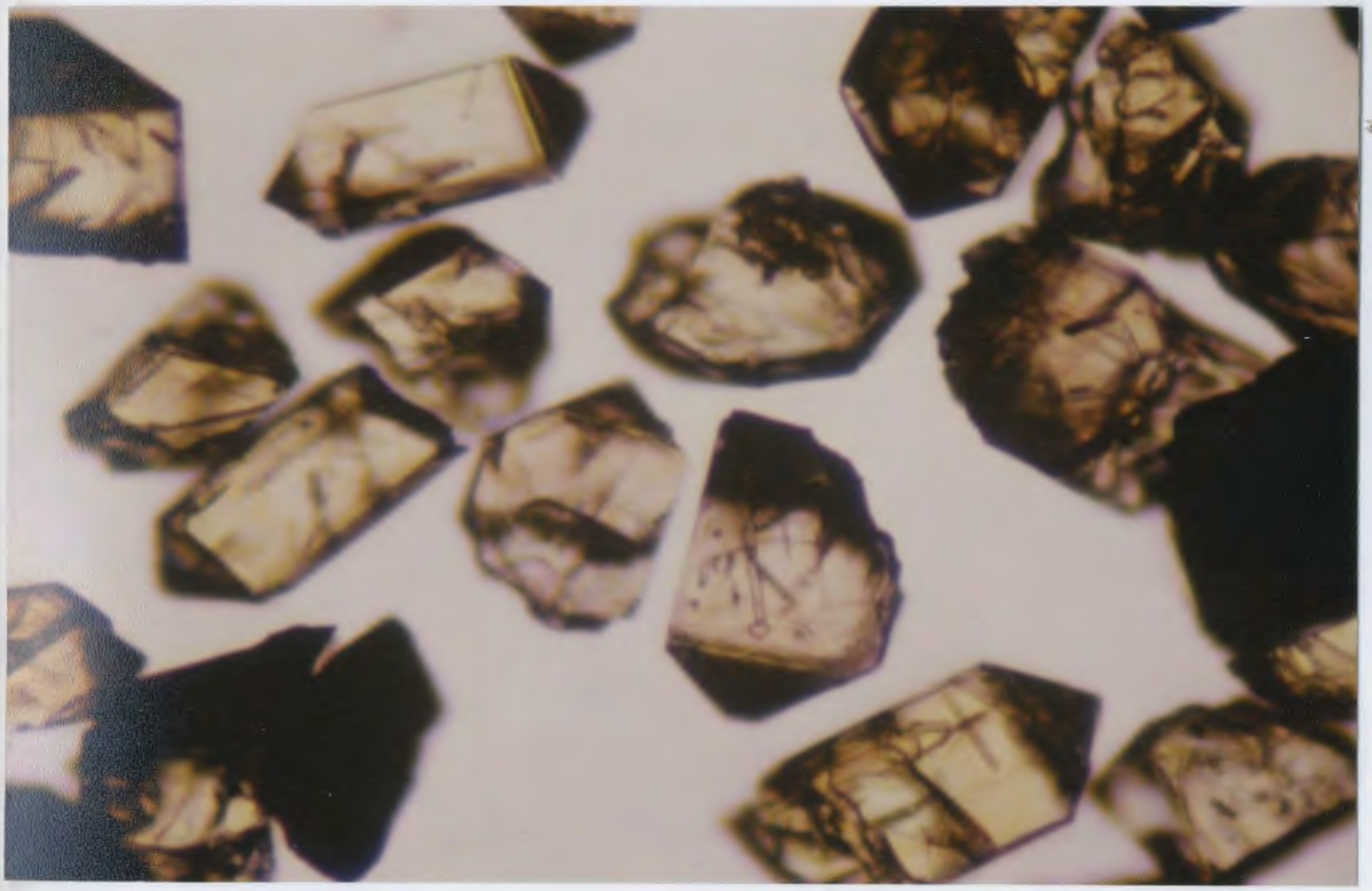

Figure 7.2. Euhedral to subhedral zircons, with small needle inclusions and original sample pyrite, of -100,+200,M1 bulk fraction; from trondhjemite, Bay of Islands Complex. 80HPAD257.

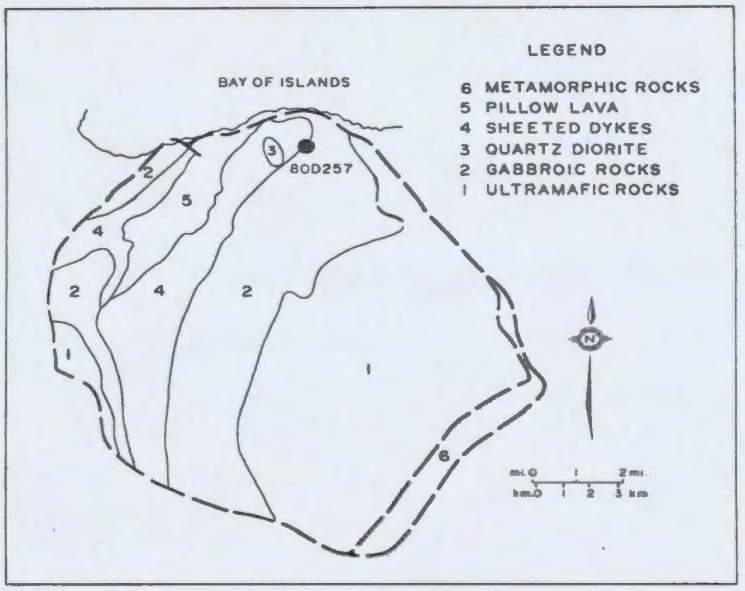

Figure 7.3. Geology of Blow Me Down Mountain of the Bay of Islands Complex after Williams (1972) showing sample location.

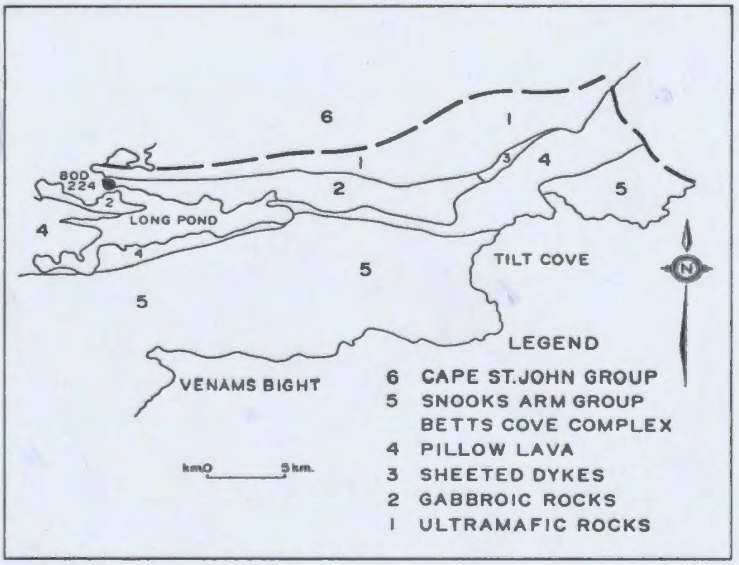

Figure 7.4. Geology of part of the Betts Cove Complex after Upadhyay (1973) showing sample location.

Five zircon fractions with differing magnetic properties and grain sizes were analysed (Table 7.1). They follow the general rule that fractions abraded to remove outer surfaces plot closer to concordia (Krogh,1982).

Two fractions (anal. 1,2, Table 7.1; Figure 7.5), both -100,+200 mesh and abraded, plot together close to concordia (1.2 and 1.3% discordant). The -200,+325, 0 degree magnetic fraction (anal. 3) is 1.7% discordant, slightly more so than the abraded fractions. The 3 degree magnetic fraction (anal. 4) is 2.2% discordant and the -325, 3 degree magnetic fraction (anal. 5), consisting in part of turbid grains is the most discordant at only 2.8%. These -325, magnetic zircons have the lowest integrity and have lost a greater proportion of their lead but even they are not greatly discordant. The age determined by fitting a line to all five points is 485.7+1.9/-1.2 Ma (2σ, Figure 7.5). This line was constrained to pass through 50 Ma +/-90% (see Appendix for discussion).

7.2.2 Betts Cove Complex

Zircons were obtained from a coarse grained quartz-bearing gabbro (0.25% quartz) of the Betts Cove Complex at Long Pond near Tilt Cove (Figure 7.4). These are clear, coarse, dark to light brown anhedral fragments which are interpreted to be pieces of larger skeletal zircons (Figures 7.7, 7.8). Zircons found in gabbro are commonly skeletal (D.W. Davis, pers. comm.,1982) and x-ray analysis confirmed their identification.

TABLE 7.1. U-Pb isotopic data

Analysis No.	Fraction and preparation	Weight (mg)[A]	Concentration (ppm)[B] U	Concentration (ppm)[B] Pb	Measured $^{206}Pb/^{204}Pb$	Atomic ratios corrected for blank and common Pb[C] $^{206}Pb/^{238}U$	Atomic ratios corrected for blank and common Pb[C] $^{207}Pb/^{235}U$	Atomic ratios corrected for blank and common Pb[C] $^{207}Pb/^{206}Pb$	Pb/Pb age
		Sample 80HPAD257 Bay of Islands Complex							
1	M1, -100 + 200[a]	6.03	318	24.6	29832	0.0773	0.6056	0.05680	484
2	NO, MO, M1, -100 + 200[a]	1.44	302	22.3	6400	0.0773	0.6055	0.05682	484
3	NO, MO, -200 + 325	0.82	264	20.2	8662	0.0769	0.6034	0.05688	487
4	M3	0.89	353	27.4	8273	0.0766	0.6000	0.05685	485
5	M3, -325, ± turbid	1.70	494	35.9	9430	0.0761	0.5966	0.05687	486
		Sample 80HPAD224 Betts Cove Complex							
6	NO, -100 + 200, clear[a]	11.61	129	10.3	7652	0.0782	0.6137	0.05693	489
7	NO, -100 + 200, bulk[a]	11.61	128	10.2	5337	0.0779	0.6104	0.05687	486
8	NO, -70 + 100, wh. frosted[a]	2.55	48	3.8	839	0.0777	0.6093	0.05688	487
9	M3, -70 + 100, cracked	2.57	131	10.2	640	0.0757	0.5923	0.05676	482
		Sample 80HPAD222 Annieopsquotch Complex							
10	NO, MO, M1, M2 - 100 + 200[a]	20.55	41	3.5	4628	0.0766	0.5993	0.05675	482
11	M3, -325, ± turbid	5.35	154	13.1	1129	0.0759	0.5932	0.05667	479
		Sample 80HPAD223 Annieopsquotch Complex							
12	NO, -40 + 70, gems[a]	15.67	46	3.4	7877	0.0768	0.5992	0.05660	476
13	NO, -70 + 100, gems[a]	7.64	49	3.6	4151	0.0765	0.5969	0.05658	475
14	NO, -70 + 100, 4 hr. HF	2.96	44	3.2	4343*	0.0764	0.5972	0.05667	479
15	NO, -70 + 100	8.65	55	4.4	14054*	0.0762	0.5955	0.05668	479
16	M2, M3, -40 + 70, cloudy	4.23	48	3.8	2176	0.0755	0.5894	0.05664	478

Notes: NO, M3 = non-magnetic, magnetic fractions; 0 and 3 indicate degrees of tilt on a Frantz isodynamic separator; both NO and MO are non-magnetic fractions; -100 + 200 = grain size between 100 and 200 mesh; [a]sample abraded. See Krogh (1982) and appendix for details of sample preparation.

A Error in weight ± 0.01 mg, 1σ.

B Error in absolute conc. approx. ± 2% defined by weight of sample and weight of tracer, but U/Pb ratios are known ± 0.25% (1σ).

C Corrected for 0.1 ng blank and common lead at the age of the sample calculated from the model of Stacey and Kramers (1975) and 36 x $10^{-12}g^{238}U$.

* Measured value corrected for common lead in 205 spike; other analyses include this lead.

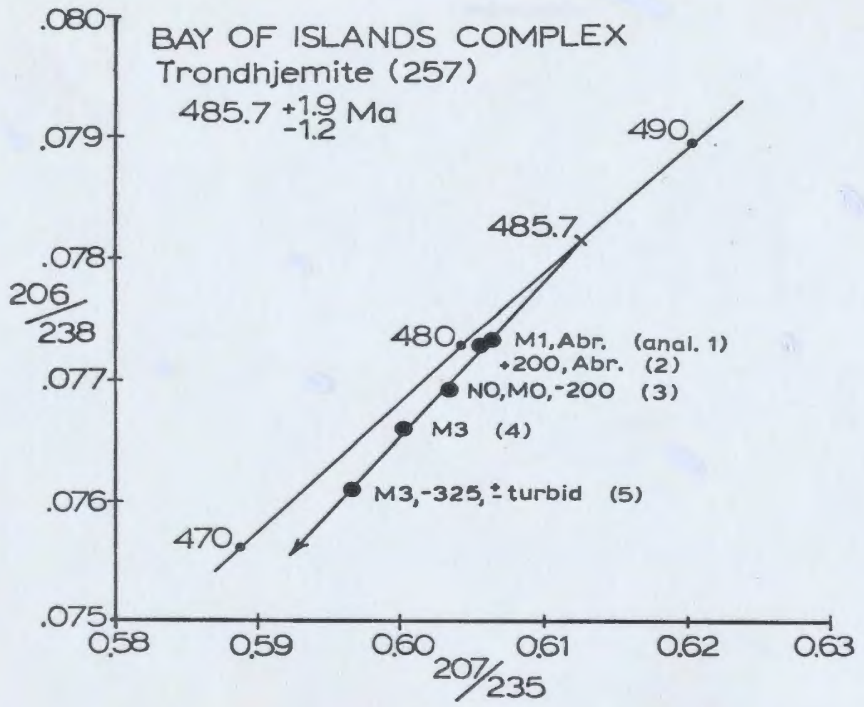

Figure 7.5. Concordia diagram showing U-Pb isotopic data from trondhjemite (80HPAD257) of the Bay of Islands Complex and the best fit line through all points.

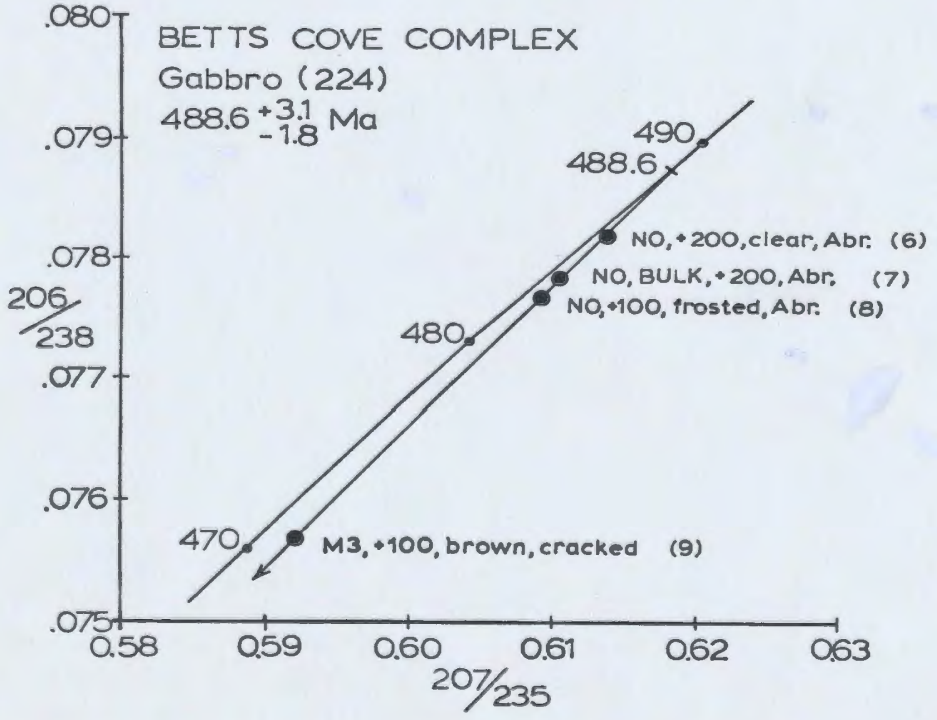

Figure 7.6. Concordia diagram showing U-Pb isotopic data from gabbro (80HPAD224) of the Betts Cove Complex and the best fit line through all points.

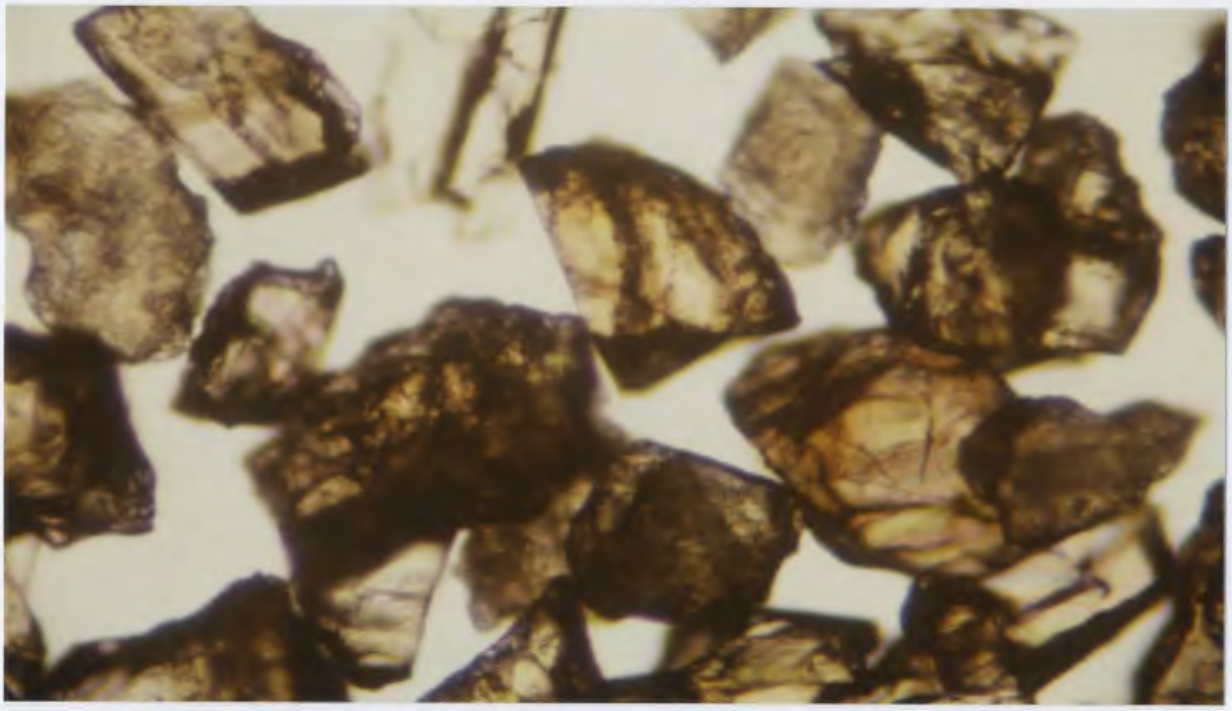

Figure 7.7. Anhedral angular zircon fragments of -100,+200,M1 bulk fraction ; from gabbro, Betts Cove Complex. 80HPAD224.

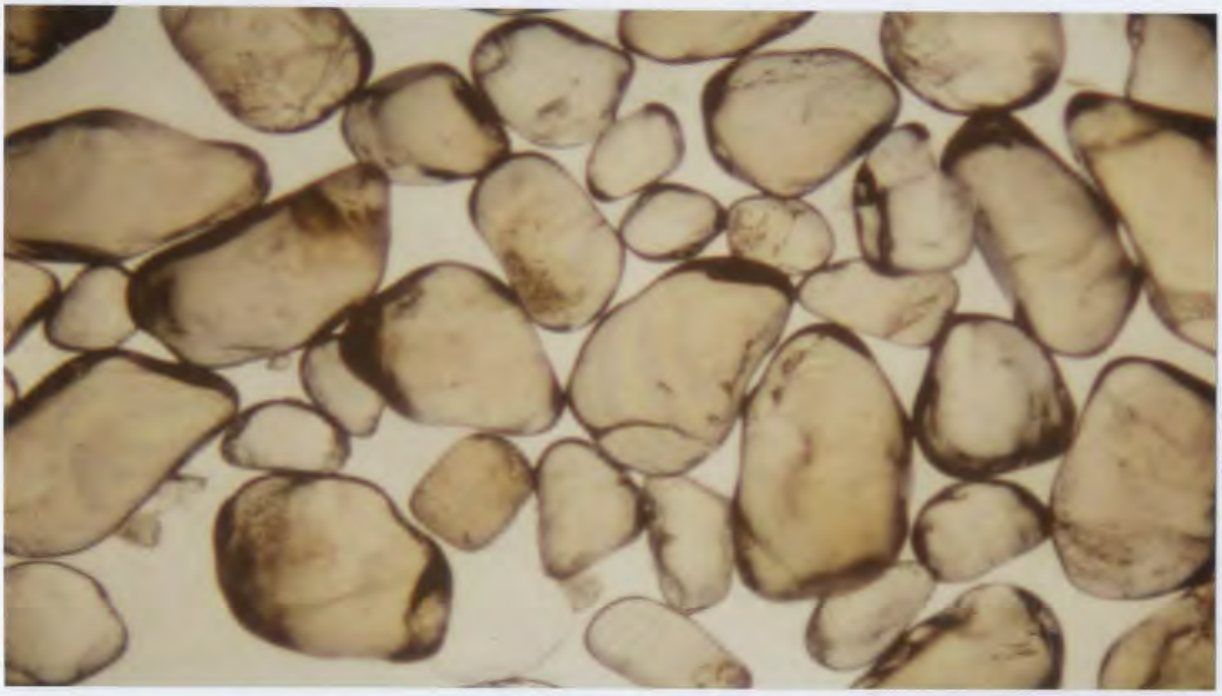

Figure 7.8. Irregular rounded zircon fragments after abrasion. Sample is clear grains picked from -70,+100,N0 fraction; from gabbro, Betts Cove Complex. 80HPAD224.

Four fractions were analysed. Three of these (anal. 6,7,8, Table 7.1) are of the 0 degree, non-magnetic fraction. After abrasion they plot near concordia at 1.0%, 1.6% and 1.9% discordant (Figure 7.6). Clear grains picked from the bulk are the closest to the upper intercept (anal. 6). Frosted grains (anal. 7) are the most discordant of the 0 degree fractions and the bulk sample (anal. 8) plots between the clear and frosted grains as expected.

All of the 0 degree abraded fractions plot close together indicating that lead loss was not significantly greater from frosted grains than from clear. This is likely due to the very low U content of these zircons (48 to 131 ppm, Table 7.1).

The 3 degree magnetic fraction (anal. 9) is 5.6% discordant. A best-fit line through all four points, constrained to pass through 50Ma+/-90%, gives an age of 488.6+3.1/-1.8 Ma (2σ, Figure 7.6). This is interpreted to be the age of crystallization of the Betts Cove gabbro.

7.2.3 Annieopsquotch Complex

Samples were collected from two trondhjemitic bodies located six kilometres apart in the gabbro zone of the Complex (Map 1, Figure 3.1).

The first sample (80HPAD222) forms the matrix of an intrusion breccia which incorporates blocks of gabbro and diabase and is strongly epidotized. It occurs next to a fault which cuts the gabbro zone and is interpreted to be a sea-floor feature (Chapter 3). The geochemistry of this

sample is consistent with differentiation from mid ocean ridge basaltic magma (Chapter 5).

Zircons from this sample are small, euhedral grains, few in number. Two fractions were analysed (anal. 10, 11, Table 7.1), the first was a collection from the non-magnetic and magnetic splits of the +200 size fraction from which turbid grains were removed. This fraction was abraded and is 1.4% discordant (Figure 7.9). The second fraction, −325, 3 degree magnetic, includes turbid grains and plots 2.5% discordant. A line through the two points, constrained to pass through 50 Ma +/-90%, gives an age of 481.4+4.0/−1.9 Ma (2σ, Figure 7.9) which is interpreted to be the age of crystallization of the trondhjemitic liquid.

The second sample (80HPAD223) is from a pegmatitic pod (Map 1) which contains hornblende crystals up to 15 centimetres long as well as abundant quartz (Figure 4.11). The pod has a core of pegmatitic trondhjemite which grades through hornblende diorite to typical 'high-level' gabbro of the ophiolite. Trace element and rare earth element geochemistry of the trondhjemite is consistent with interpretation of this pod as a differentiate of the ophiolitic gabbro (Chapter 5).

Abundant coarse, clear, euhedral 'gem' zircons were obtained from this sample and five fractions with different size and magnetic properties, both abraded and unabraded were analysed (anal. 12- 16, Table 7.1). The +70, 0 degree non-magnetic 'gem' zircons, after abrasion, plot on concordia (0.1% discordant, anal. 12, Table 7.1; Figure

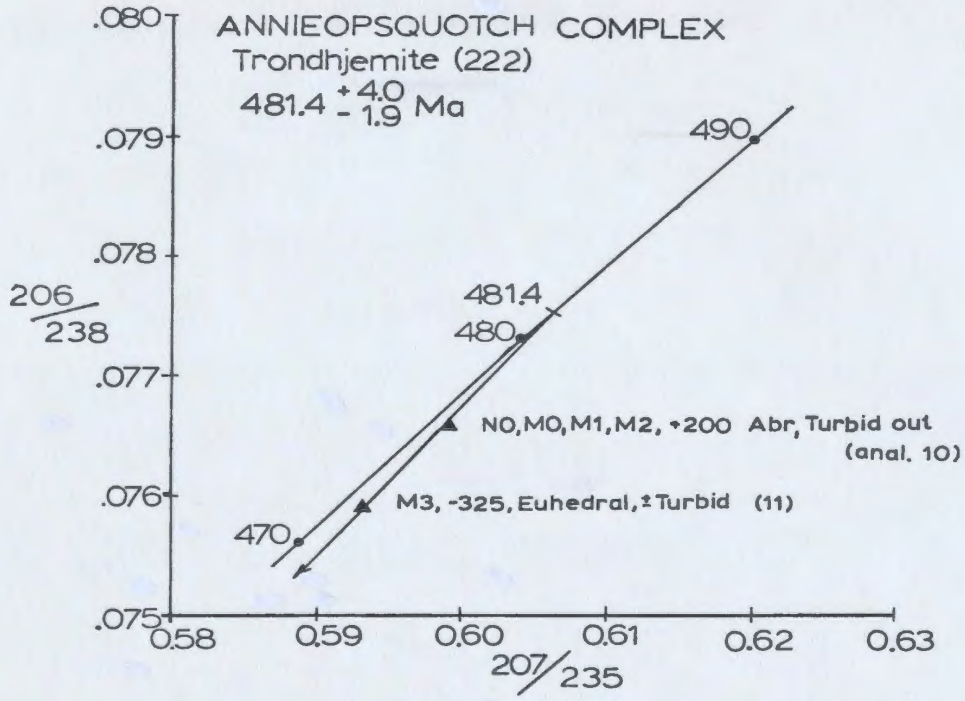

Figure 7.9 . Concordia diagram showing U-Pb isotopic data from trondhjemite (80HPAD222) of the Annieopsquotch Complex and the best fit line.

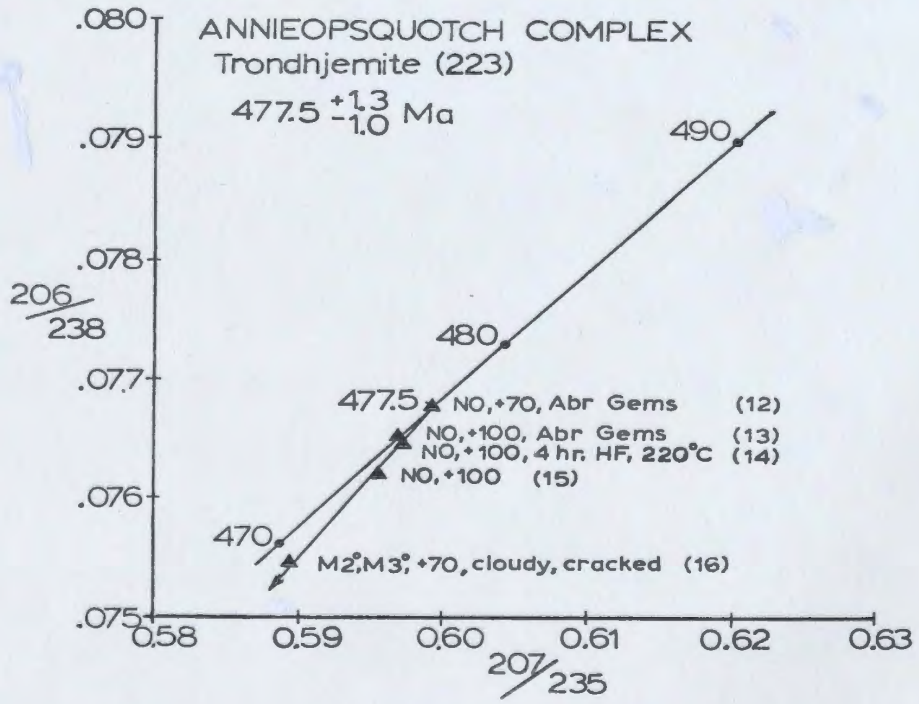

Figure 7.10. Concordia diagram showing U-Pb isotopic data from pegmatitic trondhjemite (80HPAD223) of the Annieopsquotch Complex and the best fit line through all points.

7.10). The 207Pb/206Pb age of this fraction is 476 Ma. Three +100, 0 degree non-magnetic fractions were analysed. The first (anal. 13, Figure 7.11), after abrasion, plots on concordia (0.5% discordant, Figure 7.10), slightly lower than the +70 fraction. The second +100 fraction (anal. 14) was etched in HF for four hours at 220 degrees C as an experiment to induce lead loss. The high integrity of the zircons is indicated by the fact that this leached fraction plots on the best-fit line for all points and is essentially concordant (0.6% discordant). The third +100 fraction (anal. 15), unabraded, plots more discordant (0.9%) on the best-fit line (Figure 7.10). All four 0 degree non-magnetic fractions form a tight grouping demonstrating that they have undergone little or no lead loss. This is certainly due in part to their low uranium content (44 to 55 ppm) which is among the lowest measured for zircon in the R.O.M. laboratory. The +70, 2 and 3 degree magnetic, cloudy cracked grains (anal. 16) are the most discordant. The age obtained for the best-fit line through all five analyses, well controlled by the concordant +70 abraded upper point and constrained to pass through 50 Ma +/-90%, is 477.5+1.3/-1.0 Ma (2σ, Figure 7.10).

The two ages obtained for the Annieopsquotch Complex do not overlap at the two sigma level. This may indicate a true age difference between two discrete intrusions within the gabbro zone. Alternately, it may reflect differing slow cooling rates deep in the oceanic crust over the

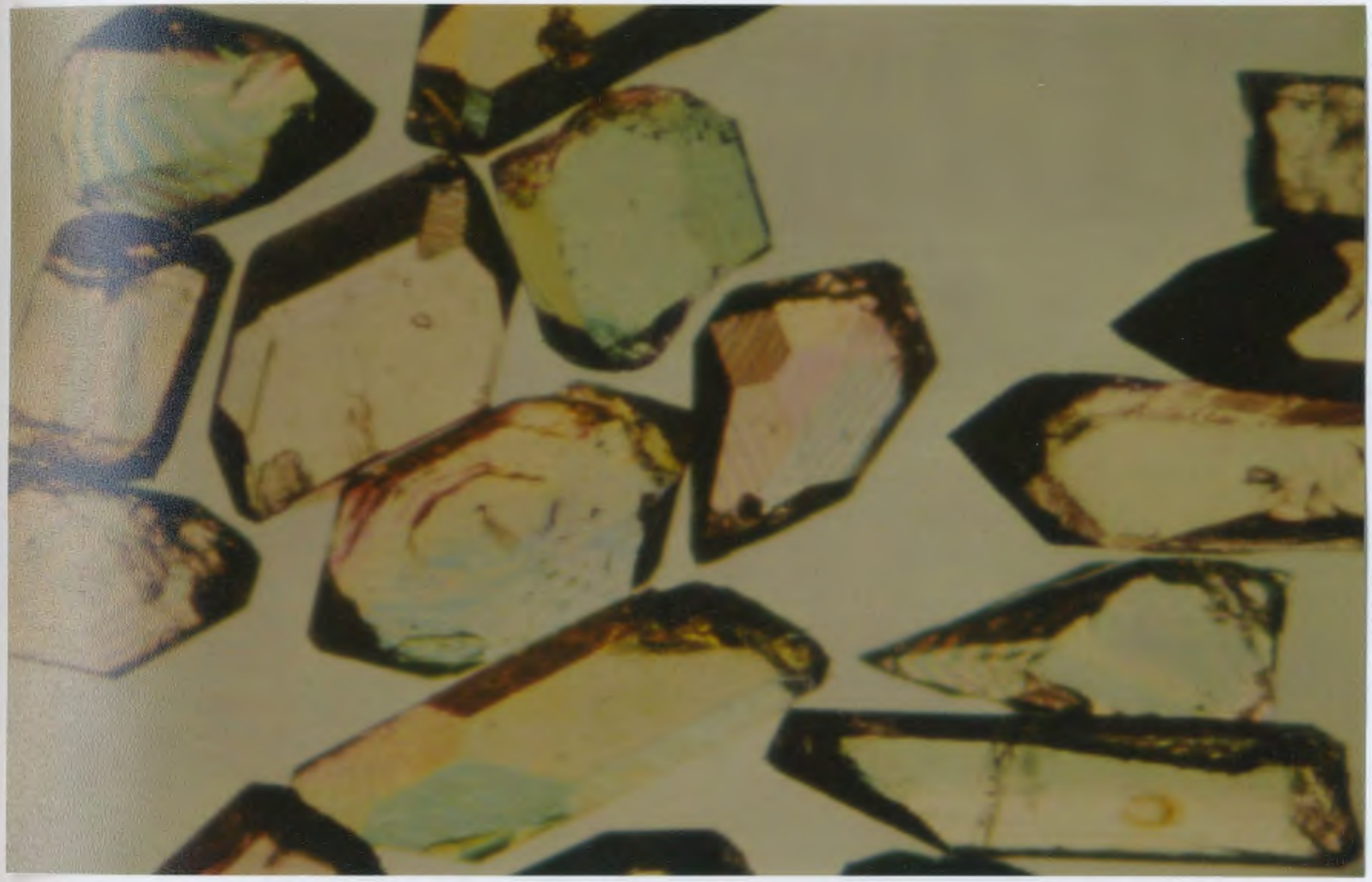

Figure 7.11. Best, picked, euhedral 'gem' zircons of the -70,+100,NO fraction; from trondhjemite, Annieopsquotch Complex. 80HPAD223.

uprising mantle diapir with its attendant high geothermal gradient.

7.3 DISCUSSION

7.3.1 Comparison to Previously Determined Ages

The new U/Pb (zircon) ages indicate that the formation of ophiolite complexes found in the Newfoundland Appalachians spans a time range from 477.5+1.3/-1.0 Ma to 488.6+3.1/-1.8 Ma rather than 463+/-6 Ma (Betts Cove Complex, U/Pb) to 504+/-10 Ma (Bay of Islands Complex, U/Pb) as previously thought. This 40 Ma age gap, initially reported by Mattinson (1976), resulted from the production of a poor discordia line for the Bay of Islands sample and the dating of a non-ophiolitic dyke at Nippers Harbour. The 207Pb/206Pb ages of individual size and magnetic fractions from the Bay of Islands Complex (480+/-7, 485+/-7, 494+/-5 Ma) determined by Mattinson (1976) are in fair agreement with the new age determination of 485.7+1.9/-1.2 Ma. They are concordant and two of the ages overlap the new intercept age, within error limits. The error in the conclusion of Mattinson (1976) resulted from projecting a line through 460 Ma based on isotopic disturbance at the time of metamorphic aureole formation (Dallmeyer and Williams,1975). High temperatures, locally of the granulite facies, achieved in the metamorphic aureole were not present throughout the ophiolite during

aureole formation, and it seems the lower metamorphic grade which affected the plutonic rocks of the Complex was insufficient to reset the zircon U/Pb isotopic system at that time.

The two Sm/Nd ages of gabbro from the Complex (Jacobsen and Wasserburg, 1979) do not overlap the new U/Pb (zircon) age. The less precise Sm/Nd age of 501+/-13 Ma is within 0.4 Ma at the maximum quoted error limits. It is suggested that the errors on the Sm/Nd ages may be larger than reported. Both are based on two point isochrons (in statistical terms) and neither has a point close to the initial 143Nd/144Nd ratio. A recent recalculation of the two Sm/Nd isochrons using Jacobsen and Wasserburg's (1979) data yielded far larger error estimates (O. van Breeman, pers. comm.,1983). In addition, it is suggested that the mineral separates analysed were not free of alteration effects. No perfectly fresh gabbros were encountered in this study and Jacobsen and Wasserburg (1979) describe their plagioclase separates as having "minor saussuritization" and one of the samples contains secondary amphibole and serpentine.

7.3.2 Bay of Islands Complex Stratigraphic Relationships

The new age for the Bay of Islands Complex is compatible with all information available on its stratigraphic relationships and time of emplacement (Figure 7.12). This age is early Arenigian according to the time scale of van Eysinga (1975). Fossil evidence indicates

that the flysch which contains ophiolitic detritus, derived from the east, is of Arenigian age (Stevens,1970). It is possible for this detritus to have been derived from a young, hot, uplifted Bay of Islands Complex, but the detritus could equally well have come from an older fragment of oceanic crust, obducted earlier and not now preserved (or not yet dated!).

Acritarchs in sedimentary rocks deposited on the Bay of Islands Complex during emplacement and termed parallochthonous by Casey and Kidd (1981) are of Llanvirnian age and final emplacement is dated as pre-Caradocian based on conodonts from the neoautochthonous Long Point Formation (Fahraeus,1973; Rodgers,1965; Stevens,1970). These data (Figure 7.12). are compatible with formation of the Bay of Islands Complex in Arenigian time and imply a history from igneous crystallization to final emplacement spanning 40 Ma using the van Eysinga (1975) time scale.

7.4 DATE OF FORMATION OF OTHER APPALACHIAN-CALEDONIAN OPHIOLITES

7.4.1 North America

In addition to the new ages for Newfoundland ophiolites reported here, Dunning and Krogh (1983) have reported a preliminary age of 495 +/-3 Ma for trondhjemite of the Pipestone Pond Complex of central Newfoundland. It

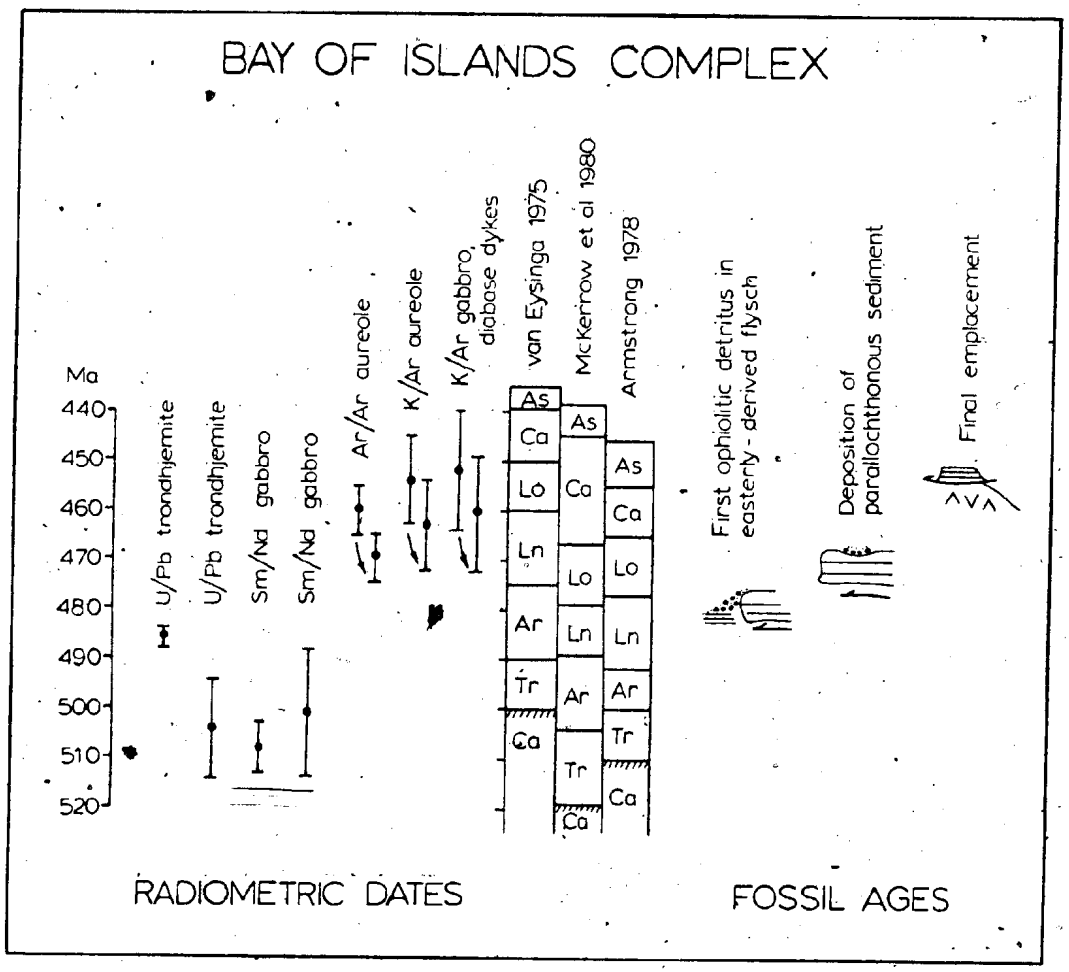

Figure 7.12. Radiometric dates for the Bay of Islands Complex and fossil age data for related sedimentary rocks compared to three Ordovician time scales. See text for sources of information. Arrows with K/Ar ages point to values recalculated with the new K decay constant. All fossil ages are plotted in relation to the van Eysinga (1975) time scale.

appears that this ophiolite, of Tremadocian age (van Eysinga, 1975), and its likely correlative the Coy Pond Complex (Colman-Sadd and Swinden, 1982) are the oldest Paleozoic ophiolites in Newfoundland.

Deformed ultramafic rocks of the Thetford Mines ophiolite are intruded by many granitic to dioritic bodies. A Rb/Sr age of 466+/-13 Ma has been determined for a tabular granitic body at Black Lake, Quebec (Wanless and Poole, 1980). This sets a minimum middle Ordovician age for the ophiolitic rocks.

Disrupted ophiolitic rocks, including sheeted dykes and pillow lava, comprise the Lushes Bight Terrane of central Notre Dame Bay. These are cut by the ophiolitic Brighton Gabbro on Pilleys Island (D.F. Strong, pers. comm., 1982). A 40Ar/39Ar age of 495+/-5 Ma, determined for the gabbro by Stukas and Reynolds (1974b) is thought to be the age of the ophiolitic rocks.

The M'Clintock West and East Ultramafic Massifs (Frisch, 1974) on northern Ellesmere Island, Arctic Canada have recently been reported as ophiolitic fragments (Trettin and Balkwill, 1979; Trettin, 1982). They are actually part of the Arctic continuation of the Greenland Caledonides and contain dioritic phases, interpreted by Frisch to be cogenetic with the ultramafic suite. The U/Pb (zircon) age of the diorite phase is 481+7/-6 Ma (Trettin, Loveridge and Sullivan, 1982).

Gaudette (1981) reported a U/Pb (zircon) age of 410+/-7 Ma for the Union ultramafic complex in Maine which

he interpreted to be an ophiolitic fragment. This age would be incompatible with the Arenigian-Tremadocian ages reported for other Appalachian ophiolites. However, Talkington and Gaudette (1983) have shown that the Union Complex is an intrusion into sedimentary rocks and consider the earlier interpretation as invalid.

7.4.2 Europe

A U/Pb (zircon) age has been determined for an ophiolite complex in the Caledonian Mountain Belt. Zircon from trondhjemite of the Ballantrae ophiolite gives an age of 483+/-4 Ma (Bluck et al., 1980). This they interpret to be the time of crystallization of the trondhjemite magma.

Thirlwall et al.(1982) have recently reported a Sm/Nd age of 490+/-14 Ma based on mineral isochrons from two samples of basalt lavas from the Southern Uplands of Scotland. These basalts have MORB chemistry, occur at the base of accreted ocean trench sedimentary sequences and are associated with transitional and alkali basalts of ocean island type. The age, while imprecise, is consistent with the data from Newfoundland ophiolites and Ballantrae.

The limited age data available for sediments unconformably overlying the Karmoy Complex in Norway indicates a pre-middle Ordovician age for that complex (Sturt et al., 1980). A Rb/Sr age of approximately 450 Ma for a granite intruding the Karmoy Complex similarly indicates a pre-middle Ordovician age for the Complex (A. Rahaeim, pers. comm., 1983)

The Storen basalts of Norway, interpreted to be ophiolitic by Gale and Roberts (1974), are overlain by middle Arenigian fossil bearing rocks. This age may closely approximate that of the ophiolitic rocks as well. However, there is evidence for erosion of the ophiolite before deposition of the middle Arenigian and younger sequence (Furnes et al.,1980).

In summary, the new ages reported here are Arenigian according to the van Eysinga (1975) time scale. Evidence from all other Appalachian-Caledonian ophiolites discussed above is consistent with their being of Arenigian or Tremadocian age as well (Figure 7.13). The minimum age range for all ophiolites that is consistent with all the age data now available is 479 to 492 Ma. This range is shown by the black bar in Figure 7.13.

7.5 TIMING OF OBDUCTION

Malpas (1979b) observed that ophiolites with well developed basal 'dynamothermal' aureoles must have been hot, possibly recently formed, when they were obducted in order to metamorphose adjacent oceanic crust as they overrode it. He suggested that these ophiolites might even represent segments of the ridge itself. With their high relief, they might be more likely to be obducted. Ophiolites preserved in the Appalachian- Caledonian Mountain Belt may thus be close to the last oceanic crust

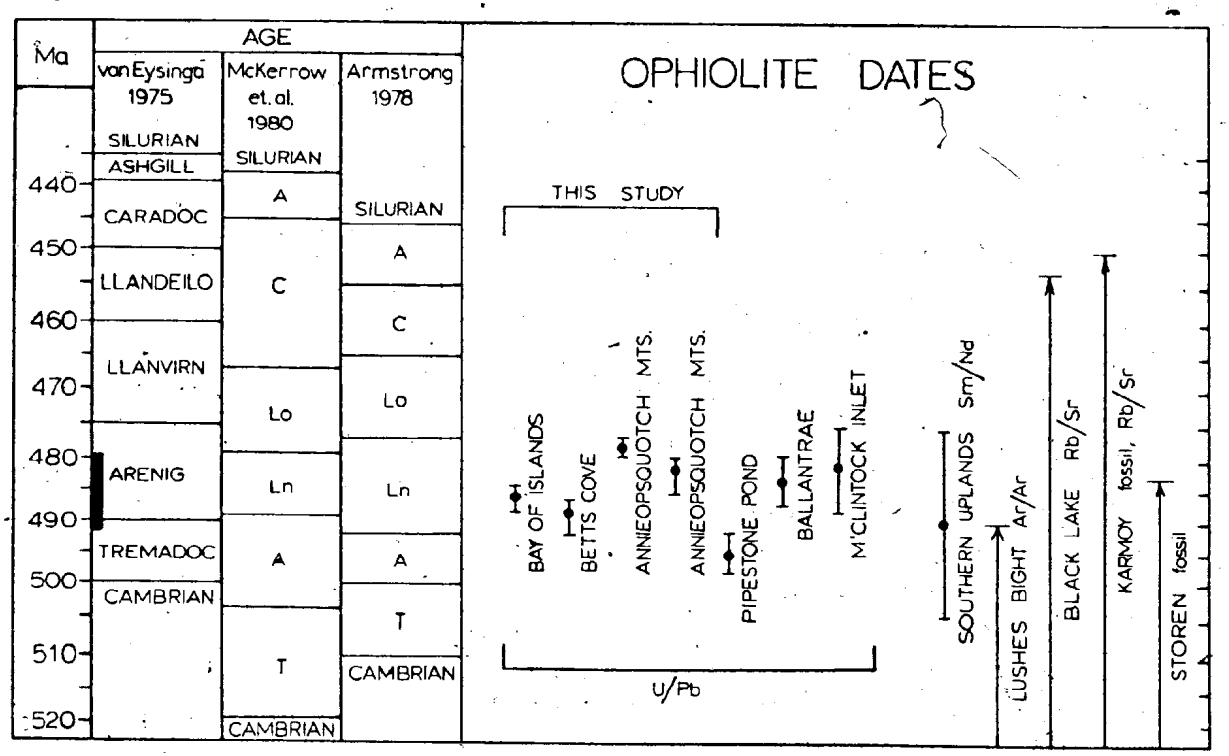

Figure 7.13. Summary of radiometric and fossil age data for ophiolitic rocks of the Appalachian - Caledonian Mountain Belt and three versions of the Ordovician time scale. Black bar shows the minimum possible age range for all the ophiolites.

formed before ocean closure.

The 40Ar/39Ar date of 469+/-5 Ma (new decay constant) for the metamorphic aureole of North Arm Mountain (Dallmeyer and Williams,1975) indicates that first obduction of the hot oceanic crust and mantle (Malpas,1979b) occurred in Llanvirnian time by the scale of van Eysinga (1975). This is later than the first indication of ophiolitic detritus in easterly derived flysch (Figure 7.13 and Stevens,1970) and implies that either older oceanic crust, or crust of the same age obducted earlier, provided some of the ophiolitic detritus in the flysch, or that the 40Ar/39Ar date for hornblende from the aureole does not indicate the time of formation of the aureole. With the present state of knowledge of age relations among Newfoundland ophiolites either of these suggestions might be correct. However, the latter interpretation is preferred.

The older 40Ar/39Ar age of 480+/-5 Ma from hornblende of the metamorphic aureole of the St. Anthony Complex led Dallmeyer (1977) to propose the diachronous obduction of ophiolites of the Humber Zone. There is some sedimentological evidence to support this hypothesis. Stevens (1970) reported that easterly-derived flysch immediately beneath the ophiolitic rocks is older in the St. Anthony area than that at Bay of Islands.

The age of 480+/-5 Ma from the aureole of the St. Anthony Complex does not require that the primary (igneous) age of the Complex be any older than that of the Bay of

Islands Complex. Obduction may have started sooner after formation of the oceanic crust at the point of origin of the St. Anthony Complex than at that of the Bay of Islands Complex.

7.6 RELEVANCE OF OPHIOLITE AGES TO THE ORDOVICIAN TIME SCALE

Ross et al. (1978) considered Mattinson's (1975) U/Pb (zircon) age of 508+/-5 Ma, which is actually for the 'Trout River ophiolite' or the Little Port Complex of current usage (Williams, 1973) to be the age of formation of the ophiolite. They considered this to be correlative with the Bay of Islands Complex but did not relate it directly to an Ordovician stage. Mattinson's (1976) age for trondhjemite of Blow Me Down Mountain was not then available.

Dallmeyer and Williams (1975) considered their age of 460+/-5 Ma from the aureole to date the Arenigian phase of obduction. Archibald and Farrar (1976) related their age of 460 Ma (not reported above) to the Arenigian as well. Yet they related the 452 Ma K/Ar age from gabbro and diabase dykes to the late Llanvirnian- early Llandeilian emplacement of the ophiolite.

Ross et al. (1978) concluded their discussion by proposing two possible time scales for the Ordovician; one involved considerable conflict with Scottish and Irish

tectonics. Their favoured scale assigned the approximately 460 Ma ages to the Llanvirnian and placed the Arenigian at 500 to 480 Ma. They assumed that most of the K/Ar ages were minimum estimates and were concerned with the origin of the dynamothermal aureole of the Bay of Islands Complex and the possiblity of later reheating.

The new zircon age of 485.7+1.9/-1.2 Ma for the Bay of Islands Complex is most reasonably interpreted to be pre-Arenigian or Arenigian to conform with the stratigraphic evidence discussed above. Of the three time scales shown in Figure 7.13, only that of van Eysinga (1975) is appropriate. If either of the other scales is correct and the fossil evidence is to be believed, the deposition of the easterly-derived flysch bearing ophiolitic detritus and of the parallochthonous sediments on North Arm Mountain would predate crystallization of the Blow Me Down trondhjemite. The latter is clearly a plutonic rock related to the ophiolite and must predate the sediments. These relationships provide strong evidence against the validity of the time scales of McKerrow et al. (1980) and Armstrong (1978) for the early Ordovician.

The aureole dates are not compatible with fossil evidence either. They are minimum (cooling) ages and the fossil evidence suggests that they are too young (Figure 7.13). However, this matter was not investigated further in this study.

Ross et al. (1978) challenged the age of 463+/-6 Ma for the Betts Cove Complex and suggested that the dyke

might be younger than the ophiolite. They were also critical of the 'slight' paleontologic evidence, as published by Snelgrove (1931), for a middle Arenigian age for the Snooks Arm Group. The new date of 488.6+3.1/-1.8 Ma for the Betts Cove Complex is compatible with the presence of Arenigian fossils in the Snooks Arm Group and provides an important point on the Ordovician time scale. This date is in agreement with the van Eysinga (1975) time scale, which places the Arenigian stage at 490 to 475 Ma.

7.7 MODERN ANALOG

These ages place no limits on the width of the early Paleozoic Iapetus Ocean. An unknown and possibly large amount of older, cold oceanic crust may have been completely subducted. If the 40Ar/39Ar age of 605+/-10 Ma (Stukas and Reynolds,1974a) is accurate for diabase dykes on the Great Northern Peninsula, the oldest oceanic crust may have been late Precambrian. Strong (1975) and earlier workers interpreted these dykes to be related to rifting and early opening of Iapetus. Certainly, a well developed continental margin sedimentary sequence was present by Cambrian time (Williams, 1979).

The ophiolites presently exposed in the Appalachian-Caledonian Mountain Belt, of a limited age range, were formed in several tectonic settings. Based on their geology and geochemistry they probably formed at a marginal

basin (or major ocean?) spreading centre, or formed the basement to island arc sequences or oceanic islands (Malpas,1976; Jenner and Fryer,1980; Furnes et al.,1980).

The evidence of an extensive continental margin by Cambrian time and early Ordovician ophiolites of many different geochemical, and by inference tectonic, affinities suggests that the Iapetus Ocean was extensive. It is suggested that this Ocean may have resembled the present day western Pacific Ocean with ridge segments, both active and inactive, island arcs and back-arc basins of various sizes present along its length (cf. Gale and Pearce,1982; Nur and Ben-Avraham,1982). The amount of strike slip movement along faults, if any, in the Iapetus Ocean before or during closure is unknown. By analogy with the western Pacific, major displacements may have occurred along such faults and the present arrangement of ophiolites and volcanic sequences may, therefore, bear little or no relationship to the Ordovician paleogeography.

CHAPTER 8 NEW DATA RELEVANT TO NEWFOUNDLAND TECTONICS AND REGIONAL SYNTHESIS AND TECTONIC INTERPRETATION

8.1 NEW DATA RELEVANT TO NEWFOUNDLAND TECTONICS

Interpretation of Newfoundland geology and Appalachian geology general is changing rapidly as a result of deep seismic profiling of the southern Appalachians (Cook et al., 1979) and, in Newfoundland, as a direct result of considerable new mapping across the island combined with structural, geochemical and isotopic studies.

In order to competently discuss the tectonic history and emplacement of the Annieopsquotch Complex, one must take in to account much of this growing body of new and largely unpublished data. Much of this has not been presented in the text of the thesis as it has been produced by others in various parts of Newfoundland or is preliminary data only.

It has long been recognized that major Taconic allochthons are present in west Newfoundland (Rodgers and Neale, 1963; Rodgers, 1965; Stevens, 1970; Williams, 1978 and many others). These, the Humber Arm and Hare Bay Allochthons, consist of a number of slices of sedimentary rocks separated by melange zones and capped by slices of ophiolitic rocks; the Bay of Islands and St. Anthony Complexes. Classically, their time of emplacement has been controlled by fossil ages in flysch interpreted to have

been derived from the east due to mass wasting of the uplifted advancing allochthons. These ages indicate disruption of the oceanic crust and assembly of allochthons from east to west occurred in Arenigian to Llanvirnian time (Stevens,1970). The time of final emplacement of the allochthons has also been determined by conodonts in the overlying 'neoautochthonous' Long Point Formation (Rodgers,1965; Stevens,1970). Fahraeus (1973) determined a Caradocian age for the conodont assemblage which implies a final emplacement of the allochthons occurred in Llandeilian to early Caradocian time (Chapter 7). This emplacement is defined (from the Taconic Allochthon of New York) as the Taconic Orogeny.

Llanvirnian - LLandeilian is the time when the Bay of Islands Complex was moving (Casey and Kidd,1981) and when many volcanic arcs of the Dunnage Zone were active. Volcanism in the Dunnage Zone has been linked by most workers to subduction of oceanic crust during closure of the Iapetus Ocean, generally synchronous with emplacement of the west Newfoundland allochthons.

Recent detailed structural mapping of cross sections from the Long Range Precambrian inlier across the Humber Allochthon to the west coast of Newfoundland strongly supports the suggestion that the entire Humber Zone is allochthonous (T.J. Calon, pers. comm.,1983). He has suggested that a basal decollment above continental crust occurs at a depth of possibly two or three kilometers.

Such a suggestion has likewise been made by C.

Beaumont (pers. comm.,1983) on the basis of the size and geometry of the Anticosti Basin west of Newfoundland. They reason that the weight of the Humber Arm Allochthon, as oulined by Stevens (1970) is insufficient to hold the basin in its downwarped position and that a far more massive allochthonous body must exist in west Newfoundland. They therefore suggest that most of the Humber Zone, including the Precambrian inlier, is allochthonous.

If correct, and the present writer favours such an interpretation, this adds a whole new dimension to the Taconic Orogeny in the Newfoundland Appalachians. It suggests that this orogeny involved tectonism and crustal shortening more on the scale of that recorded in the Caledonides of Norway, the southern Appalachians during the Alleghenian Orogeny (Cook et al., 1979), i.e.; hundreds of kilometers of movement of nappes.

Beyond this new interpretation by Calon and co-workers, even more radical models are now being suggested for the extent of Newfoundland rocks that are allochthonous and were allochthonous in Ordovician time. Evidence, mostly unpublished, is accumulating which indicates that much of the Newfoundland Appalachians may be allochthonous.

Zircons were separated from early to middle Ordovician foliated tonalite and granodiorite which intrude and include ophiolitic rocks in southwest Newfoundland (Chorlton, 1982; Dunning, Carter and Best, 1982). Analyses indicate that these zircons have cores of

approximately 1400 Ma age. High contents of large ion lithophile elements in the tonalites and the U-Pb (zircon) data (Dunning and Krogh, unpublished data) suggests that these intrusive rocks formed by partial melting of oceanic and Grenvillian (?) continental crust, or possibly sediments derived from continental crust. Wilton (1983) suggests that the generation of Devonian granites in southwest Newfoundland is due to partial melting of already depleted (once melted) Grenville granulite. It is suggested that the Ordovician tonalitic magmas were generated during the first melting episode and that under west Newfoundland a depleted, once (or twice) melted, continental crust is present.

The present writer's view is that this crust is of granulite facies metamorphic grade, dense, due to the loss of one or more melt fractions, probably hypersthene - bearing gneiss of approximately dioritic composition and with a predominant 1400 Ma age, as indicated by the U-Pb (zircon) data.

Another alternative is that sedimentary rocks, possibly of Fleur de Lys type, with a bulk composition similar to that of continental crust and containing detrital zircons of ca. 1400 Ma age are beneath the inferred basal decollment. These could have been the source, with oceanic crust, of the tonalitic melts. Or, possibly true continental crust underlies the west part of southwest Newfoundland and sedimentary rocks underlie the eastern part.

In a re-interpretation of the gravity data for Notre Dame Bay, Karlstrom (1983) indicates that it can be reconciled with an allochthonous Dunnage Zone above a decollment at approximately ten kilometers depth with continental crust beneath. So the earlier interpretation of a dense substrate, presumed to be of ultramafic composition beneath the Dunnage Zone (Miller and Deutsch, 1976) is not the only one possible for the existing data. Miller (pers. comm., 1983) now indicates that the gravity data is ambiguous and could be reconciled with an allochthonous Dunnage Zone. It is suggested that depleted granulite gneisses may be dense enough to accomodate the gravity measurements.

Inliers of foliated granodiorite in the North Bay Granite (Dickson and Tomlin, 1983) are lithologically similar to the foliated tonalite - granodiorite terrane of southwest Newfoundland (writer's observation). As zircons from these inliers (two samples) contain cores inherited from a terrane approximately 1500 Ma old (Krogh and Dickson, unpublished data), the interpretation for the generation of the tonalite terrane of southwest Newfoundland may be applied to these inliers in south-central Newfoundland as well. That is; that they formed by partial melting of a source of approximately 1500 Ma, of granitic composition at depth, or of sedimentary rocks derived from such a terrane. These two samples from the Bay d'Espoir area plus the occurrence of old inherited zircon in the Deadmans Bay Granite (Currie et al., 1982) in

the Gander Zone are east of most of the Dunnage Zone. It is therefore reasonable to suppose that similar continental crust, or sediments derived therefrom, may be continuous between all sample locations and thus under all of the Dunnage Zone. The geology seen at the surface then is likely allochthonous with respect to an underlying dense, once melted, continental crust (or sedimentary rocks from such a source). Indeed, the fossil continental margin of ancient North America may lie beneath the presumed decollment somewhere under central Newfoundland.

It has been suggested (Colman-Sadd, pers. comm., 1983) that a window exposing rocks underlying this inferred decollment occurs between the Pipestone Pond and Coy Pond Complexes of the south-central Dunnage Zone.

As a result of the above discussion it follows that, although some rock units of west Newfoundland are interpreted to be allochthonous in relation to others which are thought to be autochthonous, all might be allochthonous on the larger scale.

8.2 COMPOSITE DUNNAGE ZONE

The question of major transcurrent movement in the Dunnage Zone is now much debated. The idea that the Zone is composed simply of volcanic arc sequences built on oceanic crust, while perhaps true in a simple sense, ignores or oversimplifies complexities within the Zone. It

is more appropriate to think of the Dunnage Zone as composite, containing many discrete volcanic sequences, largely bounded by faults (and traditionally mapped as separate formations or groups) which bear uncertain relationships one to the other, and may be of different ages. The juxtaposition of some of these sequences may result from major transcurrent movement along faults in the Iapetus Ocean, some of which may be preserved in the Dunnage Zone. Thus the present relative positions of Ordovician volcanic sequences may bear no relation to the Ordovician paleogeography.

Church and Riccio (1977) and Coish and Church (1979) divided the ophiolites of Newfoundland into two groups; those of the 'External Zone' with high - Ti basalts predominant and those of the 'Internal Zone', with Ti - depleted basalts. The former are represented by the Bay of Islands Complex and the latter include Betts Cove Complex intermediate and lower lavas and Mings Bight (Point Rousse Complex) low - Ti basalts (Norman and Strong, 1975).

The distinction between these two zones was twofold; geographical and lithogeochemical. A fundamental difference was implied to exist between those ophiolites emplaced on the continental margin and those remnants present in the Dunnage Zone associated with island arc sequences. However, Lorenz and Fountain (1982) showed that many dykes of the South Lake Igneous Complex have high - Ti contents and that this Complex is geographically, within the 'Internal Zone'.

Likewise, this study clearly shows that the Annieopsquotch Complex, and related ophiolite fragments, are high - Ti ophiolites yet they are clearly associated geographically with the Victoria Lake Group. This Group is a volcanic arc sequence, at least in part, but may not be an island arc sequence as interpreted by Kean et al (1981).

This division into zones, based on the study of a small number of Newfoundland ophiolites therefore breaks down when one examines the larger picture, in particular the ophiolites of central and southwest Newfoundland. As the Dunnage Zone is composite, the relative position of most Newfoundland ophiolites in Ordovician time is unknown. Therefore any attempt to recognize patterns in the chemistry of different ophiolites and relate them to the current geography of the latter is fraught with danger!

8.3 TECTONIC HISTORY OF THE ANNIEOPSQUOTCH COMPLEX AND RELATED OPHIOLITIC FRAGMENTS

It has been demonstrated in this work that a belt of ophiolitic rocks extends from Shanadithit Brook, near Buchans, to King George IV Lake. All were previously mapped as early Paleozoic gabbro or diorite intrusions. These ophiolitic fragments are correlated (Chapter 2) with the Long Range Mafic- Ultramafic Complex (Brown, 1976) of southwest Newfoundland and a large number of additional fragments identified in the surrounding region by Chorlton

(1982).

In the region of the Annieopsquotch Mountains of southwest Newfoundland many ophiolitic fragments are present that form high - standing massifs with no visible means of support. Mapping of several of these reveals that they are bounded in whole or in part by steep faults, some of which; the Cabot, Lloyds River and Victoria Lake Faults, are structures of regional significance. The movement history of these faults is poorly known. It is suggested that the Lloyds River and Victoria Lake Faults may well have been Ordovician thrusts.

Both the foliated tonalite terrane to the west and the Victoria Lake Group to the east of the Annieopsquotch Complex are likely younger than it and intrude it (Chapter 2). Both have these major faults sited within them and are affected by further movement along them. In addition post - early Silurian uplift of the Annieopsquotch Mountains has clearly occurred (Chandler, 1982), presumably along the Lloyds River Fault. It is likely that Carboniferous or later movement has occurred on these faults as well, because Carboniferous sedimentary rocks on the west side of Red Indian Lake are tilted.

Strong (1972), and later Karson and Dewey (1978), noted that sheeted dykes in both the Bay of Islands and Betts Cove Complexes trend roughly northwest. This led them to suggest that the spreading ridge that generated these rocks was oriented northwest, at a high angle to the supposed paleo - continental margin. This model ignored

the vastly different chemistry of the two ophiolites; one MORB, the other with lavas of MORB, island arc (or ocean island) and high - Mg boninitic type.

Nevertheless, a predominantly northwest sheeted dyke trend is present and remarkably, all sheeted dykes in ophiolitic fragments of the Annieopsquotch ophiolite belt have the same northwest trend. All diabase dykes and basaltic lavas analysed from fragments in the belt, from Shanadithit Brook to King George IV Lake, have virtually identical MORB chemistry, and all plot on the same trends on most trace element variation diagrams. Therefore it is reasonable to suggest that they may be systematically related and have all formed at a single spreading ridge.

It is suggested that the ophiolitic fragments of the Annieopsquotch ophiolite belt are remnants of a once continuous sheet of Iapetus Ocean crust. The slab of oceanic crust was systematically decoupled from mantle lithologies along the layered critical zone and emplaced over the partially subducted continental margin. Partial melting of a mixed package of subducting rocks, including oceanic crust, Fleur de Lys type sediments and continental crust, generated the tonalitic magmas that intruded, in some cases engulfed, and disrupted the ophiolitic rocks. These plutons coalesced to form an Ordovician calc - alkaline batholith which enclosed the ophiolitic rocks. Locally hundreds of small (metre or less across) blocks, interpreted to be derived from ophiolite, occur bordering large ophiolite massifs and form agmatites with tonalite as

the host.

In Chapter 2 a conservative interpretation was presented of the area of ophiolitic rocks preserved in the Annieopsquotch ophiolite belt. Bodies of mafic rock that are poorly exposed or of uncertain affinity were excluded. In addition, much country with little rock exposure occurs between mapped ophiolitic fragments that could also be underlain by these rocks. So the possibility exists that some 'fragments' are actually limited exposures of a single large sheet. This is suspected to be the case especially for the area between Lloyds Lake and Southwest Brook Pond and also the northeast corner of the Puddle Pond map area.

If all the ophiolitic fragments are in their original relative positions in the sheet of oceanic crust the area outlined by them is about 1130 square kilometres. This is an area comparable to that of the entire Bay of Islands Complex. This is a minimum area because imbrication of the ophiolitic rocks (cf. Dunning and Chorlton, 1983) may have reduced their original extent, however this estimate is a useful first approximation. It indicates that a large ophiolitic sheet was emplaced in southwest Newfoundland and, if it was once continuous with the Long Range Mafic-Ultramafic Complex and associated fragments, it was by far the largest ophiolitic allochthon in Newfoundland, perhaps in the entire Appalachians!

8.4 AGE RELATIONS OF APPALACHIAN - CALEDONIAN OPHIOLITES

The ages so far determined for Newfoundland ophiolites are closely comparable. The oldest, apparently, is the Pipestone Pond Complex (495 Ma) which is central in the Dunnage Zone.

The Bay of Islands Complex is younger than previously thought (485.7 Ma) and the Betts Cove Complex older (488.6 Ma). These new ages overlap within the two sigma errors quoted. The new age for the Bay of Islands Complex refutes two previously determined late Cambrian ages, while that for the Betts Cove Complex resolves a long standing inconsistency between previous radiometric and fossil age determinations. These ages serve to refute tectonic models that relied upon a large time gap between the generation of the two complexes.

As all ophiolites dated in Newfoundland are allochthonous and fault - bounded, no model linking their ages to their present relative positions would have any meaning.

A survey of ages of ophiolitic rocks in the Appalachian - Caledonian Mountain Belt reveals that they are restricted to a narrow time range. Within errors quoted, all could have formed between 492 and 479 Ma, which covers part of the Tremadocian and Arenigian stages of the early Ordovician on the van Eysinga (1975) time scale.

Possibly only late - formed, hot or topographically high oceanic crust was able to be decoupled from the mantle

and be successfully emplaced on the continental margin. Older (colder?) topographically low oceanic crust was subducted. Therefore, no estimate of the duration of spreading or width of the Iapetus Ocean is attempted on the basis of the age data.

8.5 SUMMARY OF THE THESIS

1. The Annieopsquotch Complex of southwest Newfoundland is one of a large number of ophiolitic bodies which, including the Long Range Mafic- Ultramafic Complex, extend from Buchans to Port aux Basques. Those in the study area are included in the Annieopsquotch ophiolite belt (Dunning, 1981).

The Complex is fault- bounded and is juxtaposed to the northwest with a foliated tonalite terrane of Ordovician age and to the southeast with the Victoria Lake Group. Rocks of both of these units intrude the ophiolitic rocks. The Complex is cut by two gabbro- diorite intrusions of late Ordovician age and a granitic intrusion of presumed Devonian age, and is unconformably overlain by terrestrial sedimentary and bimodal volcanic rocks of early Silurian age (Dunning and Herd, 1980; Chandler, 1982; Chandler and Dunning, 1983).

2. The Annieopsquotch Complex dips and faces southeast and exposes a cross- section through the ophiolite stratigraphy from the critical zone to the pillow

lava zone. The sheeted dyke zone extends the full length of the ophiolite and shows transitional contacts at both its base and top.

Other ophiolite fragments in the belt expose one or more of the zones but none contains a complete section.

3. The cross section through the magma chambers of the ophiolite provides an opportunity to observe many of the features of its igneous history. These include:

a. olivine- plagioclase- clinopyroxene cumulates which crystallized from the most primitive basaltic (or picritic!) melts and which show features such as isomodal and graded layering, dropped blocks, slump folds and trough structures indicative of currents and other processes active in magma chambers;

b. zones of fine- grained, equigranular metamorphic mafic rock near the base of the ophiolite, which provide evidence of metamorphism of blocks stoped from the roof and zones of amphibolite which formed by metamorphism of coarse- grained gabbro;

c. faults that cut at a high angle across the ophiolite stratigraphy and have gabbro or trondhjemite intruded along them, indicating that they were faults active im the oceanic realm;

d. texturally heterogeneous high-level plagioclase- clinopyroxene gabbros which locally crosscut other gabbros including rocks of the critical zone;

e. stoped rocks from the roof of the magma chamber which reacted with the melt to produce hybrid zones

leading to the generation of trondhjemite locally and magnetite- rich gabbro and diorite containing hydrous minerals elsewhere;

e. a transition zone at the top of the gabbro zone, through which the percentage of diabase dykes cutting gabbro rapidly increases and where irregular patches of fine- grained diabase occur, which are interpreted to be quenched pools of basaltic liquid in the root zone of the diabase dykes.

4. The sheeted dyke zone of the Annieopsquotch Complex is continuous over a strike length (90 degrees to strike of the dykes) of twenty km. It is composed overwhelmingly of diabase dykes, many of which are plagioclase- porphyritic. With few exceptions, they strike northwest- southeast and are steeply dipping. Examination of continuous sections approximately across strike does not appear to support the use of one- way chilled margins to indicate the direction of the paleo- spreading centre. However, since no statistical data were collected, a direct comparison with the work of Kidd and Cann (1974) is not possible.

Sheeted dyke zones in the ophiolitic fragments at Shanadithit Brook and King George IV Lake, the extreme ends of the Annieopsquotch ophiolite belt, are similar in composition and orientation to that of the Annieopsquotch Complex. This suggests that all the fragments may be remnants of a once continuous sheet, and that the intrusion of the tonalitic rocks did not severely displace the

fragments. However, there may be relative movement between those fragments west of the Lloyds River Fault and those to the east. If the entire sheet was not rotated during emplacement the dyke orientations further imply that the paleo- spreading ridge was oriented approximately northwest- southeast, ie; at a high angle to the interpreted continental margin of ancient North America.

5. The major, trace and REE geochemistry of diabase dykes and pillow lavas of the Annieopsquotch Complex and of the ophiolitic fragments analysed clearly indicate that they are of Normal-type MORB affinity. The chemistry of clinopyroxenes from the Annieopsquotch Complex is consistent with this interpretation.

Dykes and lavas from all fragments show the same trends on trace element variation diagrams, suggesting that they may all have formed at a single spreading centre. This is further support for item 4 above.

6. Two U/Pb (zircon) ages for trondhjemite pods within the Annieopsquotch Complex are 477.5 +1.3/-1.0 and 481.4 +4.0/-1.9 Ma, both late Arenigian (490- 475 Ma; van Eysinga, 1975). New U/Pb (zircon) ages for trondhjemite in the Bay of Islands Complex and gabbro in the Betts Cove Complex are 485.7 +1.9/-1.2 and 488.6 +3.1/-1.8 Ma, both early Arenigian. The former refutes latest Cambrian U/Pb (zircon) and Nd/Sm ages reported by Mattinson (1976) and Jacobsen and Wasserburg (1979) respectively. The latter refutes a U/Pb zircon age of 463 +/-6 Ma reported by Mattinson (1975) and confirms the Arenigian age determined

by Snelgrove (1931) from graptolites in the overlying Snooks Arm Group.

The new ages determined in this study are tightly clustered and closely comparable to those of the Ballantrae Complex, Scotland (483 +/-4 Ma; Bluck et al, 1980) and the M'Clintock West Massif, Canada (481 +7/-6 Ma; Trettin et al,1982). Two other Newfoundland ophiolites, the Lushes Bight Terrane and the Pipestone Pond Complex (495 +/-5 Ma; Stukas and Reynolds, 1974; 495 +/-3 Ma; Dunning and Krogh, 1983) are of Tremadocian age (500- 490 Ma; van Eysinga, 1975). These data imply that oceanic crust of only a limited age range is preserved in the Appalachian - Caledonian Mountain Belt.

7. The Victoria Lake Group (Kean, 1977), in part of Llanvirnian- Llandeilian age, is a sequence of isoclinally folded and faulted basalt, dacite, rhyolite and tuffaceous sandstone, siltstone and argillite that is poorly exposed to the east of the Annieopsquotch Complex.

The Group has generally been interpreted (cf. Kean et al, 1981) to be an island arc sequence and is correlated with volcanic sequences of the Dunnage Zone exposed in Notre Dame Bay. However, the bimodal nature of the volcanic rocks and the MORB- like chemistry of the basalts is puzzling and suggests a different derivation than that of an intra- oceanic island arc. It is suggested here that many of the basalts should be correlated with those of the Annieopsquotch Complex and the King George IV Lake ophiolitic fragment, as was first suggested by Fenton

(pers. comm.; 1979) based on field relationships alone. The abundance of felsic volcanic rocks suggests derivation by partial melting of a continental source. It is suggested that the Victoria Lake Group may have formed in a transitional tectonic setting and that the basalts and rhyolites may not have a common genesis.

8. Recent regional mapping has provided much new evidence with which to construct a model for the evolution of southwest Newfoundland. The recognition of a large number of ophiolitic fragments implies that very large allochthons of N-type MORB oceanic crust were emplaced over the continental margin outboard (to the present day east) of the Humber Arm Allochthon of the Humber Zone.

The large area of Ordovician foliated tonalitic rocks outlined, which intrude the ophiolitic fragments, indicates that magmatism at the oceanic- continental interface was an important process at approximately the time of the Taconic orogeny. The variable degrees of deformation of different tonalites suggests that plutonism continued throughout and indeed outlasted the Taconic deformation.

The recognition of ophiolitic fragments and probable Fleur de Lys sedimentary rocks together, intruded and included by the tonalitic rocks (similar to those included in the Dunnage Zone elsewhere in Newfoundland), suggests that the Dunnage Zone extends through southwest Newfoundland. The accumulating evidence suggests too that both zones are allochthonous over Precambrian continental crust.

REFERENCES

Abbey, S. 1980. Studies in "standard samples" for use in the general analysis of silicate rocks and minerals. Part 6: 1979 Edition of "usable" values. Geological Survey of Canada, Paper 80- 14, 30p.

Alabaster, T., Pearce, J.A. and Malpas, J. 1982. The volcanic stratigraphy and petrogenesis of the Oman ophiolite complex. Contributions to Mineralogy and Petrology, 81, pp. 168- 183.

Archibald, D.A. and Farrar, E. 1976. K-Ar ages of amphibolites from the Bay of Islands ophiolite and the Little Port Complex, western Newfoundland, and their geological implications. Canadian Journal of Earth Sciences, 13, pp.520-529.

Armstrong, R.L. 1978. Pre- Cenozoic Phanerozoic time scale- computer file of critical dates of new and in-progress decay constant revisions. In Contributions to the Geological Time Scale, G.V. Cohee, M.F. Glaessner and H.D. Hedberg, eds. American Association of Petroloeum Geologists, Studies in Geology, 6, pp. 73- 91.

Barker, F., Arth, J.G., Peterman, Z.E. and Friedman, I. 1976. The 1.7 to 1.8 b.y.- old trondhjemites of southeastern Colorado and northern New Mexico: Geochemistry and depths of genesis. Geological Society of America Bulletin, 87, pp. 189- 198.

Basaltic Volcanism Study Project. 1981. Basaltic volcanism on the terrestrial planets. Pergamon Press, Inc., New York. 1286p.

Bence, A.E. and Albee, A.L. 1968. Empirical correction factors for the electron microanalysis of silicates and oxides. Journal of Geology, 76,pp. 382- 403.

Best, M.A. 1982. Provenance study of two sedimentary successions in the King George IV Lake area, Newfoundland. University of Ottawa, B.Sc. thesis, 76p.

Blanchard, D.P., Rhodes, J.M., Dungan, M.A., Rodgers, K.V., Donaldson, C.H., Brannon, J.C., Jacobs, J.W. and Gibson, E.K. 1976. The chemistry and petrology of basalts from Leg 37 of the Deep - Sea Drilling Project. Journal of Geophysical Research, 81, pp.4231-4246.

Bluck, B.J., Halliday, A.N., Aftalion, M. and Macintyre, R.M. 1980. Age and origin of Ballantrae ophiolite

and its significance to the Caledonian orogeny and Ordovician time scale. Geology, 8, pp.492-495.

Brown, P.A. 1975. Basement - cover relationships in southwest Newfoundland. Memorial University of Newfoundland, Ph.D. thesis, 221p.

Brown, P.A. 1976. Ophiolites in south-western Newfoundland. Nature, 264, pp.712-715.

Bryan, W.B. 1979. Regional variation and petrogenesis of basalt glasses from the FAMOUS area, Mid - Atlantic Ridge. Journal of Petrology, 20, pp.293-325.

Bryan, W.B. 1983. Systematics of modal phenocryst assemblages in submarine basalts: petrologic implications. Contributions to Mineralogy and Petrology, 83, pp. 62-74.

Bryan, W.B. and Moore, J.G. 1977. Compositional variations of young basalts in the Mid - Atlantic Ridge rift valley near 36 degrees 49'N. Geological Society of America Bulletin, 88, pp.556-570.

Bryan, W.B., Thompson, G. and Ludden, J.N. 1981. Compositional variation in normal MORB from 22- 24 degrees N, Mid- Atlantic Ridge and Kane Fracture Zone. Journal of Geophysical Research, 86, pp.11815- 11836.

Carew, W. 1979. A layered appinitic intrusion in southwest Newfoundland: A field, petrographical and geochemical investigation. Memorial University of Newfoundland, B.Sc. thesis,53p. and map.

Casey, J.F. and Karson, J.A. 1981. Magma chamber profiles from the Bay of Islands ophiolite complex. Nature, 292, pp. 295- 301.

Casey, J.F. and Kidd, W.S.F. 1981. A parallochthonous group of sedimentary rocks unconformably overlying the Bay of Islands ophiolite complex, North Arm Mountain, Newfoundland. Canadian Journal of Earth Sciences,18, pp.1035-1050.

Chandler, F.W. 1982. Sedimentology of two middle Paleozoic terrestrial sequences, King George IV Lake area, Newfoundland and some comments on regional paleoclimate. In Current Research, Part A, Geological Survey of Canada Paper 82-1A, pp.213-219.

Chandler, F.W. and Dunning, G.R. 1983. Fourfold significance of an early Silurian U-Pb zircon age from rhyolite in redbeds, southwest Newfoundland, NTS 12A/4. In Current Research, Part B, Geological Survey of Canada Paper 83-1B, pp.419-421.

Chorlton, L.B. 1982. General geology and regional significance of the Grandys Lake area (110/15). In Current Research, Mineral Development Division, Newfoundland Department of Mines and Energy, Report 82-1, pp.65-77.

Chorlton, L.B. and Dingwell, D.B. 1981. Grandys Lake (110/15), Newfoundland. In Current Research, Mineral Development Division, Newfoundland Department of Mines and Energy, Report 81-1, pp. 57-69.

Chorlton, L.B. 1983. Geology of the Grandys Lake area (110/15), Newfoundland. Mineral Development Division, Newfoundland Department of Mines and Energy, Report 83-7, Part 1, 116p.

Church, W.R. 1976. Ages of zircons from the Bay of Islands ophiolite complex, western Newfoundland: Comment. Geology, 4, pp. 623-625.

Church, W.R. and Riccio, L. 1977. Fractionation trends in the Bay of Islands ophiolite of Newfoundland: polycyclic cumulate sequences in ophiolites and their classification. Canadian Journal of Earth Sciences, 14, pp.1156-1165.

Church, W.R. and Stevens, R.K. 1971. Early Paleozoic ophiolite complexes of the Newfoundland Appalachians as mantle- oceanic crust sequences. Journal of Geophysical Research, 76, pp.1460-1466.

Clarke, D.B. 1970. Tertiary basalts of Baffin Bay: possible primary magma from the mantle. Contributions to Mineralogy and Petrology, 25, pp. 203-224.

Coish, R.A. and Church, W.R. 1979. Igneous geochemistry of mafic rocks in the Betts Cove ophiolite, Newfoundland. Contributions to Mineralogy and Petrology, 20, pp.29-39.

Coish, R.A., Hickey, R. and Frey, F.A. 1982. Rare earth element geochemistry of the Betts Cove ophiolite, Newfoundland: complexities in ophiolite formation. Geochimica et Cosmochimica Acta, 46, pp.2117-2134.

Coleman, R.G. and Peterman, Z.E. 1975. Oceanic plagiogranite. Journal of Geophysical Research, 80, pp.1099-1108.

Colman-Sadd, S.P. 1981. Geology of the Burnt Hill map area (2D/5), Newfoundland. In Current Research, Mineral Development Division, Newfoundland Department of Mines and Energy, Report 81-1, pp.40-49.

Colman-Sadd, S.P. and Swinden, H.S. 1982. Geology and

mineral potential of south-central Newfoundland. Mineral Development Division, Newfoundland Department of Mines and Energy, Report 82-8, 102p.

Cook, F.A., Albaugh, D.S., Brown, L.D., Kaufman, S., Oliver, J.E. and Hatcher, R. 1979. Thin-skinned tectonics in the crystalline southern Appalachians: COCORP seismic reflection profiling of the Blue Ridge and Piedmont. Geology, 7, pp. 563-567.

Currie, K.L., Loveridge, W.D. and Sullivan, R.W. 1982. The Deadman's Bay pluton, northeastern Newfoundland; U-Pb study of zircon reveals a Grenvillian component. In Rb-Sr and U-Pb Isotopic Age Studies, Report 5, In Current Research, Part C, Geological Survey of Canada, Paper 82-1C, pp.119-124.

Dallmeyer, R.D. 1977. Diachronous ophiolite obduction in western Newfoundland: evidence from 40Ar/39Ar ages of the Hare Bay metamorphic aureole. American Journal of Science, 277, pp.61-72.

Dallmeyer, R.D. and Williams, H. 1975. 40Ar/39Ar ages for the Bay of Islands metamorphic aureole. Their bearing on the timing of Ordovician ophiolite obduction. Canadian Journal of Earth Sciences, 12, pp.1685-1690.

Davis, D.W. 1982. Optimum linear regression and error estimation applied to U-Pb data. Canadian Journal of Earth Sciences, 19, pp.2141-2149.

DeGrace, J.R. 1974. Notes on the geology of the King George IV Lake area, southwest central Newfoundland. In Report of Activities, 1973, Mineral Development Division, Newfoundland Department of Mines and Energy, pp.43-49.

Dickson, W.L. and Tomlin, S.L. 1983. Geology of the D'Espoir Brook map area and part of the Facheux Bay map area, south-central Newfoundland. In Current Research, Mineral Development Division, Newfoundland Department of Mines and Energy, Report 83-1, pp.51-56.

Dixon, S. and Rutherford, M.J. 1979. Plagiogranites as late-stage immiscible liquids in ophiolite and mid-ocean ridge suites: an experimental study. Earth and Planetary Science Letters, 45, pp.45-60.

Dixon, T.H. and Batiza, R. 1979. Petrology and chemistry of recent lavas in the northern Marianas: implications for the origin of island arc basalts. Contributions to Mineralogy and Petrology, 70, pp.167-181.

Dostal, J. and Muecke, G.K. 1978. Trace element geochemistry of the peridotite - gabbro - basalt suite from DSDP Leg 37. Earth and Planetary Science Letters, 40, pp.415-422.

Duncan, R.A. and Green, D.H. 1980. Role of multistage melting in the formation of oceanic crust. Geology, 8, pp.22- 26.

Dunning, G.R. 1981. The Annieopsquotch ophiolite belt, southwest Newfoundland. In Current Research, Part B, Geological Survey of Canada, Paper 81-1B, pp.11-15.

Dunning, G.R., Carter, P. and Best, M.A. 1982. Geology of Star Lake (west half), southwest Newfoundland. In Current Research, Part B, Geological Survey of Canada, Paper 82-1B, pp.21-26.

Dunning, G.R. and Chorlton, L.B. 1983. Imbricate ophiolite and subduction -related intrusions in southwest Newfoundland. Geological Society of America, Northeastern Section Meeting, Abstracts with Programs,p. 188.

Dunning, G.R. and Herd, R.K. 1980. The Annieopsquotch ophiolite complex southwest Newfoundland, and its regional relationships. In Current Research, Part A, Geological Survey of Canada, Paper 80-1A, pp.227-234.

Dunning, G.R. and Krogh, T.E. 1983. Tightly clustered, precise, U/Pb (zircon) ages of ophiolites from the Newfoundland Appalachians. Geolgical Society of America, Northeastern Section, Abstracts with Programs, p.136.

Easton, R.M. 1982. Tectonic significance of the Akaitcho Group, Wopmay Orogen, Northwest Territories, Canada. Memorial University of Newfoundland, Ph.D. Thesis, 432p.

Elthon, D. 1979. High magnesia liquids as the parental magma for ocean floor basalts. Nature, 278, pp. 514 -518.

Engel, A.E.J., Engel, C.G. and Havens, R.G. 1965. Chemical characteristics of oceanic basalts and the upper mantle. Geological Society of America Bulletin, 76, pp. 719- 734.

Epstein, R.S. 1983. The eastern margin of the Burlington Granodiorite, Newfoundland. The University of Western Ontario, M.Sc. Thesis, 188p.

Erlank, A.J. and Kable, E.J.D. 1976. The significance of incompatible elements in Mid- Atlantic Ridge basalts

from 45 degrees N, with particular reference to Zr/Nb. Contributions to Mineralogy and Petrology, 54, pp.281-291.

Fahraeus, L.E. 1973. Depositional environments and conodont-based correlation of the Long Point Formation (middle Ordovician), western Newfoundland. Canadian Journal of Earth Sciences, 10, pp. 1822-1833.

Flanagan, F.J. 1976. Description and analyses of eight new USGS rock standards. United States Geological Survey, Professional Paper 840, 192p.

Frey, F.A., Bryan, W.B. and Thompson, G. 1974. Atlantic Ocean Floor: Geochemistry and Petrology of Basalts from Legs 2 and 3 of the Deep Sea Drilling Project. Journal of Geophysical Research, 79, pp. 5507- 5527.

Frisch, T.O. 1974. Metamorphic and plutonic rocks of northernmost Ellesmere Island, Canadian Arctic Archipelago. Geological Survey of Canada, Bulletin 229, 87p.

Fryer, B.J. 1977. Rare-earth evidence in iron-formations for changing Precambrian oxidation states. Geochimica et Cosmochimica Acta, 41, pp.361-367.

Furnes, H., Roberts, D., Sturt, B.A., Thon, A. and Gale, G.H. 1980. Ophiolitic fragments in the Scandinavian Caledonides. In Ophiolites, Proceedings, International Ophiolite Symposium, Cyprus,pp.582-600.

Gale, G.H. and Pearce, J.A. 1982. Geochemical patterns in Norwegian greenstones. Canadian Journal of Earth Sciences,19,pp.385-397.

Gale, G.H. and Roberts, D. 1974. Trace element geochemistry of Norwegian Lower Paleozoic basic volcanics and its tectonic implications. Earth and Planetary Science Letters,22,pp.380-390.

Gast, P.W. 1968. Trace element fractionation and the origin of tholeiitic and alkaline magma types. Geochimica et Cosmochimica Acta, 32, pp. 1057- 1086.

Gaudette, H.E. 1981. Zircon isotopic age from the Union ultramafic complex, Maine. Canadian Journal of Earth Sciences,18,pp.405-409.

Girardeau, J. and Nicolas, A. 1981. Structures in two of the Bay of Islands (Newfoundland) ophiolite massifs: a model for oceanic crust and upper mantle. Tectonophysics, 77, pp. 1-34.

Green, D.H. and Ringwood, A.E. 1967. The genesis of

basaltic magmas. Contributions to Mineralogy and Petrology, 15, pp. 103- 190.

Gregory, R.T. and Taylor, H.P. Jr. 1979. Oxygen isotope and field studies applied to the origin of oceanic plagiogranite. In International Ophiolite Symposium, Geological Survey Department, Nicosia, Cyprus, Abstracts of Papers Submitted, p.117.

Hart, S.R. and Davis, K.E. 1978. Nickel partitioning between olivine and silicate melt. Earth and Planetary Science Letters, 40, pp.203- 219.

Hellman, P.L., Smith, R.E. and Henderson, P. 1977. Rare earth element investigation of the Cliefden outcrop, N.S.W. Australia. Contributions to Mineralogy and Petrology, 65, pp.155- 164.

Herd, R.K. 1978. Geology of Puddle Pond area, Red Indian Lake map - sheet, Newfoundland. In Current Research, Part A, Geological Survey of Canada, Paper 78 - 1A, pp.195-197.

Herd, R.K. and Dunning, G.R. 1979. Geology of Puddle Pond map area, southwestern Newfoundland. In Current Research, Part A, Geological Survey of Canada, Paper 79-1A, pp.305-310.

Herrmann, A.G., Potts, M.J. and Knake, D. 1974. Geochemistry of the rare earth elements in spilites from the oceanic and continental crust. Contributions to Mineralogy and Petrology, 44, pp. 1- 16.

Hibbard, J., Compiler. 1983. Geology of the island of Newfoundland. Mineral Development Division, Newfoundland Department of Mines and Energy. Map 83-106.

Hibbard, J. in press. Geology of the Baie Verte Peninsula, Newfoundland. Newfoundland Department of Mines and Energy, Memoir Series.

Ingerson, F.E. 1935. Layered peridotitic lacoliths of the Trout River area, Newfoundland. American Journal of Science, 29, pp.422- 440.

Irvine, T.N. 1970. Crystallization sequences in the Muskox Intrusion and other layered intrusions, I. Olivine-pyroxene-plagioclase relations. Geological Society of South Africa, Special Publication 1, pp.441-476.

Irvine, T.N. 1982. Terminology for layered intrusions. Journal of Petrology, 23, pp.127-162.

Irvine, T.N. and Baragar, W.R.A. 1971. A guide to the chemical classification of the common volcanic rocks. Canadian Journal of Earth Sciences, 8,pp. 523- 548.

Jackson, E.D. 1967. Ultramafic cumulates in the Stillwater, Great Dyke and Bushveld intrusions. In Ultramafic and Related Rocks, P.J. Wyllie,ed., pp.20-38.

Jacobsen, S.B. and Wasserburg, G.J. 1979. Nd and Sr isotopic study of the Bay of Islands ophiolite complex and the evolution of the source of mid- ocean ridge basalts. Journal of Geophysical Research, 84, pp.7429-7445.

Jakes, P. and Gill, J. 1970. Rare earth elements and the island arc tholeiite series. Earth and Planetary Science Letters, 9, pp. 29- 33.

Jamieson, R.A. 1982. Metamorphism during ophiolite emplacement - the petrology of the St. Anthony Complex. Journal of Petrology, 22, pp. 397- 449.

Jenner, G.A. and Fryer, B.J. 1980. Geochemistry of the upper Snooks Arm Group basalts, Burlington Peninsula, Newfoundland: evidence against formation in an island arc. Canadian Journal of Earth Sciences, 17, pp.888-900.

Karlstrom, K.E. 1983. Reinterpretation of Newfoundland gravity data and arguments for an allochthonous Dunnage Zone. Geology, 11, pp.263-266.

Karson, J. and Dewey, J.F. 1978. Coastal Complex, western Newfoundland: An Early Ordovician oceanic fracture zone. Geological Society of America Bulletin, 89, pp.1037-1049.

Kay, R.W. and Senechal, R.G. 1976. The rare earth element geochemistry of the Troodos ophiolite complex. Journal of Geophysical Research, 81, pp.964- 970.

Kean, B.F. 1977. Geology of the Victoria Lake map area (12A/6), Newfoundland. Mineral Development Division, Newfoundland Department of Mines and Energy, Report 77-4, 11p.

Kean, B.F. 1983. Geology of the King George IV Lake map area (12A/4). Mineral Development Division, Newfoundland Department of Mines and Energy, Report 83-4,67p.

Kean, B.F., Dean, P.L. and Strong, D.F. 1981. Regional geology of the Central Volcanic Belt of Newfoundland. In The Buchans Orebodies: Fifty Years of Geology and

Mining, E.A. Swanson, D.F. Strong and J.G. Thurlow eds., Geological Association of Canada, Special Paper 22, pp.65-78.

Kean, B.F. and Jayasinghe, N.R. 1980. Geology of the Lake Ambrose (12A/10) - Noel Paul's Brook (12A/9) map areas, Central Newfoundland. Newfoundland Department of Mines and Energy, Mineral Development Division, Report 80-2, 29p.

Kean, B.F. and Strong, D.F. 1975. Geochemical evolution of an Ordovician island arc of the central Newfoundland Appalachians. American Journal of Science, 205, pp. 97- 118.

Kennedy, D.P.S. 1982. Geology of the Corner Brook Lake area, western Newfoundland. M.Sc. thesis, Memorial University of Newfoundland. 370p.

Kidd, R.G.W. 1977. A model for the process of formation of the upper oceanic crust. Geophysical Journal of the Royal Astronomical Society, 50, pp.149-183.

Kidd, R.G.W. and Cann, J.R. 1974. Chilling statistics indicate an ocean floor spreading origin for the Troodos Complex, Cyprus. Earth and Planetary Science Letters, 24, pp.515-555.

Krogh, T.E. 1973. A low contamination method for hydrothermal decomposition of zircon and extraction of U and Pb for isotopic age determinations. Geochimica et Cosmochimica Acta, 37, pp.485-494.

Krogh, T.E. 1982. Improved accuracy of U-Pb zircon ages by the creation of more concordant systems using an air abrasion technique. Geochimica et Cosmochimica Acta, 46, pp.637-649.

Krogh, T.E. and Davis, G.L. 1975. The production and preparation of 205Pb for use as a tracer for isotope dilution analyses. Carnegie Institute of Washington Yearbook, 74, pp.416-417.

Krogh, T.E. and Turek, A. 1982. Precise U-Pb zircon ages from the Gamitagama greenstone belt, southern Superior Province. Canadian Journal of Earth Sciences, 19, pp.859-867.

Kushiro, I. 1960. Si-Al relation in clinopyroxenes from igneous rocks. American Journal of Science, 258, pp.548-554.

Kushiro, I. 1968. Compositions of magmas formed by partial zone melting of the earth's upper mantle. Journal of Geophysical Research, 73, pp. 619- 634.

Langmuir, C.H., Bender, J.F., Bence, A.E. and Hanson, G.N. 1977. Petrogenesis of Basalts from the FAMOUS area: Mid- Atlantic Ridge. Earth and Planetary Science Letters, 36, pp. 133- 156.

LeBas, M.J. 1962. The role of aluminium in igneous clinopyroxenes with relation to their parentage. American Journal of Science, 260, pp.267-288.

Leeman, W.P., Budahn, J.R., Gerlach, D.C., Smith, D.R. and Powell, B.N. 1980. Origin of Hawaiian tholeiites: Trace element constraints. American Journal of Science, 280A, pp. 794-819.

LeRoex, A.P., Dick, H.J.B., Erlank, A.J., Reid, A.M., Frey, F.A. and Hart, S.R. 1983. Geochemistry, mineralogy and petrogenesis of lavas erupted along the southwest Indian Ridge, between the Bouvet triple junction and 11 degrees east. Journal of Petrology, 24, pp.267-318.

Leterrier, J., Maury, R.C., Thonon, P., Girard, D. and Marchal, M. 1982. Clinopyroxene composition as a method of identification of the magmatic affinities of paleo-volcanic series. Earth and Planetary Science Letters, 59, pp.139-154.

Lorenz, B.L. and Fountain, J.C. 1982. The South Lake Igneous Complex, Newfoundland: a marginal basin-island arc association. Canadian Journal of Earth Sciences, 19, pp.490-503.

Ludden, J.N. and Thompson, G. 1979. An evaluation of the behavior of the rare earth elements during the weathering of sea floor basalt. Earth and Planetary Science Letters, 43, pp.85-92.

Malpas, J.G. 1976. The geology and petrogenesis of the Bay of Islands ophiolite suite, W. Newfoundland (2 parts). Memorial University of Newfoundland, Ph.D. thesis, 435 p.

Malpas, J. 1978. Magma generation in the upper mantle, field evidence from ophiolite suites, and application to the generation of oceanic lithosphere. Philosophical Transactions of the Royal Society of London, Series A, 288, pp. 527- 546.

Malpas, J. 1979a. Two contrasting trondhjemite associations from transported ophiolites in western Newfoundland: initial report. In Trondhjemites, Dacites and Related Rocks, Chapter 15, F. Barker ed. Developments in Petrology 6. Elsevier, Amsterdam, pp.465-487.

Malpas, J. 1979b. The dynamothermal aureole of the Bay of Islands ophiolite suite. Canadian Journal of Earth Sciences, 16, pp.2086-2101.

Malpas, J., Stevens, R.K. and Strong, D.F. 1973. Amphibolite associated with Newfoundland ophiolite: its classification and tectonic significance. Geology, 1, pp. 45- 47.

Malpas, J. and Strong, D.F. 1975. Comparison of Cr - spinels from ophiolites and mantle diapirs of Newfoundland. Geochimica et Cosmochimica Acta, 39, pp. 1045- 1060.

Mattinson, J.M. 1975. Early Paleozoic ophiolite complexes of Newfoundland: Isotopic ages of zircons. Geology, 3, pp.181-183.

Mattinson, J.M. 1976. Ages of zircons from the Bay of Islands ophiolite complex, western Newfoundland. Geology, 4, pp.393-394.

Mattinson, J.M. 1977. U-Pb ages of some crystalline rocks from the Burlington Peninsula, Newfoundland, and implications for the age of Fleur de Lys metamorphism. Canadian Journal of Earth Sciences, 14, pp.2316-2324.

McBirney, A.R. and Noyes, R.M. 1979. Crystallization and layering of the Skaergaard Intrusion. Journal of Petrology, 20, pp.487-554.

McKerrow, W.S., Lambert, R.St.J. and Chamberlain, V.E. 1980. The Ordovician, Silurian and Devonian Time Scales. Earth and Planetary Science Letters, 51, pp.1-8.

Menzies, M., Blanchard, D. and Jacobs, J. 1977. Rare earth and trace element geochemistry of metabasalts from the Point Sal Ophiolite, California. Earth and Planetary Science Letters, 37, pp. 203- 213.

Miller, H.G. and Deutsch, E.R. 1976. New gravitational evidence for the subsurface extent of oceanic crust in north - central Newfoundland. Canadian Journal of Earth Sciences, 13, pp.459-469.

Moores, E.M. and Vine, F.J. 1971. The Troodos Massif, Cyprus and other ophiolites as oceanic crust : evaluation and implications. Philosophical Transactions of the Royal Society of London,A, 268, pp. 443-466.

Mottl, M.J. 1983. Metabasalts, axial hot springs, and the structure of hydrothermal systems at mid-ocean ridges. Geological Society of America Bulletin, 94, pp.

161-180.

Nisbet, E.G. and Pearce, J.A. 1977. Clinopyroxene composition in mafic lavas from different tectonic settings. Contributions to Mineralogy and Petrology, 63, pp. 149-160.

Norman, R.E. and Strong, D.F. 1975. Geology and Geochemistry of ophiolitic rocks exposed at Ming's Bight, Newfoundland. Canadian Journal of Earth Sciences, 12, pp. 777-797.

Nur, A. and Ben-Avraham, Z. 1982. Oceanic plateaus, the fragmentation of continents and mountain building. Journal of Geophysical Research, 87, pp. 3644- 3661.

O'Hara, M.J. 1965. Primary magmas and the origin of basalts. Scottish Journal of Geology, 1, pp. 19- 40.

O'Hara, M.J. 1977. Geochemical evolution during fractional crystallization of a periodically refilled magma chamber. Nature, 266, pp. 503-507.

O'Hara, M.J. 1982. MORB - A mohole misbegotten ? EOS, June 15, p.537.

Orcutt, J.A., Kenneth, B.L.N. and Dorman, L.M. 1975. Structure of the East Pacific Rise from an ocean bottom seismometer survey. Geophysical Journal of the Royal Astronomical Society, 45, pp. 305-320.

Osborn, E.F. and Tait, D.B. 1952. The system diopside - forsterite - anorthite. American Journal of Science, Bowen Volume, pp. 413-433.

Papike, J.J. 1980. Pyroxene mineralogy of the moon and meteorites. In Reviews in Mineralogy,7, Pyroxenes, Chapter 10, P.H. Ribbe ed., Mineralogical Society of America, Washington, D.C., pp. 495- 525.

Pearce, J.A. 1975. Basalt geochemistry used to investigate past tectonic environments on Cyprus. Tectonophysics, 25, pp. 41- 67.

Pearce, J.A. 1980. Geochemical evidence for the genesis and eruptive setting of lavas from Tethyan ophiolites. In Ophiolites, Proceedings, International Ophiolite Symposium, Cyprus, pp. 261-272.

Pearce, J.A. and Cann, J.F. 1973. Tectonic setting of basic volcanic rocks determined using trace element analyses. Earth and Planetary Science Letters, 19, pp. 290- 300.

Pearce, J.A. and Norry, M.J. 1979. Petrogenetic

implications of Ti, Zr, Y and Nb variations in volcanic rocks. Contributions to Mineralogy and Petrology, 69, pp. 33- 47.

Pearce, T. Gorman, B.E. and Birkett, J.C. 1975. The TiO2 - K20 - P205 diagram; a method of discriminating between oceanic and non- oceanic basalts. Earth and Planetary Science Letters, 24, pp. 419- 426.

Pedersen, R.B.S. 1982. The Karmoy ophiolite plutonic suite. Can. Real. thesis, University of Bergen, 419p.

Penrose Field Conference Participants. 1972. Ophiolites. Geotimes, 17, pp. 24- 25.

Perfit, M.R., Gust, D.A., Bence, A.E., Arculus, R.J. and Taylor, S.R. 1980. Chemical characteristics of island-arc basalts: implications for mantle sources. Chemical Geology, 30, pp. 227-256.

Presnall, D.C. 1979. Generation of mid- ocean ridge tholeiites. Journal of Petrology, 20, pp.3- 35.

Ramsay, J.G. 1967. Folding and fracturing of rocks. McGraw- Hill Company, New York, 568p.

Riccio, L. 1976. Stratigraphy and petrology of the peridotite - gabbro component of the western Newfoundland ophiolites. University of Western Ontario, Ph.D. Thesis, 265p.

Riley, G.C. 1957. Red Indian Lake (west half), Newfoundland. Geological Survey of Canada, Map 8 - 1957.

Robertson, A.H.F. and Fleet,A.J. 1976. The origins of rare earths in metalliferous sediments of the Troodos Massif, Cyprus. Earth and Planetary Science Letters, 28, pp. 385-394.

Rodgers, J. 1965. Long Point and Clam Bank Formations, western Newfoundland. Proceedings, Geological Association of Canada, 16, pp. 83-94.

Rodgers, J. and Neale, E.R.W. 1963. Possible 'Taconic' klippen in western Newfoundland. American Journal of Science, 261, pp. 713- 730.

Rosencrantz, E. 1983. The structure of sheeted dykes and associated rocks in North Arm Massif, Bay of Islands ophiolite complex, and the intrusive process at oceanic spreading centers. Canadian Journal of Earth Sciences, 20, pp. 787- 801.

Ross Jr., R.J., Naeser, C.W. and Lambert, R. St. J. 1978. Ordovician Geochronology. In Contributions to the Geological Time Scale, Studies in Geology,6, American Association of Petroleum Geologists, pp. 347-354.

Rothery, D.A. 1983. The base of a sheeted dyke complex, Oman ophiolite: implications for magma chambers at oceanic spreading axes. Journal of the Geological Society of London, 140, pp. 287-296.

Saunders, A.D. and Tarney, J. 1979. The geochemistry of basalts from a back-arc spreading centre in the Scotia Sea. Geochimica et Cosmochimica Acta, 43, pp. 555-572.

Sen, G. 1982. Composition of basaltic liquids generated from a partially depleted lherzolite at 9 kbar pressure. Nature, 299, pp. 336- 338.

Serri, G. 1981. The petrochemistry of ophiolite gabbroic complexes: a key for the classification of ophiolites into low-Ti and high-Ti types. Earth and Planetary Science Letters, 52, pp. 203- 212.

Shido, F., Miyashiro, A. and Ewing, M. 1971. Crystallization of abyssal tholeiites. Contributions to Mineralogy and Petrology, 31, pp. 251- 266.

Sinton, M.J. and Byerly, G.R. 1980. Silicic differentiates of abyssal oceanic magmas: evidence for late- magmatic vapor transport of potassium. Earth and Planetary Science Letters, 47, pp. 423-430.

Smewing, J.D. 1981. Mixing characteristics and compositional differences in mantle- derived melts beneath spreading axes: evidence from cyclically layered rocks in the ophiolite of north Oman. Journal of Geophysical Research, 86, pp.2645- 2659.

Snelgrove, A.K. 1931. Geology and ore deposits of the Betts Cove - Tilt Cove area, Notre Dame Bay, Newfoundland. Canadian Mining and Metallurgical Bulletin, 24, pp. 477- 519.

Sparks, R.S.J., Meyer, P. and Sigurdsson, H. 1980. Density variation amongst mid- ocean ridge basalts: implications for magma mixing and the scarcity of primitive lavas. Earth and Planetary Science Letters, 46, pp. 419- 430.

Stacey, J.S. and Kramers, J.D. 1975. Approximation of terrestrial lead isotope evolution by a two-stage model. Earth and Planetary Science Letters, 26, pp.

207-221.

Steiger, R.H. and Jager, E. 1977. Subcommission on Geochronology: Convention on the use of decay constants in geo- and cosmochronology. Earth and Planetary Science Letters, 36, pp. 359- 362.

Stern, C. 1979. Open and closed system igneous fractionation within two Chilean ophiolites and the tectonic implication. Contributions to Mineralogy and Petrology, 68, pp. 243- 258.

Stern, C. and de Wit, M.J. 1980. The role of spreading centre magma chambers in the formation of Phanerozoic oceanic crust: Evidence from Chilean ophiolites. In Ophiolites, Proceedings, International Ophiolite Symposium, Cyprus, pp. 497- 506.

Stevens, R.D., Delabio, R.N. and Lachance, G.R. 1982. Age determinations and geological studies. K-Ar isotopic ages, Report 16. Geological Survey of Canada, Paper 82-2, 48p.

Stevens, R.K. 1970. Cambro-Ordovician flysch sedimentation and tectonics in western Newfoundland and their possible bearing on a proto-Atlantic ocean. Geological Association of Canada, Special Paper No.7, pp.165-177.

Stolper, E. 1980. A phase diagram for mid- ocean ridge basalts: Preliminary results and implications for petrogenesis. Contributions to Mineralogy and Petrology, 74, pp.13- 27.

Stolper, E. and Walker, D. 1980. Melt density and the average composition of basalt. Contributions to Mineralogy and Petrology, 74, pp. 7- 12.

Strong, D.F. 1972. Ordovician sea-floor spreading in northern Newfoundland. Geological Society of America, Abstracts with Program, 4, no.1; pp. 47- 48.

Strong, D.F. 1973. Lushes Bight and Roberts Arm Groups of central Newfoundland: possible juxtaposed oceanic and island arc volcanic suites. Geological Society of America Bulletin, 84, pp.3917-3928.

Strong, D.F. 1975. Plateau lavas and diabase dykes of northwestern Newfoundland. Geological Magazine, 111, pp.501-514.

Stukas, V. and Reynolds, P.H. 1974a. 40Ar/39Ar dating of the Long Range dikes, Newfoundland. Earth and Planetary Science Letters, 22, pp.256-266.

Stukas, V. and Reynolds, P.H. 1974b. 40Ar/39Ar dating of the Brighton gabbro complex, Lushes bight terrane, Newfoundland. Canadian Journal of Earth Sciences, 11, pp.1485-1488.

Sturt, B.A., Thon, A. and Furnes, H. 1980. The geology and preliminary geochemistry of the Karmoy ophiolite, S.W. Norway. In Ophiolites, Proceedings, International Ophiolite Symposium, Cyprus, pp.538-554.

Suen, C.J., Frey, F.A. and Malpas, J. 1979. Bay of Islands ophiolite suite, Newfoundland: Petrologic and geochemical characteristics with emphasis on rare earth element geochemistry. Earth and Planetary Science Letters, 45, pp.337-348.

Sun, S.S. and Nesbitt, R.W. 1978. Geochemical regularities and genetic significance of ophiolitic basalts. Geology, 6, pp.689-693.

Swinden, H.S. and Collins, W.T. 1982. Geology and economic potential of the Great Burnt Lake area, Newfoundland. In Current Research, Mineral Development Division, Newfoundland Department of Mines and Energy, Report 82-1, pp.188-207.

Swinden, H.S. and Thorpe, R.I. in press. Variations in style of volcanism and massive sulfide deposition in Early-Middle Ordovician island arc sequences of the Newfoundland central mobile belt. Economic Geology, Special Issue.

Takahashi, E. and Kushiro, I. 1983. Melting of a dry peridotite at high pressures and basalt magma genesis. American Mineralogist, 68, pp. 859- 879.

Talkington, R.W. and Gaudette, H.E. 1983. Geology, petrogenesis and tectonic history of the Union Igneous Complex, Maine. Geological Society of America, Northeastern Section Meeting, Abstracts with Programs, p.188.

Taylor, S.R. and Gorton, M.P. 1977. Geochemical application of spark source mass spectrometry-III. Element sensitivity, precision and accuracy. Geochimica et Cosmochimica Acta, 41, pp.1375-1380.

Thirlwall, M.F., Bluck, B.J. and Leggett, J.K. 1982. Sm-Nd isotope geochemistry of early Ordovician basalts, southern Scotland, and the origin of the Ballantrae ophiolite. In Ophiolites and oceanic lithosphere, Geological Society of London, Abstract Volume, p.27.

Thurlow, J.G. 1981. Geology, ore deposits and applied

rock geochemistry of the Buchans Group, Newfoundland. Ph.D. thesis, Memorial University of Newfoundland, 305p.

Trettin, H.P. 1982. Innuitian Orogen and Arctic Platform. In Perspectives in Regional Geological Syntheses. D-NAG Special Publication 1, Geological Society of America, A.R. Palmer, ed., pp.49-55.

Trettin, H.P. and Balkwill, H.R. 1979. Contributions to the tectonic history of the Innuitian Province, Arctic Canada. Canadian Journal of Earth Sciences, 16, pp.748-769.

Trettin, H.P., Loveridge, W.D. and Sullivan, R.W. 1982. U-Pb ages on zircon from the M'Clintock West Massif and the Markham Fiord Pluton, northernmost Ellesmere Island. In Current Research, Part C, Geological Survey of Canada, Paper 82-1C, pp.161-166.

Upadhyay, H.D. 1973. The Betts Cove ophiolite and related rocks of the Snooks Arm Group, Newfoundland. Memorial University of Newfoundland, Ph.D. thesis, 224p.

van Eysinga, F.W.B. 1975. Geological Time Table, 3rd. Edition. Elsevier Publishing Company, 1978.

Walker, D. and DeLong, S.E. 1982. Soret separation of mid- ocean ridge basalt magma. Contributions to Mineralogy and Petrology, 3, pp. 231- 240.

Walker, D., Shibata, T. and DeLong, S.E. 1979. Abyssal tholeiites from the Oceanographer Fracture Zone II. Phase equilibria and mixing. Contributions to Mineralogy and Petrology, 70, pp. 111-125.

Wanless, R. and Poole, W.H. 1980. Rb-Sr age of granitic rocks in ophiolite, Thetford Mines-Black Lake area, Quebec. In Current Research, Part C, Geological Survey of Canada, Paper 80-1C, pp.181-184.

Webb, G.W. 1969. Paleozoic wrench faults in Canadian Appalachians. In North Atlantic Geology and Continental Drift. M. Kay ed., American Association of Petroleum Geologists Memoir 12, pp. 754- 788.

Wells, P.R.A. 1977. Pyroxene thermometry in simple and complex systems. Contributions to Mineralogy and Petrology, 62, pp.129-139.

Whitford, D.J., Nicholls, I.A. and Taylor, S.R. 1979. Spatial variations in the geochemistry of Quaternary lavas across the Sunda Arc in Java and Bali. Contributions to Mineralogy and Petrology, 70, pp. 341- 356.

Williams, H. 1972. Bay of Islands, Newfoundland. Geological Survey of Canada, Map 1355A.

Williams, H. 1973. Bay of Islands, Newfoundland. Geological Survey of Canada, Paper 72- 34.

Williams, H. 1978. Tectonic Lithofacies Map of the Appalachian Orogen. Memorial University of Newfoundland, Map No. 1.

Williams, H. 1979. Appalachian Orogen in Canada. Canadian Journal of Earth Sciences,16, pp.792-807.

Williams, H. and Malpas, J.G. 1972. Sheeted dikes and brecciated dike rocks within transported igneous complexes, Bay of Islands, western Newfoundland. Canadian Journal of Earth Sciences, 9, pp. 1216-1229.

Williams, H. - Mattinson, J.M. 1975. Early Paleozoic ophiolite complexes of Newfoundland: Isotopic ages of zircons: Comment and Reply. Geology, 3, p.479.

Williams, H. and Smyth, W.R. 1973. Metamorphic aureoles beneath ophiolite suites and alpine peridotites: tectonic implications with west Newfoundland examples. American Journal of Science, 273, pp.594-621.

Wilton, D.H.C. 1983. Metallogenic, tectonic and geochemical evolution of the Cape Ray Fault Zone with emphasis on electrum mineralization. Ph.D. thesis, Memorial University of Newfoundland, 618p.

Winkler, H.G.F. 1979. Petrogenesis of Metamorphic Rocks. Fifth Edition, Springer - Verlag, New York. 348 p.

Wood, D.A., Tarney, J., Varet, J., Saunders, A.D., Bourgault, H., Joron, J.L., Treuil, M. and Cann, J.R. 1979. Geochemistry of basalts drilled in the North Atlantic by IPOD Leg 49: Implications for mantle heterogeneity. Earth and Planetary Science Letters, 42, pp. 77- 97.

APPENDIX 1

Petrographic Tables

Critical Zone

Sample Number	Plagioclase	Olivine	Orthopyroxene	Clinopyroxene	Hornblende	Cummingtonite	Trem/Actin.	Biotite	Musc/Sericite	Chlorite	Serpentine	Epid/Zois.	Albite	Carbonate	K-feldspar	Quartz	Spinel	Magnetite	Sphene	Pyrite	Zircon	Apatite	Prehnite	Talc/Iddings.
78HPAD201-1	X		X	X		X	X			X		X						X						
202-1	X	X		X			X				X						X	X						
209	X	X	X	X		X	-				X	X												
212-2	X	X	X	X	X	X	X	X		X	X	X						X	X					
79HPAD015-2	X	X	X	X		X					X						X	X						
016-2	X	X	X	X	X	X	X			X	X							X						
019-1	X	X		X		X	X				X						X	X	X					X
025-2	X	X	X	X		X							X				X	X						
026-1	X			X		X	X					X						X						
026-2	X			X		X	X					X	X					X	X					
027-1	X			X			X					X	X					X	X					
031-4	X			X	X							X						X						
032-3	X		X	X			X					X	X					X						
032-5	X			X								X							X					
032-6	X			X						X		X							X					

Sample	Pl	Ol	Or	Cl	Ho	Cu	Tr	Bi	Mu	Ch	Se	Ep	Al	Ca	Ks	Qu	Sp	Ma	Sph	Py	Zi	Ap	Pr	Ta
79HPAD035-1	X			X	X	X	X			X		X							X					X
038-2	X	X		X		X	X				X	X	X				X	X						X
039-1	X	X	X		X		X				X	X					X	X						
040-2	X		X			X	X					X		X				X	X					X
046-1	X	X		X							X	X						X						
047-2	X	X	X	X								X												
049-1	X			X	X	X					X	X					X	X						X
066-1	X	X	X	X	X	X					X	X	X				X	X						X
068-1		X	X	X							X						X	X						X
079-3	X	X	X	X			X			X	X	X	X					X	X					X
080-2	X	X	X	X		X	X				X		X				X	X						X
081-1	X	X		X	X		X				X	X						X						X
082-4	X	X	X	X	X		X			X	X	X												
084-2	X	X	X	X	X					X		X						X						
248-1	X					X	X			X							X	X						
262-3	X								X					X										
263-3	X	X		X		X	X				X	X						X						
263-4	X	X	X	X		X					X							X						
265-4	X						X					X												
265-5	X	X		X	X	X					X						X	X						X
269-3	X	X	X	X		X					X						X	X						X
272-2	X	X		X			X				X							X						X
276-1	X			X	X		X					X	X					X						
276-2	X	X	X	X	X						X						X	X						
280-3	X	X	X	X		X					X	X					X	X						X

Gabbro Zone

Sample	Pl	Ol	Or	Cl	Ho	Cu	Tr	Bi	Mu	Ch	Se	Ep	Al	Ca	Ks	Qu	Sp	Ma	Sph	Py	Zi	Ap	Pr	Ta
78HPAD187	X			X	X		X					X						X						
188-1	X					X	X					X						X		X				
188-2	X				X							X						X	X					
189-1	X				X		X			X		X		X				X						
189-3	X		X	X	X	X	X			X			X				X	X						
190	X			X			X					X						X		X				
191-1	X				X		X			X								X						
192	X			X	X							X		X				X	X	X				
195	X			X			X			X		X						X						
196	X		X	X	X		X			X		X						X		X				
201-2	X				X					X		X		X				X						
202-3	X				X							X												Amphibolite
202-4	X				X	X				X		X						X	X					
203	X	X	X	X			X				X	X						X						X
206	X			X	X	X						X				X				X		X		Diorite
207	X				X							X						X		X		X		Diorite
208-1	X		X	X	X	X												X		X				Diorite
212-1	X				X			X	X	X		X						X	X	X				
79HPAD001-3	X	X	X	X	X						X	X	X				X	X						
005	X	X		X		X	X			X	X							X	X				X	
013-1	X			X			X					X						X	X					
023-1	X			X	X		X					X						X						
80HPAD054-2	X				X					X		X						X				X		

Sample	Pl	Ol	Or	Cl	Ho	Cu	Tr	Bi	Mu	Ch	Se	Ep	Al	Ca	Ks	Qu	Sp	Ma	Sph	Py	Zi	Ap	Pr	Ta
Gabbro Zone																								
80HPAD129-1	X				X		X					X		X				X	X		X			
130-2	X			X	X		X					X	X					X						
223-2	X			X	X		X					X	X					X	X		X		Diorite	
Trondhjemites																								
78HPAD191-2	X				X					X		X						X	X		X			
79HPAD003-1	X						X					X				X			X					
020-3	X											X						X						
067-2	X						X		X	X		X				X			X		X	X	X	
145-1	X				X		X					X	X			X		X	X		X			
163-2	X						X			X		X				X			X					
196-1	X									X		X				X		X	X			X		
212-2	X						X					X			X	X		X	X		X			
248-4	X						X					X			X	X			X		X			
250	X						X					X							X		X			
80HPAD222	X				X		X					X	X					X			X		U-Pb age	
223-1	X				X		X	X		X		X	X			X		X			X	X	U-Pb age	
Sheeted Dyke Zone																								
78HPAD168-1	X			X			X		X	X		X						X						
168-2	X			X			X		X	X		X						X		X				
168-4	X			X	X		X		X	X		X						X						
169-1	X			X						X		X							X	X				
169-2	X			X			X			X		X						X						
170	X			X	X		X					X	X					X	X					

Sheeted Dyke Zone

Sample	Pl	Ol	Or	Cl	Ho	Cu	Tr	Bi	Mu	Ch	Se	Ep	Al	Ca	Ks	Qu	Sp	Ma	Sph	Py	Zi	Ap	Pr	Ta	
78HPAD171-1	X				X		X					X						X							
171-2	X			X	X		X					X		X				X							
172	X				X		X		X			X						X							
173	X				X		X					X						X							
174	X			X	X				X			X						X							
176	X			X	X		X			X		X						X	X	X					
177	X			X	X		X			X		X						X							
179	X			X	X					X		X						X	X	X					
180	X			X			X			X		X						X							
181-1	X				X		X					X						X							
181-2	X			X			X					X						X	X						
182	X				X		X			X		X						X							
183	X				X		X					X						X	X	X					
184	X			X			X					X						X							Lithic fragments
185	X				X		X					X						X	X	X					
186	X			X	X							X						X	X	X					
193	X			X	X		X					X						X							Lithic fragments
194	X				X		X					X						X							
197	X			X	X		X					X						X		X					
198	X			X	X							X						X		X					
199	X									X		X		X						X					
200-1	X			X			X			X		X				X		X							
200-2	X			X			X			X		X						X							

Sheeted Dyke Zone

Sample	Pl	Ol	Or	Cl	Ho	Cu	Tr	Bi	Mu	Ch	Se	Ep	Al	Ja	Ks	Qu	Sp	Ma	Sph	Py	Zi	Ap	Pr	Ta
78HPAD201-3	X				X		X			X		X						X						
202-2	X				X							X												
79HPAD107-2	X						X			X		X						X						
108-3	X			X			X			X		X						X						
109-2	X			X			X					X						X	X					
162	X			X			X					X						X	X					
201									X	X				X		X								
237	X				X		X					X						X						
238-2	X						X		X			X						X						
240	X				X		X			X		X				X		X						
241	X				X		X					X		X		X		X						
289	X			X			X					X						X	X					
80HPAD081	X						X					X						X	X					
086-2	X				X		X					X						X						
119	X				X							X						X	X					
122	X				X							X						X	X					
81HPAD114-2	X			X			X			X		X		X				X	X					
140-2	X				X		X					X						X	X					
140-3	X						X					X						X						
141-1	X						X					X						X						
144-4	X			X			X			X								X	X					

Pillow Lava Zone

Sample	Pl	Ol	Cr	Cl	Ho	Cu	Tr	Bi	Eu	Ch	Se	Ep	Al	Ca	Ks	Qu	Sp	Ma	Sph	Py	Zi	Ap	Pr	Ta
80HPAD197-3	X			X			X			X		X	X						X					
199	X			X			X			X		X				X		X	X					
221	X			X					X	X		X						X	X					
231	X						X			X		X		X				X	X					
246	X				X													X						

APPENDIX 2 MAJOR ELEMENT ANALYTICAL PROCEDURE

Major element contents were determined at the Analytical Chemistry Laboratory of the Geological Survey of Canada by XRF techniques on fused discs composed of 1 gram of sample, 5 grams of Li2B4O7 and 0.3 grams of LiF.

Each sample was analysed with a single 20 minute reading and matrix effects were corrected by alpha coefficients. Shown in Appendix Table 2.1 are statistical data for the oxides determined. Fe2O3 and FeO were analysed by the Pratt titration method for better precision. Accuracy quoted by the analyst for this method is +/- .02 wt. % for Fe+2 and +/- .05 wt. % for Fe+3.

Appendix Table 2.2, columns 1 to 6, show major element oxide contents for 3 samples determined by fused pellet (XRF) at the GSC and by AA at MUN. Agreement is good in all cases. Columns 7 and 8 show analyses of 2 splits of powder of an olivine gabbro from the Annieopsquotch Complex, performed by XRF at the GSC.

APPENDIX TABLE 2.1

STATISTICAL DATA FOR MAJOR ELEMENT ANALYSES

BY FUSED PELLET (XRF) AT THE GSC

	Calibration Range	Total Max, Error Absolute,	Relative %	Determination Limit	Standard Deviation
SiO_2	0-100	0.30	1	0.30	0.35
TiO_2	0-3	0.01	1	0.01	0.03
Al_2O_3	0-60	0.30	1	0.30	0.31
MnO	0-1	0.01	1	0.01	0.03
MgO	0-50	0.16	1	0.16	0.17
CaO	0-35	0.05	1	0.05	0.07
Na_2O	0-10	0.10	2	0.10	0.16
K_2O	0-15	0.03	1	0.03	0.06
P_2O_5	0-1	0.01	1	0.01	0.01

APPENDIX TABLE 2:2

COMPARISON OF DUPLICATE MAJOR ELEMENT ANALYSES

	1	2	3	4	5	6	7	8
	EH7077 Kilauea tholeiite		HY.610.79 Granodiorite		HY.F405.78 Akaitcho basalt		80HPAD133-5 Olivine gabbro	
	MUN (AA)	GSC (XRF)	MUN	GSC	MUN	GSC	GSC (Duplicate)	
SiO_2	50.0	50.7	61.5	62.7	52.6	52.9	46.2	45.8
TiO_2	2.68	2.75	.60	.62	2.26	2.31	.21	.22
Al_2O_3	13.8	13.9	17.2	17.5	12.8	12.3	19.2	19.3
Fe_2O_3	12.64	2.62	5.49	1.12	16.64	3.29	.88	.76
FeO	--	9.39	--	3.92	--	11.90	4.80	4.95
MnO	.19	.19	.07	.08	.22	.24	.10	.11
MgO	6.84	6.48	1.65	1.78	3.46	3.19	11.8	12.0
CaO	10.37	10.6	3.04	3.22	6.11	6.24	13.5	13.5
Na_2O	2.29	2.3	3.26	3.3	2.76	2.5	.8	.9
K_2O	.51	.55	3.63	3.77	1.72	1.77	--	--
P_2O_5	.33	.29	.16	.17	.56	.51	.03	.02
L.O.I.	.43	.7	1.77	2.9	.51	1.74	.89	.76
Total	99.23	100.6	98.24	100.7	99.64	98.9	98.43	98.34

APPENDIX 3 TRACE ELEMENT ANALYTICAL PROCEDURE

Sample pellets consist of 10 grams (+/- 0.05 gm.) of sample powder with 1.45 grams (+/- 0.05 gm.) of bakelite resin, mixed together then pressed to bind the pellet. The pellets were baked in an oven at 200 degrees C for fifteen minutes to set the binder.

Samples were run in batches of nine with a standard of known trace element content run as a tenth sample. Mean and standard deviation were calculated from replicate analyses of standards BCR-1 and W-1 (Appendix Table 3.1).

Samples were analysed with a Phillips 1450 X-ray Flourescence Spectrometer. A monitor, saturated with trace elements was calibrated against standards and every element ratioed to it. This takes care of instrument drift between runs.

A Rh tube was used for all analyses. Th,U,Rb,Sr,Y,Zr,Nb,Cu and Ni were analysed using a LiF 220 crystal with twenty second counting times. The Compton peak was used for matrix corrections for these elements. The other elements were analysed using the LiF 200 crystal with forty second counting times.

Analyses of Pb,Th,U,Rb and Nb are accurate to within +/- 1 ppm.

APPENDIX TABLE 3.1

MEAN AND STANDARD DEVIATION OF REPLICATE ANALYSIS

OF STANDARDS BCR-1 AND W-1.

BCR-1 (10 Analyses)

	Mean	Standard Deviation	Minimum	Maximum	BCR-1 Accepted Values
Pb	14.60	4.35	6.00	22.00	14
Th	1.90	2.23	--	6.00	6.1
U	1.10	1.66	--	5.00	1.7
Rb	45.60	2.07	42.00	48.00	47
Sr	309.40	5.17	303.00	322.00	330
Y	45.40	2.12	43.00	49.00	40
Zr	179.70	3.47	175.00	186.00	185
Nb	12.00	1.15	10.00	13.00	12.9
Zn	131.20	2.36	128.00	137.00	125
Cu	--	--	--	--	16
Ni	12.40	1.35	10.00	15.00	10
La	61.00	4.85	54.00	71.00	27
Ba	767.00	18.39	741.00	799.00	763
V	409.20	6.99	399.00	421.00	420
Ce	79.90	5.55	70.00	89.00	53
Cr	15.40	1.78	12.00	18.00	15
Ga	21.00	.82	20.00	22.00	22

BCR-1 values are from Abbey (1980) except Nb, Ba are from Taylor and Gorton (1977)

APPENDIX TABLE 3.1

MEAN AND STANDARD DEVIATION OF REPLICATE ANALYSIS

OF STANDARDS BCR-1 AND W-1

W-1 (10 Analyses)

	Mean	SD	Min	Max	W-1 Accepted Values
Pb	8.10	5.11	--	15.00	7.8
Th	.80	1.14	--	3.00	2.4
U	1.90	2.56	--	7.00	.58?
Rb	19.10	1.10	18.00	21.00	21
Sr	172.00	2.11	169.00	176.00	190
Y	26.50	2.88	21.00	30.00	25
Zr	86.00	2.00	83.00	90.00	105
Nb	7.40	.97	6.00	9.00	9.5?
Zn	100.30	2.16	95.00	103.00	86
Cu	78.20	4.61	74.00	86.00	110
Ni	68.20	1.62	66.00	71.00	76?
La	32.90	6.71	23.00	43.00	9.8?
Ba	202.60	11.50	176.00	219.00	160
V	256.30	3.97	251.00	263.00	260
Ce	35.50	2.32	32.00	38.00	23?
Cr	99.90	1.52	98.00	103.00	115?
Ga	17.40	2.12	15.00	22.00	16

W-1 values from Abbey (1980)

APPENDIX 4 RARE EARTH ELEMENT ANALYTICAL PROCEDURE

REE were determined by the thin film XRF method of Fryer (1977) with modifications.

1.5 to 2.0 grams of sample was dissolved in HF and perchloric acid in Teflon beakers. The solution, in 3.1 N HCl, was passed through ion exchange columns to separate REE, Y and Ba from the other elements. Ba was then removed from the sample by precipitation as $BaSO_4$.

The solution was then concentrated by evaporation before being taken up on an ion exchange paper disc. This paper was then dried and analysed by XRF calibrated against international rock standards. Shown in Appendix Figure 4.1A are multiple REE analyses of sample BHVO-1 by Easton (1982) using the method of Fryer (1977) and the published values of Flanagan (1976) and Leeman et al. (1980). Appendix Figure 4.1B shows a comparison of REE abundances in sample EH70-77, a Hawaiian tholeiite, as determined by Easton (1982) and at MIT by neutron activation techniques.

These determinations done by XRF techniques at MUN are within 10 % of the published and neutron activation values. Therefore, the estimated accuracy of the XRF - REE method for these rocks is +/- 10% as claimed by Fryer (1977).

The Annieopsquotch Complex samples have lower abundances of the LREE by an order of magnitude than these standards, so the errors may be significantly greater. However, these depleted REE values are consistent with the

Appendix Figure 4.1A. Comparison of determinations of REE abundances in BHVO-1 by Easton (1982, MUN) and published values for the rock standard (Leeman et al., 1980; Flanagan, 1976).

Appendix Figure 4.1B. Comparison of REE abundances in sample EH70-77, a Hawaiian tholeiite, as determined at MUN by XRF and at MIT by neutron activation techniques.

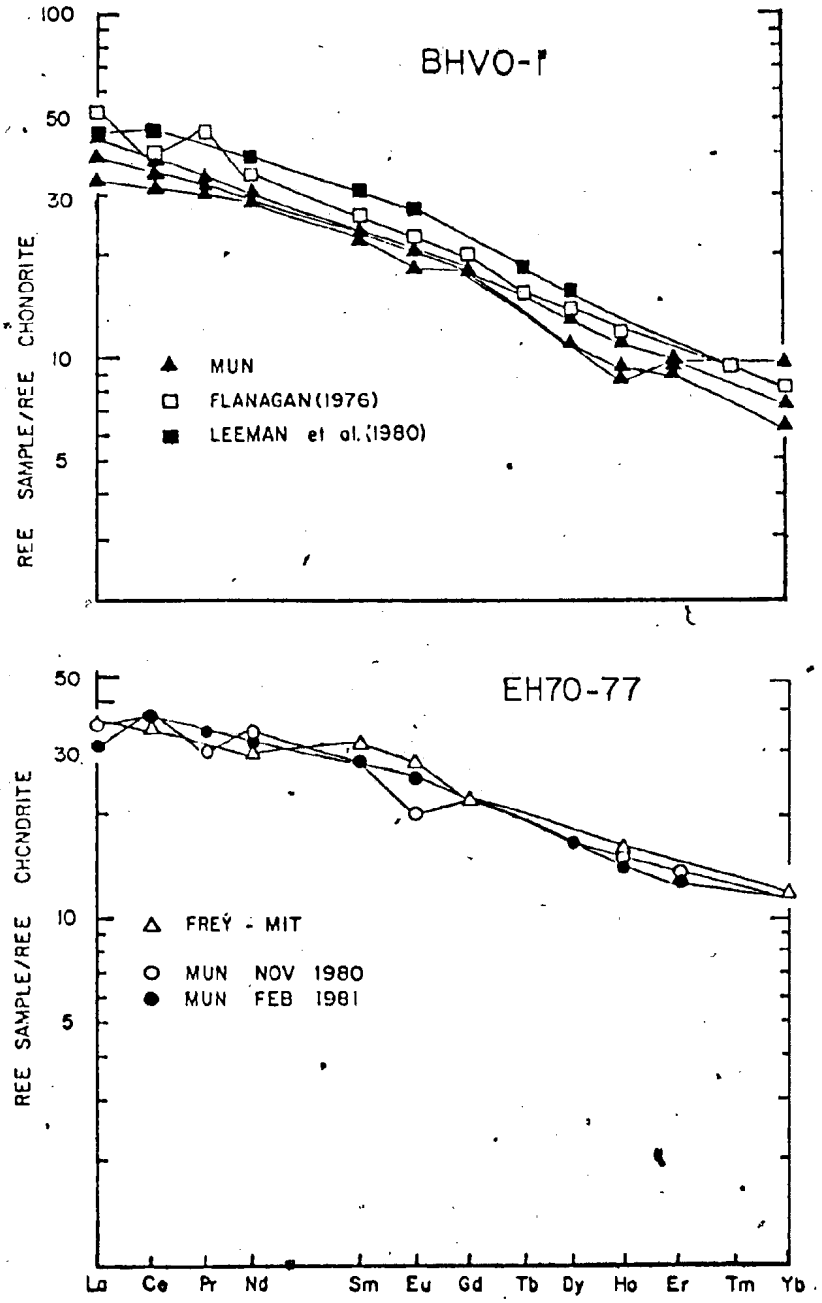
BHVO-1
100
50
30
10
5
REE SAMPLE/REE CHONDRITE
MUN
FLANAGAN(1976)
LEEMAN et al.(1980)
EH70-77
50
30
10
5
REE SAMPLE/REE CHONDRITE
FREY - MIT
MUN NOV 1980
MUN FEB 1981
La Ce Pr Nd Sm Eu Gd Tb Dy Ho Er Tm Yb

concentrations of other trace elements in the samples and the general patterns and abundances are intepreted to be real.

APPENDIX 5
ZIRCON PREPARATION AND U-Pb ANALYTICAL PROCEDURES

5.1 ZIRCON SAMPLE PREPARATION

Each sample consisted of approximately sixty kilograms of fresh hand- specimen- sized pieces collected from a single outcrop of gabbro or trondhjemite. The samples were crushed and pulverized and the powder panned on a Wilfley table.

Zircons were removed from the heavy mineral concentrate in a series of steps involving:

1. free- fall magnetic separation using a Frantz separator to remove iron filings and magnetite;

2. Bromoform heavy liquid separation to remove quartz and feldspar;

3. intitial Frantz magnetic separation, at 10 degree tilt, to remove moderately to strongly magnetic minerals, especially amphibole and epidote;

4. Methylene Iodide heavy liquid separation to remove minerals with a specific gravity less than 3.3 and;

5. final Frantz magnetic separation at tilts from 5 to 0 degrees to separate zircons (and remaining sphene, apatite and pyrite) according to their magnetic susceptibility into five fractions; N0,M0,M1,M3,M5.

Each of the five non-magnetic or magnetic separates of the zircon concentrate was seived into five size fractions:

-40,+70 mesh; -70,+100 mesh; -100,+200 mesh; -200,+325 mesh and; -325 mesh. This yields a total of twenty- five fractions of zircon, with characteristic size and magnetic properties.

5.2 ZIRCON SELECTION

The concentrates obtained by the procedures described above usually still contained pyrite and apatite as contaminating phases. For each sample, zircons for analysis were selected by picking them individually in alcohol under a binocular microscope, using tweezers. Zircon fractions analysed were selected to get a range of points with different degrees of Pb loss to define a discordia line.

Clear crack- free zircons from the non- magnetic (N0) fraction, abraded to remove outer surfaces which might have undergone Pb loss (Krogh, 1982), generally plot closest to or on concordia. The most discordant point was usually provided by analysis of the M3,-325 fraction or M3 grains which were cracked, cloudy or turbid. These features have all been shown to indicate that the zircons are of lower integrity and likely have lost more Pb.

Points intermediate between these were obtained by analysing average bulk material after abrasion or N0, fine grained material without abrasion. In general, finer grained zircons, which have a larger surface to volume ratio, will have undergone greater Pb loss and therefore be more discordant.

5.3 ZIRCON DISSOLUTION AND U-Pb LOADING

Zircons were processed by the method of Krogh (1973) with modifications. A mixed 205Pb/235U isotopic tracer (Krogh and Davis, 1975) was introduced into the teflon capsules with the zircon before dissolution. The samples were sealed, with 0.5 to 1.0 cc of HF and one drop HNO3, inside the Teflon capsules, which were placed in steel jackets and then in an oven at 220 degees C for one week.

U and Pb were separated on ion exchange columns and held as solid precipitate in sealed beakers until analysis.

U and Pb for three zircon fractions were loaded in a single sample barrel. U was loaded on an outgassed rhenium filament, crimped to form a V in the centre. The U was loaded with phosphoric acid and a slurry of tantalum pentoxide. Pb was loaded with phosphoric acid on silica gel. Samples and gel were dried by slowly raising the filament to dull red heat.

5.4 U-Pb ANALYTICAL PROCEDURE

All measurements were done using the Micromass 30 solid state mass spectrometer at the Royal Ontario Museum. Most measurements were performed by T.E. Krogh. Ratios were measured using a Faraday cup except for 207Pb/204Pb which was measured using a Daly detector in an integrating mode.

Pb ratios were measured several times with incremental increases in filament temperature in the range 1050 to about 1200 degrees C, depending on sample size. Two or

more sets of the ratios 207/206, 207/204 and 207/205 were measured. Each ratio measurement consisted of 4 blocks of 8 peaks.

U ratios were measured in the temperature range 1250 to 1400 degrees C with a 'flash' between each set of data to help average out fractionation. The flash consisted of turning the filament current slowly up to about 3 amps and quickly back to the standard range. This melts the sample, and presumably homogenizes it, while burning off part of it with resultant minor fractionation. For small samples a gentle heating of the sample was substituted for the flash.

Two sigma analytical errors of 0.5 and 0.10% were assigned to Pb/U and 207Pb/206Pb ratios respectively (cf. Krogh and Turek, 1982). As stated by these authors, these errors are of estimated overall reproducibility which includes both isotopic fractionation in the mass spectrometer and uncertainty in the common Pb correction.

5.5 METHOD OF AGE CALCULATION - CONSTRAINING THE LOWER INTERCEPT

The closely grouped data for each sample in this study, which vary from concordant to 5.6% discordant, tend to give widely varying lower intercepts because of the length of the projection.

Due to the lack of spread of points, ie; the small range of observed Pb loss, it is often not possible to use the method of Davis (1982) to calculate the best fit line. By adding a point chosen arbitrarily to lie on concordia at

a low age, with a large assigned uncertainty, one can use the linear regression technique of Davis (1982) to calculate an upper intercept age.

Forcing the line through 50 Ma +/- 90% gives a positive lower intercept in the range often seen in natural Pb loss discordia from Lower Paleozoic rocks and the assigned error of +/-90% does not unduly restrict the actual upper intercept age. A value of 50 Ma with a smaller error range, for example +/-30%, could have been used but this would restrict the error on the intercept age unreasonably. Appendix Table 5.1 shows the results of calculations limiting the range of the lower intercept error to varying degrees. If the lower intercept is not restricted in this way (with the resultant minor effect on the calculated age) and the 207Pb/206Pb age of the most concordant point for each sample is used, the result is 0 to 1 Ma younger. Therefore this procedure, though unorthodox and not to be generally used (T.E. Krogh, pers. comm., 1983) makes little or no difference to the age determined and no difference to the conclusions derived from them. Of course, since the line has been calculated using an arbitrary lower intercept, a probability of fit statistic would have no real significance.

It is perhaps ironic that the main problem in accurately determining the age of these samples from Newfoundland ophiolites has been to produce a significantly discordant analytical point. In most samples the concordant points are the hard ones to achieve! This is

APPENDIX TABLE 5.1. ERRORS (2σ) IN AGE CALCULATED BY RESTRICTING ERROR IN LOWER INTERCEPT TO VARYING DEGREES
BAY OF ISLANDS TRONDHJEMITE (80HPAD257)*

ERROR ON LOWER INTERCEPT 50 Ma	INTERCEPT AGE	CALCULATED LOWER INTERCEPT (Ma)	95% CONFIDENCE +VE ERROR	-VE ERROR
+/- 30%	486.1	45.51	1.25	1.14
+/- 45%	486.6	42.78	1.56	1.26
+/- 60%	485.9	33.97	1.64	1.23
+/- 75%	485.8	26.70	1.84	1.26
+/- 90%	485.7	16.36	1.95	1.23

*See Table 7.1 and Figure 7.5 for relevant U-Pb isotopic data and concordia diagram.

part of the larger problem that data from the lowest quality zircons (from a geologic standpoint; the most altered with the greatest degree of Pb loss) is given great emphasis in line fitting techniques which are used to determine the upper intercept age. This problem is discussed further by Krogh and Turek (1982).

APPENDIX 6

ELECTRON MICROPROBE OPERATING CONDITIONS

Pyroxene, olivine and plagioclase were analysed at Memorial University of Newfoundland using a JEOL JX-5A electron probe microanalyser with three wavelength dispersive spectrometers run automatically by the Krisel control system.

An operating voltage of 15 kv and beam current of 0.220 mA were used for all analyses. Data reduction was performed by the Alpha program provided by Krisel, using the correction scheme of Bence and Albee (1968). Pyroxene standards ACPX and FCPX (Kakanui augite, Frisch pyroxene) were used for calibration.

Appendix Table 6.1 shows the results of replicate analyses of the standard Kakanui augite with standard deviation of the oxide and homogeneity index. The latter is a measure of the homogeneity of distribution of each element in the grain. Values less than 3 are generally taken to indicate that the element has a homogeneous distribution in the grain. Elements present in small amounts (Ti, Cr, Mn and Ni) will show a inhomogeneous distribution by this measure because the calculation does not take background counts into account.

APPENDIX TABLE 6.1 REPLICATE ANALYSES OF PYROXENE STANDARD ACPX

	1. Average of 5 Spots	Standard Deviation	Homogeneity Index	2. Av. 4 spots	S.D.	H.I.	Accepted Value
SiO_2	50.71	1.71	8.65	50.45	.36	1.86	50.73
TiO_2	.87	.02	.54	.89	.02	.79	.74
Al_2O_3	8.02	.21	1.70	7.95	.26	2.07	7.86
Cr_2O_3	.12	.01	4.27	.13	.03	6.96	--
FeO	6.40	.14	1.19	6.21	.17	1.36	6.77
MnO	.11	.01	1.02	.07	.04	4.57	--
MgO	16.60	.22	1.10	16.21	.18	.99	16.65
CaO	15.73	.14	1.16	16.49	.06	.43	15.82
Na_2O	1.23	.05	.66	1.20	.07	.97	1.27
NiO	--	--	--	.05	.04	7.66	--
Total	99.79			99.65			
Si	1.84			1.835			
Al^{iv}	.16			.165			
Al^{vi}	.183			.175			
Ti	.023			.023			
Cr	.003			.003			
Fe	.193			.189			
Mn	.003			.002			
Mg	.897			.879			
Ca	.611			.643			
Na	.086			.084			
Ni	--			.001			
Total	3.999			3.999			

APPENDIX 7

In the following tables CIPW norms in weight percent, calculated using the computer program of Irvine and Baragar (1971), are presented for each table of whole rock analyses in the text. The norms were calculated with the natural Fe^{+2}/Fe^{+3} ratios.

CIPW Norms

FOR ROCKS OF THE TROCTOLITE SILL AND CRITICAL ZONE

(TABLE 5.1)

	80D 133-2	80D 133-4	80D 133-5	80D 157-1	80D 168-1	80D 181
Q	-	-	-	-	-	-
OR	.37	.24	.12	.19	.19	.06
AB	6.14	8.47	6.92	5.37	1.80	1.77
AN	40.97	50.31	49.80	18.71	20.95	19.6
DI	8.01	9.86	11.57	7.74	12.68	7.28
HE	1.22	2.03	2.61	.96	1.58	.90
EN	9.13	8.33	12.13	6.24	19.33	12.32
FS	1.59	1.96	3.14	.89	2.77	1.75
FO	24.64	13.16	8.78	45.93	27.87	44.55
FA	4.73	3.42	2.50	7.22	4.40	6.98
MT	2.28	1.28	1.30	5.03	7.38	3.05
IL	.35	.30	.41	.18	.32	.24
CR	.11	.12	.24	.72	.25	.82
AP	.07	.07	.07	.03	.07	.05
PY	.15	.23	.19	.07	.18	.15

Q=Quartz
OR=Orthoclase
AB=Albite
AN=Anorthite
DI=Diopside
C =Corundum
HE=Hedenbergite
EN=Enstatite
FS=Ferrosilite
FO=Forsterite
FA=Fayalite
MT=Magnetite
IL=Ilmenite
CR=Chromite
AP=Apatite
PY=Pyrite
CC=Calcite

CIPW Norms

FOR GABBRO ANALYSES

(TABLE 5.2)

	79D 013-1	79D 014-1	79D 027-1	79D 029-1	79D 143	79D 144-1	79D 144-2	79D 148-1
Q	-	-	-	1.34	-	-	1.27	.95
OR	.36	.54	.36	.36	.60	.36	.95	.49
AB	12.03	18.92	17.17	19.54	12.00	14.46	11.08	17.34
AN	37.51	37.67	33.07	31.93	50.53	39.07	38.74	29.43
DI	19.73	18.17	18.43	16.40	13.87	24.30	21.51	19.15
HE	5.91	7.80	6.74	6.97	4.16	5.65	6.00	8.65
EN	12.41	8.00	9.24	10.53	10.94	5.81	12.91	13.35
FS	4.27	3.94	3.88	5.13	3.77	1.55	4.13	6.92
FO	3.51	1.46	5.00	-	.69	4.32	-	-
FA	1.33	.79	2.31	-	.26	1.27	-	-
MT	2.21	1.30	3.05	4.90	1.95	2.29	2.06	2.10
IL	.60	1.08	.60	2.73	1.00	.65	.92	1.44
CR	.11	.05	.11	.03	.12	.12	.09	.03
AP	.02	.07	.05	.16	.12	.07	.14	.12
PY	-	-	.02	-	-	.08	.21	.04

	79D 150-1	79D 151	79D 152-2	79D 155	79D 156	80D 129-1	80D 130-2	80D 137-1
Q	-	.28	.94	.42	-	1.00	.51	-
OR	.36	.42	.36	.36	.66	.48	.61	.36
AB	14.52	18.76	18.96	13.81	19.60	12.07	11.27	13.01
AN	33.17	35.48	27.56	35.07	31.05	36.16	40.70	35.44
DI	24.13	19.20	18.68	23.17	23.88	21.44	15.46	21.17
HE	7.65	5.87	7.08	7.48	8.44	5.08	4.12	7.29
EN	9.38	11.90	16.02	12.01	6.40	14.44	16.79	12.89
FS	3.41	4.17	6.96	4.45	2.59	3.93	5.13	5.09
FO	2.72	-	-	-	2.87	-	-	1.54
FA	1.09	-	-	-	1.28	-	-	.67
MT	2.17	2.69	2.44	2.11	1.97	3.77	3.92	1.28
IL	1.06	.94	.79	.85	.98	1.14	.80	.66
CR	.10	.05	.03	.05	.03	.08	.14	.09
AP	.14	.09	.05	.05	.09	.07	.10	.10
PY	.10	.17	.15	.17	.17	.13	.23	.19

CIPW Norms

FOR DIABASE DYKES OF THE ANNIEOPSQUOTCH COMPLEX

(TABLE 5.3)

	79D 109-2	79D 148-2	79D 150-2	79D 153-3	79D 237	79D 240	79D 241	80D 081	80D 122	80D 130-1	80D 132-2
Q	-	-	-	-	1.68	2.11	-	5.50	3.99	1.74	.44
OR	-	.30	1.70	.60	.37	.36	.37	1.15	1.61	.54	.24
AB	20.59	14.69	16.48	15.49	15.66	31.90	21.88	22.49	16.79	19.56	11.22
AN	28.71	38.89	30.70	35.34	32.20	20.72	30.15	25.43	26.97	30.77	38.74
DI	16.77	14.39	14.85	15.13	13.56	12.16	6.75	12.13	11.83	18.70	17.82
HE	8.94	5.16	4.86	4.36	7.60	5.74	5.44	8.30	9.08	6.90	6.00
EN	11.23	10.83	17.43	7.55	14.02	8.02	13.76	7.49	9.73	9.75	15.16
FS	6.86	4.45	6.54	2.50	9.01	4.34	12.71	5.88	8.56	4.13	5.85
FO	.31	4.91	1.75	10.39	-	-	.56	-	-	-	-
FA	.21	2.22	.72	3.78	-	-	.57	-	-	-	-
MT	3.00	2.55	2.87	2.71	3.40	9.63	3.23	6.39	4.64	4.74	2.74
IL	2.27	1.44	1.48	1.62	2.05	4.41	3.11	4.21	3.78	2.56	1.12
CR	.06	.08	.15	.15	.06	.03	.05	.03	.05	.04	.09
AP	.21	.07	.26	.14	.19	.45	.26	.45	.40	.23	.12
PY	.42	.04	.21	.25	.21	.13	.09	.32	.35	.12	.23

	80D 193-1	80D 193-2	80D 193-3	80D 193-4	80D 194	80D 196-1	80D 202-2	80D 230	81D 032-1
Q	-	.99	-	-	-	-	-	-	.71
OR	.18	.36	.36	.36	.25	.43	.24	.79	.60
AB	22.82	18.97	15.49	14.59	21.03	41.70	22.67	30.48	19.56
AN	26.87	29.25	33.23	36.93	33.10	20.81	27.78	23.04	31.84
DI	13.35	13.82	16.62	17.14	20.06	6.85	15.68	14.50	14.47
HE	8.40	9.30	7.93	6.21	5.75	3.62	9.02	7.40	6.92
EN	11.47	11.77	13.38	10.85	7.32	5.61	10.46	5.86	11.89
FS	8.27	9.08	7.32	4.51	2.40	3.40	6.90	3.43	6.52
FO	.73	-	.15	3.61	3.63	7.52	.44	4.76	-
FA	.58	-	.09	1.65	1.32	5.02	.32	3.07	-
MT	3.26	3.02	2.71	2.25	3.61	2.86	3.36	2.82	4.66
IL	2.86	2.71	1.91	1.10	1.16	1.56	2.54	3.21	2.52
CR	.06	.06	.11	.11	.09	.08	.06	.05	.06
AP	.22	.26	.17	.09	.17	.17	.26	.36	.23
PY	.92	.42	.29	.15	.13	.15	.28	.25	.02

CIPW Norms

FOR DIABASE DYKES OF THE ANNIEOPSQUOTCH COMPLEX

(TABLE 5.3)

	81D 033-2	81D 033-3	81D 036-1	81D 123-1	81D 124-1	81D 128-1	81D 129	81D 136-1	81D 136-3	81D 137-1
Q	4.52	2.22	3.41	.32	2.58	4.31	3.90	2.92	3.29	.22
OR	.48	.55	.54	.54	.42	.43	.48	.89	1.58	.36
AB	18.08	19.24	16.37	25.89	20.70	19.09	20.70	18.75	13.05	31.10
AN	29.04	33.81	33.28	26.08	31.64	28.56	29.94	29.47	31.84	26.79
DI	11.72	10.91	13.68	11.88	10.96	11.66	11.04	14.61	12.82	7.63
HE	7.79	6.27	6.15	7.38	6.88	8.04	7.40	6.20	5.59	3.24
EN	10.22	11.73	11.82	11.26	11.77	10.38	10.95	14.83	18.22	17.06
FS	7.80	7.73	6.09	8.02	8.48	8.21	8.42	7.22	9.41	8.30
FO	-	-	-	-	-	-	-	-	-	-
FA	-	-	-	-	-	-	-	-	-	-
MT	6.80	4.74	5.61	4.70	3.52	5.43	4.12	3.24	2.49	3.41
IL	3.29	2.53	2.69	3.20	2.34	3.31	2.56	1.15	1.19	1.55
CR	.03	.05	.06	.05	.05	.03	.03	.09	.11	.08
AP	.24	.19	.31	.31	.19	.26	.19	.23	.31	.14
PY	-	.04	-	.15	.25	.06	.06	.17	.17	.13

	81D 137-2	81D 138-1	81D 138-2	81D 140-2	81D 140-3	81D 141-1	81D 141-2	81D 144-3	81D 144-4	81D 145
Q	.30	.06	2.73	1.82	6.13	4.45	2.11	.58	-	-
OR	.48	.54	.42	.65	.54	.54	.48	.49	.49	.62
AB	19.03	12.81	19.05	16.16	20.59	18.14	14.81	24.36	23.41	30.01
AN	34.86	39.76	29.90	34.16	27.26	28.83	34.69	27.24	27.89	22.77
DI	8.13	16.48	11.73	13.99	12.82	12.57	13.26	13.59	12.45	10.31
HE	4.57	5.15	7.64	7.56	6.43	7.84	6.36	6.85	7.64	7.21
EN	15.71	14.36	11.99	11.84	10.19	10.65	14.11	11.98	11.69	11.29
FS	10.11	5.14	8.95	7.33	5.86	7.61	7.77	6.93	8.23	9.06
FO	-	-	-	-	-	-	-	-	.32	.22
FA	-	-	-	-	-	-	-	-	.25	.20
MT	3.77	3.60	4.01	3.79	6.54	5.52	3.89	4.62	4.01	3.72
IL	2.43	1.63	3.05	2.12	2.85	3.22	2.20	2.64	2.76	2.83
CR	.08	.09	.05	.06	.03	.05	.08	.06	.05	.02
AP	.24	.09	.29	.21	.26	.28	.17	.19	.29	.24
PY	.06	.06	.21	.08	.27	.08	.08	.25	.32	1.27

CIPW Norms

FOR DIABASE DYKES FROM KING GEORGE IV LAKE AND SHANADITHIT BROOK

(TABLE 5.4)

	80D 252-1	80D 252-2	81D 210-1	81D 210-3	81D 195-2	81D 195-3
Q	-	-	.74	4.51	2.01	.91
OR	.72	.55	.66	.67	.72	.72
AB	24.09	17.63	10.35	18.16	16.27	13.71
AN	32.92	36.98	39.26	29.92	33.26	36.86
DI	12.11	12.23	15.82	9.35	12.39	8.84
HE	6.39	4.25	6.07	5.80	5.97	3.33
EN	7.07	14.61	15.27	13.28	13.77	19.46
FS	4.28	5.83	6.72	9.44	7.61	8.41
FO	4.64	.84	-	-	-	-
FA	3.09	.37	-	-	-	-
MT	2.71	3.13	3.05	5.05	4.54	4.67
IL	1.55	2.57	1.41	3.16	2.69	2.27
CR	.05	.06	.12	.08	.06	.09
AP	.31	.41	.10	.24	.26	.24
PY	.08	.06	.21	.11	.23	.27

	81D 195-4	81D 195-5	81D 196-2	81D 196-3	81D 196-4	81D 196-5
Q	8.84	5.38	3.72	-	.91	2.64
OR	1.39	.96	.71	.61	1.45	.78
AB	18.11	21.36	15.30	9.54	16.46	15.45
AN	28.92	32.00	31.27	39.40	32.45	35.70
DI	8.70	5.62	17.18	13.63	13.84	13.39
HE	7.60	4.23	7.45	4.62	5.79	5.30
EN	11.15	10.69	11.37	19.11	14.05	14.96
FS	11.16	9.23	5.65	7.44	6.74	6.79
FO	-	-	-	-	-	-
FA	-	-	-	-	-	-
MT	3.18	6.40	4.40	3.30	4.96	3.50
IL	.25	2.55	2.27	1.60	2.61	.87
CR	.03	.02	.06	.11	.06	.09
AP	.07	.26	.16	.12	.19	.14
PY	.36	1.08	.23	.30	.27	.17

CIPW Norms

FOR OPHIOLITIC INCLUSIONS IN BOOGIE LAKE INTRUSION

(TABLE 5.5)

	81D 007	81D 010-3	81D 011-1	81D 012	81D 015-1	81D 015-2	81D 018-1	81D 019	81D 042-2
Q	3.06	2.11	2.00	1.85	3.02	-	1.86	-	9.35
OR	1.26	.42	1.28	.73	4.82	2.68	.90	.55	2.62
AB	18.91	18.74	20.02	13.85	25.86	11.32	16.36	17.51	29.61
AN	30.93	30.52	28.88	35.00	29.19	38.98	33.92	33.92	26.52
DI	10.88	13.73	12.08	15.11	7.59	13.17	11.94	9.62	3.09
HE	5.96	7.98	7.01	6.61	2.56	5.05	6.81	3.64	1.97
EN	12.01	11.22	13.05	13.51	12.62	15.24	13.40	16.63	9.59
FS	7.55	7.48	8.68	6.78	4.89	6.71	8.77	7.22	7.01
FO	-	-	-	-	-	1.58	-	1.66	-
FA	-	-	-	-	-	.77	-	.79	-
MT	5.25	4.37	3.62	3.61	4.90	2.77	3.10	4.37	4.72
IL	3.03	2.85	2.68	2.22	3.43	1.60	2.46	3.32	4.03
CR	.03	.04	.08	.09	.03	.08	.06	.09	.02
AP	.33	.30	.24	.17	.80	.07	.19	.53	.84
PY	.10	.25	.17	.25	.29	-	-	.15	.17

CIPW Norms

FOR PILLOW LAVA OF THE ANNIEOPSQUOTCH COMPLEX AND KING GEORGE IV LAKE

(TABLE 5.6)

	81D 132-2	81D 132-3	81D 133-1	81D 133-2	80D 196-2	80D 197-3	80D 199	80D 231
Q	.38	-	.65	-	-	-	5.06	-
OR	.48	.37	.54	.43	.31	.25	.31	.42
AB	39.62	38.90	24.19	35.81	30.96	36.16	42.95	35.27
AN	16.80	22.80	32.87	21.09	28.21	22.80	16.36	19.91
DI	14.11	.99	7.33	4.95	5.99	3.41	5.81	16.24
HE	6.08	.47	4.23	2.50	2.42	2.48	2.85	6.85
EN	11.94	13.43	14.56	13.85	14.94	12.52	11.34	7.58
FS	5.90	7.39	9.65	8.01	6.91	10.46	6.39	3.66
FO	-	3.62	-	4.63	1.87	1.69	-	2.08
FA	-	2.19	-	2.95	.96	1.55	-	1.11
MT	2.23	6.14	3.05	2.96	3.09	4.60	3.06	4.02
IL	2.13	3.27	2.35	2.00	2.20	3.31	3.27	2.18
CR	.08	.03	.06	.06	.06	.03	.02	.05
AP	.19	.34	.21	.19	.24	.36	.41	.33
PY	.06	.06	.08	.06	1.12	.39	2.20	.06

	81D 208-1	81D 208-2	81D 208-3	81D 208-4	81D 208-5	81D 209-2
Q	.65	4.63	-	4.19	.13	4.99
OR	.61	.67	5.91	.68	2.73	4.99
AB	35.57	39.43	31.05	19.39	27.80	27.00
AN	21.68	19.16	20.08	32.29	26.19	22.79
DI	6.74	5.59	9.41	11.10	9.11	9.99
HE	3.35	2.08	5.08	4.66	4.81	4.74
EN	13.48	10.43	7.02	11.07	14.01	11.45
FS	7.69	4.44	4.35	5.32	8.48	6.23
FO	-	-	4.55	-	-	-
FA	-	-	3.10	-	-	-
MT	6.38	9.05	5.53	6.60	3.54	3.55
IL	3.04	3.54	3.20	3.38	2.42	2.01
CR	.06	.03	.05	.03	.08	.06
AP	.31	.34	.28	.36	.26	.19
PY	.23	.15	.17	.21	.21	.13

CIPW Norms

FOR TRONDHJEMITE AND DIORITE OF THE ANNIEOPSQUOTCH AND BAY OF ISLANDS COMPLEX

(TABLE 5.7)

	79D 163-2	79D 250	80D 222	80D 223-1	80D 223-2	80D 257
Q	38.47	2.39	1.90	22.77	2.30	36.93
OR	3.83	.42	4.83	1.03	1.08	.66
AB	35.09	32.53	39.25	36.28	19.78	56.40
AN	17.01	55.97	39.79	25.65	31.96	2.19
DI	.25	6.63	2.72	2.26	14.36	-
HE	.12	.42	.27	1.54	7.13	-
EN	2.03	-	5.12	3.66	10.38	.33
FS	1.14	-	.58	2.85	5.91	.21
FO	-	-	-	-	-	-
FA	-	-	-	-	-	-
MT	1.29	.35	3.04	2.13	4.47	1.99
IL	.54	.79	1.72	1.22	2.22	.29
CR	.02	.02	.02	.02	.03	.02
AP	.21	.24	.54	.26	.21	.09
PY	.02	-	-	.11	.17	.06
						Corundum .84

CIPW Norms

FOR MAFIC VOLCANIC ROCKS OF THE VICTORIA LAKE GROUP

(TABLE 7.1)

	81D 014-1	81D 0142	81D 016	81D 017-1	81D 043-1	81D 046-1	81D 047	81D 051-2	81D 051-3
Q	14.68	12.94	1.27	4.91	--	--	--	1.41	1.23
C	--	--	--	--	--	--	--	3.58	5.71
OR	7.14	6.38	.83	1.27	.84	.89	1.78	1.98	2.41
AB	30.28	35.29	17.84	35.51	33.59	28.06	24.58	63.65	53.07
AN	25.57	22.23	27.93	23.82	20.65	27.39	30.52	7.93	8.68
DI	1.92	1.71	14.07	3.76	12.87	7.90	10.80	--	--
HE	1.42	1.13	8.74	3.86	6.73	3.14	3.02	--	--
EN	7.11	7.82	10.86	5.62	8.58	16.15	14.14	9.32	13.54
FS	6.04	5.93	7.74	6.62	5.15	7.37	4.54	3.26	4.36
FO	--	--	--	--	1.57	.50	.91	--	--
FA	--	--	--	--	1.04	.25	.32	--	--
MT	2.15	2.39	6.13	6.23	5.14	4.21	5.67	4.33	6.99
IL	2.99	2.90	4.20	5.35	3.07	2.58	2.09	2.84	2.92
CR	.02	.02	.04	.02	.03	.06	.09	.03	.02
AP	.66	.61	.35	2.78	.28	.29	.14	.73	.82
PY	.04	.19	--	.25	.23	.06	.21	.02	.02
CC	--	.46	--	--	.23	1.18	1.18	.93	.24

	81D 051-4	81D 054-1	81D 057	81D 058	81D 063-1	81D 063-2	81D 065	81D 113-4
Q	1.48	10.98	--	11.51	--	.78	--	6.07
C	5.44	6.50	1.73	6.91	--	.59	--	10.08
OR	7.61	3.61	13.88	6.57	1.27	5.25	5.38	1.23
AB	51.82	47.29	22.74	35.51	39.93	38.44	39.31	43.95
AN	8.26	--	27.34	4.84	19.62	16.80	21.54	2.72
DI	--	--	--	--	2.33	--	1.48	--
HE	--	--	--	--	1.07	--	.73	--
EN	11.71	11.16	13.39	12.75	11.56	13.94	11.85	14.52
FS	4.38	2.90	4.53	7.75	6.09	9.41	6.65	12.36
FO	--	--	3.30	--	4.75	--	.35	--
FA	--	--	1.23	--	2.76	--	.22	--
MT	5.03	6.80	7.14	2.03	3.18	5.24	6.06	2.15
IL	2.92	4.78	1.51	2.60	2.20	3.14	4.67	1.76
CR	.03	.02	.02	.03	.03	.03	.02	.02
AP	.84	.79	1.08	.75	.26	.41	1.03	.12
PY	.02	--	--	.13	.04	.11	.49	.06
CC	.47	5.18	2.12	8.98	4.90	5.87	.24	4.96

CIPW Norms

FOR MAFIC VOLCANIC ROCKS OF THE VICTORIA LAKE GROUP

(TABLE 7.1)

	81D 186-1	81D 186-3	81D 188-1	81D 295-1	81D 295-2	81D 298	81D 299-3	80D 246
Q	--	.24	--	3.50	1.90	1.11	4.12	3.13
C	--	--	--	--	--	--	.27	--
OR	1.70	1.34	.92	.67	.61	2.61	.50	.73
AB	34.63	38.41	32.28	20.84	20.12	24.28	19.50	37.37
AN	24.62	24.56	26.03	25.58	26.54	30.00	42.43	16.53
DI	11.12	5.71	6.78	11.23	11.07	7.99	--	9.41
HE	4.32	2.49	3.47	6.97	8.32	4.58	--	4.95
EN	8.89	12.13	8.40	11.76	11.65	14.21	17.61	11.22
FS	3.96	6.06	4.93	8.38	10.04	9.34	1.66	6.77
FO	.78	--	6.13	--	--	--	--	--
FA	.39	--	3.96	--	--	---	---	--
MT	5.53	4.76	3.08	5.55	4.05	3.54	6.15	4.04
IL	2.78	2.88	2.70	4.03	4.04	1.01	1.57	2.99
CR	.08	.08	.08	.03	.03	.05	.09	.03
AP	.31	.26	.26	.36	.41	.24	.10	.29
PY	.21	.15	.30	.17	.28	.13	.11	2.13
CC	.70	.94	.70	.93	.94	.93	5.96	.23

CIPW Norms

FOR MAFIC DYKES AND SILLS OF THE VICTORIA LAKE GROUP

(TABLE 7.2)

	81D 013-2	81D 054-2	81D 070-1	81D 070-2	81D 070-3	81D 070-4	81D 074
Q	2.14	9.15	.12	4.55	1.14	2.65	2.00
C	--	4.64	--	--	--	--	--
OR	.92	6.28	7.64	2.66	3.35	1.36	2.52
AB	14.06	47.08	20.99	22.51	29.66	26.47	25.50
AN	39.98	--	22.56	34.19	23.38	27.39	28.03
DI	3.52	--	11.79	8.51	6.79	7.41	11.38
HE	1.31	--	6.35	2.82	3.98	3.63	4.21
EN	20.38	7.00	9.66	9.89	11.85	12.93	10.43
FS	8.68	--	5.96	3.77	7.95	7.27	4.43
FO	--	--	--	--	--	--	--
FA	--	--	--	--	--	--	--
MT	2.55	17.05	8.34	6.35	5.34	6.36	7.29
IL	2.60	4.40	5.70	2.97	3.54	3.72	3.32
CR	.08	.02	.03	.03	.03	.02	.03
AP	.41	.81	.55	.45	.43	.46	.41
PY	.32	--	.09	.15	.21	.11	.21
CC	3.07	2.34	.24	1.16	2.35	.24	.24

	81D 075-1	81D 086-3	81D 091	81D 094-3	81D 099	81D 102-2
Q	1.84	8.74	.57	--	11.71	16.93
C	--	9.88	--	3.13	3.95	1.23
OR	4.90	5.85	7.61	37.44	1.67	.56
AB	29.40	40.53	27.00	1.74	28.35	--
AN	23.51	4.89	22.04	14.85	16.78	37.89
DI	6.44	--	10.40	--	--	--
HE	3.84	--	6.18	--	--	--
EN	10.40	12.27	8.46	12.74	13.40	18.21
FS	7.12	10.16	5.76	5.50	7.32	7.49
FO	--	--	--	6.48	--	--
FA	--	--	--	3.08	--	--
MT	7.54	3.96	6.51	2.62	7.48	8.76
IL	3.98	1.74	4.24	.94	3.88	4.58
CR	.02	.03	.03	.15	.03	.05
AP	.55	.24	.65	.07	.53	.83
PY	.23	.06	.11	--	.13	.11
CC	.23	1.66	.47	11.25	4.76	3.36

CIPW Norms

FOR INTERMEDIATE AND FELSIC ROCKS OF THE VICTORIA LAKE GROUP

(TABLE 7.3)

	81D 060-1	81D 060-2	81D 076	81D 086-2	81D 064	81D 066	81D 067	81D 072-1	81D 073	81D 080-2
Q	--	9.36	5.25	17.82	5.94	3.35	25.09	5.97	5.71	8.29
C	2.76	7.10	1.86	6.68	4.27	2.63	3.73	3.43	3.65	3.37
OR	5.05	4.19	21.56	1.51	18.58	34.42	51.71	27.55	37.86	70.51
AB	40.51	32.21	49.96	50.98	56.78	47.02	12.03	46.20	38.38	6.84
AN	21.30	10.23	8.50	1.34	1.66	1.14	--	1.85	--	.16
EN	13.08	16.15	4.54	7.76	4.46	2.69	1.33	4.08	3.86	3.04
FS	6.43	13.77	3.18	4.86	6.27	3.22	.03	1.63	2.96	1.23
FO	2.89	--	--	--	--	--	--	--	--	--
FA	1.57	--	--	--	--	--	--	--	--	--
MT	4.56	4.39	3.04	3.76	.24	2.21	1.65	2.26	2.79	2.56
IL	1.13	1.91	.99	1.59	.95	.92	.81	1.27	.92	1.11
CR	.02	.03	.02	--	--	--	.02	.02	.02	--
AP	.29	.12	.61	.38	.47	.47	.38	.91	.61	.77
PY	.19	.07	.04	.06	.17	.10	.04	1.80	.04	.50
CC	.24	.48	.46	3.25	.23	1.84	3.23	3.05	3.21	1.81

	81D 081-2	81D 081-3	81D 086-4	81D 088-1	81D 090	81D 094-1	81D 094-2	81D 100	81D 109	81D 110
Q	13.46	25.79	17.68	53.39	14.97	16.82	11.73	6.28	4.89	14.16
C	2.48	2.26	6.58	2.15	1.61	.78	1.70	1.64	4.60	5.54
OR	26.95	37.59	1.93	2.08	26.14	62.60	10.48	18.07	37.52	36.00
AB	47.65	24.75	51.65	36.57	43.83	6.03	59.96	63.13	34.40	33.41
AN	1.70	1.83	.89	1.39	5.30	5.33	4.73	1.99	.66	--
EN	1.55	1.61	7.83	1.60	2.13	1.88	1.72	1.13	3.87	2.13
FS	1.40	1.53	4.95	1.30	.73	1.55	2.81	--	2.13	1.00
FO	--	--	--	--	--	--	--	--	--	--
FA	--	--	--	--	--	--	--	--	--	--
MT	.92	1.17	3.51	.88	2.11	2.11	2.10	3.87	5.73	3.02
IL	.97	.81	1.53	.29	1.02	.99	1.04	1.09	1.18	1.10
CR	.02	.02	.02	.02	.02	.02	--	.02	--	.02
AP	.33	.35	.35	.02	.47	.45	.47	.54	.78	.59
PY	.29	.23	.08	.08	.29	.08	.04	.04	.08	.04
CC	2.29	2.07	3.01	.23	1.39	1.39	3.22	1.83	4.16	2.99

Endispiece

A difficult portage to King George IV Lake.

MAP 1 GEOLOGY OF THE

LEGEND

DEVONIAN?

12 GRANITE

SILURIAN

11 RHYOLITE

10 TERRESTRIAL SEDIMENTARY ROCK

LATE ORDOVICIAN

9 GABBRO - DIORITE

MIDDLE-LATE ORDOVICIAN

8 FOLIATED TONALITE

EARLY ORDOVICIAN

7 VICTORIA LAKE GROUP

ANNIEOPSQUOTCH COMPLEX

6 PILLOW LAVA ZONE

5 SHEETED DYKE ZONE

4 TRANSITION ZONE
25 TO 75% DIABASE DYKES

3 TRONDHJEMITE

2 GABBRO ZONE

1 CRITICAL ZONE
TROCTOLITE, OLIVINE GABBRO (1A
EQUIGRANULAR METAMORPHIC RO

HE ANNIEOPSQUOTCH COMPLE

SYMBOLS

GEOLOGICAL CONTACT,
DEFINED, APPROXIMATE, A
SHEAR ZONE, FOLIATION, BE
IGNEOUS LAYERING, FLOW B
FAULT, DIABASE DYKE
LOGGING ROAD

CKS

SAMPLES

U-PB (ZIRCON), AGE IN BOX
TROCTOLITE
GABBRO, TRONDHJEMITE
DIABASE DYKE, PILLOW LAV
MINERAL ANALYSIS

2 of

EX

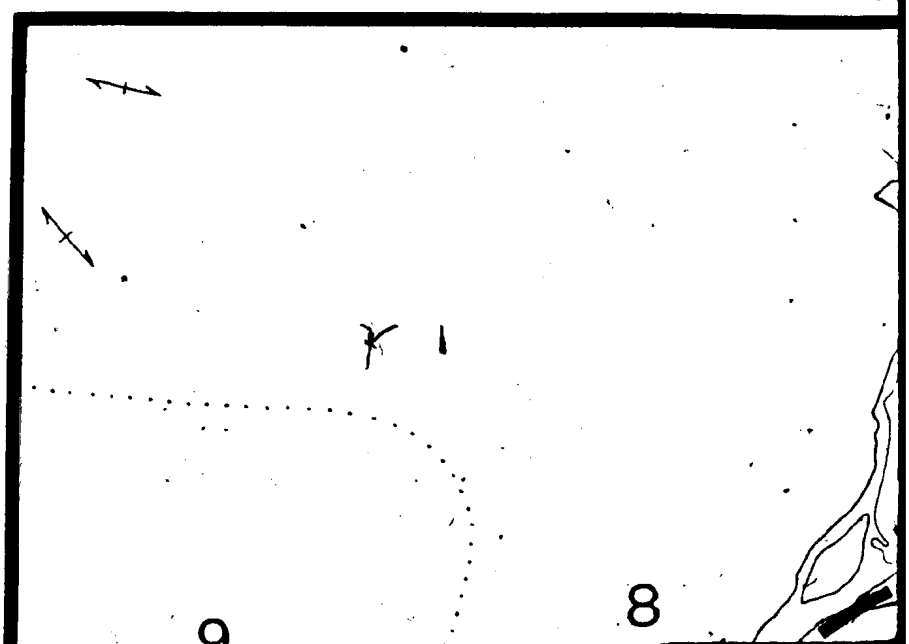

(1A)
ROCKS (1B)

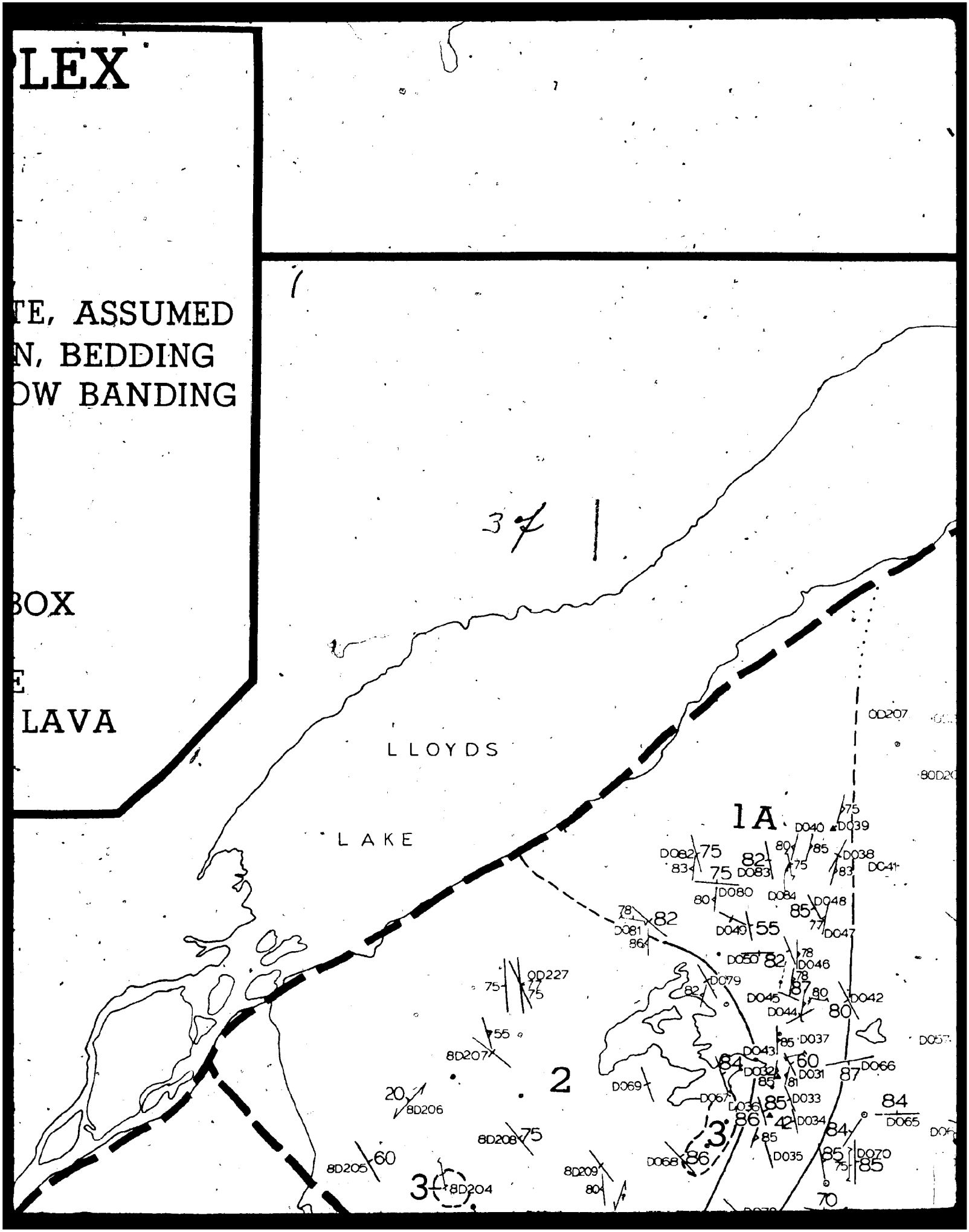
LEX
TE, ASSUMED
N, BEDDING
OW BANDING
BOX
E
LAVA
LLOYDS
LAKE
1A
2
3
3
D040
D039
D038
D041
D083
D080
D084
D048
D049
D047
D081
D050
D046
D079
D045
D044
D042
D037
D043
D032
D031
D066
D069
D067
D036
D033
D034
D035
D070
D065
OD227
OD207
8D207
8D206
8D208
8D205
8D204
8D209
D068

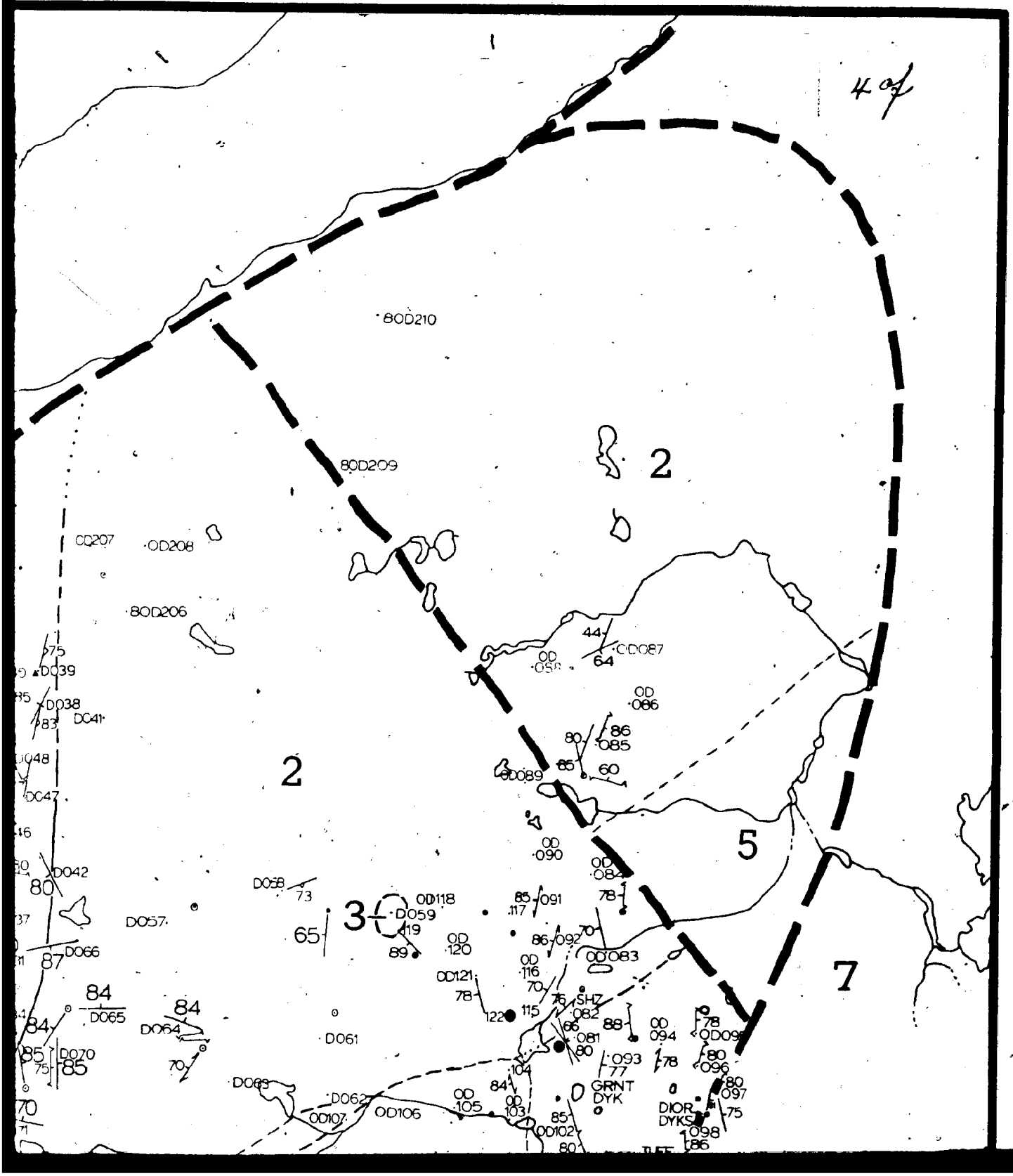
4 of
80D210
80D209
2
CD207
OD208
80D206
D039
D038
DC41
DC47
D042
80
D057
D066
87
84
D065
84
D064
84
85
D070
85
70
D068
73
65
3
OD118
D059
119
89
OD
120
OD121
78
122
115
OD
116
70
85
091
117
86
092
70
OD083
78
SHZ
082
66
081
80
88
OD
094
78
OD09
80
096
80
097
75
104
84
OD
105
OD
103
85
OD102
80
098
86
093
77
GRNT
DYK
DIOR
DYKS
D061
D062
OD107
OD106
D063
OD
090
OD
084
OD089
OD087
64
OD
086
80
86
085
85
60
44
5
7

EQUIGRANULAR METAMORPHIC RO

GEOLOGY BY G.R. DUNNING 1978

MEMORIAL UNIVERSITY OF NEWF

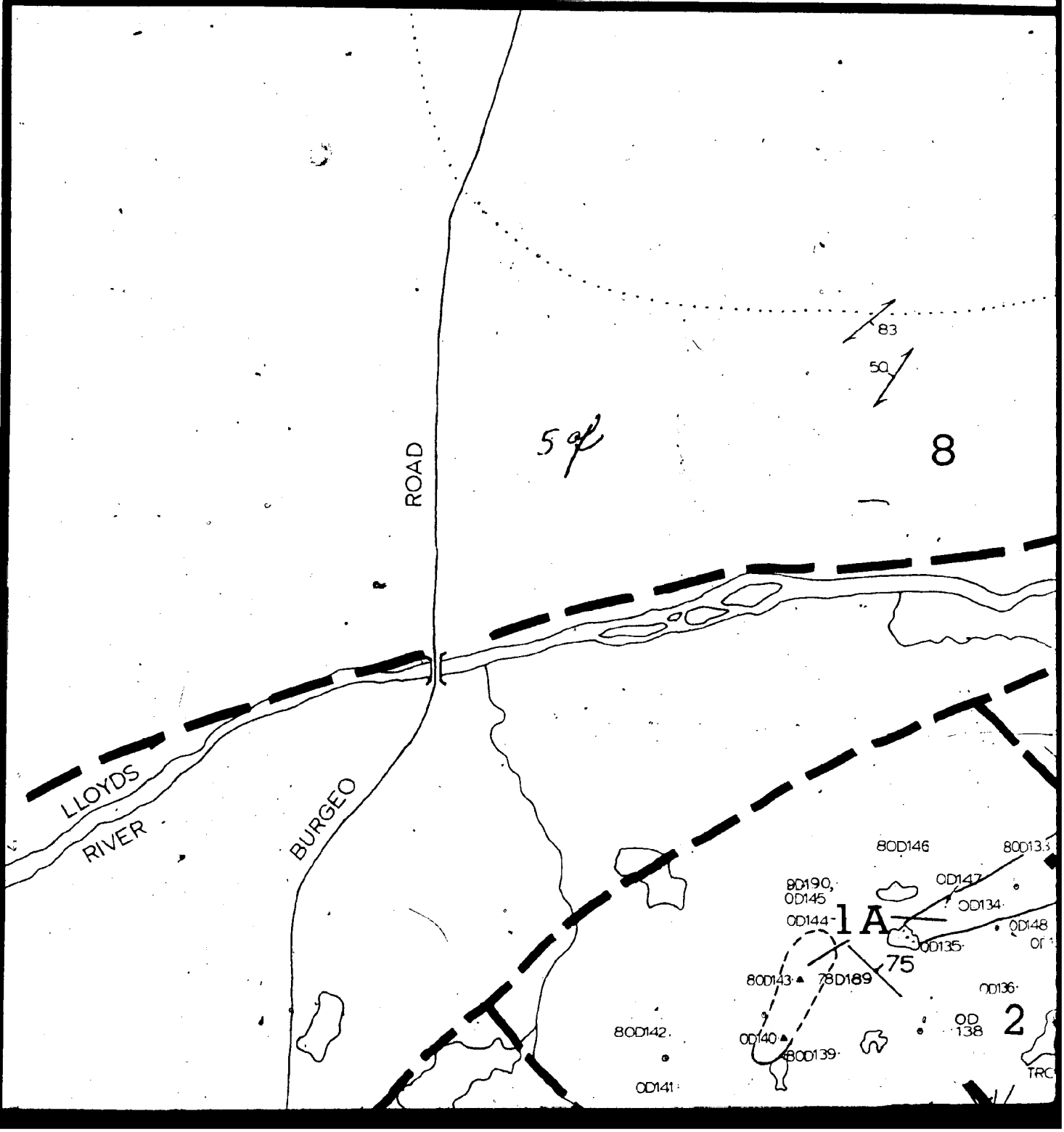

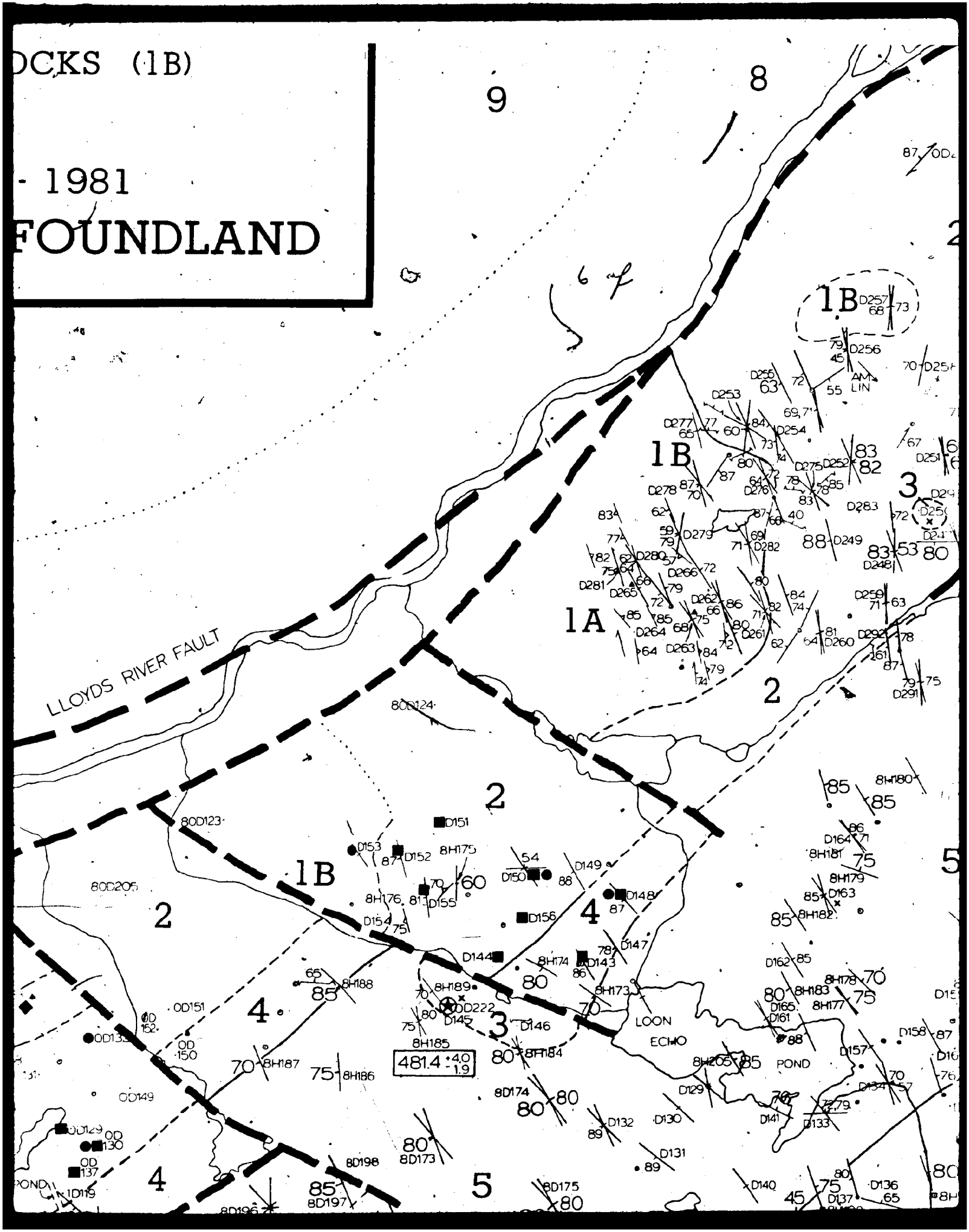
OCKS (1B)
- 1981
FOUNDLAND
LLOYDS RIVER FAULT
LOON
ECHO
POND
481.4 :40
1.9

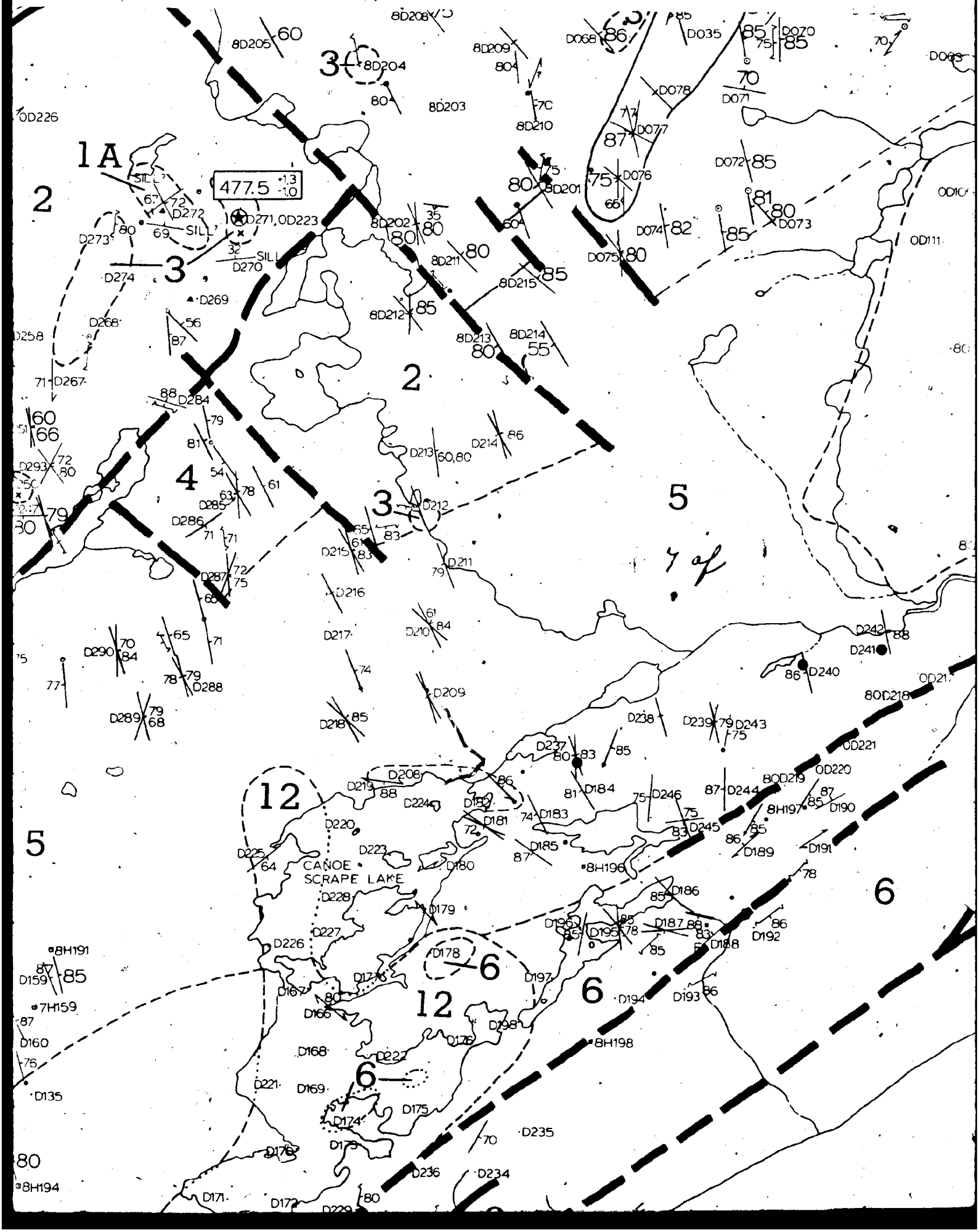
1A
2
3
4
5
6
12
477.5 +1.3 -1.0
CANOE
SCRAPE LAKE

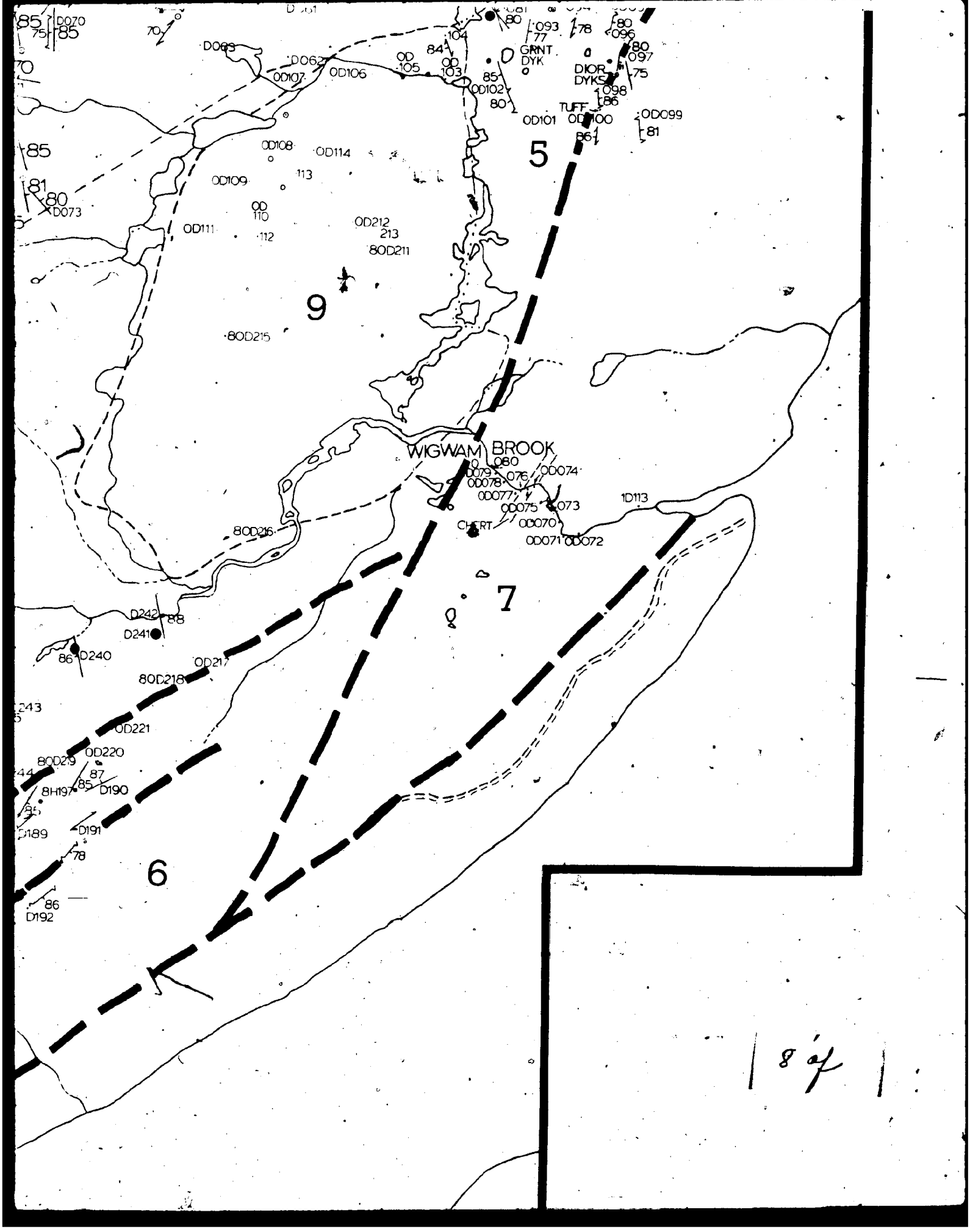
WIGWAM BROOK
GRNT DYK
DIOR DYKS
TUFF
CHERT
5
6
7
9
D070
D069
D062
OD107
OD106
OD105
OD104
OD103
OD102
OD101
OD100
OD099
OD108
OD114
OD109
OD110
OD111
OD112
OD212
213
80D211
80D215
80D216
OD074
OD078
OD077
OD075
OD070
OD071
OD072
1D113
D242
D241
D240
OD217
80D218
OD221
80D219
OD220
8H197
D190
D189
D191
D192
D073

1 of 1

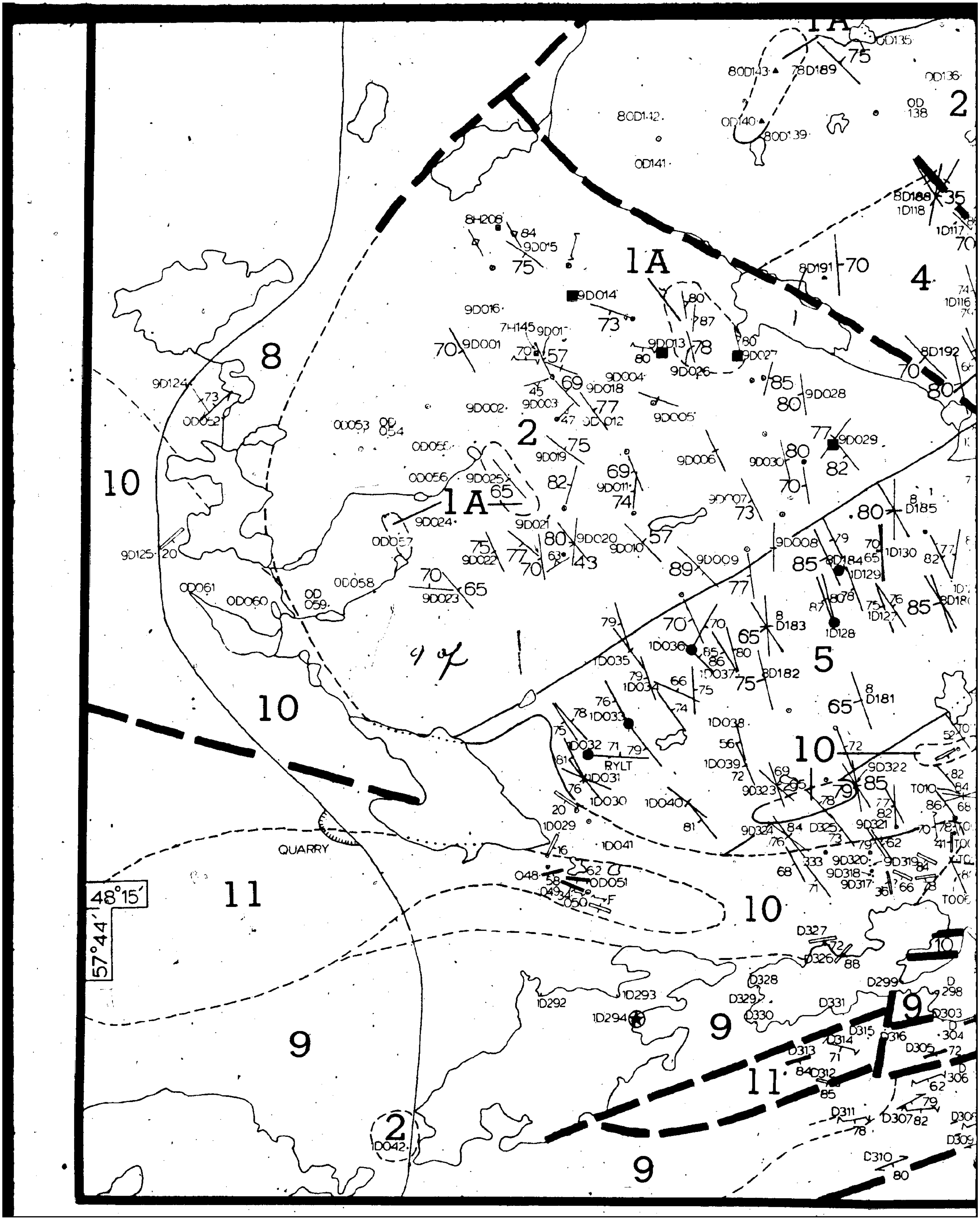

48°15′
57°44′
QUARRY
RYLT
1A
2
4
5
8
9
10
11
8H208
9D014
9D016
7H145
9D001
9D013
9D026
9D027
9D028
9D029
9D004
9D018
9D002
9D003
9D012
9D005
9D006
9D030
9D019
9D011
9D025
9D024
9D021
9D020
9D010
9D007
9D008
9D009
9D022
9D023
9D124
9D125
0D052
0D053
0D054
0D055
0D056
0D057
0D058
0D059
0D060
0D061
80D143
78D189
0D135
0D136
0D138
80D142
0D140
80D139
0D141
8D188
1D118
1D117
8D191
1D116
8D192
D185
8D184
1D129
1D130
D183
1D128
1D127
8D182
D181
1D036
1D035
1D037
1D034
1D033
1D032
1D031
1D030
1D029
1D038
1D039
1D040
1D041
9D322
9D323
9D324
D325
9D321
9D320
9D319
9D318
9D317
T010
T006
0D051
048
049
050
D327
D326
D328
D329
D330
D331
D299
D298
D303
D304
D305
D306
D313
D314
D315
D316
D312
D311
D307
D310
D309
1D292
1D293
1D294
1D042

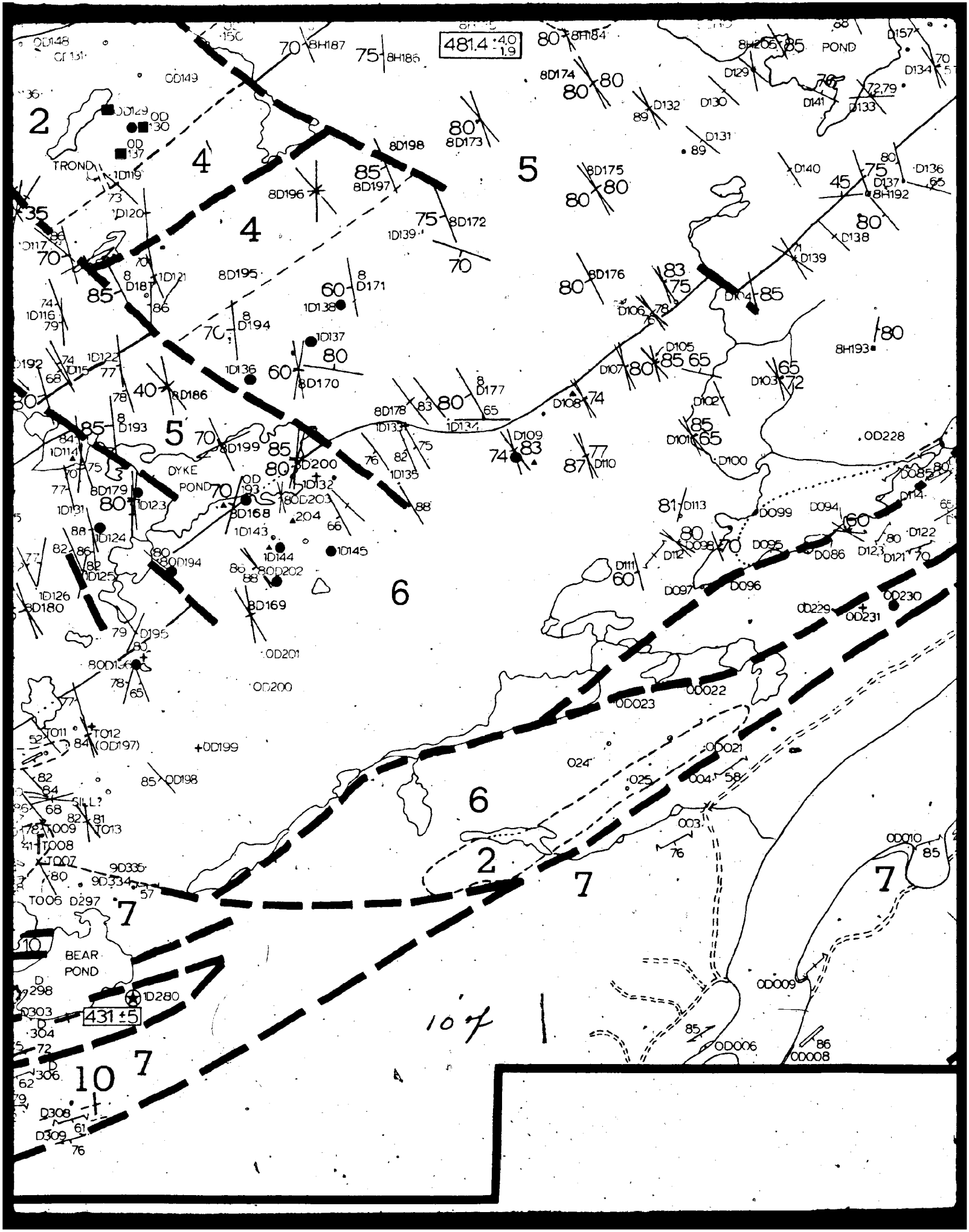
481.4 +4.0 -1.9
431 ±5
POND
DYKE POND
BEAR POND
TROND
SILL?
2
4
5
6
7
10

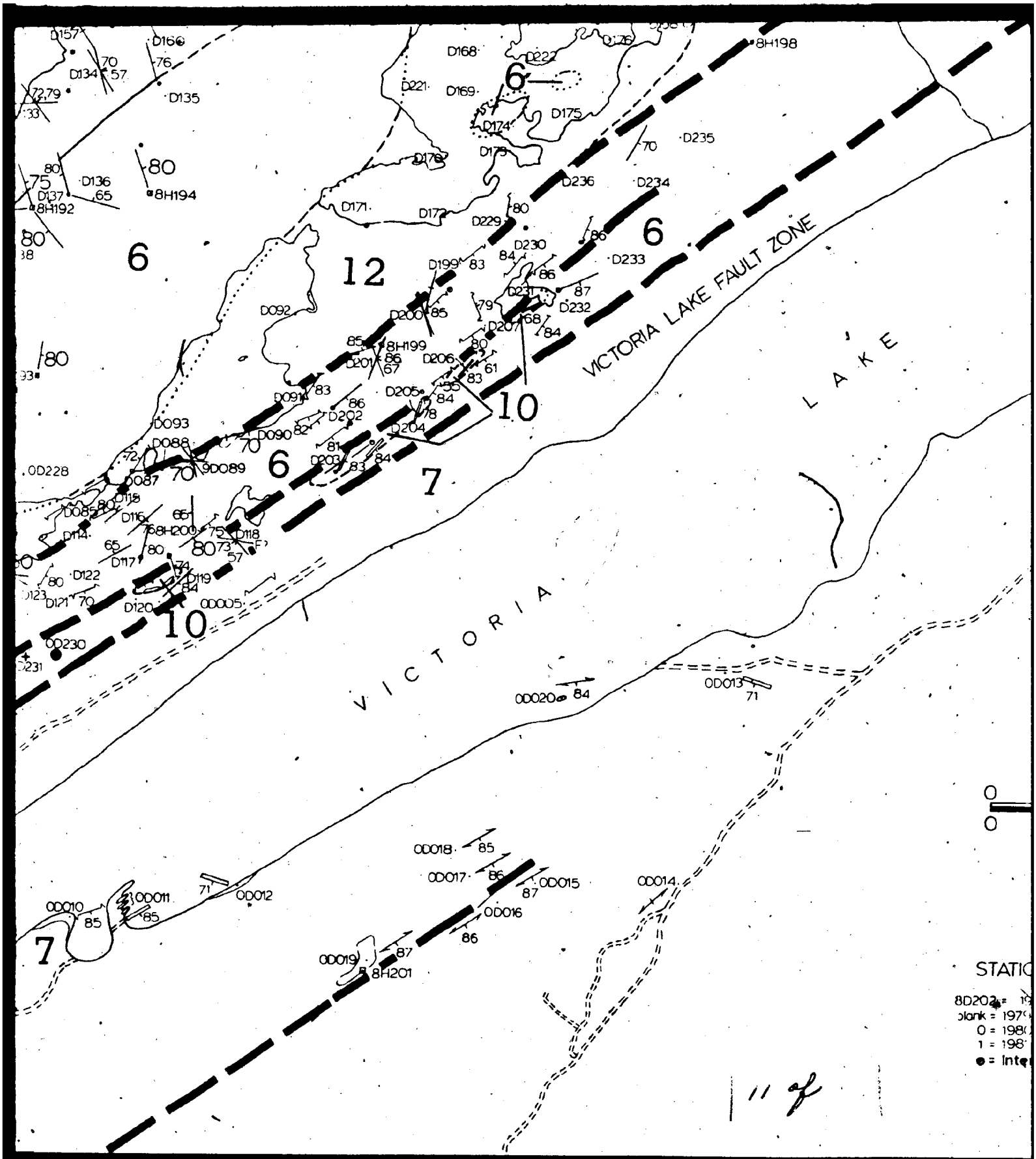
VICTORIA LAKE FAULT ZONE
VICTORIA
LAKE
D157
D160
D134
70
57
76
72,79
D135
D168
D222
D221
D169
6
D175
D174
D176
D235
70
8H198
80
75
D136
65
D137
8H192
8H194
80
D171
D172
D229
80
D236
D234
D230
84
86
D233
6
12
D199
83
D092
D200
85
D207
68
84
D231
87
D232
79
8H199
85
D201
86
67
D206
80
61
83
D205
84
D091
83
86
D202
D204
78
10
D093
D090
82
D088
70
81
D203
83
84
6
7
OD228
OD089
D087
D085
80
D115
D116
65
8H200
75
D118
D114
65
D117
80
80
73
57
D122
80
D123
D121
70
D119
84
D120
OD005
10
OD230
OD231
OD020
84
OD013
71
OD018
85
OD017
86
87
OD015
OD014
OD016
86
OD010
85
OD011
85
71
OD012
7
OD019
87
8H201
STATIC
8D202 = 19
blank = 197
0 = 198
1 = 198
● = Inte

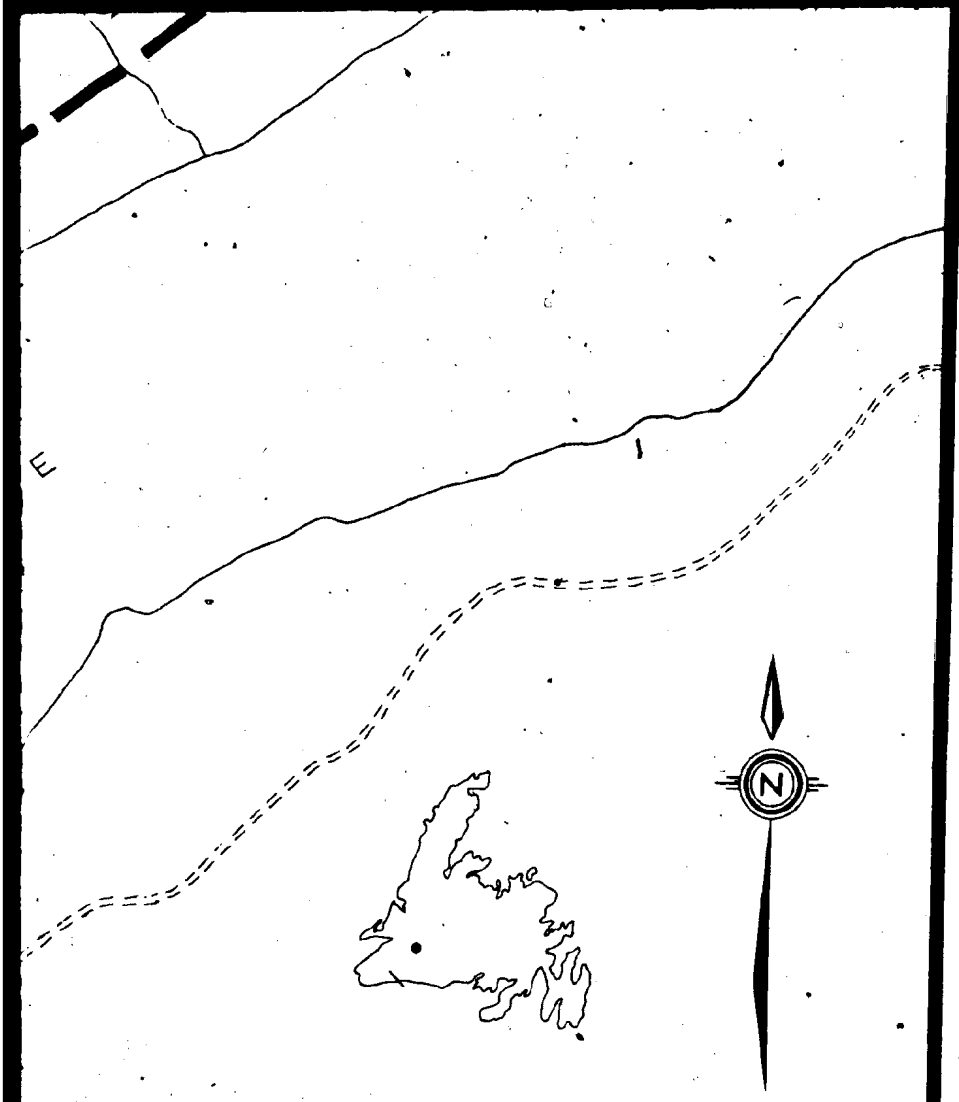

0 3000 Feet

0 .5 1.0 Kilometres

STATION NUMBERS

8D202 = 1978 DUNNING #202
blank = 1979
0 = 1980
1 = 1981
H = HERD
T = THOMPSON
● = inter-station data point

48°15'

57°29'

12 of 12